

ADAPTIVE DECISION FEEDBACK TECHNIQUES FOR MULTIUSER DETECTION IN CDMA SYSTEMS

A THESIS

*Submitted in partial fulfilment of the
requirements for the award of the degree*

of

DOCTOR OF PHILOSOPHY

in

ELECTRONICS AND COMPUTER ENGINEERING

By

AMIT KUMAR KOHLI



DEPARTMENT OF ELECTRONICS AND COMPUTER ENGINEERING
INDIAN INSTITUTE OF TECHNOLOGY ROORKEE
ROORKEE-247 667 (INDIA)

MAY, 2006

© INDIAN INSTITUTE OF TECHNOLOGY, ROORKEE 2006
ALL RIGHTS RESERVED

6th Annual Convocation- 2006
Degree conferred on 11.11.2006


Supdt. (PGS&R)



INDIAN INSTITUTE OF TECHNOLOGY ROORKEE
ROORKEE

CANDIDATE'S DECLARATION

I hereby certify that the work which is being presented in the thesis entitled "ADAPTIVE DECISION FEEDBACK TECHNIQUES FOR MULTIUSER DETECTION IN CDMA SYSTEMS" in partial fulfilment of the requirements for the award of the Degree of Doctor of Philosophy and submitted in the Department of Electronics and Computer Engineering of the Indian Institute of Technology Roorkee, Roorkee is an authentic record of my own work carried out during a period from July 2002 to May 2006 under the supervision of **Dr. D. K. Mehra**.

The matter presented in this thesis has not been submitted by me for the award of any other degree of this or any other university/Institute.

Amit Kohli

(AMIT KUMAR KOHLI)

This is to certify that the above statement made by the candidate is correct to the best of my knowledge.

Date: May 10, 2006

Bmehra

Dr. D. K. Mehra

Professor and Head,
Department of Electronics
and Computer Engineering,
Indian Institute of Technology,
Roorkee-247667, India.

The Ph.D. Via-Voce examination of **AMIT KUMAR KOHLI**, Research Scholar, has been held on 27/10/2006.

Bmehra

Signature of Supervisor

Yymin Shah

Signature of External Examiner

ABSTRACT

To satisfy the ever-increasing demand for higher data rates, as well as to allow more number of users to simultaneously access a common channel using the entire frequency spectrum allocated for transmission, interest has peaked in the direct sequence code division multiple access (DS-CDMA) techniques. In DS-CDMA transmission, the multipath propagation through linear dispersive media introduces intersymbol interference (ISI), which results in the bit error rate (BER) performance degradation. In addition to ISI, the non-orthogonal properties of signature sequences and asynchronism (*i.e.*, the random time offsets for the received signals of different users) lead to multiple access interference (MAI) along with additive white Gaussian noise (AWGN). The problem of MAI is not only due to the known intra-cell users, but also from the unknown inter-cell users. The unpredictable nature of MAI limits the capacity and performance of the multiuser system. Thus, even if the receiver thermal noise goes to zero, the error probability of the conventional receiver exhibits a non-zero floor because of MAI. Due to the propagation mechanism, the received signal from a user close to the base station can be stronger than the signal received from desired user located far from the base station. The near-far problem arises as the weaker signal can be overwhelmed by MAI.

The multiuser detection (MUD) has become a topic of extensive research interest since 1986, when Verdú formulated an optimum MUD receiver based on the maximum likelihood sequence detection criterion. However the solution involves a joint Viterbi processor with exponential complexity in the number of users, which has motivated the design of sub-optimum detectors with linear complexity. The decorrelating and minimum mean square error (MMSE) detectors are the most useful sub-optimum detectors. Though the decorrelating detector is near-far resistant, but it also enhances the background noise.

The MMSE detector, which minimizes the mean square error between the actual and estimated data bits, provides greater ability to combat noise at the cost of reduction in the near-far resistance. However the difficulty in the estimation of covariance matrix of the time-varying received signals has given rise to the use of adaptive MMSE techniques, which directly processes the samples of received signal at the chip interval without the explicit knowledge of MAI, and can be implemented using the tapped delay line filter. The adaptive MMSE techniques are analogous to the adaptive equalization of dispersive channels by virtue of the analogy between MAI and ISI. For very large loads *i.e.*, $K/N \gg 70\%$ (K = number of

strong users, and N = processing gain or signature sequence length), the substantial degradation in the performance of adaptive linear multiuser detector is observed. The adaptive non-linear MMSE techniques (decision feedback) are more effective than the linear techniques because latter is having only feedforward filter, whereas former is having feedforward as well as feedback filters to combat ISI.

In the case of a multiuser system, ISI not only originates from the past symbols of desired user, but also from the past symbols of interfering users, which can be suppressed by using the non-linear adaptive decision feedback detectors (ADFDs). At high signal to noise ratios (SNR) and loads, the non-linear techniques outperform the linear multiuser detection techniques. However the ADFDs suffer due to the error propagation problem, which leads to degradation in the BER performance. "The requirements imposed on the CDMA systems in terms of capacity and flexibility necessitate the advanced signal processing solutions for the multiuser interference suppression and data detection in the presence of ISI, MAI and AWGN. In the presented work, adaptive decision feedback structures based on the MMSE criterion are considered to solve the problems inherited in both non-adaptive and linear multiuser detection techniques."

Starting with the linear MMSE sub-optimum MUD, we focus on its probability of error performance analysis, and investigate the behavior of MAI in terms of the leakage coefficients. The MMSE linear multiuser detector considers MAI asymptotically Gaussian for a large number of users in the asynchronous DS-CDMA system. For this asymptotic condition, the MMSE detector outperforms the decorrelating detector only if the value of normalized cross-correlation (NCC) for any pair of signature sequence is less than or equal to the numerically derived upper bounded value. The available results in the literature have been derived for the two-user case. We have presented a general formula to calculate the upper bound on NCC for the arbitrary number of users under the near-far situation. The upper bound and optimum NCC ranges for $7 \geq K \geq 2$ have been derived. We also propose the Chernoff bound on the error probability of MMSE multiuser detector for Binomial as well as Gaussian distributed leakage coefficients. Its proof based on the Kullback-Leibler divergence theorem and study of the leakage coefficients for more than two users impose the stringent condition on SNR of the desired user for unbiased output of the linear MMSE MUD receiver. We have shown that the SNR of the desired user should be greater than the minimum bounded value, which depends on the number of users and NCC. The derived results depict that the MAI follows binomial distribution for a small number of users.

For adaptive implementation of the linear MMSE detector and for the channel

estimation, the least mean square (LMS) algorithm is normally used under the slowly time-varying multipath fading environment. However the Kalman filtering algorithm is used for the fast time-varying channel estimation, which increases the computational complexity of the receiver. Our motivation is to develop a novel two-step least mean square type adaptive algorithm, with low computational complexity $O[N]$, for the Markovian channel identification problem. In this work, we present a modified version of the two-step LMS-type adaptive algorithm motivated by the work of Gazor in [60]. We describe the nonstationary adaptation characteristics of this modified two-step least mean square (MG-LMS) algorithm for the system identification problem. It ensures stable behavior during convergence as well as improved tracking performance in the smoothly time-varying environments. The estimated weight increment vector is used for the prediction of weight vector for the next iteration. The proposed modification includes the use of a control parameter to scale the estimated weight increment vector in addition to a smoothing parameter used in the two-step least mean square (G-LMS) algorithm, which controls the initial oscillatory behavior of the algorithm. The analysis focuses on the effects of these parameters on the lag-misadjustment in the tracking process. The mathematical analysis for a nonstationary case, where the plant coefficients are assumed to follow a first-order Markov process, shows that the MG-LMS algorithm contributes less lag-misadjustment than the conventional LMS and G-LMS algorithms. Further, the stability criterion imposes upper bound on the value of the control parameter. These derived analytical results are verified and demonstrated with simulation examples, which clearly show that the lag-misadjustment reduces with the increasing values of smoothing and control parameters under permissible limits. It also supersedes the NLMS algorithm in tracking by combating the lag noise, which consequently reduces the lag-misadjustment at the cost of slight increase in the gradient-misadjustment. At the optimum value of control parameter, the MG-LMS algorithm provides approximately 3dB performance advantage over the G-LMS algorithm.

The G-LMS and MG-LMS are developed by exploiting the Kalman filtering algorithm. By combining the strategy used for MG-LMS and spread spectrum technique, we next present an adaptive decision feedback equalizer (ADFE) based multiuser receiver for the DS-CDMA systems over the smoothly time-varying multipath fading channels using the reduced Kalman least mean square (RK-LMS) adaptive algorithm. The frequency-selective fading channel is modelled as a tapped delay line filter with smoothly time-varying Rayleigh distributed tap-coefficients, which are considered to be auto-regressive processes varying at

the data rate. The receiver uses an adaptive MMSE multiuser channel estimator to predict the coefficients of the tapped delay line filter. We consider first the design of adaptive MMSE feedforward and feedback filters by using the estimated channel response. We next present the convergence characteristics and the tracking performance of the proposed multiuser channel estimator using the RK-LMS algorithm. Unlike the previously available Kalman filtering algorithm based approach, the incorporation of the RK-LMS algorithm reduces the computational complexity of the multiuser receiver. The computer simulation results are presented to show the substantial improvement in its tracking as well as BER performance over the conventional LMS algorithm based receiver. The simulation results depict that the performance of the proposed multiuser receiver is dependent on the channel estimation errors because the residual ISI adversely affects the BER performance. The increasing load and velocities of the mobile users deteriorates the performance of DS-CDMA system. The BER performance also degrades for a large number of multipaths because the SNR per path reduces, which results in high channel estimation errors. However for a small number of multipaths, the feedforward filter provides performance advantage by exploiting the multipath diversity. It may be inferred from the presented results that the proposed multiuser receiver proves to be robust against the nonstationarity introduced due to the channel variations, and is beneficial for the multiuser interference cancellation and data detection.

Subsequently, we consider the mitigation of error propagation effect in the decision feedback detection techniques. We present an ADFE with erasure algorithm (E-DFE) for the asynchronous DS-CDMA transmission using the LMS algorithm, which not only combats ISI and MAI but also reduces the effects of error propagation in the presence of Gaussian background noise. To reduce the possibility of feeding back the wrong decisions, the output of feedforward filter of the E-DFE is processed before it is fed back to the feedback filter. Specifically, the focus is on the performance of E-DFE using the soft-slicer based on a novel erasure algorithm. In addition, the fully connected feedback filter of E-DFE has been used to eliminate ISI due to other active users. We use the over-sampling technique to deal with the asynchronous reception of users. Comparison of the performance of conventional decision feedback equalizer and E-DFE over the slowly varying frequency-selective fading channel is presented to show the advantages of E-DFE in terms of the reduced BER. Simulation results are also presented to demonstrate the substantial improvement in its performance under the near-far and high load situations. The receiver also proves to be effective against sudden changes in the SNR of the desired user.

We next present a novel ADFD based on the parallel interference cancellation approach

(ADFD-PIC) using the LMS algorithm for the DS-CDMA system, which is motivated by the previous work on P-DFD (parallel-) in [128]. It not only combats ISI and MAI, but also suppresses other-cell interference. The multiuser P-DFD uses the estimated covariance matrix of the received signal vector, but the ill-conditioned nature of the covariance matrix introduces numerical problems. In P-DFD, the tentative decisions of K users obtained from the linear MMSE receiver are used for the parallel interference cancellation. The tentative decisions may be unreliable due to the residual MAI, which leads to error propagation in the multistage detector. The erasure algorithm may be used to generate the time-variable partial cancellation factors depending on the soft-output of multiuser linear filter. The presented ADFD-PIC structure using the channel estimator and erasure algorithm based soft-slicer (EC-ADFD-PIC) offers performance improvement by mitigating the adverse effects of error propagation. The simulation results are presented to demonstrate the substantial improvement in the BER performance of MMSE EC-ADFD-PIC over other multiuser detection techniques. Previously reported results depict that the P-DFD offers approximately 2dB gain relative to the MMSE MUD receiver. However, the presented EC-ADFD-PIC provides approximately 3dB performance advantage over the linear MMSE multiuser receiver under the smoothly time-varying multipath fading channel. The results also demonstrate that EC-ADFD-PIC may be used for the slow mobile users.

The two-stage DFD using the S-DFD (successive-) and P-DFD in concatenation (S-P-DFD) suffers due to the error propagation effect for a small number of users. In this work, we present a novel two-stage MMSE multiuser DFD for the DS-CDMA system working under the frequency-selective multipath fading environment. The first stage of the proposed cascaded structure is the noise-predictive successive DFD (NP-S-DFD), in which the active users are demodulated and detected successively using the conventional Bell Labs Layered Space-Time (BLAST) ordering criterion. The second stage includes an adaptive successive/parallel DFD (SP-DFD), which uses the tentative decisions obtained at the first stage for the multiuser interference cancellation and data detection. Therefore, the presented two-stage detector may be called the noise-predictive successive SP-DFD (NP-S-SP-DFD). The first user is detected using the linear MMSE transformation in NP-S-DFD, which may lead to the error propagation at successive stages due to the wrong detection of data symbol corresponding to the first user. However at the second stage of NP-S-SP-DFD, the first user is detected using the parallel interference cancellation approach, which leads to reduction in the bit error rate. Simulation results are presented to show the substantial improvement in the BER performance of NP-S-SP-DFD over the conventional single-stage S-, P-, NP-S-, and

cascaded S-P-DFDs. The presented DFD provides performance improvement, when the order in which the users are detected is optimized according to the BLAST ordering based on MMSE criterion. However under the low SNR conditions, significant degradation in the BER performance of NP-S-SP-DFD is observed due to the error propagation effect. On the other hand, its performance substantially improves under the high SNR conditions, and the presented results demonstrate that the NP-S-SP-DFD based on MMSE criterion outperforms the conventional single-stage and two-stage DFDs.

ACKNOWLEDGEMENTS

I wish to express my deep sense of gratitude to **Dr. D. K. Mehra** for his invaluable supervision, encouragement, constructive criticism, and suggestions during the course of work. He has been generous in undertaking comprehensive discussions and meticulously reviewing of the thesis, without which the work could not have come to its present shape. I always found him ready for resolving any of my difficulties and guiding me to the solution.

The working facilities provided by the Head, Department of Electronics and Computer Engineering, IIT, Roorkee, are highly acknowledged. I wish to express my thanks to the non-teaching staff members of Communication Lab. I sincerely acknowledge MHRD, Government of India, for sponsoring my research program.

I would like to thank Dr. Arun Kumar and Mr. S. Chakravorty for their generous, helping and friendly attitude towards me, who have shared their experiences with me during the teaching assistantship.

Special thanks to my colleague Mr. Vinay Kumar Shrivastava, presently engineer in research group of Reliance Infocomm, for fruitful technical discussions.

I wish to express my respectful tribute to **my mother Late Mrs. Kamlesh Kr. Kohli**, who passed away during my research program. With due regards, I wish to thank **my father Dr. Jagdish Chander Kohli** for motivating me during the course of study. I am grateful to my sister Mrs. Seema Kapoor for her constant support and encouragement throughout the research program, which deserves a special mention.

Thanks are due to all the fellow research scholars; especially Ajey Kumar among others for his cooperation and support.

Amit Kumar Kohli

CONTENTS

Page No.

COPYRIGHT

CANDIDATE'S DECLARATION

ABSTRACT	(i)
ACKNOWLEDGEMENTS	(vii)
TABLE OF CONTENTS	(viii)
LIST OF FIGURES	(xii)
LIST OF ACRONYMS	(xv)
LIST OF NOTATIONS	(xviii)

CHAPTER 1 INTRODUCTION

(1)

1.1 Review of the earlier work	(3)
1.2 Statement of problem	(22)
1.3 Organization of the thesis	(24)

CHAPTER 2 PROBABILITY OF ERROR ANALYSIS OF LINEAR MMSE

MULTIUSER DETECTOR

(27)

2.1 Introduction	(28)
2.2 Multiuser system model	(33)
2.3 Analysis of leakage coefficients	(40)
2.3.1 Asymptotic analysis of leakage coefficients	(40)
2.3.2 Upper bounds on the probability of error	(43)
2.4 Upper bound on signature sequence cross-correlation function	(46)
2.5 Concluding remarks	(54)

CHAPTER 3 ADAPTIVE ALGORITHMS FOR TRACKING OF SMOOTHLY TIME-VARYING CHANNELS (55)

3.1 Introduction (56)

3.2 The MG-LMS algorithm (60)

 3.2.1 Mathematical formulation (60)

 3.2.2 MG-LMS algorithm (62)

 3.2.3 Decoupling of gradient and lag components (64)

3.3 Lag-misadjustment analysis for the MG-LMS algorithm (67)

 3.3.1 Determination of control parameter for the first-order Markov process (68)

 3.3.2 Determination of lag-misadjustment for the first-order Markov process (71)

3.4 Simulation results (75)

3.5 Concluding remarks (82)

CHAPTER 4 ADAPTIVE MULTIUSER DECISION FEEDBACK EQUALIZER RECEIVERS FOR DS-CDMA SYSTEMS (84)

4.1 Introduction (85)

4.2 DS-CDMA system model (89)

4.3 Channel estimator based DFE multiuser receiver (94)

4.4 Adaptive multiuser channel estimation (95)

 4.4.1 RK-LMS algorithm based channel estimator (97)

 4.4.2 Analysis of multiuser channel estimator (100)

4.5 RK-LMS algorithm based adaptive multiuser receiver (103)

 4.5.1 Adaptive data detection procedure (103)

 4.5.2 Probability of error analysis (105)

4.6 Simulation results (107)

 4.6.1 Performance evaluation of multiuser channel estimator (107)

4.6.2 Performance evaluation of adaptive multiuser receiver	(113)
4.7 Concluding remarks	(121)
 CHAPTER 5 ADAPTIVE MULTIUSER DECISION FEEDBACK DETECTORS FOR DS-CDMA SYSTEMS USING PARALLEL INTERFERENCE CANCELLATION APPROACH	
	(123)
5.1 Introduction	(124)
5.2 Adaptive decision feedback equalizer using the erasure algorithm	(128)
5.2.1 Adaptive E-DFE structure	(128)
5.2.2 Erasure algorithm	(130)
5.3 Partial parallel interference canceller	(133)
5.4 Adaptive multiuser EC-ADFD-PIC	(137)
5.6 Simulation results	(140)
5.6.1 Performance evaluation of adaptive E-DFE	(140)
5.6.2 Performance evaluation of adaptive EC-ADFD-PIC	(145)
5.7 Concluding remarks	(150)
 CHAPTER 6 TWO-STAGE MMSE MULTIUSER DECISION FEEDBACK DETECTORS FOR DS-CDMA SYSTEMS	
	(152)
6.1 Introduction	(153)
6.2 Successive interference cancellation scheme	(158)
6.3 Noise-predictive successive DFD	(161)
6.3.1 NP-S-DFD using MMSE criterion	(161)
6.3.2 Detection ordering using MMSE criterion	(165)
6.4 Two-stage NP-S-SP-DFD	(167)
6.5 Simulation results	(170)
6.6 Concluding remarks	(176)

CHAPTER 7 CONCLUDING REMARKS	(178)
7.1 Conclusions	(178)
7.2 Suggestions for further work	(185)
APPENDIX A DETERMINATION OF THE TIME CONSTANT	(188)
APPENDIX B EQUATIONS FOR ESTIMATED WEIGHT ERROR	(190)
APPENDIX C DETERMINATION OF THE PARTIAL CANCELLATION FACTOR	(191)
REFERENCES	(192)
PUBLICATIONS BASED ON THIS WORK	(206)

LIST OF FIGURES

Fig. No.	Caption	Page No.
2.1	Lowpass equivalent representation of the DS-CDMA transmitter for K active users.	(35)
2.2	Illustration of the interference caused by the k th user to the desired user signal.	(35)
2.3	Chernoff upper bound on error probability for Binomially distributed leakage coefficients.	(45)
2.4	Upper bound on the value of NCC vs the number of users.	(53)
3.1	Unknown time-variable system.	(60)
3.2	Graphical interpretation of the proposed MG-LMS algorithm.	(63)
3.3	Relative lag-misadjustment vs a of MG-LMS algorithm for variable α ($\mu\lambda_{avg} = 0.001$ and $\beta = 0.75$).	(73)
3.4	Relative lag-misadjustment vs a of MG-LMS algorithm for variable β ($\mu\lambda_{avg} = 0.001$ and $\alpha = 0.05$).	(74)
3.5	Auto-correlation of channel tap-coefficient using the $AR(2)$ approximation with $f_d T_S = 0.001$	(77)
3.6	Convergence and tracking performance comparison of MG-LMS algorithm for various values of β in terms of MMSE (dB).	(78)
3.7	Variation of MMSE (dB) of MG-LMS algorithm for different values of control parameter β	(80)
3.8	Comparison of MG-LMS, G-LMS, NLMS and LMS algorithms for channel tracking.	(81)
4.1	Adaptive MMSE DFE multiuser receiver using the RK-LMS algorithm.	(96)

4.2	MMSE (dB) vs the number of iterations of RK-LMS algorithm for different values of Doppler frequencies.	(109)
4.3	The performance advantage of RK-LMS over the conventional LMS for different number of users.	(111)
4.4	Channel tracking performance of the RK-LMS algorithm.	(112)
4.5	BER of RK-LMS algorithm for different values of Doppler frequencies.	(116)
4.6	BER vs the number of multipaths for RK-LMS algorithm.	(117)
4.7	BER vs the number of users for RK-LMS algorithm.	(119)
4.8	BER vs SNR for RK-LMS algorithm.	(120)
5.1	Adaptive E-DFE with fully connected feedback structure for the k th user.	(129)
5.2	Graphical interpretation of the erasure algorithm for E-DFE.	(132)
5.3	Partial parallel interference cancellation using the E-slicer.	(135)
5.4	Block diagram of the proposed channel estimator based DFD using the PIC approach.	(137)
5.5	P-DFD using the E-slicer.	(138)
5.6	MMSE (dB) vs the number of iterations for adaptive E-DFE, $K = 5$	(142)
5.7	BER vs the number of users for adaptive E-DFE.	(143)
5.8	BER vs the signal-to-noise ratio (dB) of the desired user for adaptive E-DFE.	(144)
5.9	BER vs SNR for adaptive EC-ADFD-PIC.	(147)
5.10	BER vs Doppler frequency for adaptive EC-ADFD-PIC.	(148)
5.11	BER vs the number of users for adaptive EC-ADFD-PIC.	(149)
6.1	Decision feedback detector using the successive interference cancellation scheme.	(160)
6.2	Single-stage noise-predictive successive DFD.	(164)

6.3a	Two-stage NP-S-SP-DFD with adaptive successive/parallel DFD at the second stage.	(168)
6.3b	Adaptive parallel interference canceller.	(168)
6.4	Performance comparison of single-stage DFDs using the different detection ordering criteria.	(171)
6.5	Multipath channel effects on the performance of NP-S-DFD, (SNR in dB). ...	(172)
6.6	Gain of the last detected NP-S-DFD and S-DFD user relative to the linear MMSE user.	(174)
6.7	Performance comparison of the two-stage NP-S-SP-DFD with other detectors, (SNR in dB).	(175)

LIST OF ACRONYMS

ADFD	Adaptive Decision Feedback Detector
ADFE	Adaptive Decision Feedback Equalizer
AR	Autoregressive
ARMA	Autoregressive Moving Average
AWGN	Additive White Gaussian Noise
BER	Bit Error Rate
BLAST	Bell Labs Layered Space-Time
BLUE	Best Linear Unbiased Estimator
BPSK	Binary Phase Shift Keying
C-DFE	Conventional Decision Feedback Equalizer
DFD	Decision Feedback Detector
DFE	Decision Feedback Equalizer
DS-CDMA	Direct Sequence Code Division Multiple Access
E-DFE	Decision Feedback Equalizer using Erasure Algorithm based Soft-slicer
EC-ADFD-PIC	Adaptive Decision Feedback Detector based on Parallel Interference Cancellation Approach using Erasure Algorithm (soft-slicer) and Channel Estimator
EKF	Extended Kalman Filter
FDMA	Frequency Division Multiple Access
G-DFE	Generalized Decision Feedback Detector
G-LMS	Gazor's Two-step LMS-type (see [60])
HPIC	Hard-decision Parallel Interference Cancellation

IC	Interference Cancellation
ISI	Intersymbol Interference
JD	Joint Detection
KF	Kalman Filter
LMS	Least Mean Square
MAI	Multiple Access Interference
MAP	Maximum <i>a posteriori</i>
MBER	Minimum Bit Error Rate
MF	Matched Filter
MF-ML	Matched Filter Maximum Likelihood
MIMO	Multi-input Multi-output
ML	Maximum Likelihood
MLSE	Maximum Likelihood Sequence Estimation
MMSE	Minimum Mean Square Error
MMSE-ML	Minimum Mean Square Error Maximum Likelihood
MSE	Mean Square Error
MUD	Multiuser Detection
MUI	Multiuser Interference
NBI	Narrowband Interference
NCC	Normalized Cross-correlation
N-CDMA	Narrowband Code Division Multiple Access
NLMS	Normalized Least Mean Square
NP-S-DFD	Noise Predictive Successive Decision Feedback Detector
OCI	Other Cell Interference
OFDM	Orthogonal Frequency Division Multiplexing

PCF	Partial Cancellation Factor
PAM	Pulse Amplitude Modulation
PIC	Parallel Interference Cancellation
P-DFD	Parallel Decision Feedback Detector
RK-LMS	Reduced Kalman/Least Mean Square
RLS	Recursive Least Square
S-DFD	Successive Decision Feedback Detector
SIC	Successive Interference Cancellation
SIR	Signal to Interference Ratio
SNR	Signal to Noise Ratio
SPIC	Soft-decision Parallel Interference Cancellation
TDMA	Time Division Multiple Access
V-BLAST	Vertical Bell Labs Layered Space-Time
W-CDMA	Wideband Code Division Multiple Access
ZF	Zero Forcing
ZF-DFD	Zero Forcing Decision Feedback Detector

LIST OF NOTATIONS

A_k	k th user's amplitude
b_k	Data bit of k th user
c_k^j	j th chip of k th user's code sequence
E	Expectation operator
$f_D = f_d$	Maximum Doppler frequency
f_p	Spectral peak frequency
γ_k	Complex attenuation factor of k th user
γ_{lk}	Complex attenuation factor of k th user's l th path
h_{lk}	k th user's l th channel coefficient
J_{\min}	Minimum mean square error
J_{excess}	Excess mean square error
J_{lag}	Lag mean square error
$J_0(\)$	Bessel function of the first-kind and zeroth-order
K	Number of active users in a cell
K/N	Load factor
L_k	Number of multipaths for k th user
λ_p	p th eigenvalue
λ_{avg}	Average eigenvalue
λ_{max}	Maximum eigenvalue
λ_{min}	Minimum eigenvalue
μ	Step size

N	Processing gain or Spreading code sequence length
$N(\text{mean}, \text{var})$	Statistics of random process
P_k	k th user's power level
$Q_G(\)$	Complementary unit cumulative Gaussian distribution function
r_d	Pole radius corresponding to the steepness of the peaks of power spectrum
\hat{r}_k	Equivalent lowpass received signal of k th user
\hat{r}	Equivalent lowpass composite received signal
\hat{r}_{ISI}	ISI component in the composite received signal
$s_k(t)$	Spreading sequence waveform of k th user
T_b	Data bit duration
T_c	Chip interval
T_m	Multipath delay spread
T_s	Sample time
τ_k	Total delay for k th user
τ_{lk}	Total delay for k th user's l th path
v_m	Mobile velocity
ω_c	Carrier frequency
Ξ_{lag}	Lag-misadjustment
$\psi(t)$	Chip waveform
$(\)_{NF}$	Parameters under near-far situation
$(\)^H$	Hermitian operator
$(\)^*$	Conjugate operator
$[\] = [\]$	

INTRODUCTION

Direct-sequence code-division-multiple-access (DS-CDMA) systems are finding applications in wireless communications, due to the merits of spread spectrum systems over the conventional time-division-multiple-access (TDMA) and frequency-division-multiple-access (FDMA) techniques, where a number of users are assigned different code sequences (also known as signature sequences), and simultaneously transmit the information over a common channel using the entire frequency spectrum allocated for transmission [1], [2]. It has been investigated widely during 1980's, which finally led to the commercialization of N-CDMA (Narrowband-) in IS-95 standard for the cellular communications. To satisfy the ever increasing demand for the high data rates to transmit the multimedia traffic for a large number of users in the network, interest has peaked in W-CDMA (Wideband-) for the third generation (3G) wireless communication (IMT-2000 standard) due to its enhanced performance by utilizing the frequency-selective nature of channel [3]-[6].

The DS-CDMA detector receives a composite signal consisting of contributions from different users, which overlap in time as well as in frequency domain. In conventional DS-CDMA detector (matched filter receiver), the desired user's signal is detected by correlating the composite received signal with that of the desired user's code sequence waveform. However, the non-orthogonal properties of the code sequences and asynchronism (*i.e.*, the random time offsets for the received signals of different users) lead to the multiple-access-interference (MAI) along with the additive-white-Gaussian-noise (AWGN). As the number of interferers increases, the MAI becomes substantial, causing degradation in the system performance [7].

The problem of MAI is not only due to the known intra-cell users, but also from the unknown inter-cell or other-cell users. Due to propagation mechanism, the received signal from a user close to the base station can be stronger than the signal received from the desired user located far from the base station. The near-far problem arises as the weaker signal can be overwhelmed by MAI, and hence the detection is rendered unreliable. However, the unpredictable nature of MAI limits the capacity and performance of the DS-CDMA system. Thus, even if the receiver thermal noise goes to zero, the error probability exhibits a nonzero floor because of MAI.

One common strategy to deal with the near-far problem is to use power control. In a mobile cellular environment, the base station periodically sends information to each of the mobiles, directing them to adjust their transmitted power in such a manner that all the signals will be received at the base station at approximately same power level [8], causing wastage of precious bandwidth.

In addition to MAI, the multipath propagation through the linear dispersive media introduces intersymbol-interference (ISI) at the high data rates, which severely limits the performance of the conventional receiver [9], [10]. Turin [11] has shown that in a typical urban environment, the fading may cause severe performance degradation in the DS-CDMA network, because the conventional matched-filter (MF) receiver is unable to exploit the multipath diversity.

Multiuser-detection (MUD) techniques are used to overcome the effects of MAI and near-far problem. In MUD techniques, the receiver jointly detects all the active users in order to mitigate the non-orthogonal properties of spreading code sequences. The MUD techniques have become a topic of extensive research interest since 1986 when Verdú formulated an optimum multiuser detector based on the maximum-likelihood-sequence-estimation (MLSE) criterion [12]. However the solution involves a joint Viterbi processor with exponential

complexity in the number of users, which motivates the design of sub-optimum detectors with complexity linear in the number of users by applying the linear transformations to the output of matched filter bank to remove MAI [13].

However, the requirements imposed on the DS-CDMA systems in terms of the capacity and flexibility necessitate the advanced signal processing solutions for the multiuser interference suppression and detection. The adaptive minimum-mean-square-error (MMSE) techniques are analogous to the adaptive equalization of the dispersive channels by virtue of the analogy between MAI and ISI [14]. The MMSE non-linear decision feedback techniques are more effective than the linear techniques because the latter is having only feedforward filter, whereas the former is having feedforward as well as feedback filters to combat ISI [15]. Thus, the multiuser interference cancellation and detection using the decision feedback structures in the presence of MAI, ISI and AWGN may be considered as an interesting area for further research. In this thesis, adaptive decision feedback structures based on the MMSE criterion are considered to solve the problems inherited in both non-adaptive and linear multiuser detection techniques.

In the following, we present a brief summary of the earlier work carried out in the related area, followed by the statement of problem and the organization of material embodied in this thesis.

1.1 Review of the earlier work

The conventional MF receiver is vulnerable under the near-far situation. Verdú [12] proposed and analysed the optimum MUD for asynchronous CDMA system (similar work also appeared in [16]). The MUD techniques can be divided into two categories: joint-detection (JD) techniques and interference-cancellation (IC) techniques [7]. In JD techniques, the front end of the receiver is traditionally (but not necessarily) a bank of MFs followed by filters that

perform linear or non-linear transformations, which are usually computationally expensive.

Lupas and Verdú [17], [18] proposed a computationally efficient linear sub-optimum decorrelating detector (also known as decorrelator), which possesses ideal near-far resistance at the cost of noise enhancement analogous to the zero-forcing (ZF) equalizer [15]. Moreover, it requires the knowledge of interference parameters and the inverse of cross-correlation matrix. Xie *et al.* [19] first proposed the MMSE DS-CDMA receiver in 1990 using the linear transformation under the AWGN channel. The MMSE detector attempts to minimize the mean-square-error (MSE) between the transmitted and estimated bits. This receiver is non-adaptive, and requires the knowledge of the noise variance in addition to the user parameters and the inverse of correlation matrix.

The decorrelating (ZF) detector chooses the linear filter to eliminate the output MAI [18], and the MMSE detector chooses the linear filter to minimize the average mean-squared value of the output MAI-plus-noise mixture [19]. Tsatsanis and Giannakis [20] have thoroughly studied the decorrelating receiver for MAI and ISI suppression. The authors have identified the conditions under which FIR solutions are possible, and have also presented the optimal MSE solutions subject to the decorrelating constraint. However, the MMSE receiver performs better than the decorrelating receiver in the noisy environment. It has been shown in [21] that the MMSE MUD technique offers significant practical advantages, and can be adapted blindly *i.e.*, without the use of training sequence and the knowledge of interfering signature waveforms. However, since the MMSE criterion is not directly related to the error probability or to the distribution of background noise, it is of considerable interest to study the error probability of MMSE detector in an environment of back ground Gaussian noise. The design of the linear MUD techniques also depends on the distribution of MAI, which may be Gaussian or Binomial. In [22] and [23], the authors have presented a useful way to quantify the non-Gaussianness by analysing the (Kullback-Leibler) divergence of the

distribution of the random variable and the Gaussian random variable with same variance.

Monk *et al.* [24] have considered MAI as the colored noise, and have used the noise-whitening approach as well as the MAI noise rejection approach to maximize the signal-to-noise-ratio (SNR). However, the SNR maximization does not guarantee low probability of error for the non-Gaussian noise. Pursley and Geraniotis [25], [26] have analysed the spread spectrum techniques, and have also derived the probability of error by considering MAI along with AWGN.

Using the divergence theorem and the probability of error analysis, Poor and Verdú [27] have demonstrated that the MAI-plus-noise mixture at the output of MMSE linear multiuser receiver is approximately Gaussian for a large number of users, large SNR values and severe near-far scenario. This property is very useful in the performance analysis of MMSE multiuser detectors. The MMSE MUD technique supersedes the decorrelator, if the normalized cross-correlation between the signature sequences is less than $\left(\sqrt{2/\sqrt{3}}\right)/2$ for the two-user case. Similar to the intersymbol interference error bounds for the bandlimited signals presented in [28], the authors have proposed Chernoff upper bound on the error probability of linear multiuser detectors.

Moustakides and Poor [29] have shown that MMSE MUD technique does not uniformly outperform the decorrelator and the conventional MF receiver. However, the former detector provides higher spectral efficiencies under severe conditions [30]-[34]. Zhang *et al.* [35] have further extended these results to fading channels, and have demonstrated that the MAI at the output of MMSE receiver is asymptotically Gaussian for almost every realization of the signature and the received power for both synchronous and asynchronous DS-CDMA systems. However, Wang *et al.* [36], [37] have shown that the output SNR and the near-far resistance of MMSE MUD techniques depend on the cross-correlation matrix of the spreading code waveforms. Their work suggests a number of

interesting problems for further research, including the extension of the results presented in [27] for more than two-user case under the near-far situation.

A major limitation of the non-adaptive detectors is that they require the knowledge of spreading code sequences, timings and amplitudes (power) of all the active users. But unpredictable activities of some users, such as asynchronous mode of data transmission, make it more difficult to estimate their received power over a given time interval. Moreover, the use of non-adaptive receivers will result in a wasted resource of unnecessary computations if only a subset of possible users is active. An important subject in MUD is the design of adaptive detectors that self-tune the detector parameters from the observation of received signal waveform. Moreover, the difficulty in the calculation of cross-correlation matrix of the time-varying received signals has given rise to the adaptive MMSE techniques for the multiuser detection.

Adaptive multiuser DS-CDMA receivers based on the MMSE criterion have been proposed by many researchers [38]-[40]. These detectors have been implemented without the knowledge of user parameters, except the timing information of desired user and the training sequence. The typical operation of these adaptive multiuser detectors requires each transmitter to send a training sequence at start up, which the receiver uses for the initial adaptation. After the training phase, the adaptation during actual data transmission occurs in the decision directed mode. In [38], an N -tap MMSE receiver is presented, where N is the processing gain (signature sequence length). Two computationally efficient MAI suppression schemes have been considered, namely: the cyclic shifted filter bank scheme and the over-sampling technique. If the received signals from different intra-cell users are chip asynchronous, then the different timing offsets across users is an important issue. However in principle, it can be solved using the fractional chip sampling with the use of the excess bandwidth. Madhow [41] has suggested a near-far resistant time delay estimation method.

The delay is estimated by running N -parallel adaptive algorithms, and then finding the delay, which provides lowest MSE. The only requirements are a training sequence for the desired user and a finite uncertainty regarding the symbol timing.

Miller [39] has proposed an adaptive receiver for combating the near-far problem. The receiver is a chip matched filter followed by an adaptive equalizer structure to perform the despreading operation. The receiver is shown to be immune to the near-far problem in the sense that its performance without any power control is nearly identical to its performance with perfect power control. This receiver increases the capacity by two fold relative to the conventional receiver with power control. The training analysis of the adaptive MMSE receiver is given in [40].

Rapajic and Borah [42] have presented an adaptive MMSE maximum-likelihood (MMSE-ML) receiver structure, where the conventional front end of the MF maximum-likelihood (MF-ML) detector is replaced by an adaptive MMSE filter, for the generation of sufficient statistics. It is shown that the replacement of MF bank with the MMSE filter results in advantages, like ability to perform the joint synchronization, channel parameter estimation, and significant improvement in the bit-error-rate (BER) performance. However the receiver requires the knowledge of spreading sequences of all the active users, and its computational complexity increases substantially with the increasing number of users.

As real world communication channels are stressed with higher data rates in the multiuser systems, the ISI becomes a dominant limiting factor along with MAI and AWGN. The DS-CDMA systems using the non-linear interference cancellation schemes have shown even better performance if the receiver has the knowledge of spreading sequences of all the active users, the received power level of some interferers and some of the channel parameters.

To combat ISI, the decision-feedback-equalizers (DFEs) are designed to compensate

channel distortions, which consider the MAI as noise. Instead of using the direct adapting DFE, one may first estimate the channel impulse response, and then design an equalizer based on the estimated channel. The estimation of channel parameters is difficult, especially in the fast time-varying channel of mobile communications and when the SNR changes take place rapidly. Traditionally, the receivers and equalizers rely on a transmitter assisted training session to extract the desired reference signal for the channel estimation or equalization. However, the channel estimation depends on the adaptive algorithm being used in the time-varying environment.

The optimum solution for the adaptive filtering problem is provided by the Wiener-Hopf equations. For obtaining the optimum filter tap weights, the correlation matrix needs to be inverted, which involves high computational complexity $O(N_T^3)$, where N_T is the number of filter taps. The least-mean-square (LMS) and recursive-least-square (RLS) algorithms are normally used to approach this solution. The LMS algorithm is simple to implement, model-independent, and offers robust performance [43], but its main drawback is its slow rate of convergence. The LMS filter suffers from the gradient noise amplification problem, when the dimension of the tap input vector is large. The normalized-LMS (NLMS) algorithm is used to overcome these problems, in which the step size is adjusted by normalizing it with respect to the squared Euclidean norm of the tap input vector. The NLMS algorithm involves computations of the order of $O(N_T)$. On the other hand, the RLS algorithm offers faster convergence but its computational complexity is $O(N_T^2)$.

The RLS, extended RLS and Kalman algorithms are commonly used for the time-varying channel tracking [44]-[47]. Chen and Wang [48] have analysed RLS algorithm based fast fading channel tracking schemes for the multichannel MLSE equalizer. Sayed and Kailath have delineated the relationship between the RLS and the Kalman filter in [46]. Under nonstationary environment, the Kalman and RLS algorithms require the system model

parameters to solve the system identification problem [45]. They are extremely sensitive to the parametric ambiguities, and hence become unstable under the parameter mismatching situation. Sayeed and Aazhang [49], [50] have proposed an optimal technique to exploit the joint multipath-Doppler diversity for the DS-CDMA systems, which can be used to develop algorithms for the tracking of channel statistics, and thus authors provide an alternative to the Kalman filter based approaches proposed in [51] and [52]. However, the computational complexity is the main limitation for its implementation in the multiuser detection scenario. Lindbom and Ahlén *et al.* [53]-[55] have proposed adaptation algorithms with constant gains for the smooth tracking of time-varying parameters of the linear regression models with prior information. The parameters are modelled as correlated auto-regressive-moving-average (ARMA) processes with the known dynamics. The design of presented algorithm is transformed into a Weiner filtering problem. It gives improved tracking performance with computational complexity less than the Kalman and RLS algorithms. Over rapidly fading channels, the proper choice of hypermodel (model for parameters) gives significant improvement in the tracking process. This technique has found limited applications, because its complexity depends on the hypermodel.

The time-varying Rayleigh fading channels may be modelled by using the first-order autoregressive process $AR(1)$ *i.e.*, first-order Markov model [56]. Haykin [43] has shown that the LMS algorithm outperforms the RLS algorithm under typical conditions for $AR(1)$ channel. Moreover, the LMS is a model independent adaptive algorithm. But, it suffers due to the lag noise in the tracking process [57]. Under nonstationary environment, the LMS algorithm has been analysed by various authors in [43] and [58]-[64]. The degradation in its performance is observed due to the lag-misadjustment in addition to the gradient-misadjustment. Macchi and Bershad [65], [66] have evaluated its performance by using the complex chirp exponential signals buried in the AWGN, and have also developed the

tracking theory based on the random-walk model [67].

Gazor [60] has presented a two-step LMS-type adaptive algorithm for the system identification problem, which is developed by exploiting the Kalman filtering algorithm. The channel is considered to be the first-order Markov process. It supersedes the conventional LMS algorithm under the nonstationary environment (time-varying plant coefficients) by combating the lag noise. Benveniste [59] has proposed the multistep algorithms for the time-varying channel tracking. But, their designs depend on the prior information about the time-variations of the true system. However, Gazor's two-step LMS-type (G-LMS) adaptive algorithm does not require such information [60]. It is implemented using the conventional LMS algorithm in two steps, which track the moving minimum point on the MSE surface according to the Wiener theory [43]. But it suffers due to oscillatory behaviour in the convergence as well as tracking mode, which results in the longer learning period and the high value of MMSE. This work motivates the development of a modified version of the G-LMS algorithm, which may track the time-varying channels efficiently by damping the oscillatory behaviour. However for the G-LMS and the conventional LMS algorithms, a general tracking theory for the first-order Markov model is yet to be developed. This algorithm may also be applied to the direct adapting DFE structures to cancel MAI and ISI in the nonstationary environment.

George *et al.* [68] have proposed an adaptive-decision-feedback-equalizer (ADFE) to detect information transmitted by the pulse-amplitude-modulation (PAM) through a noisy dispersive linear channel, which outperforms the linear equalizers working under the slow varying environment. Further, Monsen [69] has shown that the MMSE ADFE sacrifices diversity for the interference suppression. However, the multipath reception helps to reduce the diversity sacrifice for ISI suppression provided enough equalizer taps are available. Mulgrew and Chen [70] have introduced an ADFE using the minimum-bit-error-rate

(MBER) as cost function, which may outperform the MMSE approach under the typical conditions. In general, the relative performance of equalizers designed using the MMSE and MBER criteria is dependent upon specific channel conditions. At low SNR values in particular, there may be no significant benefit in using the MBER criterion.

For DS-CDMA systems under the Rayleigh fading environment, an effort is made by Abdulrahman *et al.* [14] to solve the problem of interference suppression and equalization by using a fractionally spaced ADFE based on the MMSE criterion, as all the users are transmitting at the same chip rate. The ADFE minimizes the effects of MAI as well as ISI by trying to force zeros in the impulse response of interferers at the decision instants. The use of MMSE ADFE instead of the ZF equalizer may reduce the enhancement of background noise and sensitivity to the weight inaccuracy due to the finite number of taps and the crude power control. Like linear fractionally spaced equalizers, the feedforward filter of ADFE can act as a RAKE combiner, and also exploits the inherent multipath diversity of the spread spectrum signalling and the over-sampling techniques. Moreover, the finite length MMSE ADFE with chip matched lowpass filtering is shown to outperform the code sequence matched filtering approach under the asynchronous conditions due to the non-orthogonal properties of signature waveforms.

Chaudhary *et al.* [71] have investigated the performance of DS-CDMA system in an overlaid cellular environment, in which the processing gain is varied with data rate of the selected service. It is shown that a MMSE ADFE receiver can be used to integrate dual-rate services without adversely affecting the system capacity. Klein *et al.* [72] have proposed four sub-optimal detectors based on the MMSE and ZF equalization criteria, with and without decision feedback, to combat both MAI and ISI. The MMSE DFE receiver has been shown to perform better than the ZF DFE detector and the linear MUD techniques in terms of the probability of error performance.

In [73] and [74], the authors consider a centralized adaptive-decision-feedback-detector (ADFD) using the MMSE criterion, where in addition to a fractionally spaced feedforward filter that processes the chip matched filter output, a feedback filter processes previous decisions from all the active users to cancel both MAI and ISI. Honig and Tsatsanis [75] have reviewed adaptive techniques in the multiuser detection. At very high loads and with sufficient SNR, the MMSE ADFD offers a significant performance improvement relative to the linear MMSE receiver. The main drawback of ADFD is the error propagation, which can significantly compromise performance under the low SNR conditions.

An ADFE/MLSE structure has been suggested in [76], in which the fractionally spaced forward filter acts as (pre) error whitening matched filter, and the feedback filter acts as channel impulse response estimator using the MLSE criterion. It has lower complexity than the conventional MLSE technique, and is more efficient than the conventional DFE. But, the rapid frequency-selective fading severely affects its performance. Although extending the *maximum a posteriori* (MAP) technique to the DS-CDMA systems seems natural, yet it will not give good performance unless some kind of MAI cancellation is performed.

Wong *et al.* [77] have developed an efficient way to apply the MAP technique to the DS-CDMA systems for the time-selective flat fading channels, in which the receiver contains a code sequence matched filter, whose impulse response is matched to the signature waveform of desired user. The output samples from the matched filter are fed into a delayed-decision forward recursive MAP demodulator, which exploits the channel memory by delaying the decision and using a sequence of observations. Since the processing gain is designed to be large in most of the practical DS-CDMA systems, it is reasonable to assume that the matched filter output samples are the Gaussian random variable, which simplifies the development of MAP receiver. However its design depends on the distribution of MAI, and it can not be used for the frequency-selective fading channels. Lee and Cox [78] have proposed

the MAP selection diversity scheme for ADFE, in which the output of the branch with the lowest estimated *a posteriori* probability of bit error is used as the final decision, which is used to adapt the DFE for all diversity branches. But, its application is limited to the frequency-selective slow fading channels. The proposed scheme is suitable for indoor wireless environment.

In a different approach, Smee and Schwartz [9], [10] considered the design and the performance analysis of non-linear (feedback) MMSE detectors for the asynchronous W-CDMA/DS-SS-SSMA in the quasi-static multipath fading channel for suppressing both MAI and ISI. The feedforward filter processes samples of the chip matched filter output, and the feedback filter processes the detected symbols. It may be noted that by increasing the connectivity of the feedforward filter, so that each user has access to more received samples, additional diversity advantage can be obtained. Four different structures have been proposed based on the connectivity of feedforward and feedback filters. The error propagation severely affects the performance of decision feedback structures presented in [10].

Chiani [79], [80] has proposed E-DFE (erasure-), which reduces the effects of error propagation by using two thresholds instead of one, in contrast to the conventional-decision-feedback-equalizer (C-DFE) with single threshold slicer. A symbol is considered unreliable for feedback, if its absolute value is less than the threshold value. It performs well over channels with long memory, and gives substantial reduction in the probability of error. In case of DS-SS-SSMA systems, the threshold value may be obtained by taking the behaviour of MAI into account, and may develop an erasure algorithm to control the error propagation effect in the decision feedback receivers.

The blind deconvolution and the blind channel estimation have been developed to treat the problem of detection under the situation of unknown channel [21], [81]. In [21], Honig *et al.* have introduced a blind adaptive receiver design by minimizing the mean output energy.

Torlk and Xu [81] have employed the blind identification method to estimate the channel response by using the signal subspace technique [82]. However in the blind designs [83]-[86], the channel is assumed to be unknown but time-invariant in a transmitted frame. Therefore, their method is not suitable for the time-varying fading channel case. Diggavi *et al.* [87] have proposed an adaptive delayed-decision feedback and joint data estimation scheme to combat the time-varying multipath fading channels in the presence of undesired co-channel interference. The adaptive receiver uses the quasi-Newton algorithm for the improved channel estimation, which enhances its performance. The conventional strategy for treating the slowly fading channel problem is to design an adaptive equalizer using the LMS or the RLS algorithm [88], [89]. But, both algorithms fail to perform well in a fast fading environment.

The Kalman-filter (KF), which is known to be the best-linear-unbiased-estimator (BLUE), has been proposed in the literature for equalization and interference excision under the frequency-selective time-varying channels [90], [91]. In [92], a discrete Kalman filter has been considered for the equalization of digital binary transmission in the presence of noise and ISI. The Kalman filter has also been used in the channel estimation and demodulation of binary signals. Kozminchuk and Sheikh [93] have presented a Kalman filtering approach for the suppression of narrowband interference in the DS-CDMA communication systems. This approach is based on the digital phase-locked-loop Kalman filter. The application of this concept to the DS-CDMA detection is also described in [94], in which an extended-KF (EKF) based detector is used for the joint symbol and time delay estimation of all the active users in the tracking mode. In [95], a multiuser receiver for the asynchronous DS-CDMA signals based on the KF is introduced, in which the improved performance of this detector over the MMSE detector is demonstrated.

In [96], it has been shown that the use of KF produces symbol estimates with the lowest

possible MSE among all the linear filters in long- or short-code systems for a given detection delay, and with a complexity that is fixed for a given detection delay unlike the case of MMSE detector. Iltis [51] has described a code-tracking algorithm for a DS-CDMA receiver based on the EKF, which provides both code synchronization and joint estimation of the interferers and channel parameter. Iltis *et al.* [52] have developed a multiuser DS-CDMA detector without the knowledge of delays and amplitudes of the signals. The algorithm is made adaptive, and the likelihood function in the symbol-by-symbol metric is updated using a set of EKF innovations. However the detector possesses high computational complexity, and moreover it requires the knowledge of noise variance.

McLaughlin [97] has presented an adaptive DFE structure working under the time-varying environment using the Kalman filtering approach [98]-[100]. Chen and Chen [101] have proposed an adaptive DFE receiver design to combat the multipath fading. The time-varying channels are modelled as Rayleigh fading processes to simulate the frequency-selective fading channels. The Kalman filtering algorithm is employed to estimate the tap-coefficients of the frequency-selective fading channels. Then, an adaptive DFE receiver is developed using the Kalman algorithm. In general, the dynamic characteristics of fading channels cannot be characterised exactly by the system identification method. The presented receiver takes the channel estimation errors into consideration to improve the performance. Iltis [51] has modelled the interference as an Nth-order autoregressive process. A composite channel that is equivalent to the convolution of pre-whitening filter and multipath channel coefficients is estimated by an EKF. However in [101], the receiver is designed for multiuser detection, and the channel model can be directly derived from the Doppler spread of the fading channel.

Further, Chen *et al.* [102] have extended the above work by considering effects of both multipath time-varying fading and the impulsive noise for the design of a channel

estimation and symbol detection algorithm for the DS-CDMA systems. In contrast to the conventional autoregressive channel model [103], the proposed linear-trend channel model with a scheme for tuning the variance of the driving noise is less sensitive to the channel variations due to the changing Doppler frequency. There is no need to identify the coefficients of transition matrix of the linear-trend model. The time-varying fading channels are estimated by the Kalman algorithm based channel estimator with a self-tuning scheme to track the time-varying fading. Moreover, a decision feedback based multiuser algorithm using the Kalman algorithm is presented by taking the channel estimation errors into account.

Komninakis *et al.* [104] have used the Kalman algorithm to estimate the multi-input-multi-output (MIMO) channel response using the time-varying frequency-selective model proposed by Bello in [105], which subsequently performs the equalization task in the multiuser systems. A low order autoregressive model is used to approximate the MIMO channel variations to facilitate tracking via Kalman filtering algorithm.

The Kalman algorithm is a model dependent algorithm, and also possesses high computational complexity, particularly in the multiuser detection scenario. However, a new set of adaptive decision feedback equalizers and multiuser detectors may be developed by exploiting the Kalman filtering technique to incorporate the two-step LMS-type algorithms.

The multiuser decision feedback techniques exhibit higher spectral efficiency than the linear MUD receivers, and may handle higher load than the linear MMSE multiuser detectors [106]-[108]. In the absence of error propagation, Müller *et al.* [106], [107] have demonstrated that the capacity of DS-CDMA system with the MMSE DFD is close to the capacity of an orthogonal-frequency-division-multiple-access (OFDM) technique for the high load values, which enables power saving relative to the linear techniques. The multiuser decision feedback strategy for the DS-CDMA was first proposed in [109], and was motivated by the earlier work on MIMO DFEs [110]. Duel-Hallen [111] has presented two multiuser

DFDs: P-DFD (Parallel-) using the parallel-interference-cancellation (PIC) scheme and S-DFD (Successive-) using the successive-interference-cancellation (SIC) scheme.

Koulakiotis and Aghvami have discussed the IC techniques in [7], which are characterized by the regeneration and subtraction of definite or tentative data decisions. But, these techniques require the knowledge of channel parameters (phase, amplitude, and delay). Viterbi [112] first suggested the processing of received signal by a SIC scheme, where one interferer is cancelled at each stage from the received signal [113]. It offers less complexity, and provides reliable detection of the weak users. But its disadvantages include the long delay associated with the detection of last (weakest) user, and the error propagation if the channel parameter estimates are not reliable. Moreover, there is a need to reorder the signals ~~when ever~~ the power profile changes. Patel and Holtzman [114], [115] have analysed the SIC scheme.

On the contrary, the interference cancellation for all the active users takes place simultaneously in the PIC approach. In this scheme, all the K active users create replicas of their interference contributions to the other $K - 1$ users' signals. Then, their replicas are subtracted simultaneously from the $K - 1$ users' signals. This scheme can completely remove interference if the original interference estimates are correct. This scheme offers low delay for the detection of all users. The different PIC schemes proposed in the literature use the tentative decisions obtained from the linear MMSE MUD techniques or the conventional MF detectors for the multiuser interference suppression and data detection.

Two types of PIC schemes are classified according to the tentative decision device: hard-decision PIC (HPIC) scheme, in which the output of slicer is used for IC, and soft-decision PIC (SPIC) scheme, in which the soft-output of correlator or linear receiver is used for IC [116]. The results presented by Buehrer and Nicoloso in [117] depict that the HPIC scheme performs better than the SPIC scheme because the decision statistic is biased when

the linear estimate of the symbol or channel is used for IC. However, the BER performance degradation is observed because of the error propagation effect due to the unreliable tentative decisions.

The cancellation of spurious signals with incorrect decision feedback leads to the interference enhancement. An intuitive approach is to cancel a fraction of the estimated interference, if a symbol estimate is thought to be unreliable. Divsalar *et al.* [116] have proposed the partial PIC approach, in which the partial-cancellation-factors (PCFs) are introduced to control the interference cancellation level.

The partial HPIC scheme based on the hyperbolic tangent device (optimal from the MMSE considerations based on a Gaussian interference assumption) provides superior performance than the linear and null-zone non-linear device based HPIC schemes. On the other hand, we may improve the performance of SPIC schemes by reducing the decision statistic bias using cancellation with PCFs. The simplest approach is to multiply all the symbol estimates by the constant PCFs with value less than unity. However, this approach may be modified by using the variable PCFs based on the value of correlator output.

Renucci and Woerner [118] have presented a detailed discussion for the optimization of PCF value. Guo and Li [119] have determined the optimal PCF value under some simplifying assumptions. But, its application is limited to a small number of users. In [120] and [121], PCFs are obtained adaptively by using the LMS algorithm. However, this scheme is valid under slowly varying environment. Li *et al.* [122] have derived the optimal PCFs for the partial SPIC schemes. This method is only applicable under the perfect power control condition. Ghotbi and Soleymani [123] have presented a combination of soft and hard PIC detectors, whose performance is superior to the SIC receivers and other sub-optimum techniques. In the first few stages of this scheme, the received composite signal is refined using the partial SPIC schemes to improve the signal-to-interference-ratio (SIR), and at the

final stage, the partial HPIC scheme is used to suppress the interference. However in this technique, the multistage processing delay is more relative to the available adaptive PIC techniques.

In another adaptive scheme, Hou *et al.* [124] have proposed a recursive least square algorithm based PIC structure to improve the SIR, and to handle the MAI effect. This adaptive PIC structure includes the narrow-band-interference (NBI) cancellation filters followed by the MAI cancellation filters. In order to avoid performance degradation due to the unreliable initial detection, a robust coefficient $\bar{\gamma}$ has been introduced in the proposed design. The drawback of this method is that it is impossible to determine the theoretical optimal value of coefficient $\bar{\gamma}$. Therefore, its value is determined using the extensive simulations at the different values of SIR for the AWGN channel.

In a more sophisticated approach, Hsieh and Wu [125] have proposed a two-stage decoupled partial SPIC receiver, which outperforms not only the two-stage full SPIC receiver, but also the three-stage full SPIC. Using MBER criterion, a complete set of optimal PCFs is obtained for the periodic and aperiodic spreading codes under the AWGN and multipath channels. The respreading strategy is used in the receiver design, which requires the knowledge of spreading sequences. The optimal PCFs can be calculated online efficiently in the time-varying environment, when the exact channel response and the noise variance are assumed to be known at the receiver end. The two-ray multipath channel model has been used to verify the theoretically derived results. It has been observed that the optimal partial SPIC schemes have good immunity in the presence of channel estimation errors. However, the power control scheme imposes extra burden on the cellular system. Moreover, the respreading technique increases the complexity of the receiver.

Hou and Chen [126] have addressed the multiuser interference suppression and data detection by using the parallel interference cancellation scheme, which provides multipath

diversity and processing gain protection. The forward filter is proposed, in combination with the feedback filter, to remove the effects of MAI and ISI by parallel cancellation using the RLS algorithm. Host-Madsen and Cho [127] have analysed the linear and non-linear MMSE PIC schemes for the multiuser detection in the DS-CDMA systems. The combined MMSE/PIC detector provides considerable gain over the MMSE detector. The MMSE/PIC detector is shown to possess robustness to the large code cross-correlations. However, it requires the knowledge of code sequences at the receiver end. For asynchronous DS-CDMA system, Ratasuk *et al.* [128] have presented an adaptive P-DFD using the least-squares algorithm. But, it needs to have the knowledge of covariance matrix of the received signal vector, and it converges slowly in the time-varying environment. Further, Woodward *et al.* [129] have analysed the detection procedure of a single undetected user using the MMSE PIC scheme in the decision feedback scenario.

In all the above discussed PIC schemes, the MAI is considered as the main factor in the system performance degradation. We may use the time-variable PCF values to control the error propagation effect in the MMSE PIC scheme by replacing the tentative hard-decisions with soft-decisions. However, the PIC scheme requires a large number of regenerations/cancellations, and moreover it requires fast power control for all the active users in a particular cell *i.e.*, single stage PIC scheme is not near-far resistant. Varanasi and Aazhang first suggested a multistage PIC technique in [130], and have also studied different multistage detectors in [131] and [132], which achieve considerable improvement over the linear multiuser detectors. But they require accurate estimation of the channel parameters, which increases the complexity of multiuser receiver.

Duel-Hallen [109]-[111] has introduced the multiuser zero-forcing decision-feedback-detector (ZF-DFD). It performs linear pre-processing (partially decorrelates the users) followed by SIC detection. The interference from the strongest user is removed by the use of

decision feedback leading to the significant performance improvement as compared to the decorrelating detector. The ZF-DFD can be implemented by computing the Cholesky decomposition and the matrix inversion operation. It also requires the estimate of received signal amplitudes, as all the active users are arranged in the descending order according to their received power level.

Varanasi and Guees [133] have analysed the decision feedback multiuser equalizer with successive decoding, which achieves the total capacity of the Gaussian multiple access channel. The S-DFD is more beneficial than the P-DFD if processing delay is not the constraint. However, the detection ordering of all the active users for S-DFD in the presence of MAI, ISI and noise is an independent issue for further research. Waters and Barry [134] have proposed a noise-predictive S-DFD (NP-S-DFD) for the MIMO channels, which uses the Vertical-Bell-Labs-Layered-Space-Time (V-BLAST) ordering criterion. The MMSE based approach is shown to outperform the ZF approach in the SIC scheme.

The receiver setting of V-BLAST architecture for very high spectral efficiencies over the wireless channels with rich scattering may be viewed as the MMSE generalized-decision-feedback-equalizer (G-DFE, [135]) as applied to a MIMO channel [136], because the G-DFE employs reordering of the received sub-streams, which is an inherent feature of V-BLAST. Therefore, the G-DFE may be used to remove MAI and ISI in the DS-CDMA transmission.

Although the performance of the noncausal infinite length DFE is always better than that of the realizable (causal and stable) DFE with finite decision delay [137], yet both designs have different advantages from the viewpoint of realizability and application of adaptive algorithms for the optimum performance over the frequency-selective fading channels. Cioffi *et al.* [138] have shown that the MMSE DFE (biased or unbiased configuration) performs significantly better than the ZF DFE, particularly at moderate-to-low SNR values and on severe ISI channels. Al-Dhahir and Sayed [139] have extended the work

presented in [137] to analyse a finite length MMSE DFE in a MIMO environment. Fast and parallelizable algorithms for computing the finite length MMSE MIMO DFE are presented for the multiuser detection with the modified SIC and PIC schemes for the DS-CDMA systems. However, it requires the knowledge of multiuser multipath channel coefficient matrix.

Foschini *et al.* have introduced the V-BLAST architecture for highly spectrally efficient wireless communications in [140] and [141], in which the user's bit stream is mapped to a vector of independently modulated equal bit rate signal components that are simultaneously transmitted in the same band. A signal detection algorithm similar to the multiuser detection has been employed to detect the desired signal component in the presence of AWGN. Wai *et al.* [142] have proposed the replacement of the optimal detection order in V-BLAST by a sub-optimal one and the utilization of Gram-Schmidt orthogonalization to substitute the computations of pseudo-inverse in finding the weight vector. The V-BLAST ordering provides motivation to use this concept to order the active users in SIC schemes. Moreover, the NP-S-DFD based on MMSE criterion may be implemented for multiuser detection in the DS-CDMA systems.

1.2 Statement of problem

The presented work encompasses a study of adaptive decision feedback detection techniques based on the MMSE criterion for the multiuser interference suppression and detection of DS-CDMA signals. The aim of the work is to study and develop adaptive decision feedback architectures for the high data rate wireless transmission under the multipath fading environment, which can combat intra-cell as well as inter-cell interference (MAI and ISI) in the presence of AWGN; and to develop an adaptive algorithm, which requires low computational complexity, possesses faster convergence rate, provides efficient tracking of the smoothly time-varying channels with minimum misadjustment, and may be incorporated

in the adaptive non-linear multiuser detection techniques.

The problem, as treated in this work, may be broken up into five main parts as follows:

- i) A study of the probability of error performance in the MMSE multiuser detection for the DS-CDMA systems. The analysis of asymptotic conditions, under which the behaviour of MAI can be assumed to be Gaussian. The evaluation of bounds on the error probability of MMSE MUD technique using the SNR of desired user and the cross-correlations of code sequence waveforms under the near-far situation.
- ii) A comparative study of LMS, NLMS and two-step LMS-type adaptive algorithms in the nonstationary environment. The development of a novel two-step LMS-type adaptive algorithm to track the time-varying channels, and the study of its nonstationary characteristics.
- iii) A study of adaptive decision feedback equalizer for the multiuser detection using the two-step LMS-type algorithm obtained by exploiting the Kalman filtering algorithm under the multipath time-varying channels, which uses the adaptive multiuser channel estimator to cancel ISI.
- iv) The development of a novel erasure algorithm to control the error propagation in decision feedback structures, and its incorporation in the adaptive decision feedback equalizer for the asynchronous DS-CDMA systems. A study of adaptive multiuser decision feedback detector using a novel parallel interference cancellation approach, in which the erasure algorithm is used for the partial feedback of decisions to control the error propagation effect.
- v) A study of two-stage MMSE multiuser decision feedback detector using a novel adaptive successive/parallel interference cancellation approach, which uses the MMSE noise-predictive criterion for the successive detection procedure and the determination of detection order of all the active users.

1.3 Organisation of the thesis

Chapter 2: Probability of error analysis of linear MMSE multiuser detector

In this chapter, we first introduce MMSE and decorrelating linear sub-optimum detectors based on the linear transformation applied to the output of matched filter bank. We assume the near-far scenario. We define MAI as a function of leakage coefficients, and also investigate their distribution using the divergence theorem, which determines the behaviour of MAI at the output of sub-optimum detector. We next determine the Chernoff upper bound on the error probability of linear MUD receiver. We also obtain the upper bound on code sequence cross-correlation and the SNR of desired user using the probability of error analysis, for which MUD techniques outperform the decorrelating detector.

Chapter 3: Adaptive algorithms for tracking of smoothly time-varying channels

In this chapter, we present a two-step LMS-type adaptive algorithm for the system identification problem, where the time-varying unknown plant coefficients are modelled as the first-order Markov processes. We consider the problem of lag noise in the tracking of smoothly time-varying channels in case of the conventional LMS algorithm. We first introduce the smoothing and control parameters in the proposed algorithm to control the tracking speed and the oscillatory behaviour respectively, and also derive analytical results to determine the optimum value of control parameter using the lag and gradient decoupling theorem and the direct averaging method. We next present the lag-misadjustment analysis for the proposed algorithm, and also obtain the working range of the control parameter. The performance of the proposed two-stage LMS-type algorithm is compared with the LMS, NLMS and other two-step algorithms. The simulations are carried out, to verify the derived analytical results, and to analyse the effects of smoothing and control parameters on the performance of the proposed algorithm.

Chapter 4: Adaptive multiuser decision feedback equalizer receivers for DS-CDMA systems

In this chapter, we combine the spread spectrum technique and the two-step LMS-type adaptive algorithm considered in chapter 3 to develop an adaptive multiuser receiver for the DS-CDMA systems using the reduced Kalman/LMS (RK-LMS) algorithm. We first describe the DS-CDMA system under the multipath fading environment in the matrix form. We present the RK-LMS algorithm based multiuser channel estimator, and cancel ISI due to the past data bits from the received signal vector by using the estimated multipath channel response. We analyse the effects of smoothing and control parameters on its performance. We next propose the adaptive multiuser receiver using the RK-LMS algorithm, and also analyse its probability of error performance. We evaluate its performance by simulating a number of numerical examples, and also demonstrate that the proposed adaptive multiuser receiver outperforms the conventional LMS algorithm based approach under the smoothly time-varying multipath fading environment.

Chapter 5: Adaptive multiuser decision feedback detectors for DS-CDMA systems using parallel interference cancellation approach

We next propose a novel erasure algorithm to control the error propagation effect in the adaptive MMSE DFE for the asynchronous DS-CDMA system. We evaluate and compare its performance with the conventional adaptive DFE under the frequency-selective fading channel using simulation technique.

We then present an adaptive multiuser DFD using the parallel interference cancellation approach. The soft output of linear MMSE MUD is processed using the erasure algorithm, and subsequently fed into the PIC structure as the tentative decision. We first discuss the detection procedure for a single undetected user in a particular cell assuming all other active users have been detected. We next present the adaptive multiuser detection using the partial

parallel interference cancellation scheme under the multipath fading environment. We evaluate its performance using simulation technique, with and without channel estimator based pre-cancellation of ISI, to show its performance gain over the linear MMSE multiuser detection technique.

Chapter 6: Two-stage MMSE multiuser decision feedback detectors for DS-CDMA systems

In this chapter, we present a two-stage MMSE multiuser DFD for the DS-CDMA systems working under the multipath fading environment. We first discuss the noise-predictive successive DFD (NP-S-DFD) as the first stage of the proposed cascaded structure, in which the active users are detected successively using the MMSE noise-predictive ordering criterion. We next propose a novel adaptive DFD using the successive/parallel interference cancellation approach at the second stage, which uses the output of NP-S-DFD as the tentative decisions for the interference suppression. Numerical examples are simulated to demonstrate that the proposed adaptive multiuser DFD supersedes the conventional single-stage and two-stage DFDs.

Chapter 7: Concluding remarks

We conclude the thesis with a summary of the important results and suggestions for future work.

PROBABILITY OF ERROR ANALYSIS OF LINEAR MMSE MULTIUSER DETECTOR

DS-CDMA offers advantages over other multiple access techniques like TDMA and FDMA in terms of multipath resistance, inherent frequency diversity, interference rejection, and the potential use of advanced antenna arrays in the design of multiuser receivers [9]. In multiuser systems, two commonly used approaches for detection are the conventional matched-filter (MF) and the optimum maximum-likelihood (ML) detectors [12]. The former appears vulnerable to the near-far problem and the latter is highly complex. The decorrelating and MMSE linear sub-optimum multiuser detectors take the structure of MAI into account and provide the near-far resistance, which is ignored in the conventional matched filter detector. The decorrelating detector completely eliminates MAI but enhances the background noise [18]; whereas the MMSE detector tries to minimize the mean square error between the transmitted and estimated bit, which minimizes the average value of MAI-plus-noise at the output of linear multiuser detector in the DS-CDMA system [19], [143].

In this chapter, we first briefly review different aspects of the sub-optimum techniques used for the joint multiuser data detection and interference rejection in section 2.1. In section 2.2, we introduce the synchronous DS-CDMA system model with non-orthogonal codes, and also present details about the performance evaluation of decorrelating and MMSE multiuser detectors in terms of the leakage coefficients. Section 2.3 analyses the behaviour of leakage coefficients for equi-correlated signals, which is used to prove that as the number of users increases, then very high signal-to-noise ratio becomes the stringent condition for the desired user. In section 2.4, upper bound on the code sequence normalized-cross-correlation (NCC)

has been derived for $K > 2$ users to achieve the performance advantage in MMSE multiuser detection over the decorrelating detector. Finally, conclusions are given in section 2.5.

2.1 Introduction

In a DS-CDMA system, the transmitter multiplies each user's signal by a distinct code waveform or signature sequence. The detector receives a signal composed of the sum of intra-cell and inter-cell users' signals, which not only overlap in time domain but also in frequency domain. The multiple access interference is a major factor along with the background Gaussian noise that limits the performance of a multiuser system, which results in the near-far problem when the interfering signal is stronger than the intended signal [2]. The problem of MAI becomes severe in the asynchronous systems, where orthogonality between the spreading code sequences cannot be maintained. Moreover, it is not possible to design the code sequences for any pair of users that are orthogonal for all the time offsets. The use of code sequences such as Gold codes, which have smaller cross-correlation peak values, leads to MAI even under the synchronous conditions. Pursley *et al.* have delineated the relationship between the spread spectrum multiple access system performance and the spreading code sequence correlation function in [25], [26], [144] and [145].

In a DS-CDMA system, the conventional matched filter receiver correlates the composite received signal with the signature sequence of the desired user, ignoring the existence of MAI. One common strategy to deal with the near-far problem in the conventional receiver is to use power control. But even under a single path fading channel condition, the transmitter would have to adjust its power at least a few hundred times per second [39], causing wastage of precious bandwidth. Another strategy to overcome the MAI and near-far problem is to use the linear multiuser detection technique [13]. The optimal multiuser detector as proposed by Verdú [12] in 1986, is based on the maximum-likelihood-

sequence-estimation (MLSE) criterion. The optimum MLSE receiver requires *a priori* knowledge about the number of active users, their signature sequences, signal amplitudes and transmission delays for all the multipaths. The main drawback of this detector is its high computational complexity, which increases exponentially with the number of users.

The MAI is not an inherent flaw of the DS-CDMA system, but results from the inability of conventional MF receiver to exploit the information available from MAI [146]. The substantial performance degradation is observed with the increasing number of users due to MAI [7]. Another limitation on the performance of DS-CDMA systems is imposed by the multipath fading, which also introduces ISI due to the multipath propagation [10]. However, the multiuser detection has been shown to be a very promising method for improving the BER performance and increasing the capacity of DS-CDMA system [13].

As an alternative to the conventional MF and ML approaches, the linear sub-optimum multiuser detectors have been explored, in which the complexity of receiver grows linearly with the number of interferers. By taking into account the structure of MAI, it is possible to obtain a dramatic improvement in the BER performance of MF detector. Two key sub-optimum multiuser detectors are the decorrelating detector and the MMSE detector, in which the estimated data bits are obtained by applying the linear transformation to the output vector of a matched filter bank, involving the correlation matrix inversion operation [18], [19]. Although these linear sub-optimum multiuser detectors do not achieve the minimum BER, yet they satisfy alternative optimization criterion (minimum error probability) based on the performance indices such as the asymptotic efficiency and the near-far resistance [27].

Pursley [25] has considered the average SNR and the average error probability for the performance evaluation of DS-CDMA system in the AWGN channel. Anderson and Wintz [147] have obtained a bound on SNR at the output of correlation receiver for an asynchronous spread spectrum multiple access system by taking the cross-correlations of

signature sequences into account. It is shown in [144] that the average SNR can be computed by using only the spreading code sequence auto-correlation values. Detailed analysis of an asynchronous DS-CDMA system is presented in [25] to reveal that the code parameters have the greatest impact on the performance due to their aperiodic cross-correlation properties. Under worst conditions, the author suggests to choose that code sequence, which minimizes the maximum probability of error according to the *minmax* criterion. The upper bound on the worst case error probability has been proposed by considering the maximum magnitude of the spreading code sequence aperiodic cross-correlation. Further, the effects of mean square code sequence correlation on the error probability of the DS-CDMA system have been analysed in [144].

The upper and lower bounds on the probability of error in the multiuser system are obtained by using the convexity properties of the error probability function in [145], which are valid for the system in which the maximum value of MAI does not exceed the desired signal value. Geraniotis and Pursley [26] have analysed different error probability approximations using the periodic and aperiodic properties of the code sequence cross-correlation function. However the presented approximation is based on the integration of the characteristic-function of the MAI component at the output of correlation receiver, which is motivated by the earlier work on intersymbol interference problem in [148] using the characteristic-function method. It provides a very accurate approximation to the average probability of error. Accuracy can be improved by using this approximation to obtain an expansion point for a Taylor-series representation of the actual probability of error. Any pre-specified degree of accuracy may be achieved by employing the combination of the characteristic-function method followed by a series-expansion method. This method does not require the evaluation of higher-order moments. This feature is particularly important for the DS-CDMA systems working under the selective fading, in which higher-order moments are

difficult to compute.

For DS-CDMA systems transmitting over the time-varying multipath channels, both MAI and ISI arise. The conventional sub-optimum receiver consisting of a bank of matched filters is often insufficient because the interference is treated as noise. Klein *et al.* [72] have presented four sub-optimum detectors based on the MMSE and ZF criteria. The authors have defined signal-to-“noise and interference” ratio parameter, which takes into account not only the noise but also MAI and ISI. Using this parameter, the bit error probability for the desired user can be estimated under the time-varying environment. If the knowledge about the existing correlations is taken into account at the receiver, the estimation of error probability may be improved. The probability of error analysis demonstrates that the MMSE criterion based multiuser detectors outperform the ZF based approaches.

The MAI in a multiuser system plays an important role in the performance analysis and characterisation of fundamental system limits. Zhang *et al.* [35] have studied the behaviour of the output MAI of the MMSE multiuser receiver, under imperfect power control conditions, for a large number of users. Almost for every realization of signature sequences, the conditional distribution of the output MAI converges weakly to the same Gaussian distribution as in the unconditional case. The performance of MMSE receiver is robust to the randomness of the signature sequences. The Gaussianity justifies that from the view point of detection and channel capacity estimation, the signal-to-interference ratio is the key parameter that governs the performance of MMSE multiuser receiver.

The asymptotic multiuser efficiency and the asymptotic SIR at the output of multiuser detector have been derived in [30] and [31] respectively. Verdú [32] has considered the spectral efficiency as the fundamental figure of merit, which is a function of the number of users, processing gain and SNR. It has been shown that the optimal multiuser efficiency of the asynchronous DS-CDMA system is nonzero with unit probability of bit error. The

asymptotic analysis of the multiuser detectors can be used to prove that the MMSE receiver has higher spectral efficiency under the severe channel conditions [30]-[33]. The sensitivity of channel capacity and the worst case error probability have been analysed by taking into account the non-Gaussianness of MAI component in [22] and [23] respectively. It may be inferred from the results presented in [36] and [37] that the MMSE multiuser detector supersedes the RAKE receiver under severe conditions, including large number of users and large channel length. The output signal-to-noise ratio and the near-far resistance are also related to the cross-correlation matrix of the spreading code waveforms. Because of greater ability to combat MAI as well as noise, the MMSE multiuser detector is widely used in blind and non-blind adaptive applications.

Poor and Verdú [27] have presented the performance analysis of MMSE linear multiuser detector in an environment of non-orthogonal signalling and background Gaussian noise, in which the probability of error has been considered as a key parameter. In particular, the behaviour of MAI-plus-noise mixture at the output of MMSE detector is examined under various asymptotic conditions. As probability of error is not directly linked to the MMSE criterion, therefore the leakage coefficients have been introduced as a linking parameter. The authors have considered the probability of error in the multiuser detection as a function of the leakage coefficients and the normalized cross-correlation values, which is minimized to derive the optimum conditions. The leakage coefficients of interferers tend to zero under different asymptotic conditions like large signal-to-noise ratios; large near-far ratios; and large number of users; therefore the output MAI-plus-noise is considered to have the Gaussian distribution.

For a particular two-user case [27], it has been proved on the basis of probability of error and non-Gaussianness in the MAI-plus-noise mixture that if NCC is less than $\left(\sqrt{2/\sqrt{3}}\right)/2$, then MMSE detector is better than the linear decorrelating detector. The

Kullback-Leibler divergence theorem has been used to measure the non-Gaussianness in MAI-plus-noise mixture by comparing it with a Gaussian random variable having the same mean and the variance. Further, Moustakides and Poor [29] have shown that, contrary to the general belief, the MMSE detector does not uniformly outperform the decorrelating and matched filter detectors. But ranges of parameters, for which the performance disadvantages arise, are somewhat at the extreme of practical systems. However the analytical results are not available for arbitrary number of users ($K > 2$), in terms of the leakage coefficients, under the near-far situation.

In the present work, we analyse the behaviour of leakage coefficients, and also calculate upper bound on the spreading code sequence normalized cross-correlation value for K users under the near-far situation. The higher values of leakage coefficients indicate that their probability density function is Binomial in nature, whereas the smaller values support Gaussian nature. Therefore, we have calculated the SNR of interferers at which the leakage coefficients maximize. While divergence theorem gives a limiting value of SNR of interferers, below which the Gaussian approximation for MAI-plus-noise mixture can be used. It is that interference level, at which the non-Gaussianness maximizes. The difference in two derived values decreases with the increasing number of users, and coincides for a large number of users. This result verifies that the MAI-plus-noise mixture is asymptotically Gaussian. The above results are used to derive the upper bounds on error probability in the MMSE multiuser detection. Further, the exhaustive solution for the minimization of probability of error yields upper bound on the signature sequence normalized cross-correlation value.

2.2 Multiuser system model

In the following, we consider a spread spectrum binary communication system, employing normalized modulation waveforms $s_1(t), s_2(t), \dots, s_K(t)$, such that

$$s_k(t) = \sum_{j=0}^{N-1} c_j^k \psi(t - jT_c) \quad (2.1)$$

where c_j^k is the j th chip ($\pm 1/\sqrt{N}$) in the spreading code sequence of k th user, T_c is the chip period, N is the length of spreading code in terms of the chip periods, $1/\sqrt{N}$ is the energy normalization factor, and $\psi(t)$ is the real transmitted chip waveform shape, which has unit energy in the time interval $0 \leq t \leq T_c$ i.e., $\psi(t) = 0$ for $t \notin [0, T_c]$. The transmitted bandpass signal for the k th user may be written as:

$$x_k(t) = \text{Re} \left[\left\{ A_k \sum_i b_k(i) s_k(t - iT_b) \right\} e^{j\omega_c t} \right] = \text{Re} [\hat{x}_k(t) e^{j\omega_c t}] \quad (2.2)$$

where $b_k(i)$ is a real valued transmitted data symbol ± 1 , $s_k(t)$ is the spreading signature sequence of user k , A_k is the amplitude level ($A_k = \sqrt{2P_k}$), T_b is the symbol period (with $T_b = NT_c$), and ω_c is the carrier frequency. Each user's transmitted signal (with signal power level P_k) is assumed to pass through an independent flat fading channel, which transforms the bandpass signal for k th user as:

$$r_k(t) = \text{Re} \left[\left\{ \sqrt{2P_k} \sum_i b_k(i) \gamma_k(t) s_k(t - iT_b - \tau_k) \right\} e^{j\omega_c t} \right] = \text{Re} [\hat{r}_k(t) e^{j\omega_c t}] \quad (2.3)$$

where $\hat{r}_k(t)$ is the equivalent lowpass signal, and the complex quantity $\gamma_k(t) = |\gamma_k(t)| e^{-j\omega_c \tau_k}$ represents the complex attenuation factor for the k th user. We define the total delay as $\tau_k = \Omega_k + t_k$. For k th user, Ω_k is the delay with respect to the desired user, and t_k is the propagation delay. If K active users are present in the DS-SS-CDMA system as shown in Fig. 2.1, then the equivalent lowpass composite received signal after the demodulation is represented as:

$$\hat{r}(t) = \sum_{k=1}^K \hat{r}_k(t) + \sigma n(t) \quad (2.4)$$

where $n(t)$ is the white Gaussian noise with zero-mean and unit power spectral density, and σ is the noise scaling factor.

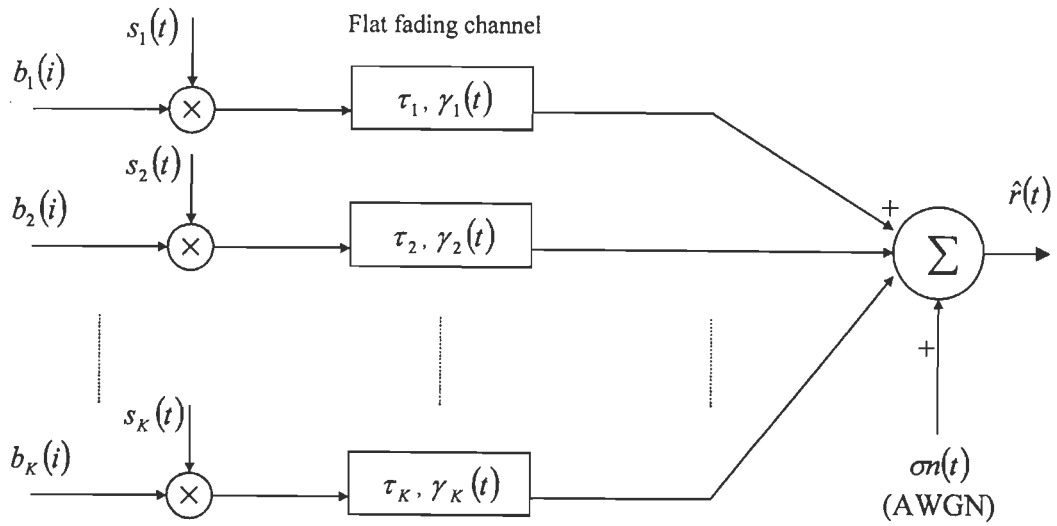


Fig. 2.1: Lowpass equivalent representation of the DS-SS transmitter for K active users.

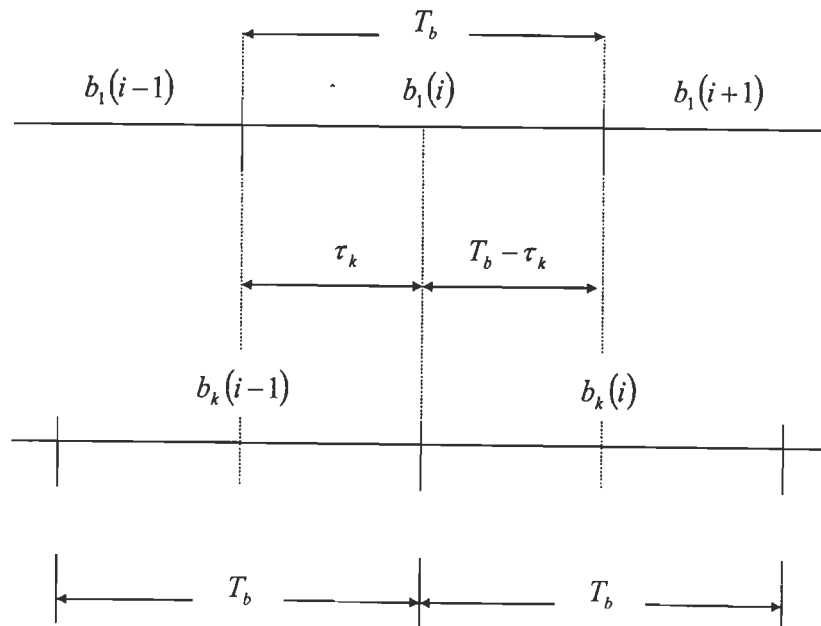


Fig. 2.2: Illustration of the interference caused by the k th user to the desired user signal.

Assuming $\gamma_k(t)=1$ for $k=1,2, \dots, K$, the composite received signal (2.4) during i th interval in the AWGN channel can be rewritten as:

$$\hat{r}(t) = \sum_{k=1}^K A_k \sum_i b_k(i) s_k(t - iT_b - \tau_k) + \sigma n(t) \quad (2.5)$$

For synchronous model, each user is assumed to have the relative delay $\{\tau_k\}$ equal to zero.

The normalized signalling waveform s_k is supported only on the interval $[0, T_b]$, with k th user's i th data bit $b_k(i)$. The output of matched filter bank is a $K \times 1$ dimensional vector y , whose k th component is the output of a filter matched to s_k in the i th data interval *i.e.*,

$$y_k(i) = \int_{iT_b}^{(i+1)T_b} s_k(t - iT_b) \hat{r}(t) dt, \quad k=1,2, \dots, K \quad (2.6)$$

For $i=0$, the sufficient vector y can be written as:

$$y = RAb + \sigma n \quad (2.7)$$

where R denotes the normalized cross-correlation matrix of the signal set s_1, s_2, \dots, s_K with

$R_{kl} = \rho_{kl} \cong \langle s_k, s_l \rangle$; $A = \text{diag}\{A_1, A_2, \dots, A_K\}$; b is the $K \times 1$ dimensional data bit vector,

whose k th component is b_k ; and n is a $N(0, R)$ random vector, independent of b . The

linear sub-optimum multiuser detectors incorporate the linear transformation ' \bar{M} ' to the output vector of matched filter bank, such that

$$\hat{b}_k = \text{sgn}\{(\bar{M}y)_k\} \quad (2.8)$$

For the decorrelating detectors, $\bar{M} = R^{-1}$. However for the MMSE detectors, the linear transformation ' M ' minimizes the second-order moment of error between the bit b_k and output \hat{b}_k .

$$\bar{M} = M \cong \{R + \sigma^2 A^{-2}\}^{-1} \quad (2.9)$$

Applying this linear transformation to the output vector of matched filter bank to detect the

desired user, we get $y_1 = (My)_1$. Therefore, the MMSE detection process for information bit of the desired user is dependent on the sign of the quantity

$$z_1 = \frac{y_1}{B_1} = b_1 + m_K + (\sigma/B_1)\tilde{n}_1 \quad (2.10)$$

where, $B_k = A_k(MR)_{1,k}$ and $\tilde{n}_1 \cong N(0, (MRM)_{1,1})$

The quantities m_K and $(\sigma/B_1)\tilde{n}_1$ are the MAI and the background Gaussian noise at the output of MMSE detector respectively. The multiple access interference comprises of *leakage coefficients* $\beta_1, \beta_2, \dots, \beta_K$, defined by

$$\beta_k = B_k / B_1 \quad (2.11)$$

which results in the discrete multiple access interference component

$$m_K = b_2\beta_2 + b_3\beta_3 + \dots + b_K\beta_K \quad (2.12)$$

Using (2.9), we can write

$$MR = I - \sigma^2 MA^{-2} \quad (2.13)$$

where, I is the identity matrix. It follows that

$$(MR)_{1,1} = 1 - \frac{\sigma^2}{A_1^2} M_{11} \quad (2.14)$$

$$\text{and } (MR)_{1,k} = -\frac{\sigma^2}{A_k^2} M_{1k} \quad (2.15)$$

Substitution of (2.14) and (2.15) in (2.11) results in

$$\beta_k = \frac{A_k (MR)_{1,k}}{A_1 (MR)_{1,1}} = \frac{\sigma}{A_1} \frac{\sigma}{A_k} \left(\frac{-M_{1k}}{1 - \frac{\sigma^2}{A_1^2} M_{11}} \right) \quad (2.16)$$

where, the values of M_{11} and M_{1k} are determined by using the following linear transformation with matrix inversion operation.

$$M = [R + \sigma^2 A^{-2}]^{-1} = \left[\begin{array}{c|c} \left(1 + \frac{\sigma^2}{A_1^2}\right) & \rho_1^T \\ \hline \rho_1 & H_1 \end{array} \right]^{-1} \quad (2.17)$$

The above partitioned form of the inverse of $[R + \sigma^2 A^{-2}]$ allows the mathematical simplification for further analysis, which results in

$$M = \begin{bmatrix} \mu_{11} & -\mu_{11}\rho_1^T H_1^{-1} \\ -\mu_{11}H_1^{-1}\rho_1 & H_1^{-1} + \mu_{11}H_1^{-1}\rho_1\rho_1^T H_1^{-1} \end{bmatrix} \quad (2.18)$$

with $\mu_{11}^{-1} = \left[\left(1 + \frac{\sigma^2}{A_1^2}\right) - \rho_1^T H_1^{-1} \rho_1 \right]$, $\rho_1 = [\rho_{12} \ \rho_{13} \ \dots \ \rho_{1K}]^T$,

and $H_1 = R_1 + \begin{bmatrix} \sigma^2/A_2^2 & & 0 \\ & \ddots & \\ 0 & & \sigma^2/A_K^2 \end{bmatrix}$ (2.19)

where, the matrix R_1 is obtained by deleting the first column and the first row from R ; such that

$$M_{11} = \mu_{11} = \left[\left(1 + \frac{\sigma^2}{A_1^2}\right) - \rho_1^T H_1^{-1} \rho_1 \right]^{-1} \quad (2.20)$$

and $M_{1k} = -M_{11}(\rho_1^T H_1^{-1})_k$ (2.21)

where, $(\rho_1^T H_1^{-1})_k$ refers to the coefficient corresponding to the k th user. Like the worst case error probability analysis for the multiuser system in [25], we consider the situation when the value of MAI overwhelms the desired signal value. We make the following assumption to obtain the value of leakage coefficients under the near-far situation.

Assumption 2.1: Assume that under the near-far problem, all other active users are at higher power level than the desired user. Such that

$$A_2 = A_3 = \dots = A_K = A_{NF} > A_1$$

$$\rho_{k,l} = \rho_{NF} \text{ (scalar) and } \rho_{k,k} = 1$$

$$\beta_2 = \beta_3 = \dots = \beta_K = \beta_{NF}$$

Under the assumed conditions, the matrix H_1 may be rewritten as:

$$H_1 = \Delta_{NF} + \rho_{NF} \underline{1} \underline{1}^T \quad (2.22)$$

where, $\Delta_{NF} = \text{diag}\left(1 + \frac{\sigma^2}{A_2^2} - \rho_{NF}, 1 + \frac{\sigma^2}{A_3^2} - \rho_{NF}, \dots, 1 + \frac{\sigma^2}{A_K^2} - \rho_{NF}\right)$ with $A_2 = \dots = A_K = A_{NF}$

and $\underline{1}$ is a $(K-1) \times 1$ dimensional column vector with all the elements equal to unity. It may be inferred from (2.22) that H_1 is a rank-1 modification of the positive definite diagonal matrix Δ_{NF} . Therefore, we can write H_1^{-1} in the closed form as [27], [149]:

$$H_1^{-1} = \Delta_{NF}^{-1} - \rho_{NF} \frac{\Delta_{NF}^{-1} \underline{1} \underline{1}^T \Delta_{NF}^{-1}}{1 + \rho_{NF} \underline{1}^T \Delta_{NF}^{-1} \underline{1}} \quad (2.23)$$

which further yields

$$\rho_1^T H_1^{-1} = \frac{\rho_{NF}}{1 + \rho_{NF} \underline{1}^T \Delta_{NF}^{-1} \underline{1}} \underline{1}^T \Delta_{NF}^{-1} \quad (2.24)$$

$$\text{and } \rho_1^T H_1^{-1} \rho_1 = \frac{\rho_{NF}^2 \underline{1}^T \Delta_{NF}^{-1} \underline{1}}{1 + \rho_{NF} \underline{1}^T \Delta_{NF}^{-1} \underline{1}} \quad (2.25)$$

Using (2.20), (2.21), (2.24) and (2.25), we obtain

$$M_{1k} = -M_{11} \left(\frac{\rho_{NF}}{1 + \frac{\sigma^2}{A_{NF}^2} + \rho_{NF}(K-2)} \right) \quad (2.26)$$

$$\text{and } M_{11} = \left(\left(1 + \frac{\sigma^2}{A_1^2} \right) - \frac{\rho_{NF}^2 (K-1)}{1 + \frac{\sigma^2}{A_{NF}^2} + \rho_{NF}(K-2)} \right)^{-1} \quad (2.27)$$

Substitution of (2.26) and (2.27) in (2.16) leads to

$$\beta_{NF} = \beta_k = \left(\frac{\rho_{NF}}{\left(1 + \frac{\sigma^2}{A_{NF}^2}\right) + \rho_{NF}(K-2) - \rho_{NF}^2(K-1)} \right) \quad (2.28)$$

2.3 Analysis of leakage coefficients

The leakage coefficients can be analysed to investigate their Gaussian or Binomial character, which determines the behaviour of MAI at the output of the linear sub-optimum detector.

2.3.1 Asymptotic analysis of leakage coefficients

Proposition 2.1: For a large number of users, the leakage coefficients follow the Gaussian distribution under worst conditions.

Proof: At boundary conditions, the following relations exist.

$$1. \quad \sigma \rightarrow \infty, \beta_{NF} \rightarrow \frac{\rho_{NF} A_{NF}}{A_1}$$

$$\sigma \rightarrow 0, \beta_{NF} \rightarrow 0$$

$$2. \quad \frac{A_{NF}}{\sigma} \rightarrow 0, \beta_{NF} \rightarrow 0$$

$$\frac{A_{NF}}{\sigma} \rightarrow \infty, \beta_{NF} \rightarrow 0$$

The leakage coefficients maximize at some intermediate value $\left(\frac{A_{NF}}{\sigma}\right)_M$, which can be

determined by differentiating β_{NF} (2.28) w.r.t. (A_{NF}/σ) ;

$$\frac{d(\beta_{NF})}{d\left(\frac{A_{NF}}{\sigma}\right)} = 0 \quad (2.29)$$

$$\text{Max}(\beta_{NF})_M = \frac{\sigma}{A_1} \frac{\rho_{NF}}{2} \left(\frac{1}{\sqrt{1 + \rho_{NF}(K-2) - \rho_{NF}^2(K-1)}} \right) \quad (2.30)$$

$$\text{which occurs at, } \left(\frac{A_{NF}}{\sigma} \right)_M = \frac{1}{\sqrt{1 + \rho_{NF}(K-2) - \rho_{NF}^2(K-1)}} \quad (2.31)$$

It is clear that as $K \rightarrow \infty$,

$$\left(\frac{A_{NF}}{\sigma} \right)_M \rightarrow 0 \text{ and } \text{Max}(\beta_{NF}) \rightarrow 0$$

Alternatively, the output MAI-plus-noise can be considered Gaussian up to a certain value

$\left(\frac{A_{NF}}{\sigma} \right)_N$, at which the non-Gaussianness maximizes. This can be calculated using (Kullback-

Leibler) divergence theorem, in which the MAI-plus-noise mixture is compared with a Gaussian random variable [22], [23]. Therefore, we can write

$$\text{MAI} - \text{plus} - \text{noise} = \sum_{k=2}^K B_k b_k + \sigma \tilde{n}_1, \text{ with the variance } \sigma_{MPN}^2 \quad (2.32)$$

$$\text{Such that, } \sigma_{MPN}^2 = \sum_{k=2}^K B_k^2 + \sigma^2 (\text{MRM})_{1,1} \quad (2.33)$$

$$\text{We have } (\text{MRM})_{1,1} = M_{11} - \sigma^2 (\text{MA}^{-2}M)_{1,1} \quad (2.34)$$

$$= M_{11} - \frac{\sigma^2}{A_1^2} M_{11}^2 - \frac{\sigma^2}{A_{NF}^2} M_{1k}^2 (K-1) \quad (2.35)$$

which results in

$$\sigma_{MPN}^2 = \sigma^2 M_{11}^2 \left(\frac{1}{M_{11}} - \frac{\sigma^2}{A_1^2} \right) = a^2 + v^2 \quad (2.36)$$

$$\text{where, } a^2 = \sum_{k=2}^K B_k^2 = \sum_{k=2}^K A_k^2 (\text{MR})_{1,k}^2 = \sigma^4 \sum_{k=2}^K \frac{M_{1k}^2}{A_k^2} \quad (2.37)$$

Using (2.26) and (2.27), the above equation can be simplified to give

$$a^2 = \frac{\sigma^4}{A_{NF}^2} (K-1) M_{11}^2 \left[\frac{\rho_{NF}}{1 + \frac{\sigma^2}{A_{NF}^2} + \rho_{NF}(K-2)} \right]^2 \quad (2.38)$$

From (2.33) and (2.36),

$$v^2 = \sigma^2 M_{11}^2 \left[\frac{1}{M_{11}} - \frac{\sigma^2}{A_1^2} \right] - a^2 \quad (2.39)$$

Since the non-Gaussianness is a monotonic function of $\frac{a^2}{v^2}$, as demonstrated in [27];

therefore we need to find $r_{NF} = \frac{A_{NF}^2}{\sigma^2}$ that maximizes this factor. Using (2.38) and (2.39), it can

be easily shown that

$$\frac{a^2}{v^2} = \frac{c r_{NF}}{(1+r_{NF} a)(1+r_{NF} b) - c r_{NF}} \quad (2.40)$$

where a , b and c are defined as:

$$a = (1 + \rho_{NF}(K-2))$$

$$b = (1 + \rho_{NF}(K-2) - \rho_{NF}^2(K-1))$$

$$c = \rho_{NF}^2(K-1)$$

$$\text{The term } \frac{a^2}{v^2} \text{ maximizes at } r_{NF} = \frac{1}{(ab)^{1/2}} = \left(\frac{A_{NF}^2}{\sigma^2} \right)_N \quad (2.41)$$

$$\text{and } \text{Max}(\beta_{NF})_N = (\beta_{NF}) \left| \left(\frac{A_{NF}^2}{\sigma^2} \right)_N \right. \quad (2.42)$$

The distance between the two derived signal-to-noise ratio values of interferers in (2.31) and (2.41), which maximizes the leakage coefficients and the non-Gaussianness respectively, may be defined as:

$$\Delta \left(\frac{A_{NF}^2}{\sigma^2} \right) = \left(\frac{A_{NF}^2}{\sigma^2} \right)_M - \left(\frac{A_{NF}^2}{\sigma^2} \right)_N = \frac{1 - \sqrt{b/a}}{b} = \left(\frac{1 - \sqrt{1 - \frac{\rho_{NF}^2(K-1)}{1 + \rho_{NF}(K-2)}}}{1 + \rho_{NF}(K-2) - \rho_{NF}^2(K-1)} \right) \quad (2.43)$$

as $K \rightarrow \infty$, it may be shown that

$$\Delta \left(A_{NF}^2 / \sigma^2 \right) \rightarrow 0 \quad (2.44)$$

The relative distance between the two points decreases with the increasing number of users, and ultimately coincides at the asymptotic condition. It is clear from above analysis that for a large number of users, the leakage coefficients follow the Gaussian distribution. Hence, we can consider the MAI-plus-noise mixture asymptotically Gaussian.

Example 2.1: For a two-user case, it can be shown by using the result (2.41) that the factor

$$\frac{\alpha^2}{\nu^2} \text{ maximizes at } r_{NF} = \left(\frac{A_{NF}^2}{\sigma^2} \right)_N = \frac{1}{\sqrt{1 - \rho_{NF}^2}}.$$

This result is same as proposed in [27]. But, the new result derived in terms of relative distance is

$$\Delta \left(\frac{A_{NF}^2}{\sigma^2} \right) = \frac{1 - \sqrt{1 - \rho_{NF}^2}}{1 - \rho_{NF}^2} \quad (2.45)$$

$$\text{as } \rho_{NF} \rightarrow 0, \quad \Delta \left(\frac{A_{NF}^2}{\sigma^2} \right) \rightarrow 0$$

$$\text{and } \rho_{NF} \rightarrow +1/-1, \quad \Delta \left(\frac{A_{NF}^2}{\sigma^2} \right) \rightarrow \infty$$

It is clear that the relative distance increases with the increasing magnitude of NCC. Moreover, the equation (2.43) can be used to show that the relative distance is maximum for $K = 2$. On the contrary, the value of $\Delta(A_{NF}^2/\sigma^2)$ approaches to zero for a large number of users (2.44). Therefore the two-user case is considered to be the worst case for nonzero NCC, in which the non-Gaussianness is maximum. Therefore, it may be inferred that the leakage coefficients follow the Binomial distribution for a small number of users.

2.3.2 Upper bounds on the probability of error

The above analysis can be used to derive the Chernoff upper bound on the probability of error in the MMSE multiuser detection. Using the MMSE detection equation (2.10), we may

partition the leakage coefficients into two sets as $Bin \cup Gau = \{2, 3, 4, \dots, K\}$. The subsets Bin and Gau consist of Binomial and Gaussian distributed leakage coefficients respectively.

Following the results presented in [28], it may be shown that the Chernoff upper bound is

$$\text{Probability of error} = Pe < \exp \left\{ - \frac{\left(1 - \sum_{k \in Bin} |\beta_k| \right)^2}{2 \left(\frac{\sigma^2}{B_1^2} (MRM)_{1,1} + \sum_{k \in Gau} \beta_k^2 \right)} \right\} \quad (2.46)$$

The above bound holds subject to the condition

$$\sum_{k=2}^K |\beta_k| < 1 \quad (2.47)$$

For a small number of users with high SNR, the multiple access interference term may be subtracted from the desired signal value. The leakage coefficients follow the Binomial distribution, and if the signature sequence normalized cross-correlation matrix is non-singular, then it can be proved by using the assumption 2.1 and $Gau = \{\emptyset\}$ in (2.46) that

$$Pe < \exp \left\{ - \frac{B_1^2 (1 - (K-1) \beta_{NF})^2}{2 (\sigma^2 (MRM)_{1,1})} \right\} \quad (2.48)$$

Under the near-far situation, the condition (2.47) can be modified as:

$$(K-1) \beta_{NF} < 1 \quad (2.49)$$

Whereas for a large number of users with $\beta_{NF} \rightarrow 0$, the leakage coefficients are considered Gaussian distributed. The Chernoff upper bound can be derived by using the assumption 2.1 and $Bin = \{\emptyset\}$ in (2.46) so that

$$Pe < \exp \left\{ - \frac{1}{2 \left(\frac{\sigma^2}{B_1^2} (MRM)_{1,1} + (K-1) \beta_{NF}^2 \right)} \right\} \quad (2.50)$$

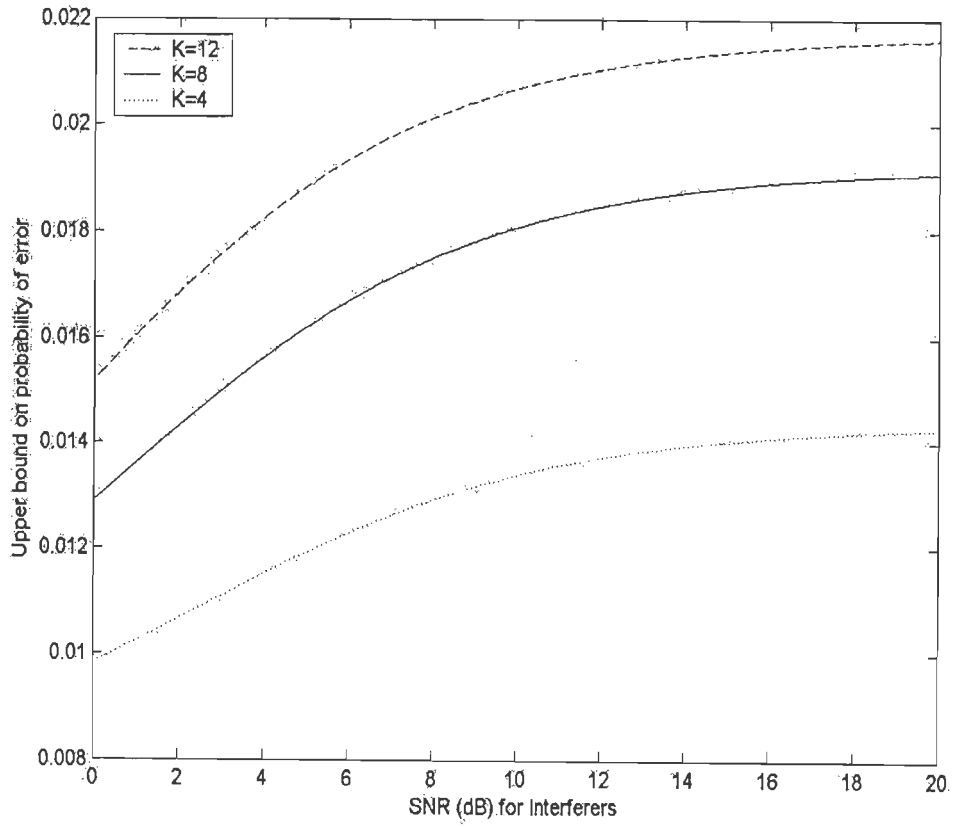


Fig. 2.3: Chernoff upper bound on error probability for Binomially distributed leakage coefficients.

The values of $Max(\beta_{NF})_M$ and $Max(\beta_{NF})_N$ can be used in (2.48) and (2.50) to evaluate the upper bounds on error probability under worst conditions. For Binomially distributed leakage coefficients and non-singular matrix R , the upper bound (2.48) on probability of error increases with the increasing number of users (as shown in Fig. 2.3). Here, we have chosen 10dB SNR for the desired user and $NCC = 0.25$.

Proposition 2.2: For unbiased performance of the MMSE linear multiuser detector, the signal-to-noise ratio of the desired user should be more than the minimum bounded value

$\left(\frac{A_1}{\sigma}\right)_{\min}$. Such that,

$$\left(\frac{A_1}{\sigma}\right)_{\min} = \frac{(K-1)}{2} \left| \frac{\rho_{NF}}{\sqrt{1 + \rho_{NF}(K-2) - \rho_{NF}^2(K-1)}} \right| \quad (2.51)$$

Proof: Using the leakage coefficient analysis discussed in subsection 2.3.1, we can replace β_{NF} with $Max(\beta_{NF})_M$ in (2.49) to obtain a tight bounding condition; which results in

$$(K-1) |Max(\beta_{NF})_M| < 1$$

Using (2.30), it can be simplified to give

$$\left(\frac{A_1}{\sigma}\right)_{\min} < \frac{A_1}{\sigma}$$

This shows that the signal-to-noise ratio of the desired user should be greater than the above defined value for the unbiased functioning of MMSE multiuser detectors.

2.4 Upper bound on signature sequence cross-correlation function

It has been shown that the performance of spread spectrum multiple access system is dependent on the signature sequence normalized-cross-correlation (NCC) values [25], [26], [144], [145]. It is apparent from the results presented in [27] that for a DS-SS system

using the non-orthogonal signalling scheme under the AWGN channel, the MMSE linear sub-optimum multiuser detectors have lesser bit error rate than the decorrelator only when the NCC is less than or equal to the upper bounded value for a two-user case [27]. This is true only if the condition (2.49) is fulfilled. For $K > 2$, this conjecture can also be proved for the worst-case conditions.

Proposition 2.3: For $K > 2$, if the normalized cross-correlation is less than the upper bounded value, then the probability of error in MMSE detection is less than or equal to the error probability of the decorrelator.

Proof: Using multiuser detection equation (2.10), the probability of error for linear multiuser detector is defined as:

$$P_1 = \Pr\left(\sum_{k=2}^K \beta_k b_k + \frac{\sigma}{B_1} \tilde{n}_1 > 1\right) \quad (2.52)$$

Under the near-far situation (assumption 2.1), it is straightforward to show that the error probability (2.52) in the linear multiuser detection is represented as [143], [150]:

$$P_1 = \frac{1}{2^{K-1}} \sum_{b_2, \dots, b_K \in \{-1, +1\}^{K-1}} Q_G \left(\frac{1 + \beta_{NF} \sum_{k=2}^K b_k}{\sqrt{\frac{(MRM)_{1,1} \sigma^2}{B_1^2}}} \right) \quad (2.53)$$

where, Q_G denotes the complementary unit cumulative Gaussian distribution. In above

equation, we may use $p = \sum_{k=2}^K b_k$.

The simple arithmetic operations show that

$$p = [-(K-1), \dots, -2, 0, +2, \dots, +(K-1)] \text{ for } K = \text{odd}$$

$$p = [-(K-1), \dots, -1, +1, \dots, +(K-1)] \text{ for } K = \text{even}$$

Now, the probability of error for the MMSE multiuser detector can be rewritten as:

$$P_1 = \frac{1}{2^{K-1}} \sum_{\substack{|p| \in \{0, 2, \dots, K-1\} \{K=ODD\} \\ \dots \in \{1, 3, \dots, K-1\} \{K=EVEN\}}} \left\{ Q_G \left(\frac{1 + \beta_{NF}|p|}{\sqrt{\frac{(MRM)_{1,1} \sigma^2}{((MR)_{1,1} A_1)^2}}} \right) + Q_G \left(\frac{1 - \beta_{NF}|p|}{\sqrt{\frac{(MRM)_{1,1} \sigma^2}{((MR)_{1,1} A_1)^2}}} \right) \right\} \quad (2.54)$$

$$\text{Here, } (MRM)_{1,1} = M_{11} - \sigma^2 \sum_{k=1}^K \frac{M_{1k}^2}{A_k^2}$$

$$\text{and } (MR)_{1,1} = \left(1 - \frac{\sigma^2}{A_1^2} M_{11} \right)$$

Using $(MRM)_{1,1}$ and $(MR)_{1,1}$ in (2.54), it can be shown that

$$P_1 = \frac{1}{2^{K-1}} \sum_{\substack{|p| \in \{0, 2, \dots, K-1\} \{K=ODD\} \\ \dots \in \{1, 3, \dots, K-1\} \{K=EVEN\}}} \{f_1(\bar{x}, \bar{y}, z) + f_2(\bar{x}, \bar{y}, z)\} \quad (2.55)$$

$$\text{where } f_1(\bar{x}, \bar{y}, z) = Q_G \left(\frac{\bar{x} + \bar{y}|p|}{z} \right), f_2(\bar{x}, \bar{y}, z) = Q_G \left(\frac{\bar{x} - \bar{y}|p|}{z} \right),$$

$$\phi_1 = \frac{\sigma^2}{A_1^2}, \phi_2 = \frac{\sigma^2}{A_{NF}^2} + \rho_{NF}(K-2), \quad (2.56)$$

$$\bar{x} = \frac{1 + \phi_2 - \rho_{NF}^2(K-1)}{\sqrt{\phi_1}}, \quad (2.57)$$

$$\bar{y} = \rho_{NF} \sqrt{\phi_2}, \quad (2.58)$$

$$z = \sqrt{(1 - \rho_{NF}^2(K-1))(1 + 2\phi_2) + \phi_2^2 + \Delta}, \quad (2.59)$$

$$\Delta = \rho_{NF}^3(K-2)(K-1) \quad (2.60)$$

Assumption 2.2: Let us consider the case, when $|p| = (K-1)$ in (2.55). For this boundary condition, $f_1(\bar{x}, \bar{y}, z)$ has MAI in the favourable condition, which is considered to be the best case. Whereas, all the leakage coefficients are having opposite sign in $f_2(\bar{x}, \bar{y}, z)$, which leads to the worst case.

Applying above assumption in (2.55), we get

$$\tilde{P}_1 = \frac{1}{2} \left\{ \mathcal{Q}_G \left(\frac{\bar{x} + \bar{y}(K-1)}{z} \right) + \mathcal{Q}_G \left(\frac{\bar{x} - \bar{y}(K-1)}{z} \right) \right\} \quad (2.61)$$

The probability of error for the decorrelator for above case is $\tilde{P}_1^D = \tilde{P}_1 \Big|_{\phi_2 = \rho_{NF}(K-2)}$ *i.e.*, the error

probability with $\frac{\sigma^2}{A_{NF}^2} = 0$. For a two-user case,

$$\tilde{P}_1^D = \mathcal{Q}_G \left(\frac{A_1}{\sigma} \sqrt{1 - \rho_{NF}^2} \right) \quad (2.62)$$

As NCC tends to unity, the performance of decorrelator approaches the conventional MF detector *i.e.*, $\tilde{P}_1^D \rightarrow 1/2$. It is clear that its error probability is independent of the noise variance. But, this is not true for the MMSE multiuser detector. Now, we will show that for the given normalized cross-correlation range in the minimum mean square error detection,

$$\frac{\partial}{\partial \phi_2} \tilde{P}_1 \leq 0 \text{ for } \phi_2 \geq 0 \quad (2.63)$$

$$\begin{aligned} \frac{\partial}{\partial \phi_2} \tilde{P}_1 = & \left[\frac{z^2 - \bar{x}\sqrt{\phi_1}u}{z^3\sqrt{\phi_1}} \right] \times \frac{1}{2} \left[\mathcal{Q}'_G \left(\frac{\bar{x} + \bar{y}(K-1)}{z} \right) + \mathcal{Q}'_G \left(\frac{\bar{x} - \bar{y}(K-1)}{z} \right) \right] \\ & + \left[\frac{\rho_{NF}(K-1)z^2 - 2\bar{y}(K-1)\sqrt{\phi_2}u}{2z^3\sqrt{\phi_2}} \right] \times \frac{1}{2} \left[\mathcal{Q}'_G \left(\frac{\bar{x} + \bar{y}(K-1)}{z} \right) - \mathcal{Q}'_G \left(\frac{\bar{x} - \bar{y}(K-1)}{z} \right) \right] \end{aligned} \quad (2.64)$$

where, $u = (1 - \rho_{NF}^2(K-1) + \phi_2)$. We now make use of the following

$$z^2 - \bar{x}\sqrt{\phi_1}u = \rho_{NF}^2(K-1)[1 + \rho_{NF}(K-2) - \rho_{NF}^2(K-1)] \quad (2.65)$$

and

$$\rho_{NF}(K-1)z^2 - 2\bar{y}(K-1)\sqrt{\phi_2}u = \rho_{NF}(K-1)[1 - \rho_{NF}^2(K-1)\{1 - \rho_{NF}(K-2)\} - \phi_2^2] \quad (2.66)$$

The substitution of (2.65) and (2.66) in (2.64) yields

$$\frac{\partial}{\partial \phi_2} \tilde{P}_1 = -\frac{\rho_{NF}^2(K-1)}{2z^3\sqrt{2\pi\phi_2}} e^{-\frac{(\bar{x} + \bar{y}(K-1))^2}{2z^2}} H \cosh \left(\frac{\bar{x} - \bar{y}(K-1)}{z} \right) (2\xi - f(\phi_2)) \quad (2.67)$$

where, $H = 1 - \rho_{NF}^2(K-1) + \rho_{NF}^3(K-1)(K-2) \geq 0$

$$\xi = \sqrt{\frac{\phi_2}{\phi_1}} \left(\frac{b}{H} \right) \quad (2.68)$$

$$f(\phi_2) = \frac{1}{\rho_{NF}} \left(1 - \frac{\phi_2^2}{H} \right) \tanh \left(\frac{\bar{x} \bar{y} (K-1)}{z^2} \right) \quad (2.69)$$

The condition $\frac{\partial}{\partial \phi_2} \tilde{P}_1 \leq 0$ is fulfilled only if $(2\xi - f(\phi_2))$ in (2.67) is a non-negative term. It is

clear from (2.68) that for $\xi \geq 0$ (positive value), the following relation should exist.

$$\frac{b}{H} \geq 0 \quad (2.70)$$

Let us consider the favourable positive range of NCC for the condition (2.70) i.e.,

$$0 < \rho_{NF} < 1 \quad (2.71)$$

Consider the case $\xi > 0$

Case 2.1: If $\phi_2 \geq \sqrt{H}$, then $(2\xi - f(\phi_2))$ depends on the non-negativity of term ξ , and which is true for (2.70) and (2.71).

Case 2.2: For $0 \leq \phi_2 \leq \sqrt{H}$, the optimum conditions can be found out by investigating the argument of 'tanh' term in (2.69), under which $f(\phi_2)$ is maximum. Here,

$$f(\phi_2) = \frac{1}{\rho_{NF}} \left(1 - \frac{\phi_2^2}{H} \right) \tanh \left(\rho_{NF} \sqrt{\frac{\phi_2}{\phi_1}} r(\phi_2) \right)$$

For smaller values of argument, the following approximation can be used.

$$\lim_{m \rightarrow 0} \tanh(m) \rightarrow m \quad (2.72)$$

Consider the term $r(\phi_2)$ for further analysis, which is given by

$$r(\phi_2) = \left(\frac{(1 + \phi_2 - \rho_{NF}^2(K-1))(K-1)}{(1 + 2\phi_2)(1 - \rho_{NF}^2(K-1)) + \phi_2^2 + \Delta} \right) \quad (2.73)$$



$$\text{Such that, } r(0) = \frac{(1 - \rho_{NF}^2 (K-1))(K-1)}{(1 - \rho_{NF}^2 (K-1)) + \Delta} \quad (2.74)$$

The $r(\phi_2)$ maximizes at

$$\phi_{2\max} = d - (1 - \rho_{NF}^2 (K-1)) \geq 0 \quad (2.75)$$

where,

$$d = (\rho_{NF} \sqrt{K-1}) \sqrt{b} \quad (2.76)$$

Substitution of (2.75) in (2.73) results in

$$r(\phi_{2\max}) = \left(\frac{K-1}{2d} \right) \quad (2.77)$$

The condition (2.75) can be rewritten as:

$$-2\rho_{NF}^4 (K-1)^2 + \rho_{NF}^3 (K-1)(K-2) + 3\rho_{NF}^2 (K-1) - 1 \geq 0 \quad (2.78)$$

If NCC is equal to unity, then $r(\phi_{2\max})$ approaches infinite value. To avoid this situation, the condition $b > 0$ imposes a bound on the value of NCC *i.e.*,

$$-\frac{1}{(K-1)} < \rho_{NF} < 1 \quad (2.79)$$

The NCC range (2.71) satisfies the condition (2.79). For this case, the solution of

$$(2\xi - f(\phi_2)) \Big|_{\phi_{2\max}} \geq 0 \text{ gives}$$

$$4d^3 - \rho_{NF}^2 (K-1)^2 H \geq 0 \quad (2.80)$$

We can use (2.71), (2.78) and (2.80) to determine the optimum range for the spreading code sequence normalized cross-correlation value, which is explained with the help of following example.

Example 2.2: For $K = 2$, we can show that (2.78) and (2.80) reduce to give the following conditions respectively.

$$\rho_{NF} \sqrt{1 - \rho_{NF}^2} - (1 - \rho_{NF}^2) \geq 0 \quad (2.81)$$

$$4 \geq \frac{1}{\rho_{NF} \sqrt{1 - \rho_{NF}^2}} \quad (2.82)$$

From (2.81) and (2.82), it can be proved that

$$\frac{1}{\sqrt{2}} < \rho_{NF} \leq \frac{1}{\sqrt{2}} \sqrt{1 + \frac{\sqrt{3}}{2}} \quad (2.83)$$

The results are same as the equations (113) and (114) in [27].

Example 2.3: For $K > 2$, the solution can be found out using the numerical analysis techniques. For $K = 3$, the resulting NCC range is $0.4314 < \rho_{NF} \leq 0.8203$. The upper bound on the value of NCC for the different number of users is shown in Fig. 2.4. The analysis shows that the conditions (2.78) and (2.80) are sufficient to derive the results for $K \leq 7$. But for a large number of users, the argument of \tanh in (2.69) being large, we can not apply the approximation (2.72).

The above examples show that the upper bound on the value of NCC decreases with the increasing number of users. Under near-far situation, the probability of error in the MMSE multiuser detection can be calculated for worst NCC ($\rho_{NF} \rightarrow 1$) *i.e.*,

$$\tilde{P}_1 = \frac{1}{2} \left\{ \mathcal{Q}_G \left(\frac{A_1 + A_{NF}(K-1)t}{\sigma} \right) + \mathcal{Q}_G \left(\frac{A_1 - A_{NF}(K-1)t}{\sigma} \right) \right\} \quad (2.84)$$

$$\text{where, } t = \sqrt{1 + (K-2) \frac{A_{NF}^2}{\sigma^2}} \quad (2.85)$$

For a large number of users and $A_{NF} > A_1$,

$$\tilde{P}_1 \cong \frac{1}{2} \mathcal{Q}_G \left(\frac{A_{NF}^2}{\sigma^2} (K-1) \sqrt{(K-2)} \right) + \frac{1}{4} \quad (2.86)$$

From the results proposed in [27], it is evident that the error probability of decorrelator approaches $\frac{1}{2}$, as the value of NCC tends to unity. This clearly shows that $\tilde{P}_1 < \tilde{P}_1^D$ *i.e.*, the

MMSE multiuser detector is more robust.

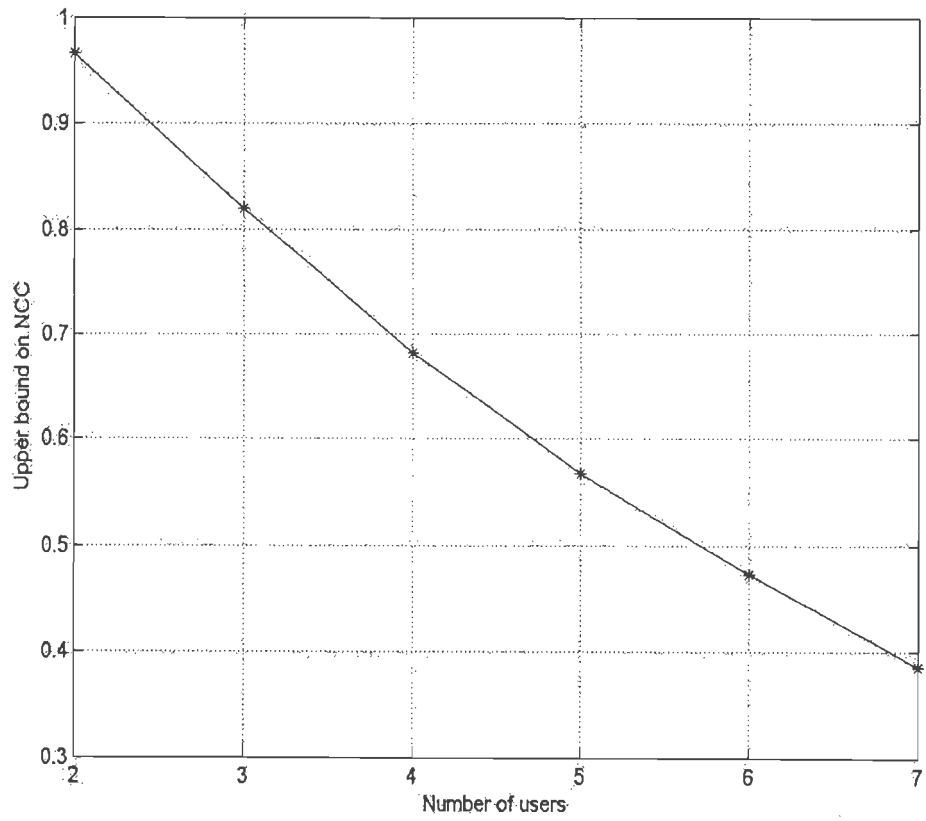


Fig. 2.4: Upper bound on the value of NCC vs the number of users.

2.5 Concluding remarks

In this chapter, we have analysed the MMSE linear multiuser detector under worst conditions. The behaviour of MAI at the output of sub-optimum multiuser detector has been investigated in terms of the leakage coefficients, and we have also shown that the signal-to-noise ratio of the desired user should be greater than the minimum bounded value, which depends on the number of users and the value of signature sequence normalized cross-correlation. It may be inferred from the derived analytical results that the leakage coefficients follow the Gaussian distribution, for a large number of users, under the near-far scenario. On the contrary, the Binomial distribution may be used for a small number of users. The two-user case is shown to be the worst case with maximum non-Gaussianness in the MAI-plus-noise mixture at the output of linear MMSE multiuser detector. The Chernoff upper bounds on the error probability of MMSE multiuser detector have been proposed for the Binomial as well as the Gaussian distributed leakage coefficients. In [27], upper bound on the normalized cross-correlation function has been presented for $K = 2$. Here, we have derived the upper bound and the optimum NCC ranges for $7 \geq K \geq 2$ under the near-far situation. The MMSE multiuser detector exhibits lower probability of error in comparison to the decorrelator only if the value of NCC is less than or equal to the upper bounded value. In the end of section 2.4, it has been shown that the MMSE detector outperforms the decorrelating detector under worst conditions.

ADAPTIVE ALGORITHMS FOR TRACKING OF SMOOTHLY TIME-VARYING CHANNELS

Adaptive signal processing techniques are finding increasing applications in DS-CDMA systems for equalization and interference excision, which may require the use of the estimated value of the time-varying channel parameters. The adaptive algorithm is the backbone of the channel estimator/predictor, using the pilot signals, in such adaptive multiuser interference suppression techniques. The time-varying Kalman filter constitutes the MSE-optimal linear algorithm for estimating the regression parameters based on the linear model of their behaviour [156], and it can be used for channel tracking [53]. Unfortunately, its computational complexity is high, and it also suffers due to the numerical instability problem. On the other hand, the LMS algorithm has been found suitable for tracking slow varying channels. It motivates the extension and optimization of the structure of LMS-like adaptation laws for tracking the smoothly time-varying channel parameters with low computational complexity. For the system identification problem, we present a modified version of the two-step LMS-type adaptive algorithm motivated by the work of Gazor [60], and also describe the nonstationary adaptation characteristics of this modified two-step least-mean-square (MG-LMS) algorithm.

In this chapter, we first briefly review different adaptive algorithms used for the tracking of time-varying channels in section 3.1. In section 3.2, we describe the smoothly time-varying system model, and also present details about the mathematical formulation of the nonstationary environment arising due to the variations in system parameter values. We next introduce the proposed MG-LMS adaptive algorithm, and also discuss its nonstationary

adaptation characteristics. In section 3.3, we assume that the time-varying system is governed by an independent stationary ergodic first-order Markov process. The analytical results are derived to show the different aspects of the presented algorithm in terms of the lag-misadjustment. Simulation results validating mathematical analysis are presented in section 3.4. Finally, conclusions are given in section 3.5.

3.1 Introduction

In the field of adaptive signal processing, the LMS is an extensively explored algorithm, and has found wide applications for the stationary environments due to its implementation simplicity [43]. However, its performance degrades substantially in the time-varying environment (nonstationary case) [58]-[64]. This degradation arises mainly because of the lag noise in addition to the gradient noise, which is measured in terms of the dimensionless quantity, called “Misadjustment” [57].

The quality of adaptive algorithm is also defined in terms of the misadjustment, the ratio of excess mean square error in an adaptive system to the minimum possible MSE [43]. The higher the misadjustment, the lower is the quality. The misadjustment is caused by three errors in the adaptive weight vector [65]: i) the noise-misadjustment, which is due to the noisy character of the input signal; ii) the lag-misadjustment, which is independent of the additive noise and is due to the time-varying nature of the optimal weights; iii) the gradient-misadjustment, which is due to the presence of gradient noise in the stochastic gradient adaptive algorithms.

The random-walk model has been used for developing the tracking theory for the LMS algorithm in [67]. Macchi *et al.* have evaluated the performance of LMS algorithm in the nonstationary environment, where the nonstationarity is introduced by using the complex chirp exponential signal buried in AWGN [65], [66]. In [151], Haykin *et al.* have presented

the modular learning strategy for the detection of a target signal of interest, when the transmitted signal is considered to be corrupted by the interference with unknown statistics (a source of nonstationarity). However in the present work, we are considering the system identification problem for the tracking of wireless channel, in which the channel response is time-varying.

In a recent paper [44], it is shown that the time-varying fading channel may be accurately modelled by using the second-order autoregressive *i.e.*, $AR(2)$ process. The analytical and simulation results presented in [56] depict that the first-order Markov channel provides a mathematically tractable model for the time-varying Rayleigh fading channels. However for the LMS algorithm, a general tracking theory of the first-order Markov model is yet to be developed.

For a first-order Markov channel, the LMS algorithm performs better than the RLS algorithm under typical conditions [43]. It produces a minimum level of misadjustment that is smaller than the corresponding value produced by the RLS algorithm. Moreover, the model independent design of the LMS algorithm provides an additional advantage over the RLS algorithm. In [46], Sayed *et al.* have presented the RLS algorithm as a special case of the Kalman filtering algorithm. In nonstationary environment, the substantial degradation in the tracking performance of the RLS algorithm is observed due to the design constraints. Subsequently the extended RLS algorithm has been proposed in [45] for the adaptive systems under the time-varying environment, which provides better tracking performance than the LMS algorithm. However, the limitation of this technique is that it requires the knowledge about the original dynamical system model to solve the system identification problem.

The Kalman filtering algorithm is considered to be optimum for such applications [46], [47]. In multiuser scenario, Chen *et al.* have presented the Kalman filtering algorithm for channel estimation [102]. A simple linear-trend channel model is proposed for the efficient

channel estimation in the time-varying channel case. However, the computational complexity and requirement of the knowledge of system model may often preclude the above Kalman filter based approaches. To avoid the online Riccati updating in the ordinary Kalman adaptation laws, Lindbom *et al.* have proposed the Wiener-LMS algorithm for the improved tracking performance [53]-[55]. It requires prior information about the model of the dynamics of time-varying parameters (hypermodel). The major drawback of this technique is that its implementation depends on the knowledge of covariance matrix of the regressors. Moreover, the complexity of this algorithm is directly coupled to the choice of hypermodel. Therefore, this technique has found limited applications.

In another approach, Gazor has simplified the Kalman algorithm to obtain a two-step LMS-type (G-LMS) adaptive algorithm for the system identification problem, in which the nonstationarity has been introduced by considering the plant coefficients to be time-varying according to a first-order Markov process [60]. This algorithm supersedes the conventional LMS algorithm because of its ability to combat the lag noise. Unlike the Wiener-LMS and other multistep algorithms [59], this adaptive algorithm does not require any prior information about the time-variations of the true system. However it requires relatively longer training period for the initial learning, during which, the oscillatory behaviour of algorithm accounts for the high value of residual MMSE.

The G-LMS algorithm is implemented in two stages [60]. The first stage includes the conventional LMS algorithm, which approaches unique minimum point on the mean square error-surface according to the Wiener theory [43]. This introduces the lag-misadjustment as well as the gradient-misadjustment. It is apparent that the adaptive filter has a quadratic bowl-shaped error-surface, whose position in the weight-space is in a permanent state of motion. The second stage is estimation of the weight increment vector using another independent conventional LMS algorithm with a smoothing parameter, which is used to predict the weight

vector for the next iteration of first stage. The two stage processing reduces the misadjustment due to the lag noise by tracking the moving minimum point. The above procedure uses the information that the weight increment vector is correlated to the weight vector for the next iteration. However for the first-order Markov channel, the analytical results for misadjustment due to the lag noise have not been reported so far in literature for the G-LMS algorithm.

In the following, we propose a modified version of the G-LMS algorithm, where a control parameter is incorporated for the prediction of weight vector for the next iteration. This control parameter is used to suppress oscillations during the convergence mode in the training period. Instead of relying on the intuitive justification as in [60], we formulate a stability criterion for the proposed algorithm. It ensures stable behaviour during convergence as well as improved tracking performance in the smoothly time-varying environments. The mathematical analysis for a nonstationary case, where the plant coefficients are assumed to follow a first-order Markov process, shows that the MG-LMS algorithm contributes less lag-misadjustment than the conventional LMS and G-LMS algorithms. Further, the stability criterion imposes upper bound on the value of control parameter. The analysis focuses on the impact of smoothing and control parameters on the lag-misadjustment in the tracking process. These derived analytical results are verified and demonstrated with simulation examples, which clearly show that the lag-misadjustment reduces with increasing values of the smoothing and control parameters under permissible limits. Moreover, the MG-LMS algorithm reduces to the conventional LMS algorithm under typical conditions, which signifies its flexibility.

3.2 The MG-LMS algorithm

3.2.1 Mathematical formulation

In this section, we consider a time-variable system as an example of the nonstationary environment (as shown in Fig. 3.1). If the input signal is $X(n)$ and the corresponding desired weight vector is $H_o(n)$, then the desired signal is defined as:

$$d(n) = H_o^H(n)X(n) + e(n) \quad (3.1)$$

where, $e(n)$ is AWGN with $N(0, J_{\min})$ and $()^H$ is the complex Hermitian operator. The input signal is assumed to satisfy the following basic assumptions.

Assumption 3.1: The sequence $X(n)$ is stationary with finite moments.

Assumption 3.2: $X(n)$ is independent of the noise sequence $e(n)$ i.e., $E[X(n)e^H(n)] = 0$, where $E[]$ is the expectation operator.

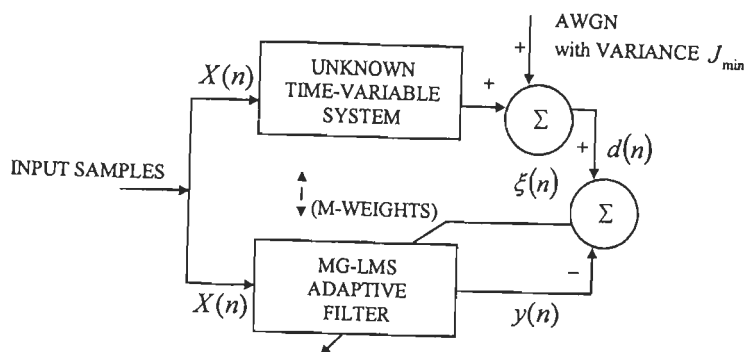


Fig. 3.1: Unknown time-variable system.

For tracking the variations in the system response, we consider a discrete-time filter with $M \times 1$ dimensional input vector $X(n)$ at time n . Using the principle of linear combining, the output of adaptive filter with $M \times 1$ dimensional weight vector $H(n)$ is given as:

$$y(n) = H^H(n)X(n) \quad (3.2)$$

which gives the measurement noise $\xi(n)$ corresponding to the desired signal $d(n)$, such that

$$\xi(n) = d(n) - y(n) \quad (3.3)$$

Using the above assumptions, the optimum solution of Wiener-Hopf equation in the matrix form yields $H_o(n) = R^{-1}P(n)$. The $M \times M$ dimensional correlation matrix of the input signal is defined as $R = E[X(n)X^H(n)] = Q\Lambda Q^H$ (Toeplitz), where $\Lambda = \text{diag}(\lambda_1, \lambda_2, \dots, \lambda_M)$ is a diagonal matrix of eigenvalues and Q is the matrix containing eigenvectors. The $M \times 1$ dimensional cross-correlation vector between the input signal and the desired response is $P(n) = E[X(n)d^*(n)]$. The mean square error in the adaptation process is denoted as $J(n)$, and is given as $J(n) = E[\xi(n)\xi^*(n)]$. If J_{\min} is the minimum MSE, then $J(n)$ can be defined as:

$$J(n) = J_{\min} + (H(n) - H_o(n))^H R (H(n) - H_o(n)) = J_{\min} + J_{\text{excess}}(n) \quad (3.4)$$

In the above equation, $J_{\text{excess}}(n)$ is the excess mean square error at time n . Therefore, the constant quantity J_{\min} always prevents a perfect match between the unknown system and the adaptive system. The MSE quadratic bowl varies in position with changing impulse response of the unknown system, and $H(n)$ attempts to match the unknown $H_o(n)$ on a continual basis while tracking. Using the method of steepest descent, the changing weight vector is represented as:

$$H(n+1) = H(n) + 2\mu E[X(n)\xi^H(n)] \quad (3.5)$$

where the scalar parameter μ is step size, which controls the convergence and stability.

It is clear from (3.4) and (3.5) that the adaptive process tracks the bottom of the MSE bowl, which is moving. Therefore, we can assume that the total excess noise is due to the lag in tracking process *i.e.*, $J_{\text{excess}}(n) \cong J_{\text{lag}}(n)$, which can be measured in terms of the

misadjustment as:

$$Lag - Misadjustment = \Xi_{lag} = \frac{E[J_{lag}(n)]}{J_{min}} \quad (3.6)$$

This dimensionless quantity is an index of mismatch between the impulse responses of unknown system and the adaptive system. The lag-misadjustment is the only factor, which can be used to determine the efficiency of MG-LMS algorithm in the nonstationary environment.

3.2.2 MG-LMS algorithm

In the two-step LMS-type (G-LMS) adaptive algorithm [60], the first-order and second-order increment weight vectors are $\dot{H}_o(n-1) \cong H_o(n) - H_o(n-1)$ and $\ddot{H}_o(n-1) \cong \dot{H}_o(n) - \dot{H}_o(n-1)$ respectively. For further analysis, we assume

Assumption 3.3: $\dot{H}_o(n)$ and $\ddot{H}_o(n)$ are modelled as zero-mean processes [60], [64]. The corresponding auto-correlation matrices are $E[\dot{H}_o(n)\dot{H}_o^H(k)] = \delta(n-k)Cov(\dot{H}_o)$ and $E[\ddot{H}_o(n)\ddot{H}_o^H(k)] = \delta(n-k)Cov(\ddot{H}_o)$ respectively, where $\delta(\cdot)$ is the Koroneker function.

Assumption 3.4: $\dot{H}_o(n)$, $\ddot{H}_o(n)$, $e(n)$ and $X(n)$ are statistically independent.

The vectors $\dot{H}_o(n-1)$ and $H_o(n)$ are considered to be correlated. Both increment vectors are taken into account to simplify the Kalman filter as:

$$H(n+1) = \hat{H}(n+1) + 2\mu X(n) \mathcal{E}^H(n) \quad (3.7)$$

where, $\hat{H}(n+1)$ is *a priori* estimated weight vector.

$$\dot{H}(n+1) = \dot{H}(n) + 2\alpha\mu X(n) \mathcal{E}^H(n) \quad (3.8)$$

In (3.7) and (3.8), the Kalman gains or blending factors are replaced by 2μ and $2\alpha\mu$ respectively. Where $0 \leq \alpha < 1$ is a smoothing parameter, which controls the lag in tracking

the time-varying system. The *a priori* estimated weight vector in (3.7) is defined as:

$$\hat{H}(n+1) = H(n) + \dot{H}(n) \quad (3.9)$$

Since the second stage (3.8) includes the conventional LMS algorithm without the *a priori* estimated weight vector, therefore under the optimum condition *i.e.*,

$$\dot{H}(n) \rightarrow \dot{H}_o(n) = H_o(n+1) - H_o(n) \quad (3.10)$$

Equation (3.7) can be rearranged by using (3.9) and (3.10) as:

$$H(n+1) \cong H_o(n+1) + \Delta H(n) + 2\mu X(n)\xi^H(n) \quad (3.11)$$

where, the tracking weight error vector is

$$\Delta H(n) = H(n) - H_o(n) \quad (3.12)$$

It may be inferred from the above equation that the sum of weight error vector $\Delta H(n)$ and gradient vector $2\mu X(n)\xi^H(n)$ oscillates about the optimum weight value, which prevents the matching of the tracking weight vector and the optimum weight vector.

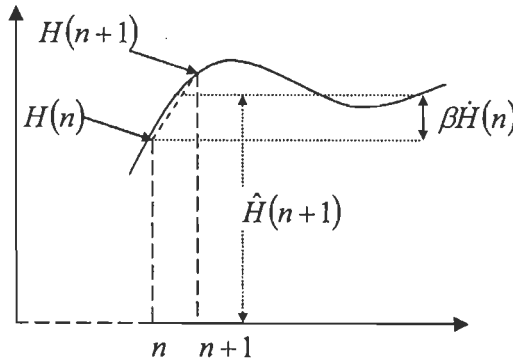


Fig. 3.2: Graphical interpretation of the proposed MG-LMS algorithm.

In the proposed MG-LMS algorithm, the first-order estimated increment weight vector is scaled with a control parameter to control the oscillatory behaviour. Therefore, (3.9) can be redefined as:

$$\hat{H}(n+1) = H(n) + \beta \dot{H}(n) \quad (3.13)$$

where, $0 \leq \beta < 1$ is a real valued parameter. Using (3.10) and (3.13) for $\beta \neq 1$, the tracking equation (3.7) can be modified as:

$$H(n+1) \cong \hat{H}_o(n+1) + \Delta H(n) + 2\mu X(n)\xi^H(n) \quad (3.14)$$

where, $\hat{H}_o(n+1) = H_o(n) + \beta\dot{H}_o(n)$ is the *a priori* estimated weight vector. In the above situation, the control parameter β adjusts the location of poles to damp the oscillations (described in section 3.3). Therefore by adjusting the values of α and β parameters, we obtain a modified version of the G-LMS algorithm with same computational complexity. The parameter α influences the tracking of time-varying system, while the parameter β provides stability.

The MG-LMS algorithm belongs to the family of stochastic gradient adaptive algorithms. The estimation of the first-order increment weight vector helps in reducing the lag noise during tracking, but application of the conventional LMS algorithm in step (3.8) contributes minor gradient noise in addition to the residual lag noise because the value of smoothing parameter is small. However, the major reduction in lag noise points toward the improved tracking in the time-varying nonstationary environment.

3.2.3 Decoupling of gradient and lag components

Using *a priori* estimated weight vector (3.13) and the second-order increment weight vector i.e., $\ddot{H}(n) = \dot{H}(n+1) - \dot{H}(n)$, the tracking weight vector (3.7) at time $n+1$ can be rewritten as:

$$H(n+1) = H(n) + \beta\dot{H}(n+1) + 2\mu X(n)\xi^H(n) - \beta\dot{H}(n) \quad (3.15a)$$

Substitution of (3.8) in (3.15a) results in

$$H(n+1) = H(n) + 2\mu(1 + \alpha\beta)X(n)\xi^H(n) + \beta[\dot{H}(n) - \ddot{H}(n)] \quad (3.15b)$$

The corresponding weight error vector is derived using $\xi(n) = e(n) - \Delta H^H(n)X(n)$ and (3.12)

in (3.15b) as:

$$\begin{aligned} \Delta H(n+1) = & [I - 2\mu(1 + \alpha\beta)X(n)X^H(n)]\Delta H(n) \\ & + 2\mu(1 + \alpha\beta)X(n)e^H(n) - [\dot{H}_o(n) - \beta\{\dot{H}(n) - \ddot{H}(n)\}] \end{aligned} \quad (3.16)$$

Using assumption 3.4, the weight error may be decoupled into the gradient ()^s and the lag ()^l components [64]. The two decoupled adaptation algorithms appear as:

$$\Delta H^s(n+1) = [I - 2\mu(1 + \alpha\beta)X(n)X^H(n)]\Delta H^s(n) + 2\mu(1 + \alpha\beta)X(n)e^H(n) \quad (3.17)$$

$$\Delta H^l(n+1) = [I - 2\mu(1 + \alpha\beta)X(n)X^H(n)]\Delta H^l(n) - [\dot{H}_o(n) - \beta\{\dot{H}(n) - \ddot{H}(n)\}] \quad (3.18)$$

It is apparent from the above equations that the tracking speed of the MG-LMS algorithm may be increased by increasing the value of α or β parameter, which reduces the lag noise in (3.18) at the cost of small increase in the gradient noise component in (3.17).

The step size μ is assigned a small value in order to realize good tracking performance. Under this condition, we may replace the stochastic difference equation (3.18) with the following stochastic difference equation by invoking the *direct-averaging method* [152].

$$\Delta H^l(n+1) = [I - 2\mu(1 + \alpha\beta)R]\Delta H^l(n) - [\dot{H}_o(n) - \beta\{\dot{H}(n) - \ddot{H}(n)\}] \quad (3.19)$$

Premultiplying both sides of (3.19) by Q^H and using the property of unitary matrix $Q^H = Q^{-1}$, we obtain

$$\Delta c(n+1) = [I - 2\mu(1 + \alpha\beta)\Lambda]\Delta c(n) - [\dot{c}_o(n) - \beta\{\dot{c}(n) - \ddot{c}(n)\}] \quad (3.20)$$

where $\Delta H^l(n) = [\Delta H_1^l(n) \dots \Delta H_p^l(n) \dots \Delta H_M^l(n)]^T$, $\Delta c(n) = Q^H \Delta H^l(n)$, $\dot{c}_o(n) = Q^H \dot{H}_o(n)$, $\dot{c}(n) = Q^H \dot{H}(n)$ and $\ddot{c}(n) = Q^H \ddot{H}(n)$. The p^{th} element of the vector $\Delta c(n+1)$ is

$$\Delta c_p(n+1) = [1 - 2\mu(1 + \alpha\beta)\lambda_p]\Delta c_p(n) - [\dot{c}_{o,p}(n) - \beta\{\dot{c}_p(n) - \ddot{c}_p(n)\}] \quad (3.21)$$

For convergence of the MG-LMS algorithm, the magnitude of $1 - 2\mu(1 + \alpha\beta)\lambda_p$ must be less than unity for all p . Similarly, it may be proved for the gradient-component that the same condition is required to be fulfilled. Therefore,

$$-1 < 1 - 2\mu(1 + \alpha\beta)\lambda_p < 1 \quad \text{for all } p \quad (3.22)$$

Since eigenvalues of the covariance matrix R are all real and positive, it follows that

$$0 < \mu < 1/((1 + \alpha\beta)\lambda_{\max}) \quad (3.23)$$

where, λ_{\max} is the largest eigenvalue of matrix R . In the design of MG-LMS algorithm, the values of α and β parameters are kept less than unity. Therefore, the above inequality can be redefined as:

$$0 < \mu < 1/(2\lambda_{\max}) \quad \text{as } \alpha\beta \rightarrow 1 \quad (3.24)$$

When the steady state is achieved for the recursive equation (3.21), it can be shown as in [60] that $E[\Delta c(n)] = 0$. We further assume that

Assumption 3.5: $\Delta c(n)$, $\dot{c}_o(n)$, $\dot{c}_p(n)$ and $\ddot{c}(n)$ are zero-mean processes, and are statistically independent.

Let us define the weight error covariance matrix as $\Gamma(n+1) = E[\Delta c(n+1)\Delta c^H(n+1)]$. Using (3.21) and assumption 3.5, the p^{th} diagonal element of $\Gamma(n+1)$ can be written as:

$$\begin{aligned} E[\Delta c(n+1)\Delta c^H(n+1)]_{pp} &= (1 - 2\mu(1 + \alpha\beta)\lambda_p)^2 E[\Delta c_p(n)\Delta c_p^*(n)] \\ &\quad + E[\dot{c}_{o,p}(n)\dot{c}_{o,p}^*(n)] + \beta^2 [E[\dot{c}_p(n)\dot{c}_p^*(n)] + E[\ddot{c}_p(n)\ddot{c}_p^*(n)]] \end{aligned} \quad (3.25)$$

Under steady state condition, we may write $\sigma_{\Delta p}^2 = E[\Delta c_p(n)\Delta c_p^*(n)]$, $\dot{\sigma}_{o,p}^2 = E[\dot{c}_{o,p}(n)\dot{c}_{o,p}^*(n)]$, $\dot{\sigma}_p^2 = E[\dot{c}_p(n)\dot{c}_p^*(n)]$ and $\ddot{\sigma}_p^2 = E[\ddot{c}_p(n)\ddot{c}_p^*(n)]$. Therefore, (3.25) can be rearranged as:

$$\sigma_{\Delta p}^2 = \frac{\dot{\sigma}_{o,p}^2 + \beta^2(\dot{\sigma}_p^2 + \ddot{\sigma}_p^2)}{1 - (1 - 2\mu(1 + \alpha\beta)\lambda_p)^2} \quad (3.26)$$

The variance $\sigma_{\Delta p}^2$ minimizes at an optimum value of the control parameter *i.e.*, β_{optimum}^p ,

which is obtained by differentiating (3.26) *w.r.t.* β and equating it to zero. It leads to

$$\beta_{optimum}^p = \frac{1 - \mu\lambda_p (1 - \alpha^2 \dot{\sigma}_{o,p}^2 / (\dot{\sigma}_p^2 + \ddot{\sigma}_p^2))}{\alpha(1 - 2\mu\lambda_p)} \left[\sqrt{1 + \frac{(1 - 2\mu\lambda_p)^2 \alpha^2 \dot{\sigma}_{o,p}^2 / (\dot{\sigma}_p^2 + \ddot{\sigma}_p^2)}{(1 - \mu\lambda_p (1 - \alpha^2 \dot{\sigma}_{o,p}^2 / (\dot{\sigma}_p^2 + \ddot{\sigma}_p^2)))^2}} - 1 \right] \quad (3.27)$$

The value of $(\dot{\sigma}_{o,p}^2 / (\dot{\sigma}_p^2 + \ddot{\sigma}_p^2)) \rightarrow 0$, when the variance of the first-order weight increments is very high *i.e.*, $\dot{\sigma}_p^2 \rightarrow \infty$. Under this condition, the value of $\beta_{optimum}^p$ approaches zero. This indicates that the second stage (3.8) of the MG-LMS algorithm is not required. The general

optimum value of β may be obtained by considering $\lambda_{avg} = \frac{1}{M} \sum_{p=1}^M \lambda_p$ and

$$(\dot{\sigma}_{o,p}^2 / (\dot{\sigma}_p^2 + \ddot{\sigma}_p^2)) = (\dot{\sigma}_{o,avg}^2 / (\dot{\sigma}_{avg}^2 + \ddot{\sigma}_{avg}^2)) \quad i.e.,$$

$$\beta_{optimum} = \frac{1 - \mu\lambda_{avg} (1 - \alpha^2 \dot{\sigma}_{o,avg}^2 / (\dot{\sigma}_{avg}^2 + \ddot{\sigma}_{avg}^2))}{\alpha(1 - 2\mu\lambda_{avg})} \left[\sqrt{1 + \frac{(1 - 2\mu\lambda_{avg})^2 \alpha^2 \dot{\sigma}_{o,avg}^2 / (\dot{\sigma}_{avg}^2 + \ddot{\sigma}_{avg}^2)}{(1 - \mu\lambda_{avg} (1 - \alpha^2 \dot{\sigma}_{o,avg}^2 / (\dot{\sigma}_{avg}^2 + \ddot{\sigma}_{avg}^2)))^2}} - 1 \right] \quad (3.28)$$

The value of $\beta_{optimum}$ depends on the factor $(\dot{\sigma}_{o,avg}^2 / (\dot{\sigma}_{avg}^2 + \ddot{\sigma}_{avg}^2))$.

3.3 Lag-misadjustment analysis for the MG-LMS algorithm

For the lag-misadjustment analysis, which has been defined earlier in section 3.2, we can eliminate the gradient noise from consideration by using the expectation operator $E[\]$ in the MG-LMS algorithm [57]. Like the method of steepest descent algorithm (3.5), the ensemble average nullifies the stochastic effect [43]. Therefore, (3.7) and (3.8) are redefined as:

$$\dot{H}(n+1) = \hat{H}(n+1) + 2\mu E[X(n)\xi^H(n)] = \hat{H}(n+1) + 2\mu[RH_o(n) - RH(n)] \quad (3.29)$$

$$\dot{H}(n+1) = \dot{H}(n) + 2\alpha\mu E[X(n)\xi^H(n)] = \dot{H}(n) + 2\alpha\mu[RH_o(n) - RH(n)] \quad (3.30)$$

Under zero gradient noise situation, the ensemble average of the excess MSE due to the lag noise at time n is

$$E[J_{lag}(n)] \cong E[(H(n) - H_o(n))^H R(H(n) - H_o(n))] \quad (3.31)$$

$$= E\left[\left(\tilde{H}(n) - \tilde{H}_o(n)\right)^H \Lambda \left(\tilde{H}(n) - \tilde{H}_o(n)\right)\right] \quad (3.32)$$

where, $Q^H H = \tilde{H}$ and the above equation can be solved for the p^{th} eigenvalue λ_p as:

$$E[J_{\log}(n)] \cong \sum_{p=1}^M \left[E\left[\left(\tilde{H}_p(n) - \tilde{H}_{o,p}(n) \right)^* \left(\tilde{H}_p(n) - \tilde{H}_{o,p}(n) \right) \right] \right] \lambda_p = \sum_{p=1}^M \varepsilon_p \lambda_p \quad (3.33)$$

where, ε_p is the weight error energy corresponding to the p^{th} eigenvalue (independent sub-channel). The quantity $\Delta\tilde{H}(n) = \left(\tilde{H}(n) - \tilde{H}_o(n)\right)$ is the weight tracking error vector, whose elements are used to determine the energy in p^{th} sub-channel. Using (3.7), (3.13) and (3.29)-(3.30), the composite quantity $\tilde{H}(n+1)$ is represented as:

$$\tilde{H}(n+1) = (1 + \beta)\tilde{H}(n) - \beta\tilde{H}(n-1) + 2\mu\left[\Lambda\tilde{H}_o(n) + \alpha\beta\Lambda\tilde{H}_o(n-1)\right] - 2\mu\left[\Lambda\tilde{H}(n) + \alpha\beta\Lambda\tilde{H}(n-1)\right] \quad (3.34)$$

The z-transform of the above equation is

$$z\tilde{H}[z] = (1 + \beta - z^{-1}\beta)\tilde{H}[z] - 2\mu(\Lambda + z^{-1}\alpha\beta\Lambda)\left(\tilde{H}[z] - \tilde{H}_o[z]\right) \quad (3.35)$$

The weight tracking error in the discrete frequency-domain is

$$\Delta\tilde{H}[z] = [\Psi[z]]^{-1} \left[(1 + \beta - z)I - z^{-1}\beta I \right] \tilde{H}_o[z] \quad (3.36)$$

where, $\Psi[z] = [z^{-1}\beta I + 2\mu(1 + z^{-1}\alpha\beta)\Lambda - (1 + \beta - z)I]$

$\Psi[z]$ is a non-singular $M \times M$ dimensional matrix and I is the identity matrix.

3.3.1 Determination of control parameter for the first-order Markov process

If it is assumed that the time-varying $\tilde{H}_o(n)$ is a first-order Markov process, which originates from the independent stationary ergodic white noise excitation with $N(0, \sigma^2)$, such that

$$\tilde{H}_o(n) = a\tilde{H}_o(n-1) + W(n) \quad (3.37)$$

where, the $M \times 1$ dimensional process noise vector is $W(n) = [w_1(n) \ w_2(n) \ \dots \ w_M(n)]^T$.

Subsequently, the z-transform of recursive relation (3.37) is

$$\tilde{H}_o[z] = \frac{W[z]}{(1-az^{-1})} \quad (3.38)$$

Substitution of (3.38) in (3.36) gives

$$\Delta\tilde{H}[z] = F[z]\tilde{H}_o[z] = [\Psi[z]]^{-1}[(1+\beta-z)I - z^{-1}\beta I] \frac{W[z]}{(1-az^{-1})} \quad (3.39)$$

Since $F[z]$ in (3.39) is a $M \times M$ dimensional diagonal matrix, the scalar transfer function of its p^{th} diagonal element (sub-channel) may be written as:

$$F_p[z] = \frac{[(1+\beta-z) - z^{-1}\beta]}{[z^{-1}\beta + 2\mu(1+z^{-1}\alpha\beta)\lambda_p - (1+\beta-z)]} \quad (3.40)$$

From the above analysis, the p^{th} component of the weight tracking error is

$$\Delta\tilde{H}_p[z] = (\tilde{H}_p[z] - \tilde{H}_{o,p}[z]) = \frac{-z(z-\beta)(z-1)w_p[z]}{[z^2 - (1+\beta-2\mu\lambda_p)z + (1+2\alpha\mu\lambda_p)\beta](z-a)} \quad (3.41)$$

The poles of this component are determined by solving the quadratic term in the denominator of above equation as:

$$(z - P_1)(z - P_2) = 0 \quad (3.42)$$

where, $P_2 = P_1^*$ and

$$P_1 = \frac{1}{2}(1+\beta-2\mu\lambda_p) + j\frac{1}{2}\sqrt{4\beta(1+2\alpha\mu\lambda_p) - (1+\beta-2\mu\lambda_p)^2} \quad (3.43)$$

Therefore, the poles are located at a , P_1 and P_2 respectively.

$$z = P_1 = P_2^* = \frac{1}{2}(1+\beta-2\mu\lambda_p) + j\frac{1}{2}\sqrt{8\mu\lambda_p(1+\alpha)(1+2\alpha\mu\lambda_p) - (\beta - (1+2\mu\lambda_p(1+2\alpha)))^2} \quad (3.44)$$

The upper bound on the value of β is derived by keeping the magnitude of complex poles within unit circle *i.e.*, $|z| < 1$, such that

$$\beta_{upper} < \frac{1}{(1+2\alpha\mu\lambda_p)} \quad (3.45)$$

For real and equal poles, the imaginary parts of poles should be zero. This condition is fulfilled for a certain value of $\beta = \beta_{threshold}$, which is given as:

$$\beta_{threshold} = -\sqrt{8\mu\lambda_p(1+\alpha)(1+2\alpha\mu\lambda_p)} + (1+2\mu\lambda_p(1+2\alpha)) \quad (3.46)$$

This threshold value determines the behaviour of poles as:

$$\left[\begin{array}{ll} 0 \leq \beta < \beta_{threshold} & \longrightarrow \text{real and unequal poles} \\ \beta = \beta_{threshold} & \longrightarrow \text{real and equal poles} \\ \beta_{threshold} < \beta < \beta_{upper} & \longrightarrow \text{complex conjugate poles} \end{array} \right. \quad (3.47)$$

where, β_{upper} is upper limit on the value of control parameter. If the value of $\mu\lambda_p$ decreases, then $\beta_{threshold}$ shifts towards unity. However its value can not be equal to one because at $\beta = 1$ and $\mu\lambda_p < 1$, the complex poles are

$$z = (1 - \mu\lambda_p) \pm j\sqrt{2\mu\lambda_p(1+\alpha) - (\mu\lambda_p)^2} \quad (3.48)$$

For the smoothing parameter $\alpha \neq 0$ in the above equation, the magnitude of poles is $|z|_{\beta=1} = \sqrt{1+2\alpha\mu\lambda_p}$, which is greater than unity. Using Routh-Hurwitz stability criterion, the location of poles out side the unit circle is responsible for instability of the algorithm. Thus by adjusting the value of β to a value below its threshold value, we can control the oscillatory behaviour during the convergence mode. The design equation (3.46) can be rewritten in terms of λ_{avg} as:

$$\beta_{threshold} = -\sqrt{8\mu\lambda_{avg}(1+\alpha)(1+2\alpha\mu\lambda_{avg})} + (1+2\mu\lambda_{avg}(1+2\alpha)) \quad (3.49)$$

Hence for stable functioning of the MG-LMS adaptive algorithm, the smoothing and control parameters are tuned in such a way that poles must be real because the complex conjugate poles will give rise to the damped oscillations, which will result in high MSE during the convergence and tracking modes.

3.3.2 Determination of lag-misadjustment for the first-order Markov process

The above analysis of the smoothing and control parameters shows that the poles P_1 and P_2 are complex for the value of control parameter in the range $\beta_{threshold} < \beta < \beta_{upper}$, such that

$$\Delta\tilde{H}_p[z] = \frac{-z(z-\beta)(z-1)w_p[z]}{(z-P_1)(z-P_2)(z-a)} \quad (3.50)$$

Using Parseval's relation, the weight error energy of the p^{th} sub-channel can be calculated in the frequency-domain as:

$$\varepsilon_p = \frac{1}{2\pi j} \oint_C v^{-1} \Delta\tilde{H}_p[v] \Delta\tilde{H}_p^*[1/v^*] dv \quad (3.51)$$

$$= \frac{\sigma^2}{2\pi j} \oint_C \frac{(v-1)(v-\beta)(1-\beta v)(1-v)}{(1-av)(1-P_1^*v)(1-P_2^*v)(v-a)(v-P_1)(v-P_2)} dv \quad (3.52)$$

where, the contour of integration C is the unit circle. If the poles a , P_1 and P_2 are inside the contour of integration [153], the Cauchy residue theorem gives

$$\varepsilon_p = \sigma^2 f_p(\alpha, \beta, a, P_1, P_2) \quad (3.53)$$

$$\text{where, } f_p(\alpha, \beta, a, P_1, P_2) = \left[\hat{f}_1 + (P_1 - P_2)^{-1} (\hat{f}_2 - \hat{f}_3) \right] \quad (3.54)$$

$$\text{and } \hat{f}_1 = \frac{(1-a)(1-a\beta)(\beta-a)}{(1+a)(1-aP_1^*)(1-aP_2^*)(a-P_1)(a-P_2)} \quad (3.55)$$

$$\hat{f}_2 = \frac{(1-P_2)^2(1-P_2\beta)(\beta-P_2)}{(1-aP_2^*)(a-P_2)(1-P_1^*P_2)(1-|P_2|^2)} \quad (3.56)$$

$$\hat{f}_3 = \frac{(1-P_1)^2(1-P_1\beta)(\beta-P_1)}{(1-aP_1^*)(a-P_1)(1-P_1P_2^*)(1-|P_1|^2)} \quad (3.57)$$

From (3.33) and (3.53), the average excess MSE is

$$E[J_{lag}(n)] \cong \sigma^2 \sum_{p=1}^M f_p(\alpha, \beta, a, P_1, P_2) \lambda_p \quad (3.58)$$

If all the eigenvalues are considered equal *i.e.*, λ_{avg} , then the weight error energy of all the

sub-channels becomes equal *i.e.*, $f_1 = \dots = f_M = f_{avg}$. It leads to

$$\Xi_{lag} = \frac{\sigma^2 M}{J_{\min}} f_{avg}(\alpha, \beta, a, P_1, P_2) \lambda_{avg} \quad (3.59)$$

$$\text{Relative Lag - Misadjustment} = \frac{\Xi_{lag}}{\Xi_N} = 4\mu\lambda_{avg} f_{avg}(\alpha, \beta, a, P_1, P_2) \quad (3.60)$$

where, the normalization factor is defined as:

$$\Xi_N = \left(\frac{\sigma^2 M}{4\mu J_{\min}} \right) \quad (3.61)$$

Under special case ($\alpha = \beta = 0$), the values of poles are $P_1 = (1 - 2\mu\lambda_{avg})$ and $P_2 = 0$ respectively (see example 2 in appendix A). Consequently, the value of $f_{avg}(\alpha, \beta, a, P_1, P_2)$ is

$$f_{avg}(0, 0, a, P_1, P_2) = \frac{2}{(1+a)(1+P_1)(1-aP_1)} \quad (3.62)$$

$$f_{avg}(0, 0, a, P_1, P_2) \Big|_{a \rightarrow 1} \approx \frac{1}{4\mu\lambda_{avg}} \quad (3.63)$$

Under the above assumed condition, the lag-misadjustment is

$$\Xi_{lag} = \frac{\sigma^2 M}{4\mu J_{\min}} \quad \text{as } a \rightarrow 1 \quad (3.64)$$

This derived result is similar to the result presented in [57] for the conventional LMS algorithm working under the nonstationary environment. From (3.64) and (A.9), it is apparent that the conventional LMS algorithm is a special case of the MG-LMS algorithm.

For different values of the parameters α and β , the expected performance of the MG-LMS algorithm is next analysed using (3.60) in terms of the relative lag-misadjustment (index of excess MSE). The initial oscillatory behaviour is controlled by keeping the value of control parameter less than $\beta_{threshold}$ (3.49). The values of $\mu\lambda_{avg} = 0.001$ and $\beta = 0.75$ have been used in (3.60), and results are given in Fig. 3.3.

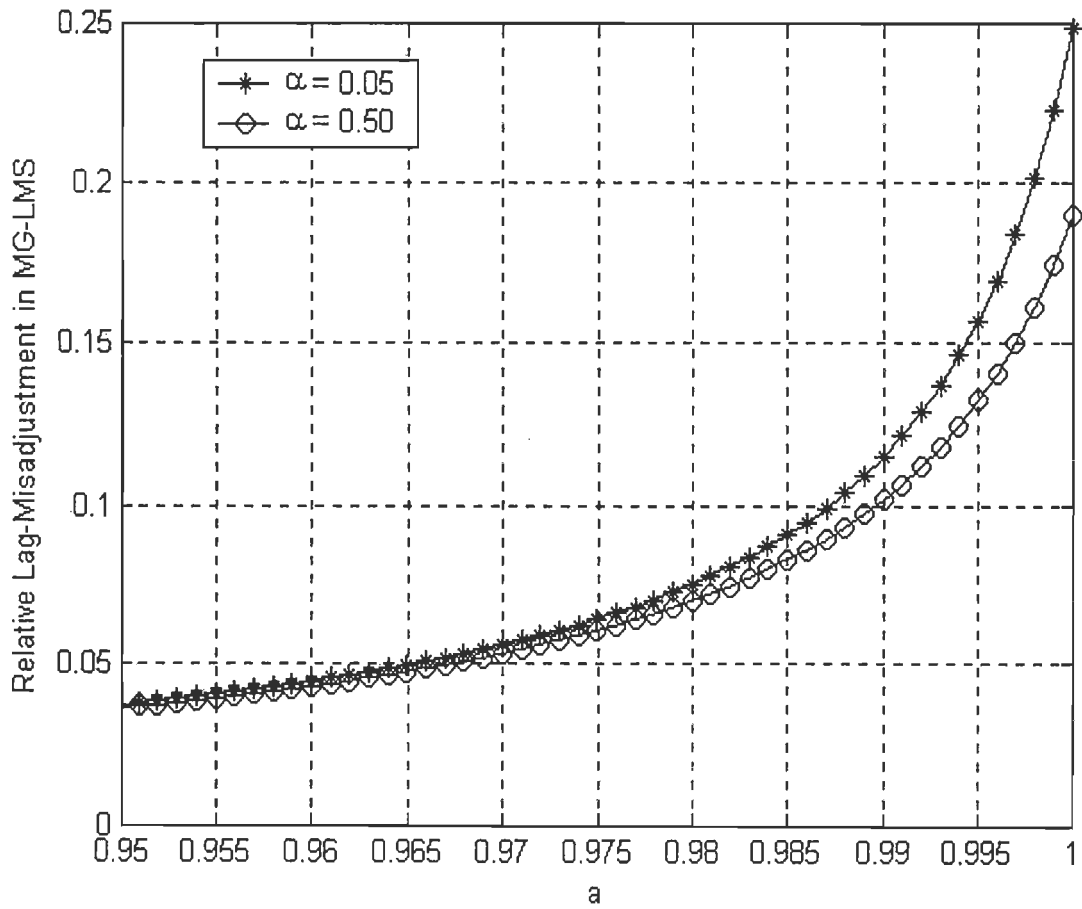


Fig. 3.3: Relative lag-misadjustment vs a of MG-LMS algorithm for variable α ($\mu\lambda_{avg} = 0.001$ and $\beta = 0.75$).

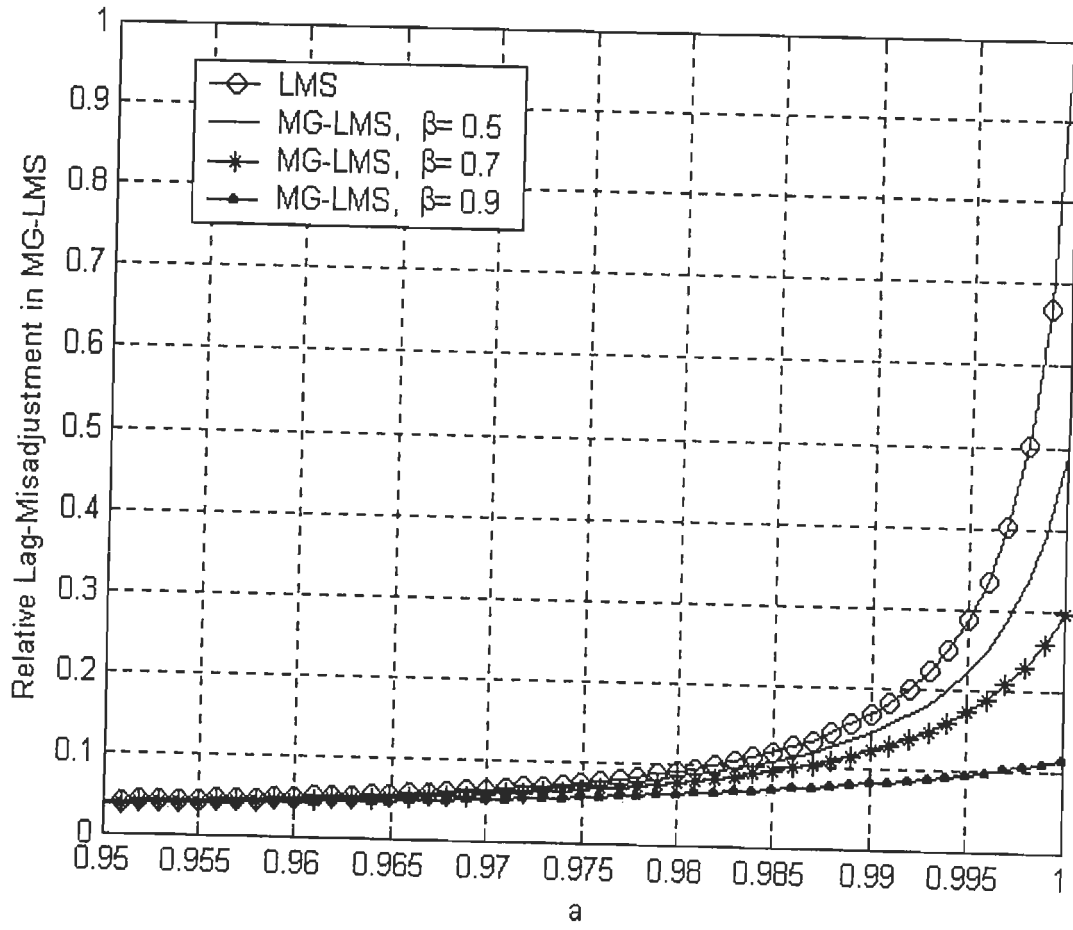


Fig. 3.4: Relative lag-misadjustment vs α of MG-LMS algorithm for variable β ($\mu\lambda_{avg} = 0.001$ and $\alpha = 0.05$).

It may be observed from Fig. 3.3 that the relative lag-misadjustment gradually reduces with the increasing value of α for real and unequal poles. For $\mu\lambda_{avg} = 0.001$ and $\alpha = 0.05$, Fig. 3.4 depicts that the value of relative lag-misadjustment also reduces with the increasing value of β . However when poles are complex, the lag-misadjustment is expected to increase again because of the instability of the algorithm in above situation. The effects of smoothing and control parameters on the performance of the proposed algorithm are verified by simulations in the next section.

3.4 Simulation results

We shall investigate the behaviour of the proposed MG-LMS algorithm, in convergence and tracking mode, to analyse the effects of the smoothing and control parameters on its performance. We shall also compare its performance with the conventional LMS, NLMS and G-LMS algorithms. The variation in lag-misadjustment is analysed in terms of the variation in minimum MSE. The value of the step size μ is kept lower than its maximum bounded value (described in section 3.2).

For parameter tuning of the MG-LMS algorithm, the value of $\beta_{threshold}$ is obtained by using (3.49) for a fixed value of α . First the value of smoothing parameter $0 \leq \alpha < 1$ is set to provide *coarse tuning*, and then adjustment of the control parameter β results in *fine tuning* of the proposed algorithm. Since we require the knowledge of $(\dot{\sigma}_{o,avg}^2 / (\dot{\sigma}_{avg}^2 + \ddot{\sigma}_{avg}^2))$ in (3.28) to obtain the optimum value of β , at which the MSE minimizes. Therefore, the value of $\beta_{optimum}$ is determined by simulations at the fixed values of other parameters. However, its value must be less than $\beta_{threshold}$ because the real poles provide stability in $\beta \leq \beta_{threshold}$ domain (described in section 3.3).

To generate the nonstationary environment, $H_o(n)$ is considered to be the fast fading

mobile communication channel (Rayleigh). The auto-correlation function of the $AR(2)$ process is close to that of a Rayleigh fading process [154]. The Jakes model is widely accepted as the realistic fading channel model, which is simulated by using the $AR(2)$ process [equation (1), 103], such that

$$H_o(n) = -K_1 H_o(n-1) - K_2 H_o(n-2) + U(n) \quad (3.65)$$

where, $U(n)$ is a complex zero-mean white Gaussian process. The scalar coefficients in the above equation are $K_1 = -2r_d \cos(\sqrt{2}\pi f_D T_s)$ and $K_2 = r_d^2$, which take account of the maximum Doppler frequency f_D of the underlying fading channel, sampling time T_s and pole radius r_d corresponding to the steepness of the peaks of power spectrum with the spectral peak frequency $f_p = f_D/\sqrt{2}$ [equation (9), 155]. For accurate modelling [equation (70), 44], the value of pole radius is

$$r_d = (1 - 2f_D T_s) \quad (3.66)$$

The auto-correlation of the channel tap-coefficient is shown in Fig 3.5, in which the fading parameters are $f_d = 10\text{Hz}$ and $1/T_s = 10\text{kHz}$. Note that we have kept 20dB signal-to-noise ratio in each of the following cases. The BPSK *i.i.d.* data is considered to be input. The presented results are based on an ensemble average of 150 independent simulation runs.

Case 3.1: The variation of MMSE with respect to the control parameter β is analysed by fixing $\alpha = 0.05$ and $\mu = 0.005$. In this case, we consider the fading channel with $f_D = 75\text{Hz}$ and $1/T_s = 10\text{kHz}$. The convergence and tracking performance of the adaptive filter with ten weights is shown in Fig. 3.6. The observed average eigenvalue is $\lambda_{avg} = 0.0752$, which is used to calculate $\beta_{threshold} = 0.9446$ for the above fixed values of α and μ . With increasing value of β , the performance of the MG-LMS algorithm substantially improves.

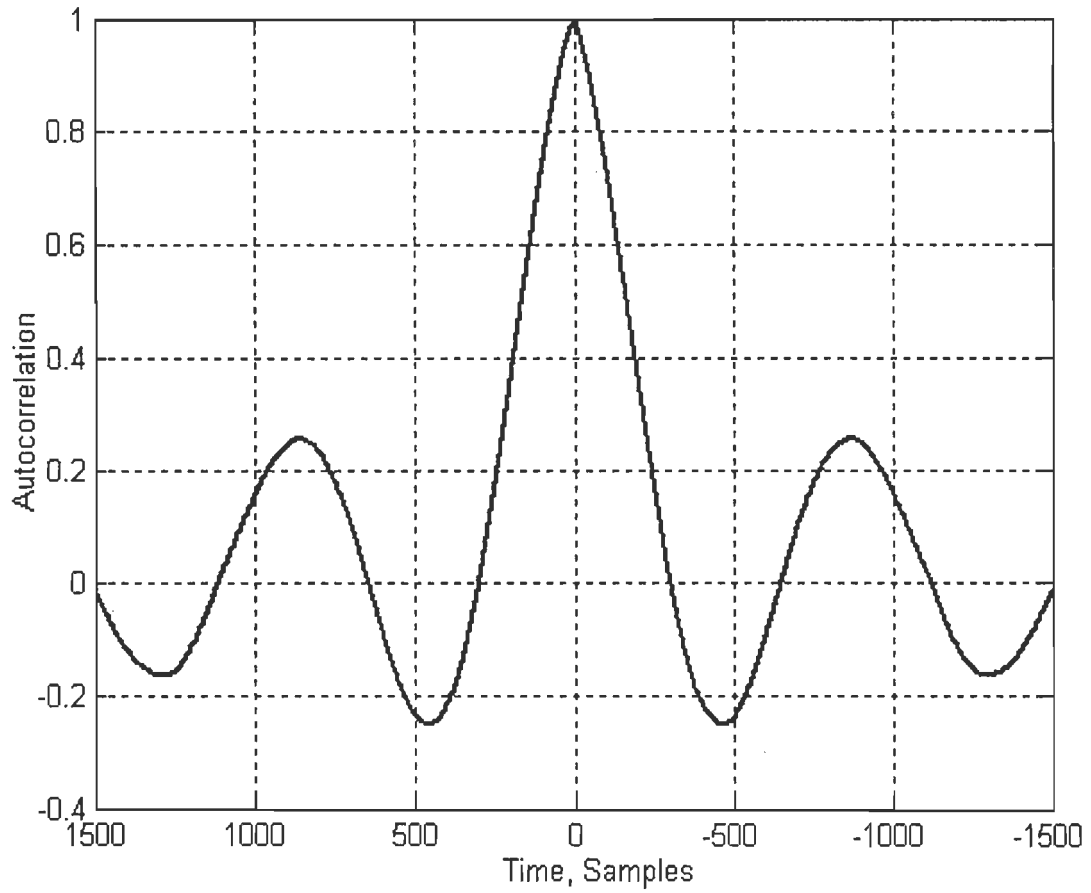


Fig. 3.5: Auto-correlation of channel tap-coefficient using the $AR(2)$ approximation with $f_d T_s = 0.001$.

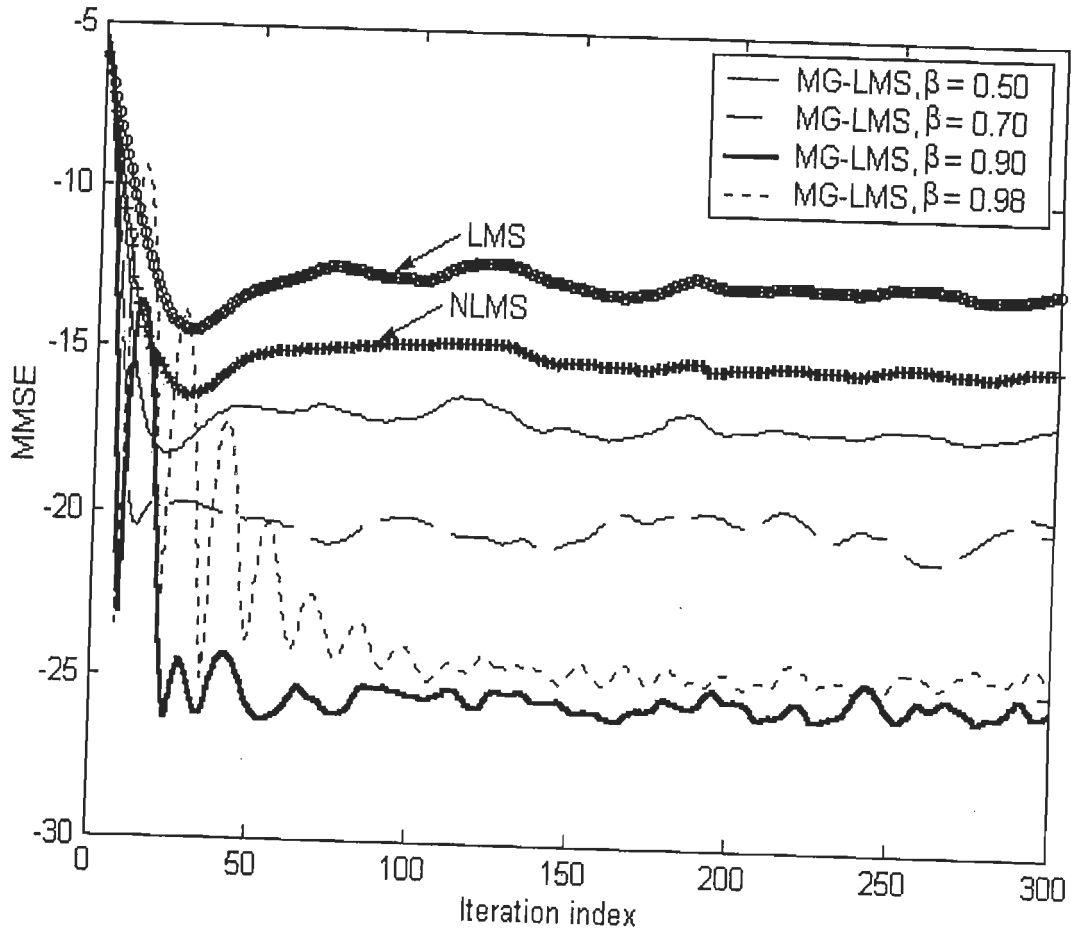


Fig. 3.6: Convergence and tracking performance comparison of MG-LMS algorithm for various values of β in terms of MMSE (dB).

But beyond the optimum value of control parameter $\beta_{optimum} \cong 0.92$ (as measured by simulations), the performance starts degrading. At $\beta = 0.98$, the increase in MSE and oscillatory behaviour during the convergence mode indicate instability because the poles are complex. In section 3.3, the mathematical analysis demonstrates that for $\beta_{threshold} < \beta$ domain, the MSE will start increasing because of the damped oscillations.

Therefore, the simulation results justify the analytical results described earlier. The results presented in Fig. 3.6 and Fig. 3.7 depict that the NLMS algorithm gives approximately 2.5dB performance advantage over the conventional LMS algorithm. However, the proposed MG-LMS algorithm performs better than the LMS and NLMS algorithms under same nonstationary environment.

For analysing the effects of control parameter on the stability of the proposed algorithm, the above experiment is repeated for different values of β and the resulting MMSE is plotted in Fig. 3.7. For comparison, performance of the conventional LMS and NLMS algorithms are also shown. The G-LMS algorithm gives approximately 11dB improvement over the conventional LMS algorithm [60]. It may be seen from Fig. 3.7 that the performance of the MG-LMS algorithm compared with the conventional LMS improves by approximately 14dB at the optimum value of β . The proposed algorithm provides an additional 3dB advantage in performance than the G-LMS algorithm at $\beta_{optimum}$. In addition, the increasing value of smoothing parameter α leads to reduction in the output MSE. However in $\beta_{threshold} < \beta$ domain, the generation of damped oscillations overwhelms the advantages of the increasing value of α .

Case 3.2: To show the tracking performance of the proposed algorithm over the time-varying wireless channels, we consider a filter with eight tap weights. Under fading conditions, the maximum Doppler frequency f_D and sampling rate are 50Hz and $1/T_s = 10kHz$ respectively.

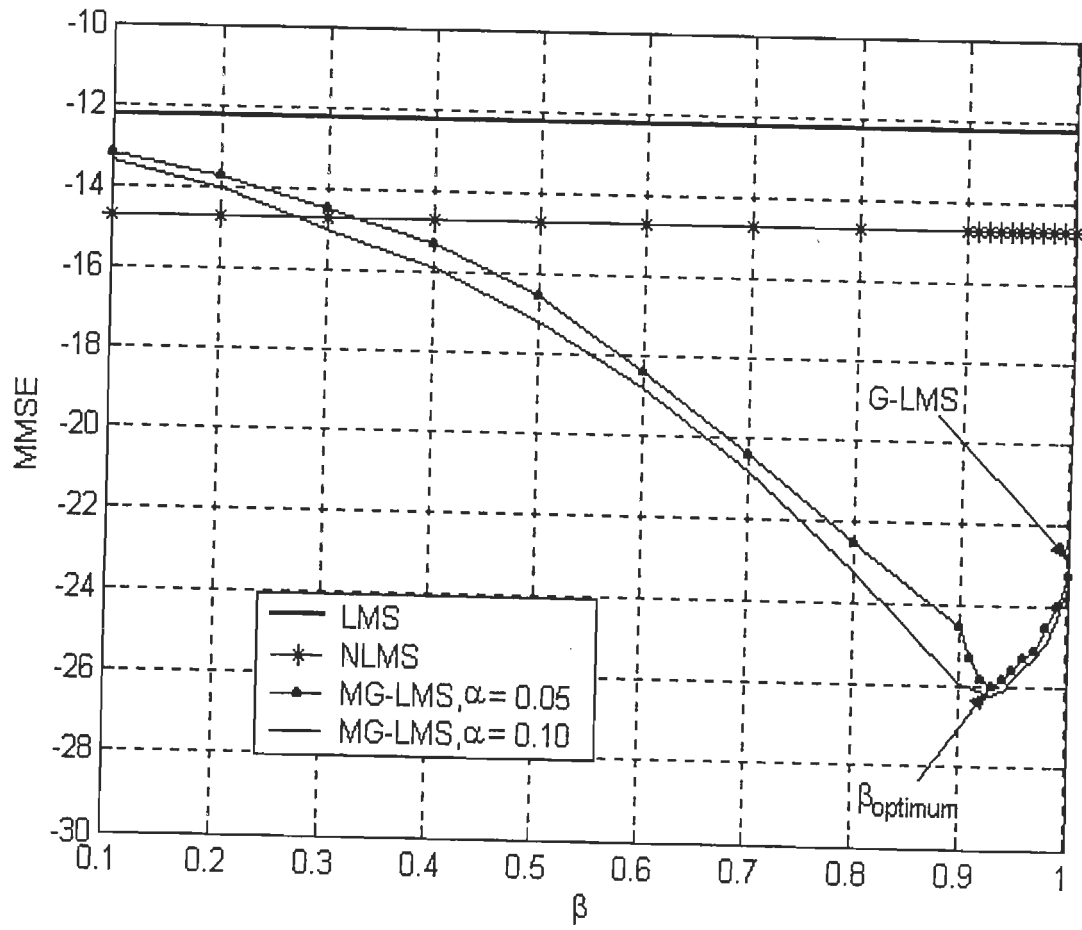


Fig. 3.7: Variation of MMSE (dB) of MG-LMS algorithm for different values of control parameter β .

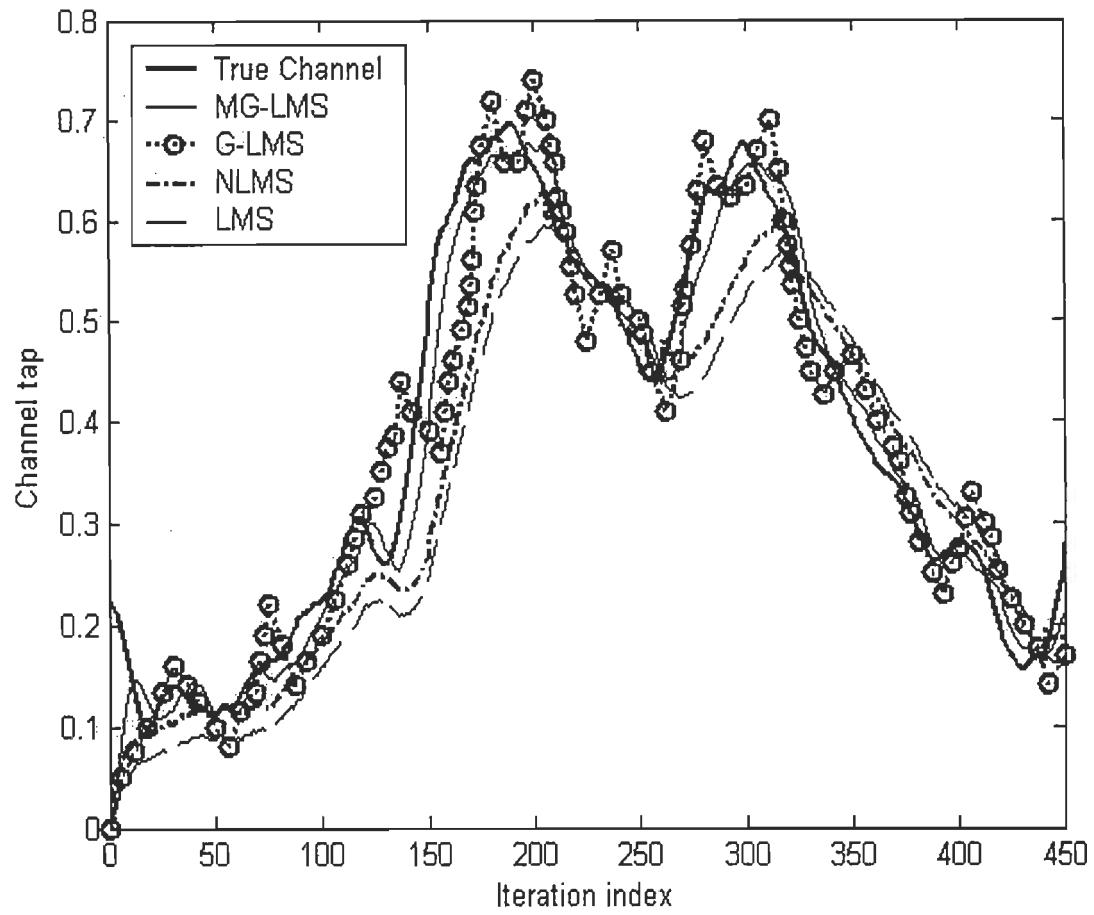


Fig. 3.8: Comparison of MG-LMS, G-LMS, NLMS and LMS algorithms for channel tracking.

With pole radius $r_d = 0.99$, the true time-varying channel is shown in Fig. 3.8. The adaptive MG-LMS algorithm is tuned with $\alpha = 0.01$ and $\beta = 0.75$. Its performance is compared with the conventional LMS, NLMS and G-LMS algorithms by using the same step size $\mu = 0.005$. It is clear from results in Fig. 3.8 that the conventional LMS and NLMS algorithms lag behind the true channel. The channel tap-coefficient value estimated by the G-LMS algorithm oscillates about the true channel coefficient value, which results in high MSE. However, the MG-LMS algorithm gives improved tracking performance by reducing lag.

Therefore, it may be inferred from simulation results that the performance of MG-LMS algorithm improves over the conventional LMS, NLMS and G-LMS adaptive algorithms by tuning the smoothing and control parameters. However, the incorporation of variable step size in the proposed algorithm is expected to further improve its performance.

3.5 Concluding remarks

In this chapter, we have presented a two-step MG-LMS adaptive algorithm, which outperforms the existing G-LMS algorithm [60] under the nonstationary conditions like time-varying fading channels. The proposed algorithm combats the lag noise while tracking, which consequently reduces the total misadjustment. Though it increases the gradient-misadjustment slightly, but it eliminates a large amount of the lag-misadjustment.

We have derived analytical results for the lag-misadjustment, which mainly depend on the smoothing and control parameters. The increasing value of former improves its tracking performance, whereas latter provides stability in the convergence mode. Up to optimum value of the control parameter, MSE at the output decreases, but after that it starts increasing. In practice $\beta_{optimum} \leq \beta_{threshold}$ because beyond the threshold value, the complex poles induce damped oscillations. At $\beta_{optimum}$, the MG-LMS gives approximately 3dB performance

advantage over the G-LMS algorithm. The simulation results have evidenced the superiority of proposed algorithm at adequate values of the smoothing and control parameters. It also validates the derived analytical results.

In the next section, we incorporate the concept of two-step LMS-type MG-LMS algorithm in the adaptive multiuser interference suppression and detection technique for the DS-CDMA system.

ADAPTIVE MULTIUSER DECISION FEEDBACK EQUALIZER RECEIVERS FOR DS-CDMA SYSTEMS

During the last two decades the commercial use of DS-CDMA has increased, due to the demand for large capacity in terms of the number of users and for the efficient usage of bandwidth. It was previously confined to only military communication systems as it provides protection against interference and jamming. But, major limiting factors for capacity in the multiuser systems are multiple access interference and intersymbol interference. In this chapter, we present an adaptive decision feedback equalizer based multiuser receiver for the DS-CDMA systems over smoothly time-varying multipath fading channels using the reduced Kalman/LMS (RK-LMS) adaptive algorithm by exploiting the Kalman filtering algorithm. This is motivated by the work on two-step LMS-type algorithms presented in [60] and chapter 3.

In section 4.1, we first briefly review different adaptive time-varying channel estimation techniques and adaptive decision feedback equalization structures with or without the knowledge of estimated channel response to suppress ISI and MAI. In section 4.2, we describe the DS-CDMA system model, and also give details about the mathematical formulation of frequency-selective channel model for the multipath fading environment. The fading channel is modelled as a tapped-delay-line filter with smoothly time-varying Rayleigh distributed tap-coefficients, which are considered to be autoregressive (*AR*) processes. In section 4.3, we consider a channel estimator based MMSE DFE multiuser receiver structure, which uses the channel estimates obtained from the multiuser channel estimator to cancel out ISI due to the multipath transmission [101]. We next introduce the RK-LMS adaptive

algorithm based multiuser channel estimator, and also present the analytical results for its convergence and tracking characteristics in section 4.4. Section 4.5 includes details about the proposed adaptive DFE multiuser receiver using the RK-LMS algorithm. The computer simulation results are presented in section 4.6 to show the substantial improvement in tracking as well as bit error rate performance of the proposed multiuser receiver over the conventional LMS algorithm based receiver under the smoothly time-varying environment. Finally, conclusions are given in section 4.7.

4.1 Introduction

Over the multipath fading channel with additive white Gaussian noise, the adaptive non-linear MMSE techniques (decision feedback) are more effective than the linear techniques [38], because the latter is having only feedforward filter, whereas the former is having feedforward as well as feedback filters to combat ISI. An adaptive decision feedback equalizer proposed by Abdulrahman [14] is commonly used for interference cancellation and data detection on the forward link from base station to mobile. It is apparent from the presented results that the forward filter of adaptive DFE also performs the function of RAKE receiver to exploit diversity resulting from the multipath transmission. However its application is limited to the detection of a single desired user, and it partially suppresses ISI and MAI by forcing zeros in the impulse response of the interferers.

On the reverse link from mobile to base station, the received composite signal includes ISI due to the past data symbols of other active users. As information about the past detected symbols of all users is available at the base station, therefore adaptive DFE multiuser receiver is used for the multiuser interference cancellation and data detection at the base station. A centralized detection process can be performed at a base station, which is assigned the task of detecting the data from all the users in a cell. Rapajic *et al.* [73] have considered a

centralized MMSE decision feedback detector, where in addition to a fractionally spaced feedforward filter that processes the chip matched filter output, the feedback filter processes previous decisions from all the users to cancel both ISI and MAI. But, authors have presented only single-user adaptation of the filter coefficients. Smee *et al.* [9], [10] have proposed adaptive feedforward/feedback architectures for multiuser detection in the high data rate wireless CDMA networks by extending the work of [73], in which the LMS, NLMS and RLS algorithms can be incorporated to determine the coefficients of multiuser detector. The cyclostationarity of the MAI and ISI is exploited through a feedforward filter, which processes the samples at the output of parallel chip matched filters, and a feedback filter, which processes detected symbols. In blind and non-blind adaptive receiver designs [21], [82], the channel is assumed to be unknown, but time-invariant in a transmitted time frame. Therefore, these techniques are not applicable for the time-varying multipath fading channel situations.

The conventional strategy for handling the time-varying fading channel is to design an adaptive equalizer using the Kalman filtering algorithm [100]. In [97], McLaughlin has employed a channel estimator for the design of Kalman algorithm based equalizer. The performance of this equalizer depends on the accuracy of the channel estimation. Iltis *et al.* have proposed a technique for the joint estimation of PN code delay and channel using the extended Kalman filter [51], [52]. They have also used the QR-decomposition technique in channel estimation for the quasi-synchronous DS-SS system [157]. Recent research has been devoted to the design of multiuser detection using the MMSE adaptive DFE under the time-varying environment [101], [102], [158].

In [101], Chen *et al.* have proposed a multiuser receiver by taking into account the channel model directly obtained from the Doppler spread of the fading channel. In general, the dynamic characteristics of fading channel can not be characterized exactly by system

identification method. Therefore for robust adaptive design, this Kalman filtering algorithm based approach considers the channel estimation errors and model's uncertainties to improve the performance. But, it requires the knowledge of maximum Doppler spread of the multipath fading channel accurately at receiver. Further in [102], Chen *et al.* have proposed a linear-trend tracking algorithm and a multiuser detection algorithm, which uses the self-tuning scheme to automatically adjust the variance of the driving noise in the state-space model to cope with the time-varying Doppler frequency. Moreover, a non-linear limiting function is embedded into the multiuser channel estimator and detector to mitigate the noise effects. A robust Kalman algorithm based DFE detection algorithm is proposed to prevent severe error propagation due to impulsive noise and channel estimation errors under the time-varying fading channel and impulsive noise. The robustness is achieved by using the hard-decision feedback and non-linear limiting function, but at the cost of increased computational complexity. It is seen in above techniques that the channel estimator plays an important role in the overall performance of the multiuser receiver.

Cao *et al.* [159] have proposed a polynomial approach for the MMSE estimation of the time-varying channel parameters in the DS-CDMA system. But, its dependency on the knowledge of system model may often preclude its use. The two-step G-LMS algorithm [60] does not require prior information about the time-variations of the true system, which supersedes the conventional LMS algorithm because of its ability to combat the lag noise [57]. The drawback of G-LMS algorithm is that it requires relatively longer training period, during which, the oscillatory behaviour of algorithm accounts for the high value of residual MMSE. However, the MG-LMS algorithm presented in chapter 3 may be used to circumvent these problems.

In another approach [158], the chip-level equalization can be used to mitigate the MAI together with a despreader. The despreader restores the orthogonality of signature sequences

after equalization. Choi *et al.* [158], have used the feedback filter at the chip rate so that adaptive algorithm can be used to find the filter coefficients of the DFE. It has been shown that the use of soft-decisions has an advantage in effective updating of the chip-level DFE to track the time-variant channels. However, this approach is computationally inefficient due to despreading operation. Traditionally, adaptive equalizers using the RLS algorithm are used for treating the smoothly fading channel problem [88], [89]. Under the quasi-static environment, the multiuser RLS algorithm and direct matrix inversion approach determine the coefficients more efficiently than the single-user algorithms [10]. However to reduce the computational complexity, the two-step LMS-type algorithms (see chapter 3) can be used in the adaptive equalization and multiuser detection techniques (see [101] and [102]) under the smoothly time-varying multipath fading channels.

In the present work, an adaptive multiuser receiver is developed by using the two-step RK-LMS algorithm, which combats the nonstationarity introduced by the channel variations. The receiver uses an adaptive MMSE multiuser channel estimator to predict the coefficients of tapped-delay-line filter. We consider first the design of adaptive MMSE feedforward and feedback filters by using the estimated channel response to cancel out ISI. We next present the convergence characteristics and the tracking performance of the proposed multiuser channel estimator using the RK-LMS algorithm. Unlike the previously available Kalman filtering algorithm based approach [101], [102], the incorporation of the RK-LMS algorithm reduces the computational complexity of the multiuser receiver. It can be inferred from simulation results that the proposed multiuser receiver with the RK-LMS algorithm outperforms the conventional LMS algorithm based approach by reducing the lag noise during tracking [57], and it proves to be an efficient approach for the multiuser interference cancellation and data detection in the DS-CDMA wireless communication systems.

4.2 DS-CDMA system model

In the following spread spectrum binary communication system, each user's transmitted signal (with signal power level P_k) is assumed to pass through an independent frequency-selective Rayleigh fading channel, which transforms the bandpass signal for k th user (2.2) as:

$$r_k(t) = \text{Re} \left[\left\{ \sqrt{2P_k} \sum_i b_k(i) \sum_{l=0}^{L_k-1} \gamma_{lk}(t) s_k(t - iT_b - \tau_{lk}) \right\} e^{j\omega_c t} \right] = \text{Re} [\hat{r}_k(t) e^{j\omega_c t}] \quad (4.1)$$

$$\text{with } s_k(t) = \sum_{j=0}^{N-1} c_j^k \psi(t - jT_c)$$

where $\hat{r}_k(t)$ is the equivalent lowpass signal, $s_k(t)$ is the spreading signature sequence of user k , c_j^k is the j th chip ($\pm 1/\sqrt{N}$) in the code sequence of k th user, T_c is the chip period, N is the length of code sequence in terms of the chip periods, $1/\sqrt{N}$ is the energy normalization factor, $\psi(t)$ is the real transmitted chip waveform shape, which has unit energy in the time interval $0 \leq t \leq T_c$ i.e., $\psi(t) = 0$ for $t \notin [0, T_c]$, $b_k(i)$ is a real valued transmitted data symbol ± 1 , A_k is the amplitude level ($A_k = \sqrt{2P_k}$), T_b is the symbol period (with $T_b = NT_c$), ω_c is the carrier frequency, L_k is the number of multipaths for k th user, and the complex quantity $\gamma_{lk}(t) = |\gamma_{lk}(t)| e^{-j\omega_c \tau_{lk}}$ represents the complex attenuation factor of l th path.

We assume that the fading channel response changes at the symbol rate. The channel order ($L_k - 1$) is kept less than the processing gain N (i.e., the maximum delay spread of channel is smaller relative to the symbol period). The system suffers from severe ISI, as the value of ($L_k - 1$) approaches N [81]. We define the total delay as $\tau_{lk} = \Omega_k + t_{lk}$. For k th user, Ω_k is the delay with respect to the desired user, and t_{lk} is the propagation delay. At the receiver end, the demodulated equivalent lowpass signal for k th user can be written as:

$$\hat{r}_k(t) = \sqrt{2P_k} \sum_i \sum_{j=0}^{N-1} b_k(i) c_j^k g_k(t; t - (iN + j)T_c) \quad (4.2)$$

where $g_k(t; \tau) = \sum_{l=0}^{L_k-1} \gamma_{lk}(t) \psi(\tau - \tau_{lk})$, which is the convolution of the equivalent lowpass impulse response $\sum_{l=0}^{L_k-1} \gamma_{lk}(t) \delta(\tau - \tau_{lk})$ of the multipath fading channel and the lowpass chip waveform $\psi(\tau)$. Therefore, this fading channel model is analogous to the tapped-delay-line filter model (as used in [101]) for the time-varying frequency-selective channel by virtue of analogy between the multipath transmission [102] and ISI [101] respectively. The L_k coefficients of the tapped-delay-line filter are assumed to be time-varying according to an autoregressive process. Assume that $g_k(t; \tau)$ has finite support of length LT_c for $k = 1, 2, \dots, K$ i.e., $g_k(t; \tau) = 0$ for $\tau \notin [0, LT_c]$. As chip level processing is considered in this work, therefore the data symbol at chip level is defined as $b_k(i) = b_k(iN) = b_k(iN + 1) = \dots = b_k(iN + j)$ for $0 \leq j \leq N - 1$. For mathematical simplicity, we replace $b_k(i)$ with $b_k(iN + j)$ in (4.2). Such that,

$$\hat{r}_k(t) = \sqrt{2P_k} \sum_i \sum_{j=0}^{N-1} b_k(iN + j) c_j^k g_k(t; t - (iN + j)T_c) \quad (4.3)$$

If K active users are present in the system, then the equivalent lowpass composite received signal after demodulation is represented as:

$$\hat{r}(t) = \sum_{k=1}^K \hat{r}_k(t) + z(t) \quad (4.4)$$

where, $z(t)$ is the zero-mean lowpass AWGN with two-sided power spectral density N_0 (due to the presence of thermal noise at receiver), which does not include interference due to other users.

The demodulated lowpass signal is filtered using the chip waveform matched filter [85]

and subsequently sampled within the spreading limit (implicitly) at the chip rate to give

$$\hat{r}(iN+n) = \int_{iN+n}^{(iN+n+1)T_c} \hat{r}(t) \nu(t - (iN+n)T_c) dt = \sum_{k=1}^K \hat{r}_k(iN+n) + z(iN+n) \quad (4.5)$$

Since the short codes used in the above described DS-CDMA system are cyclic (periodic) in nature, therefore the received signal sample $\hat{r}(iN+n)$ is a cyclostationary process. Moreover, the transmission through the multipath fading channel is also periodically time-varying. For k th user, the discrete-time received signal in i th data symbol interval's n th chip is represented as:

$$\hat{r}_k(iN+n) = \sqrt{2P_k} \sum_{l=0}^{L-1} h_{lk}(iN+n-l) b_k(iN+n-l) c_{((n-l)_N)}^k \quad \text{for } n = 0, 1, 2, \dots, N-1 \quad (4.6)$$

$$z(iN+n) = \int_{iN+n}^{(iN+n+1)T_c} z(t) \nu(t - (iN+n)T_c) dt \quad (4.7)$$

where, the expression $(x)_N$ denotes “ $x \bmod N$ ” and

$$h'_k(iN+n, l) = \int_0^{T_c} g_k(t + (iN+n)T_c; t + lT_c) \nu(t) dt \quad (4.8)$$

We can rearrange the above equation to give

$$h_{lk}(iN+n-l) = h'_k(iN+n-l, l) = \int_{lT_c}^{(l+1)T_c} g_k(t' + (iN+n-l)T_c; t') \nu(t' - lT_c) dt' \quad (4.9)$$

In the above equation, the channel coefficient h_{lk} is assumed to be constant for the data symbol duration T_b i.e., $h_{lk}(i) = h_{lk}(iN) = h_{lk}(iN+1) = \dots = h_{lk}(iN+n)$ for $0 \leq n \leq N-1$. If

$z(n)$ has auto-correlation $\frac{1}{2} E[z(n)z^*(m)] = N_0 \delta(n-m)$, then the resulting average signal-to-

noise ratio (SNR) of k th user is given by

$$[SNR]_k^{avg} = \frac{P_k \sum_{l=0}^{L-1} E|h_{lk}(i)|^2}{N_0} \quad (4.10)$$

where, $(\cdot)^*$ denotes the complex conjugate operator. Without the loss of generality, we assume that all the active users are transmitting at the same signal power level, such that

$$A_1 = A_2 = \dots = A_k = 1 \text{ i.e., } \sqrt{2P_k} = 1.$$

The received signal vector $\hat{r}_k(i)$ consists of N consecutive stacked samples, where i is the data symbol index. The $N \times 1$ dimensional vector $\hat{r}_k(i)$ can be written as $\hat{r}_k(i) = [\hat{r}_k(iN) \ \hat{r}_k(iN+1) \ \dots \ \hat{r}_k(iN+j) \ \dots \ \hat{r}_k(iN+N-1)]^T$. The $N \times 2L$ dimensional signature-sequence-matrix $C^k(i)$, $2L \times 2L$ dimensional data-symbol-matrix $B^k(i)$, and $2L \times 1$ dimensional multipath channel coefficient vector $h^k(i)$ for the k th user's i th data symbol can be defined as:

$$C^k(i) = \begin{bmatrix} c_0^k & \dots & 0 & 0 & c_{N-1}^k & \dots & c_{N-L+1}^k \\ c_1^k & \dots & 0 & 0 & 0 & \dots & \vdots \\ \vdots & \dots & \vdots & \vdots & \vdots & \dots & \vdots \\ \vdots & \dots & c_0^k & \vdots & \vdots & \dots & c_{N-1}^k \\ \vdots & \dots & c_1^k & 0 & \vdots & \dots & 0 \\ \vdots & \dots & \vdots & \vdots & \vdots & \dots & \vdots \\ c_{N-1}^k & \dots & c_{N-L}^k & 0 & 0 & \dots & 0 \end{bmatrix} = [C^k \parallel \tilde{C}^k]$$

$$B^k(i) = \text{diag}[b_k(i)I_L, b_k(i-1)I_L], \text{ and } h^k(i) = [\bar{h}_k^T(i) \parallel \bar{h}_k^T(i-1)]^T.$$

where, I_L is the $L \times L$ dimensional identity matrix and $\bar{h}_k(i) = [h_{0k}(i) \ h_{1k}(i) \ \dots \ h_{(L-1)k}(i)]^T$.

Using (4.6), the received signal vector $\hat{r}_k(i)$ can be rewritten in the matrix form as:

$$\hat{r}_k(i) = [C^k(i)B^k(i)]h^k(i) = D^k(i)h^k(i) \quad (4.11)$$

where, $D^k(i)$ is the $N \times 2L$ dimensional chip-data-matrix. The composite signal vector $\hat{r}(i)$ can be written as:

$$\hat{r}(i) = [\hat{r}(iN) \ \hat{r}(iN+1) \ \dots \ \hat{r}(iN+j) \ \dots \ \hat{r}(iN+N-1)]^T$$

$$\begin{aligned}
&= \sum_{k=1}^K \hat{r}_k(i) + \hat{z}(i) = \sum_{k=1}^K C^k(i) B^k(i) \hat{h}^k(i) + \hat{z}(i) \\
&= [\hat{C}(i) \hat{B}(i)] \hat{h}(i) + \hat{z}(i) = \hat{D}(i) \hat{h}(i) + \hat{z}(i)
\end{aligned} \tag{4.12}$$

where, $\hat{C}(i) = [C(i) \parallel \tilde{C}(i)] = [C^1 \ C^2 \dots \ C^K \parallel \tilde{C}^1 \ \tilde{C}^2 \dots \ \tilde{C}^K]$

is a $N \times 2KL$ dimensional matrix,

$$\hat{B}(i) = \text{diag}[b_1(i)I_L, b_2(i)I_L, \dots, b_K(i)I_L \parallel b_1(i-1)I_L, b_2(i-1)I_L, \dots, b_K(i-1)I_L]$$

is a $2KL \times 2KL$ dimensional matrix,

$$\hat{h}(i) = [\bar{h}_1^T(i) \ \bar{h}_2^T(i) \dots \ \bar{h}_K^T(i) \parallel \bar{h}_1^T(i-1) \ \bar{h}_2^T(i-1) \dots \ \bar{h}_K^T(i-1)]^T$$

is a $2KL \times 1$ dimensional matrix,

$$\hat{D}(i) = [C^1 \{b_1(i)I_L\} \dots C^K \{b_K(i)I_L\} \parallel \tilde{C}^1 \{b_1(i-1)I_L\} \dots \tilde{C}^K \{b_K(i-1)I_L\}]$$

is a $N \times 2KL$ dimensional matrix, and

$$\hat{z}(i) = [z(iN) \ z(iN+1) \dots \ z(iN+j) \dots \ z(iN+N-1)]^T$$

The $N \times 1$ dimensional matrix $\hat{z}(i)$ denotes the noise sample vector. The equation (4.12) is used for the channel estimation. We next define the data symbol detection equation using the composite signal vector $\hat{r}(i)$ as:

$$\hat{r}(i) = \hat{C}(i) \hat{H}(i) \hat{b}(i) + \hat{z}(i) = C(i) H(i) b(i) + \tilde{C}(i) H(i-1) b(i-1) + \hat{z}(i) \tag{4.13}$$

where, $\hat{b}(i) = [b^T(i) \parallel b^T(i-1)]^T$ with $b(i) = [b_1(i) \ b_2(i) \dots \ b_K(i)]^T$

$$\hat{H}(i) = \text{diag}[H(i), H(i-1)] \text{ with } H(i) = \text{diag}[\bar{h}_1(i), \bar{h}_2(i), \dots, \bar{h}_K(i)]$$

We use (4.12) to estimate the multipath fading channel response using the signature-sequence-matrices and data-symbol-matrices of all the active users, and then design the adaptive DFE multiuser receiver using the RK-LMS algorithm for the multiuser interference cancellation and data detection (4.13).

4.3 Channel estimator based DFE multiuser receiver

In this section, we present details about the MMSE DFE multiuser receiver design using the multiuser channel estimates. Let the input vector to the decision device be

$y(i) = [y^1(i) \ y^2(i) \ \dots \ y^K(i)]^T$, and the corresponding estimated data symbol vector at the

slicer output is $b_e(i) = [b_{e1}(i) \ b_{e2}(i) \ \dots \ b_{eK}(i)]^T$, such that

$$y(i) = F_f(i)\hat{r}(i) - F_b(i)b_e(i-1) \quad (4.14a)$$

$$= F_f(i)[C(i)H(i)b(i) + \tilde{C}(i)H(i-1)b(i-1) + \hat{z}(i)] - F_b(i)b_e(i-1) \quad (4.14b)$$

where, the $K \times N$ dimensional matrix $F_f(i)$ and the $K \times K$ dimensional matrix $F_b(i)$ are the feedforward filter (FFF) and the feedback filter (FBF) weight matrices respectively. For simplification, we assume that no error propagation in the decision feedback loop takes place *i.e.*, $b_e(i-1) = b(i-1)$ in (4.14a) and (4.14b). The filtering error of the DFE multiuser receiver is a $K \times 1$ dimensional vector $e_1(i) = b(i) - y(i)$. The corresponding error covariance matrix is $\varepsilon_1(i) = E[e_1(i)e_1^H(i)]$, where E is the ensemble average operator. The cost function is defined as the sum of all diagonal elements of the matrix $\varepsilon_1(i)$ *i.e.*, $J_1(i) = E[e_1^H(i)e_1(i)]$.

The optimum MMSE receiver is derived by minimizing the scalar cost function. Using the

partial derivatives $\frac{\partial J_1(i)}{\partial F_f} = 0$ and $\frac{\partial J_1(i)}{\partial F_b} = 0$ [160], we derive the optimum solution as:

$$F_f(i) = H^H(i)C^H(i)[C(i)H(i)H^H(i)C^H(i) + R_z]^{-1} \quad (4.15a)$$

where, the noise covariance matrix is $R_z = E[\hat{z}(i)\hat{z}^H(i)]$.

$$F_b(i) = F_f(i)\tilde{C}(i)H(i-1) \quad (4.15b)$$

where, $()^H$ is the Hermitian operator. Since we are using the channel estimates in the design of feedback filter, therefore the matrix $H(i-1)$ is replaced by the estimated channel

coefficient matrix $H(i-1|i-1)$ in (4.15b). Substituting (4.15b) in (4.14a), the input vector $y(i)$ to the decision device can be redefined as:

$$y(i) = F_f(i) \hat{r}_{eq}(i) \quad (4.16)$$

where, the equivalent input signal vector to the feedforward filter is $\hat{r}_{eq}(i) = \hat{r}(i) - \hat{r}_{ISI}(i)$. The ISI term $\hat{r}_{ISI}(i) = \tilde{C}(i)H(i-1|i-1)b_e(i-1)$ is generated and cancelled from the composite signal vector $\hat{r}(i)$ by using the estimated channel response $H(i-1|i-1)$. It is apparent from (4.16) that we can replace $F_f(i)$ with an adaptive feedforward filter of the same dimension.

The proposed adaptive multiuser receiver is shown in Fig. 4.1, in which the feedforward filter $F_f(i)$ is replaced by the RK-LMS algorithm based adaptive FFF $W_f(i)$ (described in section 4.5), and the estimated multiuser channel response $H(i-1|i-1)$ is obtained by using the RK-LMS algorithm (described in next section). It may be noted that the performance of adaptive multiuser channel estimator influences the intersymbol interference cancellation.

4.4 Adaptive multiuser channel estimation

In the literature, the unknown channel coefficients are often assumed to be a first-order Markov process for the tracking performance analysis of the LMS-based adaptive algorithms [57], [60], [101]. Therefore, the multipath channel coefficient vector of the k th user can be modelled by using the $AR(1)$ process as:

$$\bar{h}_{k,o}(i) = \hat{\rho} \bar{h}_{k,o}(i-1) + \hat{w}_k(i) \quad (4.17)$$

where, the $L \times L$ dimensional channel correlation coefficient matrix is $\hat{\rho} = \text{diag}[a_{0k}, a_{1k}, \dots, a_{(L-1)k}]$. The above model is valid for the fading channel only if the channel coherence time is large enough to estimate the channel response. The subscript $()_o$ denotes the optimum value.

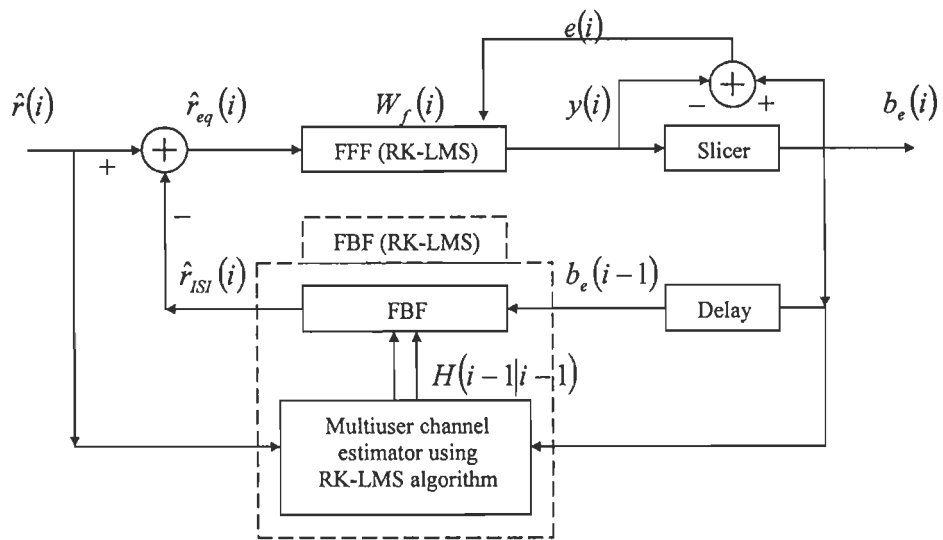


Fig. 4.1: Adaptive MMSE DFE multiuser receiver using the RK-LMS algorithm.

(The non-adaptive FFF $F_f(i)$ is replaced by an adaptive FFF (RK-LMS) $W_f(i)$)

The scaling factor a_{lk} denotes the state transition coefficient of the k th user in l th path. According to Jakes model presented in [154], this factor may be defined as the correlation coefficient. In (4.17), $\hat{w}_k(i) = [\hat{w}_k^0(i) \ \hat{w}_k^1(i) \ \dots \ \hat{w}_k^{L-1}(i)]^T$ is a zero-mean white noise process vector with the covariance matrix $\sigma_{\hat{w}_k}^2 I_L$, which results in the uncorrelated tap-coefficients of the multipath fading channel (wide-sense stationary uncorrelated scattering channel).

If we consider the first-order weight increment vector $\dot{\bar{h}}_{k,o}(i-1) \cong \bar{h}_{k,o}(i) - \bar{h}_{k,o}(i-1)$ correlated with the vector $\bar{h}_{k,o}(i)$, then this redundant information may be used to predict the vector $\bar{h}_{k,o}(i)$ because $\bar{h}_{k,o}(i) \cong \hat{d} \left\{ \hat{\rho} \bar{h}_{k,o}(i-1) + \hat{w}_k(i) \right\}$; where the $L \times L$ dimensional scaling matrix is $\hat{d} = \text{diag} \left[(1 - a_{0k})^{-1}, (1 - a_{1k})^{-1}, \dots, (1 - a_{(L-1)k})^{-1} \right]$. Similarly, the second-order weight increment vector $\ddot{\bar{h}}_{k,o}(i-1) \cong \dot{\bar{h}}_{k,o}(i) - \dot{\bar{h}}_{k,o}(i-1)$ may be used to approximate the state equation for the time-varying fading environment. In the following, we assume that $a_{lk} = a$ i.e., the correlation coefficients of all the fading channels are equal. Such that, the optimum channel coefficient vector used in the channel estimation equation (4.12) is $\hat{h}_o(i) = A \hat{h}_o(i-1) + \hat{W}(i)$ with $A = aI$, where $\hat{W}(i)$ is a $2KL \times 1$ dimensional zero-mean white noise process vector, and I is a $2KL \times 2KL$ dimensional identity matrix. In the multiuser scenario, the state equation may be defined in terms of the first-order and second-order weight increment vectors as:

$$\begin{bmatrix} \hat{h}_o(i) \\ \dot{\hat{h}}_o(i) \end{bmatrix} = \begin{bmatrix} I & I \\ 0 & I \end{bmatrix} \begin{bmatrix} \hat{h}_o(i-1) \\ \dot{\hat{h}}_o(i-1) \end{bmatrix} + \begin{bmatrix} 0 \\ \ddot{\hat{h}}_o(i-1) \end{bmatrix} \quad (4.18)$$

4.4.1 RK-LMS algorithm based channel estimator

The application of Kalman algorithm for the multiuser channel estimation is based on the following equations.

$$\hat{h}(i) = \hat{h}(i|i-1) + \hat{K}(i)[\hat{r}(i) - \hat{r}_e(i)] \quad (4.19)$$

where the Kalman gain or blending factor is $\hat{K}(i) = P(i|i-1)\hat{D}^T(i)[\hat{D}(i)P(i|i-1)\hat{D}^T(i) + R_z]^{-1}$, and the estimated signal vector using (4.12) is denoted as:

$$\hat{r}_e(i) = [\hat{C}(i)\hat{B}(i)]\hat{h}(i|i-1) = \hat{D}(i)\hat{h}(i|i-1) \quad (4.20)$$

The covariance matrix of the prediction error (in time update) is $P(i|i-1) = AP(i-1|i-1)A^T + Q_w$ and the covariance matrix of the estimation error (in measurement update) is $P(i|i) = [I - \hat{K}(i)\hat{D}(i)]P(i|i-1)$, where $R_z = E[\hat{z}(i)\hat{z}^H(i)]$ and $Q_w = E[\hat{W}(i)\hat{W}^H(i)]$ are the measurement noise and the process noise covariance matrices respectively. It is clear that the above described Kalman adaptive algorithm based approach is computationally complex.

Therefore, the Kalman algorithm is reduced to give a computationally efficient two-step LMS-type algorithm, which eliminates the matrix inversion operation in the Riccati update equation. The new RK-LMS algorithm based multiuser channel estimator is as follows

$$\hat{h}(i) = \hat{h}(i|i-1) + \mu\hat{D}^T(i)[\hat{r}(i) - \hat{r}_e(i)] \quad (4.21)$$

where the scalar parameter μ is step size, which controls the convergence and stability of the adaptive algorithm. The Kalman gain $\hat{K}(i)$ is replaced by $\mu\hat{D}^T(i)$, and the *a priori* estimate $\hat{h}(i|i-1)$ of $\hat{h}(i)$ is defined as:

$$\hat{h}(i|i-1) = \hat{h}(i-1|i-1) + \beta\hat{h}(i-1|i-1) \quad (4.22)$$

In the above equation, the first-order weight increment vector is estimated as:

$$\hat{h}(i) = \hat{h}(i-1|i-1) + \alpha\mu\hat{D}^T(i)[\hat{r}(i) - \hat{r}_e(i)] \quad \text{with } \hat{h}(i|i-1) = \hat{h}(i-1|i-1) \quad (4.23)$$

where $0 \leq \alpha < 1$ is a smoothing parameter, which controls the lag in tracking the time-varying system [60]; and the estimated first-order weight increment vector is scaled with a real valued

control parameter $0 \leq \beta < 1$, which controls the oscillatory behaviour of algorithm. The analytical and simulation results presented in chapter 3 show that the value of β should be tuned below the threshold value (depending on the value of α and μ), which ensures stability in the convergence mode. Further it has been shown by computer simulations that for a single-user system, the proposed algorithm provides approximately 14dB performance advantage in channel estimation over the conventional LMS algorithm by reducing the mean square error in tracking mode.

Let $E[\hat{h}(i)]$ is the ensemble average of $\hat{h}(i)$ (see [57] and chapter 3). The estimated multiuser channel coefficient vector can be defined in terms of the optimum channel coefficient vector $\hat{h}_o(i)$, tracking noise vector $\hat{h}_T(i) = \hat{h}(i) - E[\hat{h}(i)]$ and lag noise vector $\hat{h}_L(i) = E[\hat{h}(i)] - \hat{h}_o(i)$ as:

$$\hat{h}(i) = \hat{h}_o(i) + \hat{h}_T(i) + \hat{h}_L(i)$$

For the above procedure, the estimation of the first-order weight increment vector (4.23) helps in reducing the lag noise *i.e.*, $\hat{h}_L(i)$ in tracking, but application of the conventional LMS algorithm in steps (4.21) and (4.23) contributes minor gradient noise in addition to the residual lag noise. The reduction in the lag noise results due to the improved tracking in the time-varying nonstationary environment.

Therefore, the equations (4.20 – 4.23) are used to estimate the multipath channel response for K users. The reduced Kalman/LMS algorithm is computationally comparable to the conventional LMS adaptive algorithm. Moreover, the RK-LMS algorithm does not require the knowledge of channel correlation coefficient α . In addition, the substitution of variable step size $\mu(i)$ results in development of a new family of the two-step LMS-type algorithm based adaptive channel estimators.

4.4.2 Analysis of multiuser channel estimator

In this section, we study the mean convergence behaviour and tracking characteristics of the RK-LMS algorithm based adaptive multiuser channel estimator. Using the channel estimation equation (4.12), we redefine the received composite signal vector in terms of the optimum weight vector as $\hat{r}(i) = \hat{D}(i)\hat{h}_o(i) + \hat{z}(i)$. Let the state (channel coefficient) error vector be

$$\Phi(i) \cong \begin{bmatrix} \Delta\hat{h}(i) \\ \Delta\hat{h}(i) \end{bmatrix} \cong \begin{bmatrix} \hat{h}(i|i) - \hat{h}_o(i) \\ \hat{h}(i|i) - \hat{h}_o(i) \end{bmatrix} \quad (4.24)$$

The equation (4.24) is solved using the RK-LMS algorithm (see appendix B) to give

$$\Phi(i) \cong T(i)\Phi(i-1) + N(i) \quad (4.25)$$

$$\text{where, } T(i) \cong \begin{bmatrix} I - \mu\hat{R}(i) & I - \mu\hat{R}(i) \\ -\alpha\mu\hat{R}(i) & I - \alpha\mu\hat{R}(i) \end{bmatrix} \quad \text{with } \hat{R}(i) = \hat{D}^T(i)\hat{D}(i) \quad (4.26)$$

$$N(i) \cong \begin{bmatrix} \mu\hat{D}^T(i)\hat{z}(i) + \{(1-\beta)\mu\hat{R}(i)\}\hat{h}(i-1|i-1) - (1-\beta)\hat{h}(i-1|i-1) \\ \alpha\mu\hat{D}^T(i)\hat{z}(i) + \{\alpha(1-\beta)\mu\hat{R}(i)\}\hat{h}(i-1|i-1) - \hat{h}_o(i-1) \end{bmatrix} \quad (4.27)$$

The above weight error vector may be considered as the output of a recursive linear system with the state transition matrix $T(i)$ and the input vector $N(i)$.

Since $\hat{z}(i)$ is a zero-mean statistically independent random process vector *i.e.*, $E[\hat{z}(i)] = 0$ and $\hat{R} = E[\hat{D}^T(i)\hat{D}(i)]$ is the average value of matrix $\hat{R}(i)$, therefore the ensemble average of the weight error vector $\Phi(i)$ gives the mean error variation. We can write,

$$E[\Phi(i)] \cong \hat{T}(i)E[\Phi(i-1)] + \hat{N}(i) \quad (4.28)$$

$$\text{where, } \hat{T}(i) \cong \begin{bmatrix} I - \mu\hat{R} & I - \mu\hat{R} \\ -\alpha\mu\hat{R} & I - \alpha\mu\hat{R} \end{bmatrix} \quad \text{and } \hat{N}(i) \cong \begin{bmatrix} -(1-\beta)\{I - \mu\hat{R}\} & 0 \\ + (1-\beta)\{\alpha\mu\hat{R}\} & -I \end{bmatrix} \begin{bmatrix} E[\hat{h}(i-1|i-1)] \\ E[\hat{h}_o(i-1)] \end{bmatrix} \quad (4.29)$$

The square matrix \hat{R} is spectrally factorized to give $Q^{-1}\Lambda Q$, where Q is the modal matrix consisting of eigenvectors as column vectors and Λ is the spectral matrix with only eigenvalues at its main diagonal *i.e.*, $\Lambda = \text{diag}\{\lambda_1, \lambda_2, \dots, \lambda_q, \dots, \lambda_{2KL}\}$. The multiplication of the modal matrix \hat{Q} on the both sides of (4.28) leads to

$$\hat{Q}E[\Phi(i)] \cong \hat{T}_Q(i)[\hat{Q}E[\Phi(i-1)]] + \hat{Q}\hat{N}(i) \quad (4.30)$$

where $\hat{Q} = \begin{bmatrix} Q & 0 \\ 0 & Q \end{bmatrix}$, $\hat{T}_Q(i) = \begin{bmatrix} I - \mu\Lambda & I - \mu\Lambda \\ -\alpha\mu\Lambda & I - \alpha\mu\Lambda \end{bmatrix}$ and

$$\hat{Q}\hat{N}(i) \cong [\hat{S}(i) + \hat{M}(i)]\hat{O}(i) \quad (4.31)$$

where $\hat{S}(i) = \begin{bmatrix} -\{I - \mu\Lambda\} & 0 \\ (1 - \beta)\{\alpha\mu\Lambda\} & -I \end{bmatrix}$, $\hat{M}(i) = \begin{bmatrix} \beta\{I - \mu\Lambda\} & 0 \\ 0 & 0 \end{bmatrix}$ and $\hat{O}(i) = \begin{bmatrix} QE[\hat{h}(i-1|i-1)] \\ QE[\hat{h}_o(i-1)] \end{bmatrix}$

(4.32)

The matrix $\hat{T}_Q(i)$ may be considered as the transfer function in the system defined by (4.30).

The transfer function of its q th sub-channel is

$$[\hat{T}_Q(i)]_q = \begin{bmatrix} 1 - \mu\lambda_q & 1 - \mu\lambda_q \\ -\alpha\mu\lambda_q & 1 - \alpha\mu\lambda_q \end{bmatrix} \quad (4.33)$$

The eigenvalues of the above transfer function for the q th sub-channel are

$$\gamma_q = 1 - \mu\lambda_q \frac{1 + \alpha}{2} \pm \sqrt{\left(\mu\lambda_q \frac{1 + \alpha}{2}\right)^2 - \alpha\mu\lambda_q} \quad (4.34)$$

For complex eigenvalues, the RK-LMS algorithm will exhibit damped oscillations, which results in the high mean square error during the initial learning mode. However the real eigenvalues provide stability to algorithm, which can be achieved by keeping

$$\left(\mu\lambda_q \frac{1 + \alpha}{2}\right)^2 - \alpha\mu\lambda_q \geq 0 \quad (4.35)$$

The rearrangement of the above equation results in the lower bound on the value of smoothing parameter *i.e.*,

$$\alpha \geq \frac{\mu\lambda_{\max}}{\left(1 + \sqrt{1 - \mu\lambda_{\max}}\right)^2} \approx \frac{\mu\lambda_{\max}}{4} \quad (4.36)$$

For real and equal eigenvalues, the mean time constant is defined as:

$$\zeta_q = \frac{1}{1 - |\gamma_q|} = \frac{2}{\mu\lambda_q(1 + \alpha)} \quad (4.37)$$

Since the value of α is kept small, therefore the mean time constant for convergence is approximated as $\zeta_q \cong 2/\mu\lambda_q$. The value of ζ_q is comparable to the mean time constant for the conventional LMS algorithm as α approaches unity *i.e.*, $\zeta_q \rightarrow 1/\mu\lambda_q$. Therefore, the mean time constant can be adjusted by tuning the value of smoothing parameter.

The state error vector $\Phi(i)$ converges to zero for null values of $E\left[\hat{h}(i-1|i-1)\right]$ and $E\left[\tilde{\tilde{h}}_o(i-1)\right]$, which results in the unbiased adaptive multiuser channel estimator. The input vector $\hat{Q}\hat{N}(i)$ depends on the value of β , which is fed to the recursive system (4.30) with transfer function $\hat{T}_Q(i)$ to give the output vector $\hat{Q}E[\Phi(i)]$. Therefore, the criterion of the bounded input and the bounded output stability is applied for the stable functioning of system. For q th sub-channel, the magnitude of the off-diagonal elements of matrix $[\hat{S}(i)]_q$ should be less than one *i.e.*, $-1 < (1 - \beta)\alpha\mu\lambda_q < +1$. For stable convergence behaviour, the stringent condition on the control parameter β may be defined as $1 - (\alpha\mu\lambda_q)^{-1} < \beta < 1 + (\alpha\mu\lambda_q)^{-1}$. For the large values of $(\alpha\mu\lambda_q)$ *i.e.*, $(\alpha\mu\lambda_q)^{-1} \ll 1$, the corresponding operating range of the control parameter can be redefined as:

$$1 - (\alpha\mu\lambda_q)^{-1} < \beta < 1 \quad (4.38)$$

From the above equation, it is clear that the value of β can be varied in a small range for the large values of $(\alpha\mu)$. As the value of $(\alpha\mu\lambda_q)^{-1} \gg 1$, the above operating range is constrained to $0 \leq \beta < 1$. This range is considered for the RK-LMS algorithm in previous subsection because the value of $(\alpha\mu)$ is kept small. However the increasing value of β increases the elements of matrix $\hat{M}(i)$ in (4.32), which enhances the amplitude of damped oscillations by increasing the input vector $\hat{Q}\hat{N}(i)$.

It may be inferred from (4.23) that the tracking speed may be increased by increasing the value of α , which reduces the lag noise during tracking mode. However, this improvement is achieved at the cost of slight increase in damped oscillations. Under this condition, the reduction in the value of β suppresses the amplitude of oscillations to minimize the MMSE in tracking. Unlike the G-LMS algorithm [60], this parameter tuning provides stability in the convergence mode of the proposed RK-LMS algorithm.

Thus, the RK-LMS algorithm based adaptive channel estimator is used in the time-varying environment by tuning the smoothing and control parameters at the optimum values. The estimated multipath channel coefficients of K active users are used in the multiuser data detection equation (4.13), which is incorporated in the proposed multiuser receiver (described in next section).

4.5 RK-LMS algorithm based adaptive multiuser receiver

4.5.1 Adaptive data detection procedure

In this section, we propose the RK-LMS algorithm based adaptive MMSE DFE multiuser receiver, which uses the estimated multipath channel information. The Kalman algorithm based multiuser receiver (as described in section 4.3) is computationally complex due to the matrix inversion operation in (4.15a). The computational complexity in the calculation of the

feedforward filter weight matrix $F_f(i)$ i.e., the equation (4.15a) is reduced by using the adaptive feedforward filter $W_f(i)$ (the $K \times N$ dimensional weight matrix), which results in $b_e(i) = \text{sgn}[y(i)]$.

$$\text{where, } y(i) = W_f(i)\hat{r}_{eq}(i) \quad (4.39)$$

Under no error propagation condition, it is assumed that $b_e(i) = b(i)$ at the slicer output. The error vector at the slicer output is $e_2(i) = b(i) - y(i)$. The corresponding error covariance matrix is $\varepsilon_2(i) = E[e_2(i)e_2^H(i)]$. The scalar cost function for this case is defined as the trace of matrix $\varepsilon_2(i)$ i.e., $J_2(i) = E[e_2^H(i)e_2(i)]$. The $K \times N$ dimensional gradient matrix

$\frac{\partial J_2(i)}{\partial W_f} = -2E[e_2(i)\hat{r}_{eq}^H(i)]$ is used to derive the weight update equation for the forward filter as:

$$W_f(i) = W_f(i-1) + \hat{\mu}e_2(i)\hat{r}_{eq}^H(i) \quad \text{with step size } \hat{\mu} \quad (4.40)$$

The above weight update equation is governed by the conventional LMS adaptive algorithm.

The adaptive multiuser channel estimator (as shown in Fig. 4.1) provides the estimated multipath channel coefficients, which suffers from the estimation errors. Therefore, the presence of residual ISI (which also introduces nonstationarity) can not be ignored in the equivalent input signal vector $\hat{r}_{eq}(i)$. Under such situation, we incorporate the RK-LMS adaptive algorithm (see [60] and chapter 3) for updating the feedforward filter weight matrix as:

$$W_f(i|i) = W_f(i|i-1) + \hat{\mu}e_2(i)\hat{r}_{eq}^H(i) \quad (4.41)$$

The *a priori* estimate $W_f(i|i-1)$ is updated as:

$$W_f(i|i-1) = W_f(i-1|i-1) + \hat{\beta}\dot{W}_f(i-1|i-1) \quad (4.42)$$

where $\dot{W}_f(i|i)$ is the first-order weight increment matrix, which is defined as:

$$\dot{W}_f(i|i) = \dot{W}_f(i-1|i-1) + \hat{\alpha}\hat{\mu}e_2(i)\hat{r}_{eq}^H(i) \quad (4.43)$$

where $0 \leq \hat{\alpha} < 1$ is a smoothing parameter, which combats nonstationarity in the time-varying multipath fading environment; and the real valued control parameter $0 \leq \hat{\beta} < 1$ is used to provide stability in the initial learning period. In the proposed RK-LMS algorithm based DFE multiuser receiver, the smoothing and control parameters are tuned to give the optimum performance. The adaptive feedforward filter also acts like RAKE, and thus provides the diversity gain. The feedback filter partially cancels ISI using the channel estimates, while the forward filter suppresses the residual ISI as well as MAI. Hence, the proposed DFE multiuser receiver is used for the multiuser interference cancellation and data detection.

4.5.2 Probability of error analysis

Using (4.39), the signal vector at slicer input (as shown in Fig. 4.1) can be written as:

$$\begin{aligned} y(i) &= [y^1(i) \ y^2(i) \ \dots \ y^K(i)]^T \\ &= W_f(i) [C(i)H(i)b(i) + \tilde{C}(i)H(i-1)b(i-1) - \tilde{C}(i)H(i-1|i-1)b_e(i-1) + \hat{z}(i)] \end{aligned} \quad (4.44)$$

where, the output corresponding to the first user is $y^1(i)$. Let $W_f^1(i)$ be the first row vector in the matrix $W_f(i)$. Such that,

$$y^1(i) = W_f^1(i) \begin{bmatrix} C^1 \bar{h}_1(i) b_1(i) + \sum_{k=2}^K C^k \bar{h}_k(i) b_k(i) + \sum_{k=1}^K \tilde{C}^k \bar{h}_k(i-1) b_k(i-1) \\ - \sum_{k=1}^K \tilde{C}^k \bar{h}_k(i-1|i-1) b_{ek}(i-1) + \hat{z}(i) \end{bmatrix} \quad (4.45)$$

In the above equation, we can write the weight vector as:

$$W_f^1(i) = W_{f,T}^1(i) + W_{f,L}^1(i) + W_{f,o}^1(i) \quad (4.46)$$

where $W_{f,T}^1(i) = W_f^1(i) - \bar{W}_f^1(i)$, $W_{f,L}^1(i) = \bar{W}_f^1(i) - W_{f,o}^1(i)$ and $W_{f,o}^1(i)$ are the tracking error weight vector, lag error weight vector and optimum weight vector respectively [57]. The vector $\bar{W}_f^1(i)$ is the average value of the weight vector. Using (4.24), the estimated multipath channel vector is

$$\bar{h}_k(i-1) = \bar{h}_k(i-1|i-1) - \Delta\bar{h}_k(i-1) \quad (4.47)$$

where, the vector $\Delta\bar{h}_k(i-1)$ denotes the channel estimation errors for k th user. Substitution of (4.46) and (4.47) in (4.45) leads to

$$\begin{aligned} y^1(i) &= W_f^1(i) \left[\begin{array}{l} C^1 \bar{h}_1(i) b_1(i) + \sum_{k=2}^K C^k \bar{h}_k(i) b_k(i) + \sum_{k=1}^K \tilde{C}^k \bar{h}_k(i-1) \{b_k(i-1) - b_{ek}(i-1)\} \\ - \sum_{k=1}^K \tilde{C}^k \Delta\bar{h}_k(i-1) b_{ek}(i-1) + \hat{z}(i) \end{array} \right] \\ &= y_o^1(i) \left[b_1(i) + \{y_o^1(i)\}^{-1} \left\{ \left(W_{f,T}^1(i) + W_{f,L}^1(i) \right) C^1 \bar{h}_1(i) \right\} b_1(i) + y_{MUI}^1(i) + y_{ES}^1(i) + y_{\hat{z}}^1(i) + y_{EP}^1(i) \right] \end{aligned} \quad (4.48)$$

where, $y_o^1(i) = W_{f,o}^1(i) C^1 \bar{h}_1(i)$ (Scaling factor)

$y_{MUI}^1(i) = \{y_o^1(i)\}^{-1} \sum_{k=2}^K W_f^1(i) C^k \bar{h}_k(i) b_k(i)$ (Multiuser interference with $N(0, \sigma_{MUI}^2)$)

For probability of error analysis of the proposed multiuser receiver, the multiuser-interference (MUI) can be considered Gaussian process for a large number of users [27], where $b_k(i)$ is a collection of independent equi-probable ± 1 random variables.

$y_{ES}^1(i) = -\{y_o^1(i)\}^{-1} \sum_{k=1}^K W_f^1(i) \tilde{C}^k \Delta\bar{h}_k(i-1) b_{ek}(i-1)$ (Channel estimation error with $N(0, \sigma_{ES}^2)$)

The channel estimation error vector is considered to be a zero-mean random process.

$y_{\hat{z}}^1(i) = \{y_o^1(i)\}^{-1} [W_f^1(i) \hat{z}(i)]$ (Noise component with $N(0, \sigma_{\hat{z}}^2)$)

Since tracking and lag error weight vectors are random, therefore the mean and variance of the component $\{y_o^1(i)\}^{-1} \left\{ \left(W_{f,T}^1(i) + W_{f,L}^1(i) \right) C^1 \bar{h}_1(i) \right\} b_1(i)$ are $N(0, \sigma_{TL}^2 = \sigma_T^2 + \sigma_L^2)$.

$y_{EP}^1(i) = \{y_o^1(i)\}^{-1} \sum_{k=1}^K W_f^1(i) \tilde{C}^k \bar{h}_k(i-1) \{b_k(i-1) - b_{ek}(i-1)\}$ (Error propagation component)

Under worst conditions *i.e.*, $b_k(i-1) = -b_{ek}(i-1)$, the error propagation severely effects the

performance of receiver because $y_{EP}^1(i) = 2\{y_o^1(i)\}^{-1} \sum_{k=1}^K W_f^1(i) \tilde{C}^k \bar{h}_k(i-1) b_k(i-1)$. The cross-

correlation in the signature sequences implicitly randomises the value of $y_{EP}^1(i)$ [38], which is assumed to be a stochastic process with $N(0, \sigma_{EP}^2)$. Therefore, the probability of bit error under worst condition is defined as:

$$\text{Max}\{Pb_e^1\} = Q_G \left(\frac{1}{\sqrt{\sigma_{TL}^2 + \sigma_{MUI}^2 + \sigma_{ES}^2 + \sigma_{\dot{z}}^2 + \sigma_{EP}^2}} \right) \quad (4.49)$$

where, Q_G denotes the complementary unit cumulative Gaussian distribution function. The above equation can be used to derive the conditional probability of bit error for a known channel. However, the equation (4.49) can be averaged for the different channel realizations to calculate the unconditional probability of bit error.

The zero error propagation condition *i.e.*, $b_k(i-1) = b_{ek}(i-1)$ results in $\sigma_{EP}^2 = 0$ and $\min\{Pb_e^1\}$. We have demonstrated analytically in previous sections and verified by computer simulations in next section that the application of the two-step RK-LMS adaptive algorithm reduces the lag noise *i.e.*, $\sigma_{TL}^2 \rightarrow \sigma_T^2$. But the conventional LMS algorithm fails to reduce the lag noise in nonstationary environment. Therefore, it may be inferred that

$$Pb_e^1|_{RK-LMS} < Pb_e^1|_{LMS} .$$

4.6 Simulation results

4.6.1 Performance evaluation of multiuser channel estimator

We shall investigate the behaviour of the proposed RK-LMS algorithm based multiuser channel estimator in the convergence and tracking modes to confirm the analytically derived results. For simulating DS-CDMA system, the Gold-sequences of length $N=31$ are generated. For all the active users, we have considered frequency-selective multipath fading channel. Each Rayleigh channel tap-coefficient is assumed to be time-varying according to $AR(1)$ process (4.17), which does not change during the data symbol transmission period *i.e.*,

$T_s = T_b$. As the sample rate is $R_s = 1/T_b \text{ Hz}$ at the maximum Doppler spread $f_D = v_m f_c / c$, the correlation coefficient is chosen as $a_k = a = J_0(2\pi f_D T_b)$ [101], [154]; where f_c is the carrier frequency, v_m is the relative speed of mobile user *w.r.t.* the position of receiver, c is the velocity of light and $J_0(\cdot)$ denotes the Bessel function of the first-kind and zeroth-order.

Three simulation examples are presented to illustrate the superiority of the proposed adaptive multiuser channel estimator using the RK-LMS algorithm over the conventional LMS algorithm based approach. We have calculated the ensemble average of 150 independent trials. The values of smoothing parameter $\alpha = 0.01$, control parameter $\beta = 0.75$ and step size $\mu = 0.0025$ are kept lower than their maximum bounded values (described in previous sections). These parameters are tuned at their optimum values using the computer simulations. We have considered 20dB signal-to-noise ratio, the carrier frequency $f_c = 2\text{GHz}$ and sample rate $1/T_b = 100\text{kHz}$ ($T_c = 0.3226\mu\text{sec}$) in each of the following examples.

Example 4.1: In this example, we investigate the convergence and tracking performance of the proposed multiuser channel estimator for a four-user system. First, we consider the fading channel with the maximum Doppler spread $f_D = 10\text{Hz}$ (*i.e.*, $v_m = 5.4\text{Km/Hr}$). For the multipath delay spread $T_m = 0.5\mu\text{sec}$, the number of multipaths is $L = (T_m/T_c) + 1 \cong 3$ for each user's transmission channel. Next, we increase the Doppler spread $f_D = 100\text{Hz}$ (*i.e.*, $v_m = 54\text{Km/Hr}$) at the same data symbol rate, which increases the channel variation and consequently results in the high MMSE (as shown in Fig. 4.2). At lower fading rate *i.e.*, $f_D T_b = 0.0001$, the RK-LMS algorithm gives approximately 3dB performance advantage over the conventional LMS algorithm because the RK-LMS algorithm combats the lag noise in tracking mode.

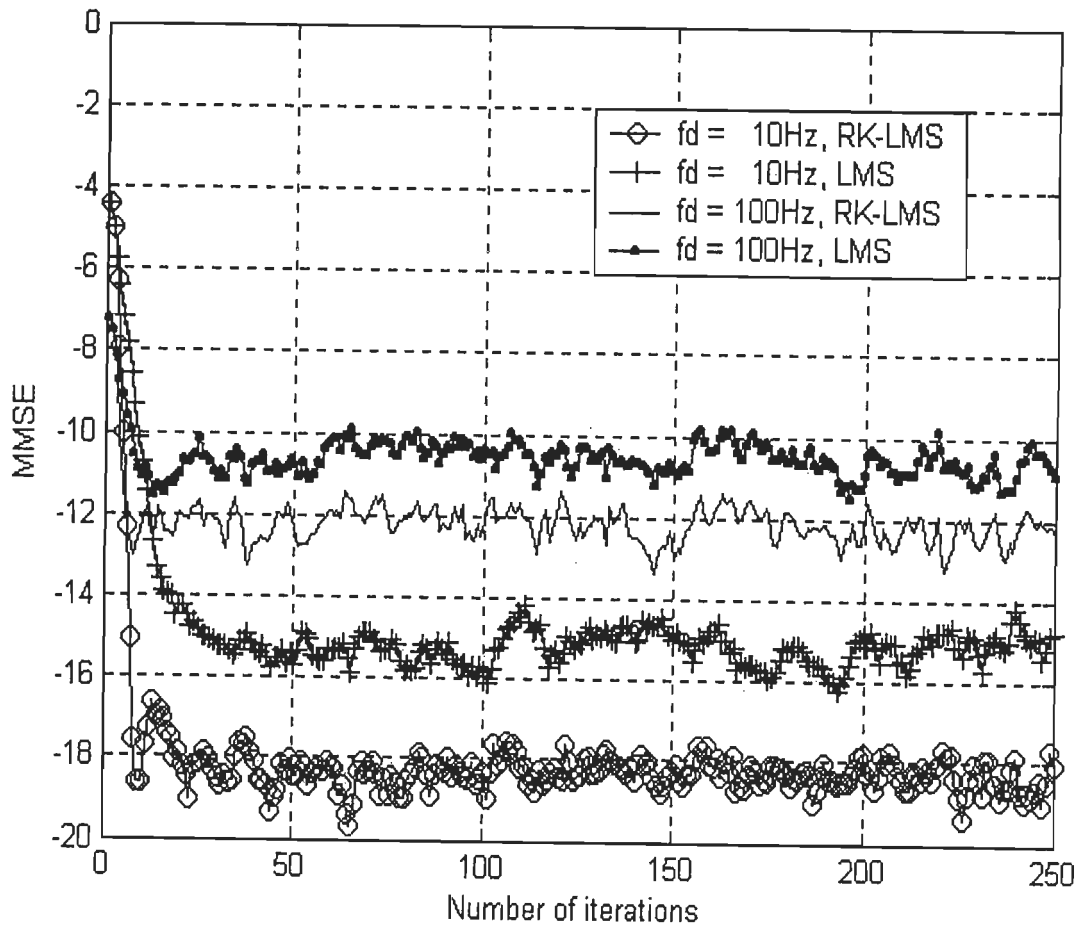


Fig. 4.2: MMSE (dB) vs the number of iterations of RK-LMS algorithm for different values of Doppler frequencies.

However, the performance advantage reduces to approximately 1.5dB for the fading rate $f_D T_b = 0.001$ due to the lag noise. Unlike the G-LMS algorithm [60], the control parameter $\beta < 1$ controls the initial oscillatory behaviour of the RK-LMS algorithm.

Example 4.2: We next consider the performance comparison of the RK-LMS and the conventional LMS algorithm based multiuser channel estimators for different number of active users. In this example, the maximum Doppler spread is $f_D = 50\text{Hz}$ (i.e., $v_m = 27\text{Km/Hr}$). The two different values of the multipath delay spreads $T_m = 0.5\mu\text{sec}$ and $T_m = 1.5\mu\text{sec}$ are considered, which correspond to $L \cong 3$ and $L \cong 6$ respectively. The computer simulation results shown in Fig. 4.3 demonstrate that the performance advantage of the RK-LMS algorithm deteriorates with the increasing number of users. This degradation is due to the presence of residual MAI, which increases with the increasing number of users. Moreover, it may be inferred from Fig. 4.3 that the RK-LMS algorithm gives better performance for three multipaths. For $L \cong 6$, the signal-to-noise ratio per path reduces, which adversely affects the performance of the proposed multiuser channel estimator.

Example 4.3: For a five-user case, we analyse channel tracking performance of the two multiuser channel estimators under the time-varying environment. The Doppler spread is considered to be $f_D = 100\text{Hz}$ (i.e., $v_m = 54\text{Km/Hr}$) with the multipath delay spread $T_m = 0.25\mu\text{sec}$ (i.e., $L \cong 2$). The adaptive channel tracking performance in Fig. 4.4 shows that the channel estimated by using the RK-LMS algorithm is comparable to the true channel. However, the estimated channel coefficient by using the conventional LMS algorithm is lagging behind the true channel coefficient. Both adaptive algorithms use the same step size, but the RK-LMS algorithm based channel estimator supersedes because it removes the lag noise by using the estimated first-order weight increment vector.

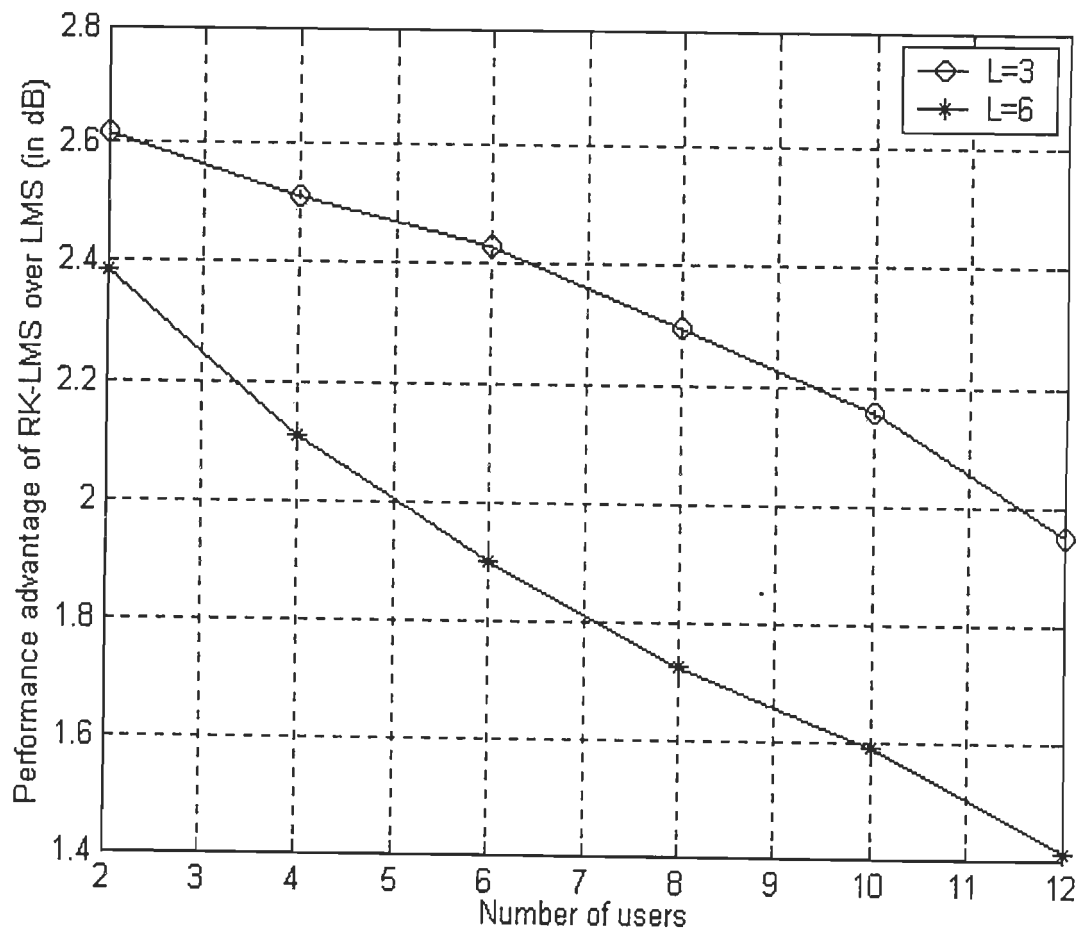


Fig. 4.3: The performance advantage of RK-LMS over the conventional LMS for different number of users.

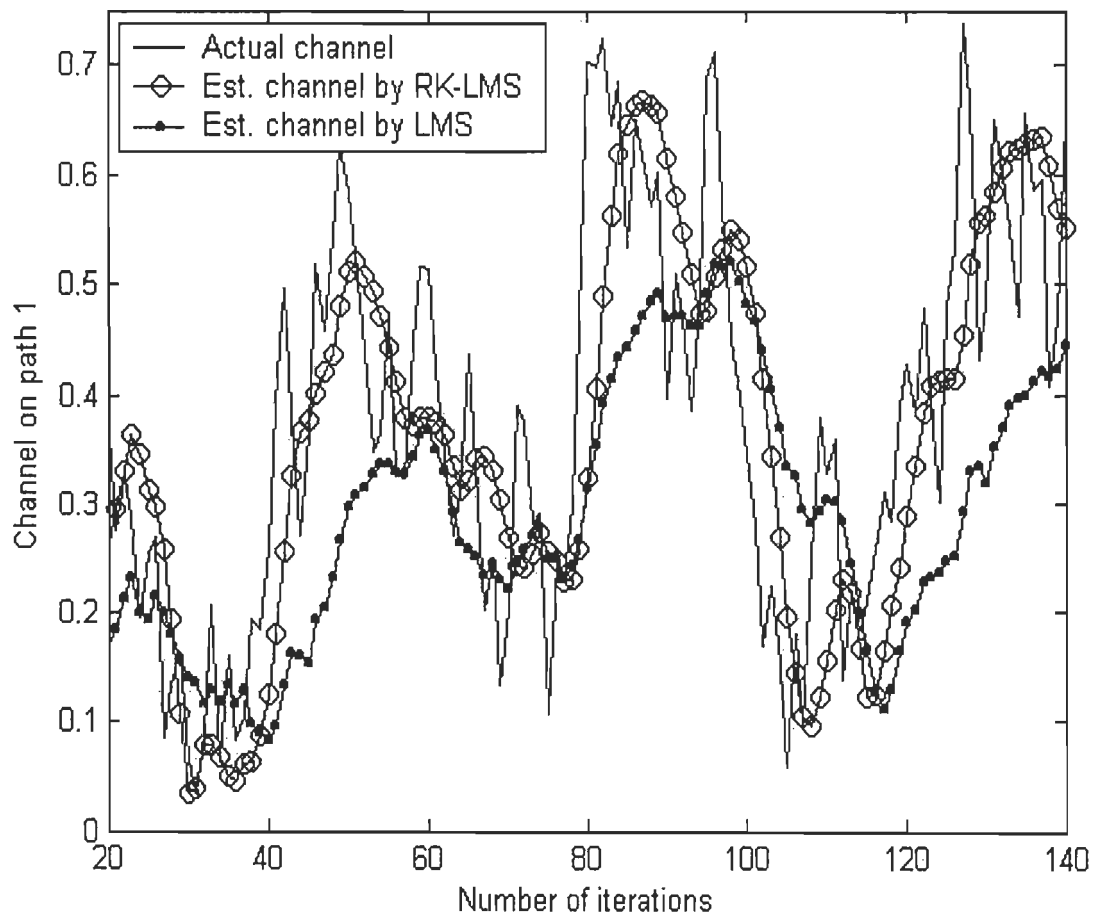


Fig. 4.4: Channel tracking performance of the RK-LMS algorithm.

Moreover, it is observed that we can increase the tracking speed by increasing the value of smoothing parameter, and can also reduce the oscillatory behaviour by reducing the value of control parameter. The channel tracking results shown in Fig. 4.4 are at the optimum values of α , β and μ (as described earlier).

4.6.2 Performance evaluation of adaptive multiuser receiver

We next investigate the performance of the proposed adaptive MMSE DFE multiuser receiver under the time-varying frequency-selective multipath fading channels, which utilizes the estimated channel information in the design of feedback filter (FBF) (as shown in Fig. 4.1). The multiuser channel estimator uses the RK-LMS algorithm and the FBF generates $\hat{r}_{ISI}(i)$ using the estimated channel coefficients. This feedback unit is denoted as FBF (RK-LMS). The feedforward filter of the proposed receiver also uses the RK-LMS algorithm, which is denoted as FFF (RK-LMS). To generate the time-varying environment, the $L \times 1$ dimensional vector $\bar{h}_{k,o}(i)$ is considered to be a smoothly fading mobile communication multipath channel (Rayleigh). The Jakes model is widely accepted as the realistic fading channel model, which is simulated by using $AR(2)$ process [equation (1), 103] as:

$$\bar{h}_{k,o}(i) = -K_1 \bar{h}_{k,o}(i-1) - K_2 \bar{h}_{k,o}(i-2) + U(i) \quad (4.50)$$

where $U(i) = [u_0(i) \ u_1(i) \ \dots \ u_{L-1}(i)]^T$, such that $u_l(i)$ is a complex zero-mean white Gaussian process. The scalar coefficients in the above equation are $K_1 = -2r_d \cos(\sqrt{2}\pi f_D T_b)$ and $K_2 = r_d^2$ (see section 3.4), which take account of the maximum Doppler frequency f_D of the underlying fading channel, sampling time $T_s = T_b$ and pole radius r_d corresponding to the steepness of the peaks of power spectrum. The value of pole radius is given as $r_d = (1 - 2f_D T_b)$ [equation (70), 44].

Three simulation examples are presented to investigate the performance of the proposed

adaptive DFE multiuser receiver, in which we have considered the carrier frequency $f_c = 2GHz$, sample rate $1/T_b = 10kHz$ ($T_c = 3.226\mu sec$), smoothing parameter $\alpha = \hat{\alpha} = 0.01$, control parameter $\beta = \hat{\beta} = 0.75$, step size of the channel estimator $\mu = 0.001$ in (4.21) and step size of the adaptive multiuser receiver $\hat{\mu} = 0.05$ in (4.41). Note that the DFE receiver is switched to the decision directed mode after transmission of 500 training bits. Moreover, the multiuser channel estimation equation (4.12) uses the estimated chip-data-matrix $\hat{D}_e(i) = \hat{C}(i)\hat{B}_e(i)$ in the decision directed mode, where $\hat{B}_e(i)$ is the estimated data-symbol-matrix. We have considered all the active users moving at the same speed. We compare the bit error rate (*BER*) performances of the following six adaptive DFE multiuser receiver configurations using the RK-LMS and the conventional LMS algorithms in the simulation examples.

- i) FFF (LMS) \rightarrow The recursive feedforward filter $W_f(i)$ uses the LMS algorithm. No channel estimator based feedback unit is used to cancel ISI due to the past symbols.
- ii) FFF (LMS), FBF (LMS) \rightarrow The recursive feedforward filter $W_f(i)$ uses the LMS algorithm. The LMS algorithm based channel estimator is used in the feedback unit to cancel ISI due to the past symbols.
- iii) FFF (LMS), FBF (RK-LMS) \rightarrow The recursive feedforward filter $W_f(i)$ uses the LMS algorithm. The RK-LMS algorithm based channel estimator is used in the feedback unit to cancel ISI due to the past symbols.
- iv) FFF (RK-LMS) \rightarrow The recursive feedforward filter $W_f(i)$ uses the RK-LMS algorithm. No channel estimator based feedback unit is used to cancel ISI due to the past symbols.
- v) FFF (RK-LMS), FBF (LMS) \rightarrow The recursive feedforward filter $W_f(i)$ uses the RK-LMS algorithm. The LMS algorithm based channel estimator is used in the feedback

unit to cancel ISI due to the past symbols.

- vi) FFF (RK-LMS), FBF (RK-LMS) → The recursive feedforward filter $W_f(i)$ uses the RK-LMS algorithm. The RK-LMS algorithm based channel estimator is used in the feedback unit to cancel ISI due to the past symbols.

Example 4.4: In this simulation, we analyse the affects of maximum Doppler spread on the performance of the proposed multiuser receiver. The increase in Doppler spread is due to the increasing speed of mobile user (*i.e.*, $v_m = 0.54 \text{ Km/Hr}$ to 5.4 Km/Hr). In the present case, the multipath channel response is time-varying due to the movement of the desired user. The time-varying channel tracking suffers due to the lag noise when LMS algorithm is used (see chapter 3). For a five-user system at $SNR = 20\text{dB}$ and $L = 2$, the results are presented in Fig. 4.5. It is clear that the use of the RK-LMS algorithm in the channel estimator FBF (RK-LMS) improves the performance of multiuser receiver because the channel estimation errors are small. In addition, the incorporation of the RK-LMS algorithm in the FFF leads to better results in comparison to FFF (LMS) as the FFF (RK-LMS) suppresses residual ISI (nonstationarity) in the time-varying environment. As the Doppler spread increases, the *BER* performances of all the proposed configurations degrade due to the inability of LMS algorithm to adapt under the fast time-varying channel. Moreover, the error propagation effect also degrades the performance of non-linear detectors [75]. However, the adaptive receiver using FFF (RK-LMS), FBF (RK-LMS) configuration outperforms the other five configurations (as shown in Fig. 4.5).

Example 4.5: In this example, the effect of increasing number of multipaths *i.e.*, L on the performance of the presented multiuser receiver is analysed. We keep $SNR = 10\text{dB}$ at the Doppler spread $f_D = 1\text{Hz}$ (*i.e.*, $v_m = 0.54 \text{ Km/Hr}$) in a five-user system.

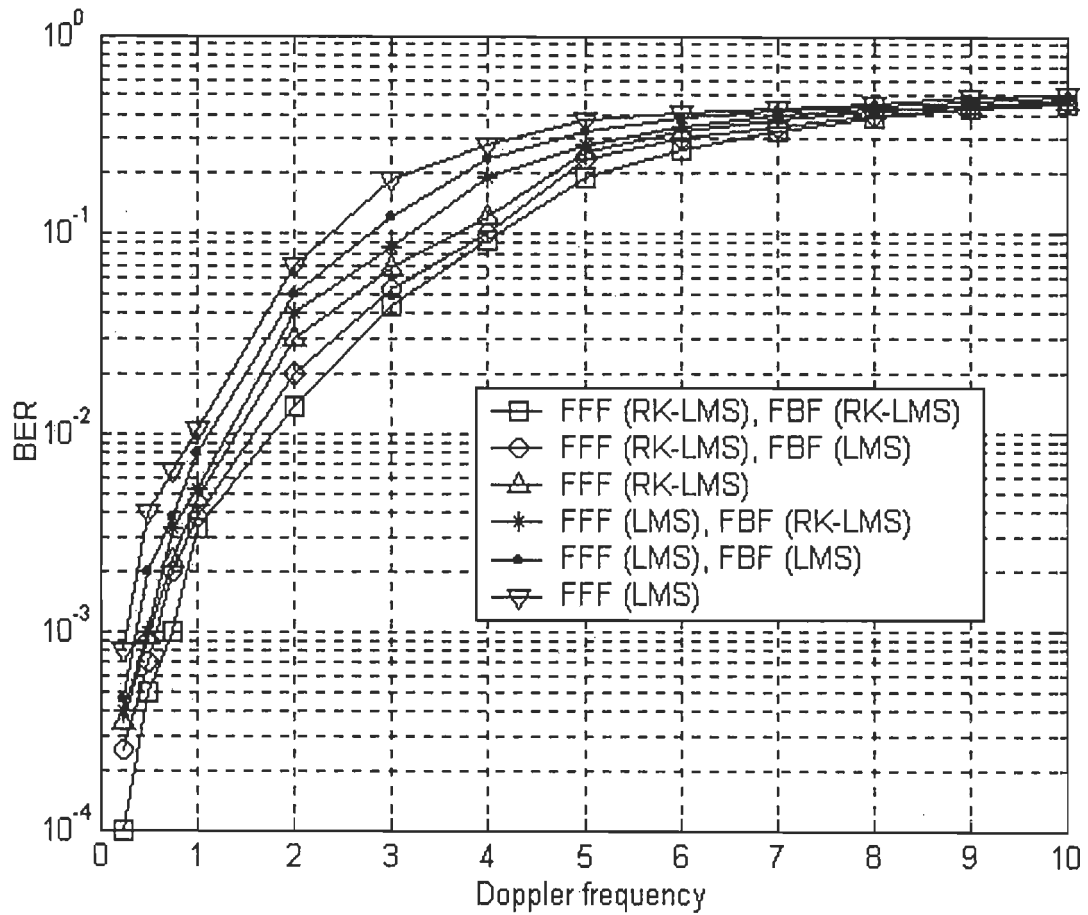


Fig. 4.5: BER of RK-LMS algorithm for different values of Doppler frequencies.

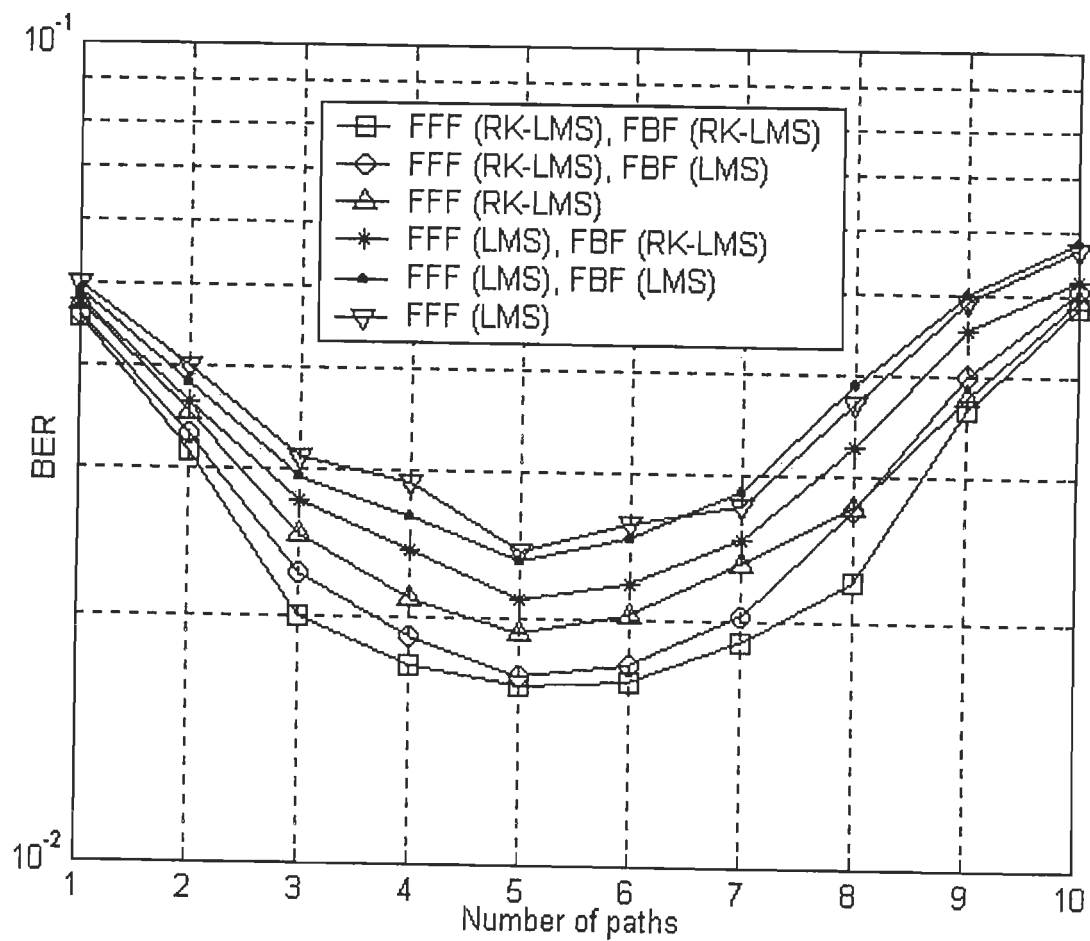


Fig. 4.6: BER vs the number of multipaths for RK-LMS algorithm.

The results presented in Fig. 4.6 show that for a small number of multipaths, the performance of the proposed receiver improves because the FFF of the proposed receiver also works as RAKE [14], and thus improves SNR by providing the diversity gain. However, as the number of paths become large (*i.e.*, SNR per path reduces), the BER performance deteriorates substantially. The observed degradation is due to the increasing magnitude of residual ISI and MAI as the channel estimation errors are large. It is evident from Fig. 4.6 that for a large number of multipaths, the configurations using LMS algorithm for the channel estimation in the feedback unit (as shown in Fig 4.1) *i.e.*, using FBF (LMS) show inferior performance. Therefore, the FFF (RK-LMS), FBF (RK-LMS) configuration for the presented multiuser receiver supersedes the other configurations.

Example 4.6: In this simulation, we investigate the performance of the proposed receiver for the different number of users and for the different values of SNR . We first consider the Doppler spread $f_D = 1Hz$ at $SNR = 15dB$. The multipath delay spread is considered to be $T_m = 5\mu sec$ (*i.e.*, the number of multipaths is $L \cong 3$). The bit error rate increases with the increasing number of users (as shown in Fig. 4.7) because the load factor (*i.e.*, K/N) increases [73], which results in the high magnitude of residual MAI at the output of adaptive FFF. The increase in the magnitude of residual MAI also deteriorates the tracking performance of multiuser channel estimator, which severely affects the BER performance of the presented multiuser receiver due to the presence of channel estimation errors.

We next simulate a four-user system and vary the SNR at the same values of Doppler spread and multipath delay spread. It is clear from Fig. 4.8 that the increase in the value of SNR improves the BER performance of all the multiuser receivers. However at the $BER = 0.006$, the proposed FFF (RK-LMS), FBF (RK-LMS) multiuser receiver provides approximately $3dB$ performance gain over the conventional FFF (LMS) configuration.

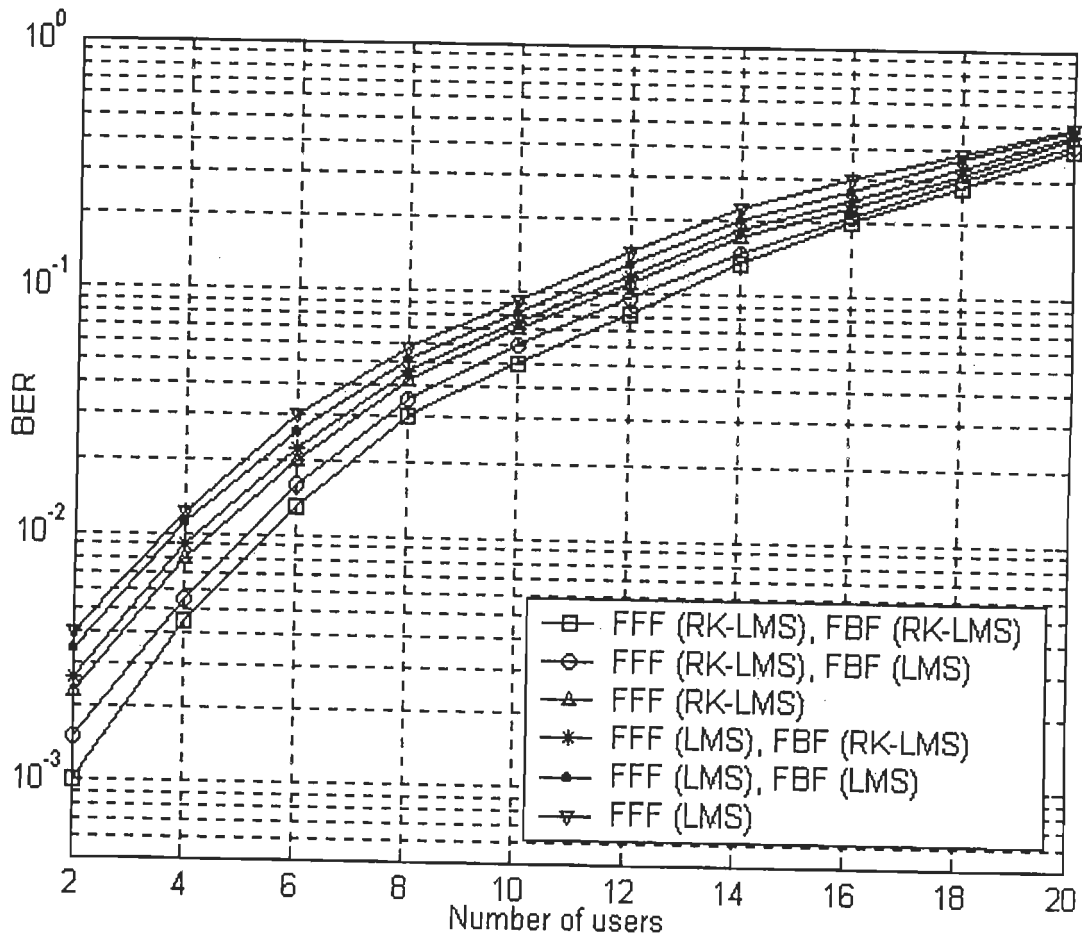


Fig. 4.7: BER vs the number of users for RK-LMS algorithm.

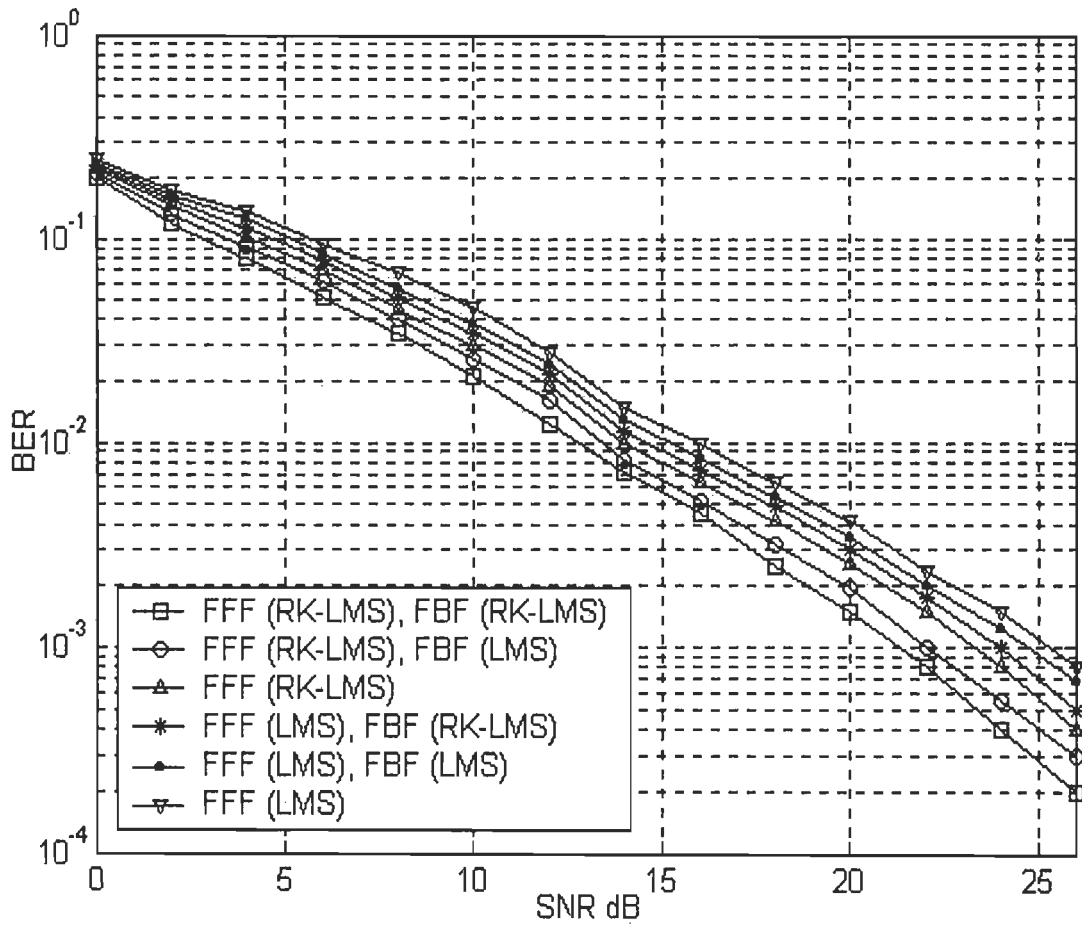


Fig. 4.8: BER vs SNR for RK-LMS algorithm.

From Fig. 4.7 and Fig. 4.8, it may be inferred that the FFF (RK-LMS), FBF (RK-LMS) is the best suited configuration for an adaptive multiuser receiver under the smoothly time-varying fading conditions.

4.7 Concluding remarks

In this chapter, we have presented an adaptive MMSE DFE multiuser receiver using the two-step LMS-type reduced Kalman/LMS algorithm under the frequency-selective smoothly time-varying multipath fading channels. The proposed receiver uses an adaptive multiuser channel estimator to design the feedback filter of DFE. The estimated weight increment matrix is used in the weight update equation to track the time-varying channels. The values of the smoothing parameter, control parameter and step size are kept less than their respective maximum values. The optimum values of these parameters are determined using the computer simulations. We can improve the tracking speed of adaptive channel estimator by increasing the value of α , which in turn enhances the oscillatory behaviour of the RK-LMS algorithm. Since, it has been analytically proved that the reduction in the value of parameter β reduces the amplitude of oscillations. Therefore, the value of β may be reduced to control the instability of the proposed algorithm.

Simulation results show that the performance of the presented multiuser receiver is dependent on the channel estimation errors because the residual ISI adversely affects the *BER* performance. The increasing number of users and the velocities of moving users deteriorate the *BER* performance, as the error propagation effect and the residual interference (ISI and MAI) overwhelm the decision process. For a small number of multipaths, the FFF provides performance advantage by exploiting the multipath diversity. However, the *BER* performance degrades for a large number of multipaths because the *SNR* per path reduces, which results in the high channel estimation errors. The computer simulation results have

evidenced that the performance of FFF (RK-LMS), FBF (RK-LMS) configuration for the proposed adaptive multiuser receiver is superior to the conventional LMS algorithm based configurations.

It is known that the error propagation may severely affect the performance of decision feedback multiuser receivers. In the next chapter, we focus on the error propagation problem arising in the decision feedback structures used to combat ISI and MAI.

ADAPTIVE MULTIUSER DECISION FEEDBACK DETECTORS FOR DS-CDMA SYSTEMS USING PARALLEL INTERFERENCE CANCELLATION APPROACH

Multipath propagation through linear dispersive media introduces intersymbol interference that distorts the wireless transmission and degrades the bit error rate performance of the multiuser systems. In addition to ISI, the non-orthogonal properties of signature sequence waveforms and asynchronism result in the generation of multiple access interference along with AWGN at the multiuser receiver. In DS-CDMA system, the problem of MAI is not only due to the known intra-cell users, but also from the unknown inter-cell users. In such situations, the adaptive non-linear (decision feedback) MMSE techniques [9], [10], [14], [73] are more effective than the linear techniques (without feedback) [38]. However, the error propagation adversely affects the performance of decision feedback multiuser detectors under the low SNR conditions (see [75] and chapter 4).

In this chapter, we first briefly review different schemes to control the error propagation effect in the adaptive decision feedback equalizers in section 5.1. We also review different parallel-interference-cancellation (PIC) techniques used in the adaptive-decision-feedback-detectors (ADFDs) for the efficient multiuser interference cancellation and data detection under the controlled error propagation conditions. Using the multiuser system model described in section 4.2, we introduce an adaptive decision feedback equalizer using the erasure algorithm (E-DFE) with fully connected feedback filter in section 5.2, which also includes details about the proposed erasure algorithm. We next present the DS-CDMA system model in terms of the detected and undetected users, which is used to design the

partial parallel interference canceller in section 5.3. We present an adaptive decision feedback detector based on the parallel interference cancellation approach using the erasure algorithm and channel estimator (EC-ADFD-PIC) in section 5.4. The simulation results are presented in section 5.5 to demonstrate the improved performance of the proposed adaptive E-DFE over the conventional DFE (C-DFE) under the slowly time-varying frequency-selective fading channel. We also provide simulation results on the performance of the proposed adaptive EC-ADFD-PIC. Finally, conclusions are given in section 5.6.

5.1 Introduction

On the forward link of DS-CDMA multiuser system, adaptive decision feedback equalizer is used to detect the desired user by considering MAI as noise [14]. The forward filter of adaptive DFE improves the signal-to-noise ratio, as it performs the function of RAKE. If the received signals are chip asynchronous, then the problem of different timing offsets across the active users can be solved by using the fractional chip sampling along with the use of excess bandwidth [41]. As the information about past detected symbols of all the active users is available at the base station on reverse link, therefore the backward filter of adaptive DFE can be used in fully connected mode to cancel out ISI due to other active intra-cell users (interferers) [10]. However there is a possibility of wrong decisions due to the presence of residual MAI, which leads to error propagation due to the use of decision feedback loop.

Previously, erasures have been introduced in the decision feedback equalizer for the detection of binary pulse-amplitude-modulation (PAM) and quadrature-amplitude-modulation (QAM) signals to reduce the effect of error propagation [79], [80]. In this scheme, a symbol is considered unreliable if the corresponding absolute value of sample at the slicer input is below a pre-determined threshold value. Subsequently, these uncertain symbols are erased in the feedback unit. This erasure process leads to complete loss of the

low amplitude received symbols along with the spurious signals. Moreover, this technique is not directly applicable to the adaptive DFE structures used in the DS-CDMA system because under no power control condition, the absolute value of the residual MAI may dominate the decision process. These drawbacks can be overcome by modifying the non-linear function used in the soft-slicer. In this chapter, we present a novel erasure algorithm based soft-slicer (E-slicer) for adaptive decision feedback equalizer in the DS-CDMA system for interference suppression. However this single-user detection scheme is not beneficial on the reverse link (at the base station), therefore we next focus on the multiuser interference suppression and data detection techniques.

Duel-Hallen has presented two multiuser decision feedback detectors in [109]-[111] *i.e.*, S-DFD (successive-) and P-DFD (parallel-). Previously presented work on MMSE DFDs using the successive interference cancellation scheme in [139] depicts that the total delay involved in the decision process of S-DFD is more in comparison to the P-DFD, which limits the application of the former multiuser detector. In P-DFD, the tentative decisions of K users obtained from the linear MMSE receiver are simultaneously used for the parallel interference cancellation. The tentative decisions may be unreliable due to the overwhelming nature of MAI, which leads to error propagation in the subsequent stages of multistage detector. Divsalar *et al.* have proposed the partial PIC approach in [116], in which the constant partial-cancellation-factors (PCFs) are introduced to cancel a fraction of the estimated interference. The MMSE/PIC decision feedback detector supersedes the linear MMSE detector even for the large values of signature sequence cross-correlation [127]. However, the RLS algorithm based PIC approach used in the non-linear detection results in the high computational complexity [126].

During the last decade, different PIC schemes have been proposed in the literature for the multiuser interference suppression and data detection [116]-[132]. However the simplest

approach is to multiply all the symbol estimates by the constant PCFs less than unity, and subsequently subtract the interference term from the received signal using the PIC scheme. This approach may be modified by using the variable PCFs based on the value of correlator or linear MMSE receiver output. The optimal PCF values are determined either by theoretical analysis under some simplifying assumptions [122], or by using the LMS adaptive algorithm [120]. However the former method is only valid for a small number of users, and the latter adaptive method is not applicable in the fast time-varying multipath fading environment. Using the perfect power control and respreading technique [125], the optimal PCFs can be calculated efficiently online under the known time-varying channel conditions. In the above discussed PICs, the BER performance degradation is observed due to the presence of MAI in the asynchronous DS-CDMA receiver. However the erasure algorithm may be used to generate the variable PCFs depending on the soft-output of multiuser linear filter, which reduces the effects of residual MAI in the decision process.

In BPSK transmission, we transmit chip waveforms at the chip rate in the DS-CDMA wireless systems. At the receiver end, the detection takes place at the data rate. Therefore the intersymbol interference is not only due to the chip waveforms of past data bits, but also due to the chip waveforms of present data bits of all the intra-cell active users. For the asynchronous DS-CDMA system, Ratasuk *et al.* have proposed the P-DFD structure for the slowly time-varying channels, which attempts to cancel all the interference (ISI and MAI) simultaneously [128]. This is an adaptive structure based on embedding the received signal vector in a higher dimensional space. For the known intra-cell users' signature sequences and channel parameters, the filter coefficients are estimated without a training sequence. On the contrary, when channel parameters are unknown, a training sequence is required to estimate the filter coefficients. These estimates have been obtained by minimizing the least-squares cost function. Under the time-varying environment, it is difficult to estimate the covariance

matrix of the received signal vector. Moreover the ill-conditioned covariance matrix introduces numerical problems, and the covariance matrix inversion operation also increases the computational complexity.

It has been shown that the P-DFD consists of a linear MMSE filter followed by an error-estimation filter, in which the lower-diagonal constraint on the feedback filters is removed [129]. The simulation results presented in [129] depict that the error propagation effect severely degrades the performance of P-DFD. In a multiuser system, the detection procedure of a single undetected user has been discussed using the PIC approach. However, adaptive multiuser P-DFD based on partial parallel interference cancellation scheme for the multipath fading channel has not been reported so far in the literature.

In this chapter, we propose two methods for interference cancellation. In the first method, the received signal vector is directly fed to the adaptive decision feedback detector based on the PIC approach (ADFD-PIC), which suppresses noise and interference without the knowledge of spreading signature sequences and the estimated channel response. In the second method, we first estimate the multiuser channel response and then cancel the interference term (due to the past detected data bits) from the received signal vector. The resultant received signal vector is fed to the ADFD-PIC, which considers the residual ISI as noise. The second method may be called the C-ADFD-PIC scheme. Therefore, four different decision feedback configurations with or without the E-slicer are

- i) ADFD-PIC \rightarrow adaptive P-DFD or adaptive decision feedback detector based on the parallel interference cancellation approach.
- ii) E-ADFD-PIC \rightarrow ADFD-PIC using the E-slicer.
- iii) C-ADFD-PIC \rightarrow ADFD-PIC using the channel estimator.
- iv) EC-ADFD-PIC \rightarrow ADFD-PIC using the E-slicer and channel estimator.

In the following, we first propose an adaptive E-DFE for the asynchronous DS-CDMA using a novel erasure algorithm to reduce the effects of error propagation in the non-linear detection techniques. To reduce the possibility of feeding back the wrong decisions, the output of the feedforward filter of the E-DFE is processed before it is fed back to the feedback filter. In addition, the fully connected feedback filter of E-DFE has been used to eliminate ISI due to the intra-cell users. We next propose an ADFD-PIC for the DS-CDMA transmission, which not only combats ISI and MAI but also suppresses the other-cell-interference (OCI). Under the smoothly time-varying multipath fading channels, the presented ADFD-PIC structure is motivated by the work of Ratasuk *et al.* in [128] and [129], which offers significant performance improvement by using the multiuser channel estimator. We also incorporate the erasure algorithm based soft-slicer in C-ADFD-PIC to mitigate the adverse effects of error propagation in the presented non-linear decision feedback technique (EC-ADFD-PIC), which outperforms the hard-slicer based approach and also proves to be beneficial for the inter- and intra-cell interference suppression. Comparison of the performance of C-DFE and E-DFE is presented to show the advantages of the proposed adaptive E-DFE in terms of the reduced average BER performance, under the near-far situations and the sudden change in the signal power of the desired user. The simulation results are also presented to demonstrate the substantial improvement in the BER performance of the proposed MMSE EC-ADFD-PIC over other multiuser detection techniques.

5.2 Adaptive decision feedback equalizer using the erasure algorithm

5.2.1 Adaptive E-DFE structure

At the DS-CDMA receiver, a lowpass filter with bandwidth equal to the chip signal bandwidth is normally used for the demodulation [14] (as shown in Fig. 5.1) as the matched filtering and noise-whitening approach does not give any exclusive benefit [24]. If K active

users are present in the multiuser system as shown in Fig. 2.1, then the equivalent lowpass composite received signal is represented as:

$$\hat{r}(t) = \sum_{k=1}^K \hat{r}_k(t) + \sigma n(t) \quad (5.1)$$

where, $\hat{r}_k(t)$ is the equivalent lowpass signal of k th user and $\sigma n(t)$ is the zero-mean lowpass AWGN due to the presence of receiver thermal noise (as described in section 2.2).

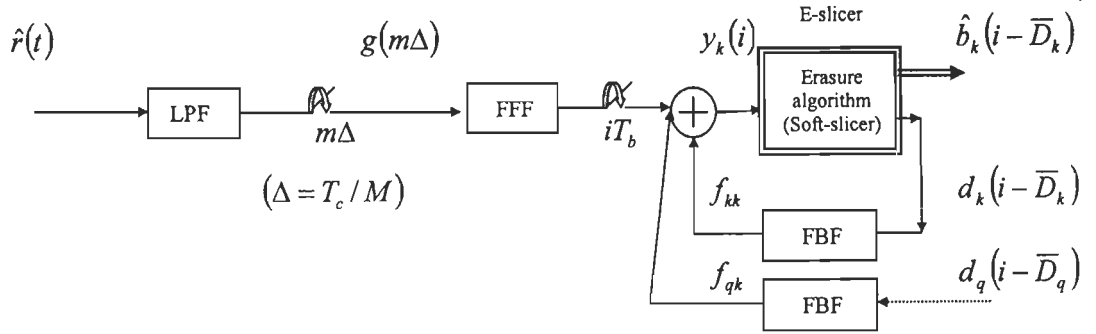


Fig. 5.1: Adaptive E-DFE with fully connected feedback structure for the k th user.

(Only the q th user is considered as the strong interferer)

In the proposed adaptive E-DFE, the received signal $\hat{r}(t)$ is sampled after passing it through a lowpass filter, where M is the number of over-samples used to tackle the problem of asynchronous reception [38], $g(m\Delta)$ is input to the fractionally spaced feedforward filter, such that $\Delta = T_c / M$. The data bit duration is $T_b = NT_c$, where N and T_c are the processing gain and chip duration respectively. The input to the soft-slicer (E-slicer) may be written as:

$$y_k(i) = \sum_{m=0}^{N_{Fk}} F_k^*(m) g(iT_b - m\Delta) - \sum_{h=1}^{N_{fk}} f_{kk}^*(h) d_k(i - h - \bar{D}_k) - \sum_{\substack{q=1 \\ q \neq k}}^K \sum_{h=1}^{N_{fq}} f_{qk}^*(h) d_q(i - h - \bar{D}_q) \quad (5.2)$$

For k th user, $N_{Fk} + 1$ and N_{fk} are the numbers of forward and feedback taps with coefficients F_k and f_{kk} respectively. In addition, N_{fq} is the number of feedback taps with

coefficients f_{qk} used to cancel the intersymbol interference due to q th user. The forward filter acts like RAKE in the adaptive E-DFE and combines the energy of desired user received through different paths [14].

The E-slicer gives two outputs \hat{b}_k and d_k as shown in Fig. 5.1; where \hat{b}_k is the final decision *i.e.* ($-A_k$ or $+A_k$), while its other output d_k is fed back to the respective FBF. It is assumed that \bar{D}_k is the net decision delay in the system. The outputs of soft-slicers of other strong interferers are also fed back to their respective feedback filters (FBF of the q th user is shown in Fig. 5.1). In order to optimize the performance of the adaptive E-DFE receiver, the forward and feedback filter taps are optimized using the minimum mean square error criterion; where the error is defined as:

$$\varepsilon_k = \hat{b}_k - y_k \quad \text{where, } \hat{b}_k = \text{sgn}(y_k) \quad (5.3)$$

Under the practical situations, the C-DFE receiver suffers from the problem of error propagation due to the feedback of wrong decisions. This problem can be controlled by using the erasure algorithm in E-DFE (described in next section), which makes its performance superior in comparison to the conventional DFE.

5.2.2 Erasure algorithm

In the conventional approach, the output of the forward filter of C-DFE is fed to the slicer circuit to decide in favour of $-A_k$ or $+A_k$ (with zero threshold level), which is subsequently fed back to the feedback filter. The slicer circuit can be replaced by a soft-slicer unit, which can erase the decisions with high uncertainty in the feedback unit [79]. In [80], Chiani has presented analytical results for a single-bit memory channel and determined the optimum threshold level ($|\bar{\gamma}_k|$) using computer simulations for different signal-to-noise ratio values. The signals falling below $|\bar{\gamma}_k|$ are erased, which leads to the removal of weak but useful

information signals along with the unreliable signals. Moreover, the adjustment of $|\bar{y}_k|$ becomes a tedious procedure for the long-memory slowly time-varying channels.

But in the proposed erasure algorithm, no such “threshold level determination” procedure is followed. An alternate novel method has been presented to remove the drawbacks of previous erasure technique, in which the E-slicer (as shown in Fig. 5.1) gives appropriate weight to the decision according to the level of uncertainty and erases the highly uncertain decisions.

The adaptive MMSE decision feedback equalizer reduces the mean square error between the actual data bit b_k and its estimate y_k . The first key observation in the conventional adaptive DFE is that if y_k is close to the threshold value (*i.e.*, zero in this case), the corresponding output of the slicer is not reliable. Secondly, when the estimated value $|y_k|$ is close to $|A_k|$, the results of estimation theory [161] can be used to infer that the slicer output is reliable. The increasing distance between the value of $|y_k|$ and $|A_k|$ makes the output of slicer more unreliable. These two facts have been used to design the erasure algorithm, which suggests the possibility of reducing the error propagation by giving appropriate weight to each detected data bit in the feedback loop. The weights are adjusted according to the level of uncertainty in the estimated value y_k . The erasure algorithm can be stated as follows

$$\begin{cases} |y_k| > |2A_k| \text{ or } \left(1 - \frac{|\varepsilon_k|^2}{|A_k|^2}\right) < 0 \longrightarrow w_k = 0 \\ 0 < |y_k| \leq |2A_k| \longrightarrow w_k = \left(1 - \frac{|\varepsilon_k|^2}{|A_k|^2}\right) \end{cases} \quad (5.4)$$

where w_k is the weight, which varies according to the changes in the squared error. If $\varepsilon_k \rightarrow 0$, then the value of assigned weight tends to one (maximum); whereas for $|\varepsilon_k| \rightarrow |A_k|$,

its value approaches zero (minimum). Thus the value of weight is constrained to the limit $[0,1]$. Using the above criterion, the weighted feedback is

$$d_k = w_k \times \hat{b}_k \quad (5.5)$$

The proposed system is coincident with the conventional DFE if we let $w_k = 1$ and becomes the linear equalizer if we fix $w_k = 0$.

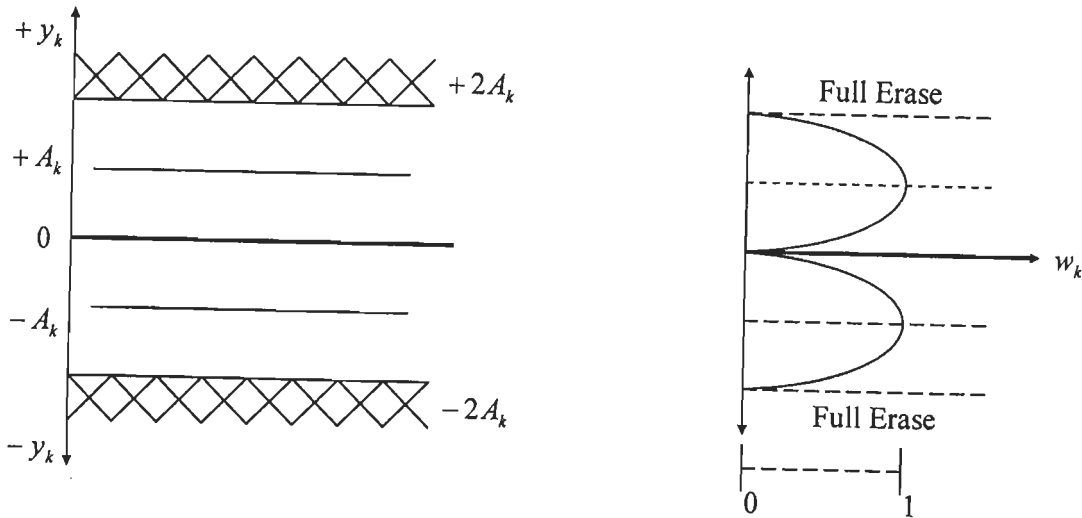


Fig. 5.2: Graphical interpretation of the erasure algorithm for E-DFE.

The graphical interpretation of the above algorithm is shown in Fig. 5.2. It may be inferred that if $|y_k| > |2A_k|$ or $|\varepsilon_k| > |A_k|$, then there is a possibility that the residual MAI dominates the decision process, since the near-far problem is unavoidable in the absence of power control. Therefore, the value of w_k is constrained to zero in this region *i.e.*, the feedback signal is fully erased. It is a well-known fact that the feedback of a wrong decision almost doubles the error in C-DFE. However it is apparent from the erasure algorithm that the assigned weight decreases with the increasing value of error, which proves to be beneficial in reducing the error propagation effect. The resulting single-user detection scheme may be called, “adaptive

MMSE decision feedback equalizer with erasure algorithm”, and has been incorporated in the DS-CDMA receiver for obtaining the performance improvement over C-DFE.

In the next section, we discuss the multiuser system model in terms of the detected and undetected users, which is used to develop a partial parallel interference canceller.

5.3 Partial parallel interference canceller

Using the multiuser system model described in section 4.2, the composite received signal vector (in the discrete-domain) at the base station can be written as:

$$\hat{r}(i) = \sum_{k=1}^K \hat{r}_k(i) + \hat{z}(i) \quad (5.6)$$

where $N \times 1$ dimensional received signal vector corresponding to the k th user's i th data symbol is $\hat{r}_k(i)$, and $\hat{z}(i)$ is the zero-mean additive white Gaussian noise vector. For the multiuser system model under the multipath fading environment [102], we can define the $K \times 1$ dimensional data symbol vector $b(i)$ with binary elements (± 1), $L \times 1$ dimensional channel coefficient vector $\bar{h}_k(i)$, and $N \times L$ dimensional signature sequence matrices C^k , \tilde{C}^k as:

$$b(i) = [b_1(i) \ b_2(i) \ \dots \ b_K(i)]^T, \quad \bar{h}_k(i) = [h_{0k}(i) \ h_{1k}(i) \ \dots \ h_{(L-1)k}(i)]^T, \text{ and}$$

$$C^k = \begin{bmatrix} c_0^k & \dots & 0 \\ c_1^k & \dots & 0 \\ \vdots & \dots & \vdots \\ c_{N-1}^k & \dots & c_{N-L}^k \end{bmatrix}, \quad \tilde{C}^k = \begin{bmatrix} 0 & c_{N-1}^k & c_{N-L+1}^k \\ 0 & 0 & \vdots \\ \vdots & \vdots & c_{N-1}^k \\ \vdots & \vdots & \vdots \\ 0 & 0 & \dots & 0 \end{bmatrix}$$

where c_j^k is the j th chip ($\pm 1/\sqrt{N}$) in the signature sequence of k th user, and the number of multipaths L is considered equal for all the active users. The fading coefficient $h_{lk}(i)$ is considered to be $AR(2)$ *i.e.*, second-order autoregressive process varying at the data rate. It

can be shown that the data symbol detection equation is

$$\hat{r}(i) = C(i)H(i)b(i) + \tilde{C}(i)H(i-1)b(i-1) + \hat{z}(i) \quad (5.7)$$

where $b(i) = [b_1(i) \ b_2(i) \ \dots \ b_K(i)]^T$ is a $K \times 1$ dimensional vector,

$H(i) = \text{diag}[\bar{h}_1(i), \bar{h}_2(i), \dots, \bar{h}_K(i)]$ is a $KL \times K$ dimensional matrix,

$C(i) = [C^1 \ C^2 \ \dots \ C^K]$ and $\tilde{C}(i) = [\tilde{C}^1 \ \tilde{C}^2 \ \dots \ \tilde{C}^K]$ are the $N \times KL$ dimensional matrices.

Further, we can divide all the active users (in a particular cell) into two sets of the detected 'D' and the undetected 'U = K - D' users respectively [129], which results in

$$C(i) = [C^D(i) \parallel C^U(i)] \quad (5.8)$$

where, $C^D(i) = [C^1 \ C^2 \ \dots \ C^D]$ and $C^U(i) = [C^{D+1} \ C^{D+2} \ \dots \ C^K]$. Similarly, the multiuser channel coefficient matrix may be written as:

$$H(i) = \text{diag}[H^D(i), H^U(i)] \quad (5.9)$$

where, $H^D(i) = \text{diag}[\bar{h}_1(i), \bar{h}_2(i), \dots, \bar{h}_D(i)]$ and $H^U(i) = \text{diag}[\bar{h}_{D+1}(i), \bar{h}_{D+2}(i), \dots, \bar{h}_K(i)]$.

The data bit vector is written as:

$$b(i) = [b^{DT}(i) \parallel b^{UT}(i)]^T \quad (5.10)$$

where, $b^D(i) = [b_1(i) \ b_2(i) \ \dots \ b_D(i)]^T$ and $b^U(i) = [b_{D+1}(i) \ b_{D+2}(i) \ \dots \ b_K(i)]^T$. The substitution of (5.8)-(5.10) in (5.7) leads to

$$\hat{r}(i) = C^D(i)H^D(i)b^D(i) + C^U(i)H^U(i)b^U(i) + \tilde{C}(i)H(i-1)b(i-1) + \hat{z}(i) \quad (5.11)$$

The first two terms on the right hand side of above equation include not only the desired signal but also ISI due to the chip waveforms of present data bits of active users. In addition, the third term is ISI due to the chip waveforms of past data bits. We next present details about the MMSE multiuser P-DFD receiver design, which uses the estimated multiuser channel response $H(i|i)$ to suppress ISI.

Let the input vector to the decision device be $\hat{y}(i) = [\hat{y}^1(i) \hat{y}^2(i) \dots \hat{y}^K(i)]^T$ and the corresponding estimated data symbol vector at the slicer output is $b_e(i) = [b_{e1}(i) b_{e2}(i) \dots b_{eK}(i)]^T$. If the past decisions and channel estimates of all the active users are available at the receiver end, the intersymbol interference due to the previous data symbols can be cancelled as:

$$\hat{r}_{eq}(i) = \hat{r}(i) - \hat{r}_{ISI}(i) \quad \text{with } \hat{r}_{ISI}(i) = \tilde{C}(i)H(i-1|i-1)b_e(i-1) \quad (5.12)$$

Under no error propagation condition in the decision feedback loop *i.e.*, $b_e(i-1) = b(i-1)$, the above equation may be written as:

$$\hat{r}_{eq}(i) = C^D(i)H^D(i)b^D(i) + C^U(i)H^U(i)b^U(i) - \tilde{C}(i)\Delta H(i-1)b(i-1) + \hat{z}(i) \quad (5.13)$$

where, the channel estimation error is $\Delta H(i-1) = H(i-1|i-1) - H(i-1)$. For simplification, we assume zero channel estimation error. It follows that

$$\hat{r}_{eq}(i) = C^D(i)H^D(i)b^D(i) + C^U(i)H^U(i)b^U(i) + \hat{z}(i) \quad (5.14a)$$

$$= C(i)H(i)b(i) + \hat{z}(i) \quad (5.14b)$$

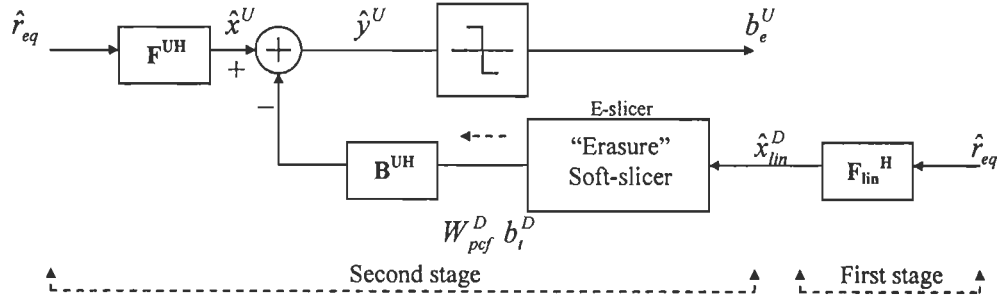


Fig. 5.3: Partial parallel interference cancellation using the E-slicer.

Let us assume that the present data bit tentative decisions of D users (strong) are $b_i^D(i) = [b_{i1}(i) b_{i2}(i) \dots b_{iD}(i)]^T$, as shown in Fig. 5.3. The soft-output of $N \times D$ dimensional

MMSE multiuser linear detector (F_{lin}) *i.e.*, $\hat{x}_{lin}^D(i) = [\hat{x}_{lin,1}(i) \hat{x}_{lin,2}(i) \dots \hat{x}_{lin,D}(i)]^T$ is fed to the E-slicer to generate $W_{pcf}^D b_i^D$. The $D \times D$ dimensional partial cancellation factor matrix is defined as $W_{pcf}^D(i) = \text{diag}[w_{pcf}^1(i), w_{pcf}^2(i), \dots, w_{pcf}^D(i)]$, where w_{pcf}^k is the PCF assigned to the tentative decision of k th detected user. Using (5.14a) in this decision feedback detection structure, the input to slicer for the i th data symbol is

$$\hat{y}^U(i) = F^{UH}(i)\hat{r}_{eq}(i) - B^{UH}(i)[W_{pcf}^D(i)b_i^D(i)] \quad (5.15)$$

where, F^U and B^U are the $N \times U$ dimensional feedforward and the $D \times U$ dimensional feedback matrices respectively. Since all the PCF values are real, therefore $W_{pcf}^D = W_{pcf}^{DH}$. We assume that all the tentative decisions of detected users are correct *i.e.*, $b_i^D(i) = b^D(i)$. The above equation may be rewritten as:

$$\hat{y}^U(i) = F^{UH}(i)\hat{r}_{eq}(i) - B_w^{UH}(i)b^D(i) \quad \text{with } B^{UH}W_{pcf}^{DH} = B_w^{UH} \quad (5.16)$$

The $U \times 1$ dimensional error vector at the DFD output is $e_{dfa}^U(i) = b^U(i) - \hat{y}^U(i)$. The corresponding error covariance matrix of the undetected users is defined as:

$$\Gamma_{dfa}^U(i) = E[e_{dfa}^U(i)e_{dfa}^{UH}(i)] \quad (5.17)$$

The cost function *i.e.*, $J_{dfa}^U(i)$ is defined as the trace of matrix $\Gamma_{dfa}^U(i)$. The optimum MMSE DFD is derived by minimizing the scalar cost function. Using the partial derivatives

$$\frac{\partial J_{dfa}^U(i)}{\partial F^U} = 0 \quad \text{and} \quad \frac{\partial J_{dfa}^U(i)}{\partial B^U} = 0, \quad \text{we obtain}$$

$$R_{eq}F^U(i) - C^U(i)H^U(i) - C^D(i)H^D(i)W_{pcf}^{DH}(i)B^U(i) = 0$$

This leads to the optimum solution as:

$$F^U(i) = [R_U + R_z]^{-1}C^U(i)H^U(i) \quad \text{with } R_z = E[\hat{z}(i)\hat{z}^H(i)] \quad (5.18)$$

$$\text{and } C^D(i)H^D(i)W_{pcf}^{DH}B^U(i) = R_D F^U(i) \quad (5.19a)$$

The above equation can be simplified to give

$$B_w^U(i) = W_{perf}(i)B^U(i) = H^{DH}(i)C^{DH}(i)F^U(i) \quad (5.19b)$$

where, the covariance matrix of the input signal vector $\hat{r}_{eq}(i)$ is defined as

$$R_{eq} = E[\hat{r}_{eq}(i)\hat{r}_{eq}^H(i)] = R_D + R_U + R_z. \text{ The covariance matrices corresponding to the detected}$$

users, undetected users and noise vector are R_D , R_U and R_z respectively.

We consider the case of a single undetected k th user in a particular cell *i.e.*, set of undetected users $U = \{k\}$ and set of detected users $D = \{1, 2, \dots, k-1, k+1, \dots, K\}$. Using (5.18) and (5.19b), the optimum feedforward and feedback matrices may be written as:

$$F^k(i) = [R_k + R_z]^{-1} C^k \bar{h}_k(i) \quad (5.20)$$

$$B_w^k(i) = H^{DH}(i)C^{DH}(i)F^k(i) \quad (5.21)$$

The above results for a single undetected user are used in the next section for deriving the adaptive multiuser P-DFD structure for the multiuser interference suppression and data detection on the reverse link in mobile communication systems.

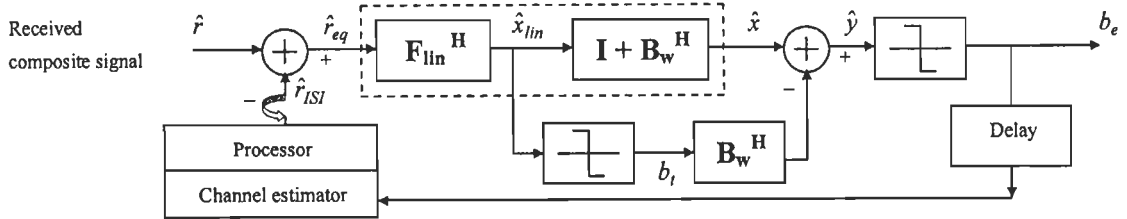


Fig. 5.4: Block diagram of the proposed channel estimator based DFD using the PIC approach.

5.4 Adaptive multiuser EC-ADFD-PIC

The block diagram shown in Fig. 5.4 represents the proposed channel estimator based DFD using the PIC approach. Its equivalent structure (P-DFD using the E-slicer) is shown in Fig.

5.5, where F and B denote the $N \times K$ dimensional feedforward and the $K \times K$ dimensional feedback matrices respectively. The $K \times 1$ dimensional vectors \hat{x}_{lin} , b_t and \hat{y} in Fig. 5.4 are the soft-output of MMSE linear multiuser receiver (F_{lin}), tentative decisions and input to the slicer respectively. The \hat{x}_{lin} is fed to the E-slicer to generate the real PCF matrix (see appendix C) *i.e.*, $W_{pcf}(i) = \text{diag}[w_{pcf}^1(i), w_{pcf}^2(i), \dots, w_{pcf}^K(i)]$.

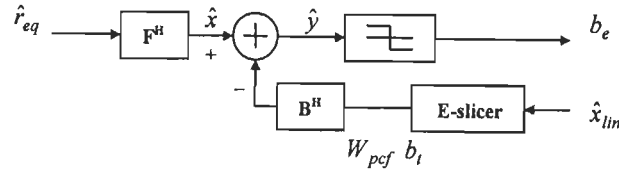


Fig. 5.5: P-DFD using the E-slicer.

From Fig. 5.5, it may be seen that the input to the decision device is

$$\hat{y}(i) = F^H(i)\hat{r}_{eq}(i) - B^H(i)[W_{pcf}(i)b_t(i)] \quad \text{where, } W_{pcf}(i) = W_{pcf}^H(i) \quad (5.22a)$$

$$\hat{y}(i) = F^H(i)\hat{r}_{eq}(i) - B_w^H(i)b_t(i) \quad \text{where, } B_w(i) = B(i)W_{pcf}(i) \quad (5.22b)$$

The $K \times 1$ dimensional error vector at the output of DFD is $e_{dfd}^F(i) = b_e(i) - \hat{y}(i)$ with the error covariance matrix $\Gamma_{dfd}^F(i) = E[e_{dfd}^F(i)e_{dfd}^{FH}(i)]$. The optimum feedforward and feedback filters are derived by minimizing the trace of $\Gamma_{dfd}^F(i)$ *w.r.t.* $F(i)$ and $B(i)$ using the MMSE criterion, and are given as:

$$F(i) = F_{lin}(i)[I_K + B_w(i)] \quad \text{with } F_{lin}(i) = [R_{eq}]^{-1}C(i)H(i) \quad (5.23)$$

$$B_w(i) = [H^H(i)C^H(i)C(i)H(i)]^{-1}H^H(i)C^H(i)R_{eq}F(i) - I_K \quad (5.24)$$

where, $R_{eq} = E[\hat{r}_{eq}(i)\hat{r}_{eq}^H(i)]$ is the $N \times N$ dimensional covariance matrix of the input signal vector and I_K is the $K \times K$ dimensional identity matrix. It may be inferred from (5.23) that the optimum forward filter is a concatenation of the linear MMSE filter $F_{lin}(i)$ and the error-

estimation filter $[I_K + B_w(i)]$ (as shown in Fig. 5.4). Since each column of $F(i)$ represents the weight vector corresponding to a particular user, therefore we can use the single-user forward filter $F^k(i)$ (5.20) to obtain the optimum feedforward filter as $F(i) = [F^1(i) F^2(i) \dots F^K(i)]$ (see [129]). The implementation of P-DFD requires the estimation of covariance matrix R_{eq} , which is usually difficult to compute in the time-varying environment. Therefore in EC-ADFD-PIC, we obtain filter coefficients by using the LMS adaptive algorithm as:

$$F_{lin}(i+1) = F_{lin}(i) + \mu \hat{r}_{eq}^H(i) e_{lin}^H(i) \quad \text{with step size } \mu \quad (5.25)$$

where, $e_{lin}(i) = b(i) - \hat{x}_{lin}(i)$ in the training mode. For the single-user detection scenario, the input to decision device is

$$\hat{y}^k(i) = \tilde{F}^{kH}(i) \hat{r}_{dfe}^k(i) \quad (5.26)$$

with $\tilde{F}^k(i) = [F^{kT}(i) \quad -\tilde{B}^{kT}(i)]^T$, $\hat{r}_{dfe}^k(i) = [\hat{r}_{eq}^T(i) [W_{pcf}^D(i) b_i^D(i)]]^T$ and $e_{dfe}^k(i) = b_{ik}(i) - \hat{y}^k(i)$ in the decision directed mode; where the $(K-1) \times (K-1)$ dimensional matrix W_{pcf}^D and the $(K-1) \times 1$ dimensional vector b_i^D are obtained by eliminating the k th element from W_{pcf} and b_i respectively. The $(K-1) \times 1$ dimensional output vector of the E-slicer is pumped into the $(K-1) \times 1$ dimensional single-user feedback filter $\tilde{B}^k(i)$. It follows that

$$\tilde{F}^k(i+1) = \tilde{F}^k(i) + \mu \hat{r}_{dfe}^k(i) e_{dfe}^{k*}(i) \quad (5.27)$$

The single-user forward filter $F^k(i)$, which is the k th column of $F(i)$, is obtained by using the first N elements of $\tilde{F}^k(i)$. Using the Moore-Penrose pseudo-inverse of matrix F_{lin} [162], the equation (5.24) may be rearranged as:

$$B_w(i) = [F_{lin}^H(i) F_{lin}(i)]^{-1} F_{lin}^H(i) F(i) - I_K \quad (5.28)$$

The feedback matrix $B_w(i)$ is obtained by substituting $F_{lin}(i)$ and $F(i)$ in (5.28). The estimation of R_{eq} is not required in the implementation of the presented EC-ADFD-PIC. It is

apparent that the linear filter F_{lin} partially cancels interference and noise. However, the feedback filter B_w suppresses the residual interference.

5.6 Simulation results

5.6.1 Performance evaluation of adaptive E-DFE

Three simulation examples are presented to illustrate the superiority of the proposed adaptive E-DFE over C-DFE. For simulating the asynchronous DS-CDMA system, the Gold-sequences of length $N = 31$ are generated. The square-root raised-cosine pulses are used for the transmission of information over a dispersive channel. For the k th desired user, we have considered frequency-selective multipath fading channel with $L = 3$ (number of taps), and the channel tap-coefficients do not change during the data bit transmission period because these tap-coefficients are assumed to be slowly time-varying. In all the examples, the number of forward filter taps is fixed at $N_{zk} = 3N$ and the number of feedback filter taps is two *i.e.*, $N_{jk} = N_{jq} = \dots = 2$. The NLMS adaptive algorithm has been used to update the coefficients of forward and feedback filter taps of the decision feedback equalizers *i.e.*, C-DFE and E-DFE.

Since we are implementing the adaptive DFE structures for the data detection and interference cancellation, therefore no power control scheme has been used. In the following examples, we have taken the ensemble average of 200 independent trials, and each DFE is switched to the decision directed mode after the transmission of 500 training bits.

Example 5.1: In this example, we investigate the influence of sudden changes in the signal-to-noise ratio of the desired user on the *BER* performance of the proposed adaptive E-DFE. Because under this situation, there is a strong likelihood that the wrong decisions will be fed back. In a five-user system, the signal-to-noise ratios of the desired user and other intra-cell users are kept at $25dB$ and $5dB$. After the transmission of 5000 data bits, the weight vector

of adaptive filter is assumed to be set at its optimum value. The SNR of the desired user is next changed to $5dB$. This change results in the high mean square error for C-DFE as compared to the E-DFE, which is clearly shown in Fig. 5.6. This is due to the error propagation in the conventional DFE, but this disadvantage has been controlled by the use of erasure algorithm in E-DFE.

Example 5.2: We next consider the performance comparison of C-DFE and E-DFE, when the number of active users changes. For analysing the behaviour of E-DFE, we have kept SNR for all the active users equal to $10dB$. The computer simulation results shown in Fig. 5.7 demonstrate that for both equalizers, the bit error rate increases with the increasing value of K/N ratio *i.e.*, load factor [73].

For a single-user situation, the maximum performance advantage of the proposed adaptive E-DFE over C-DFE is obtained as the erasure algorithm reduces the error propagation effect. As the number of users increases, this performance gap reduces gradually. The reason for this observed degradation is that the increasing value of load factor in the asynchronous DS-CDMA system results in the increase of residual MAI, which deteriorates the BER performance of both equalizers. But, it is observed that the E-DFE still outperforms the C-DFE when the number of users is $K \leq 20$. However for $K > 20$ (*i.e.*, load factor > 0.645), the residual MAI limits the BER performance of the multiuser system. Consequently, the adaptive E-DFE performs marginally better than the C-DFE for a large number of active users.

Example 5.3: For an eight-user case, the near-far situation is introduced in the DS-CDMA system by keeping other active interferers at 20% higher power level than the desired user. The BER performance improvement has been observed for both equalizers with the increasing value of SNR (as shown in Fig. 5.8).

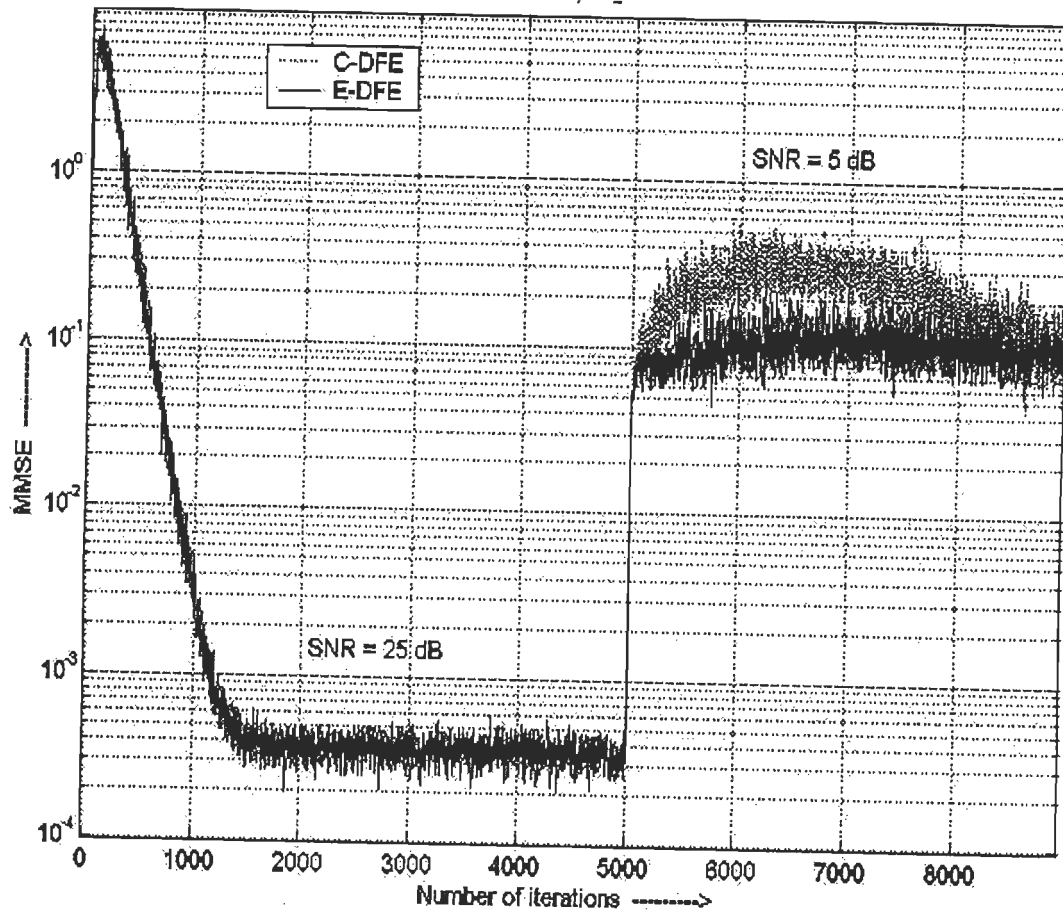


Fig. 5.6: MMSE (dB) vs the number of iterations for adaptive E-DFE, $K = 5$.

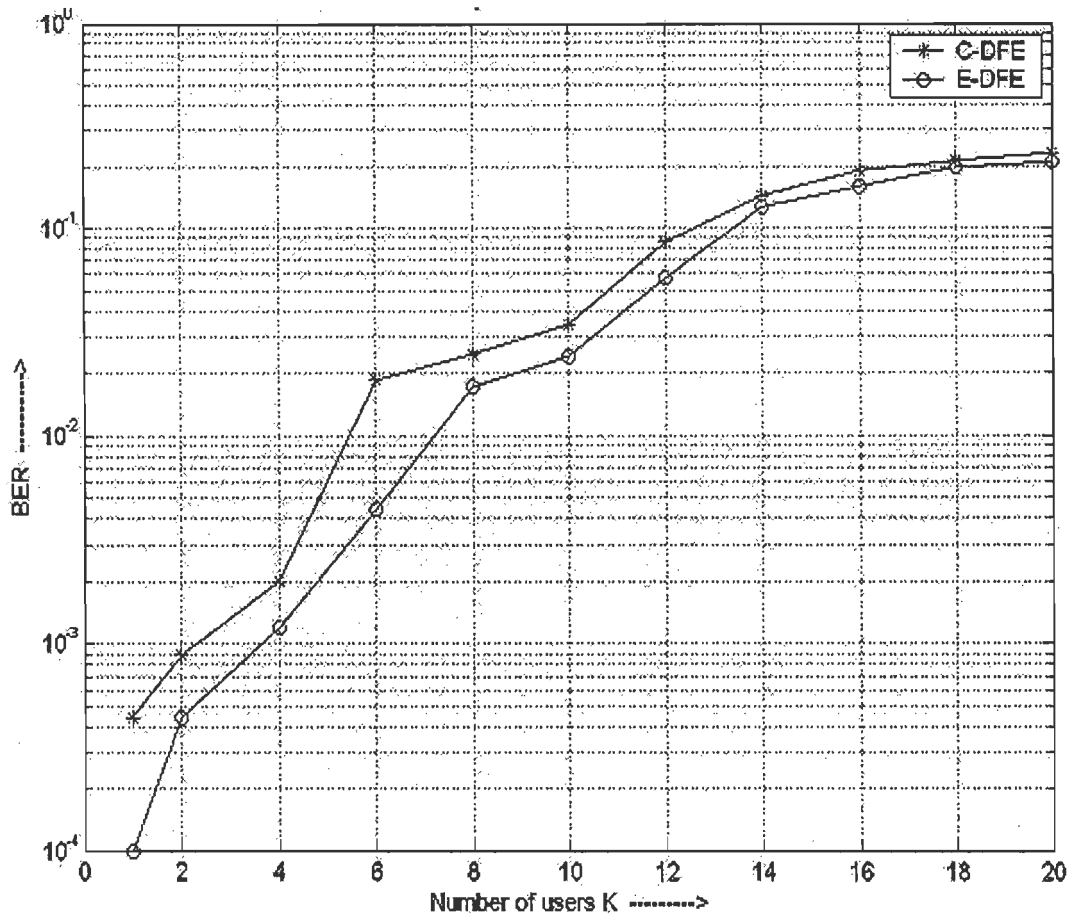


Fig. 5.7: BER vs the number of users for adaptive E-DFE.

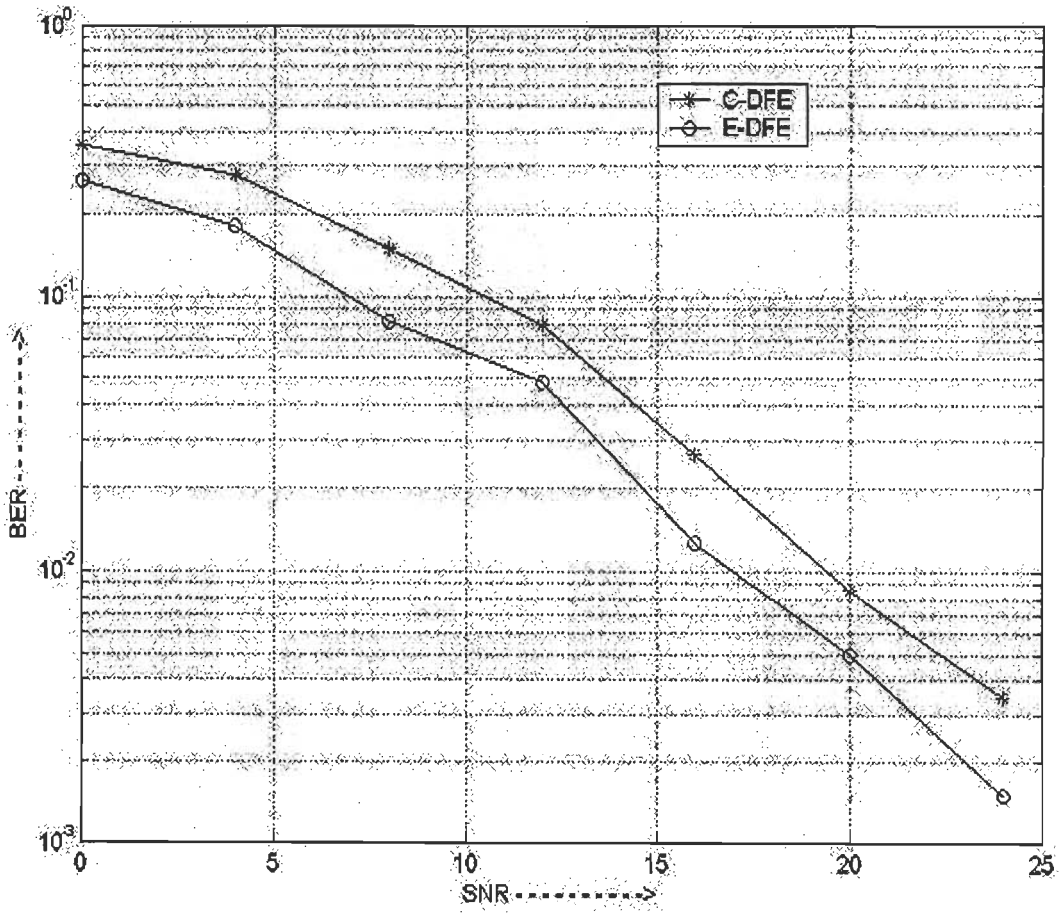


Fig. 5.8: BER vs the signal-to-noise ratio (dB) of the desired user for adaptive E-DFE.

The simulation results at the different values of SNR of the desired user have evidenced that the bit error rate increases under the near-far situation, but the proposed adaptive E-DFE supersedes the conventional equalizer because the error propagation severely affects the performance of C-DFE. At $BER = 0.01$, E-DFE provides approximately $2.5dB$ performance gain over the conventional DFE.

5.6.2 Performance evaluation of adaptive EC-ADFD-PIC

We shall investigate the performance of the proposed EC-ADFD-PIC under the frequency-selective smoothly time-varying fading channels. The $L \times 1$ dimensional channel coefficient vector $\bar{h}_k(i)$ is considered to be a smoothly fading multipath channel (Rayleigh), which is simulated by using the second-order autoregressive process (see subsection 4.6.2). We have used the LMS adaptive algorithm to update the filter coefficients.

Two simulation examples are presented, in which we have considered the carrier frequency $f_c = 2GHz$, sample rate $1/T_b = 10kHz$ ($T_c = 3.226\mu sec$) and step size $\mu = 0.01$. In the training mode, we consider $b_i(i) = b_e(i) = b(i)$. Note that the DFD is switched to the decision directed mode after the transmission of 500 training bits. For the multipath delay spread $T_m = 9\mu sec$, the number of multipaths is $L = (T_m/T_c) + 1 \cong 4$ for each user's transmission channel. We consider the maximum Doppler spread $f_D = 1Hz$ for all the active users. No power control scheme has been used.

We propose two methods to cancel ISI due to the past data bits of K active users. In the first method, we directly feed the received composite signal vector to ADFD-PIC *i.e.*, $\hat{r} = \hat{r}_{eq}$. However in the second method, we estimate the ISI term \hat{r}_{ISI} using the multiuser channel estimator, and then cancel the intersymbol interference from the received composite signal vector before feeding it to ADFD-PIC (as shown in Fig. 5.4). We compare the BER performances of both methods by using the E-slicer in the following examples. The presented

results are based on an ensemble average of 150 independent simulation runs. We have shown the average bit error rate for each detector, which is defined as $BER = \sum_{k=1}^K BER_k / K$.

Example 5.4: In this simulation, the effects of signal-to-noise ratio on the performance of the proposed ADFD-PICs are analysed. For a four-user system, the results shown in Fig. 5.9 depict that the BER reduces with the increasing value of SNR. The effects of other-cell interference are observed by considering the two inter-cell interferers (with $L = 4$ and $f_D = 1Hz$). The BER performance of all the multiuser detectors degrades. However, the EC-ADFD-PIC outperforms other detectors with and without inter-cell interferers. It may be inferred from the results presented in [128] that the P-DFD offers approximately $2dB$ gain relative to the linear receiver. However at $BER = 0.04$, the proposed EC-ADFD-PIC provides approximately $3dB$ performance gain over the linear MMSE receiver in the smoothly time-varying environment.

Example 5.5: For a four-user system, we analyse the effects of maximum Doppler spread on the performance of the proposed multiuser receiver. In this case, the maximum Doppler spread is varied up to $f_D = 5Hz$ at $SNR = 6dB$. The simulation results presented in Fig. 5.10 show that the bit error rate substantially increases with the increasing value of f_D . Therefore, the proposed technique is valid for the slow moving mobile users. This performance degradation is due to the incorporation of LMS algorithm in the presented ADFD-PIC, which does not adapt in the fast fading environment (see chapter 4). However, the EC-ADFD-PIC outperforms other detectors in the time-varying environment.

We next increase SNR to $15dB$ and observe the effects of increasing number of users. The application of the MMSE multiuser linear detector is limited to a specific range of loads *i.e.*, $K/N < 70\%$ [73].

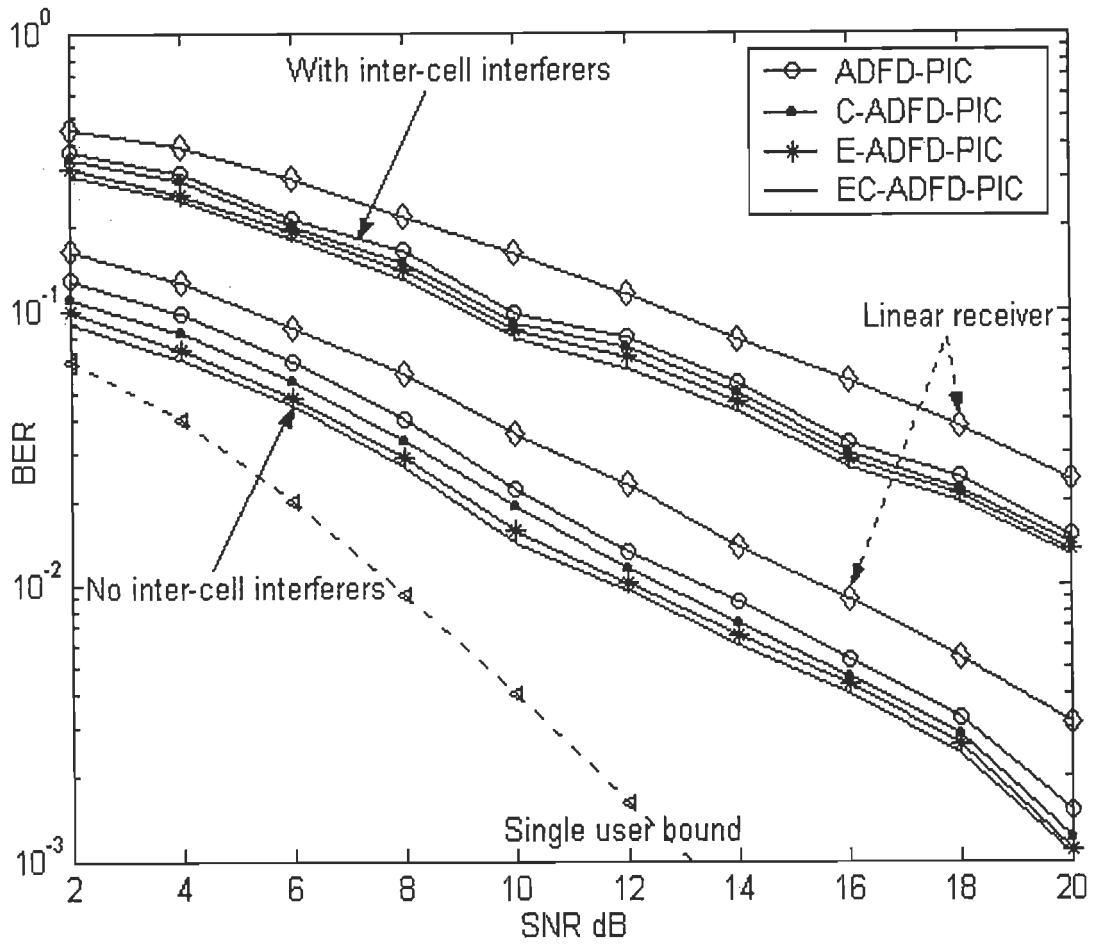


Fig. 5.9: BER vs SNR for adaptive EC-ADFD-PIC.

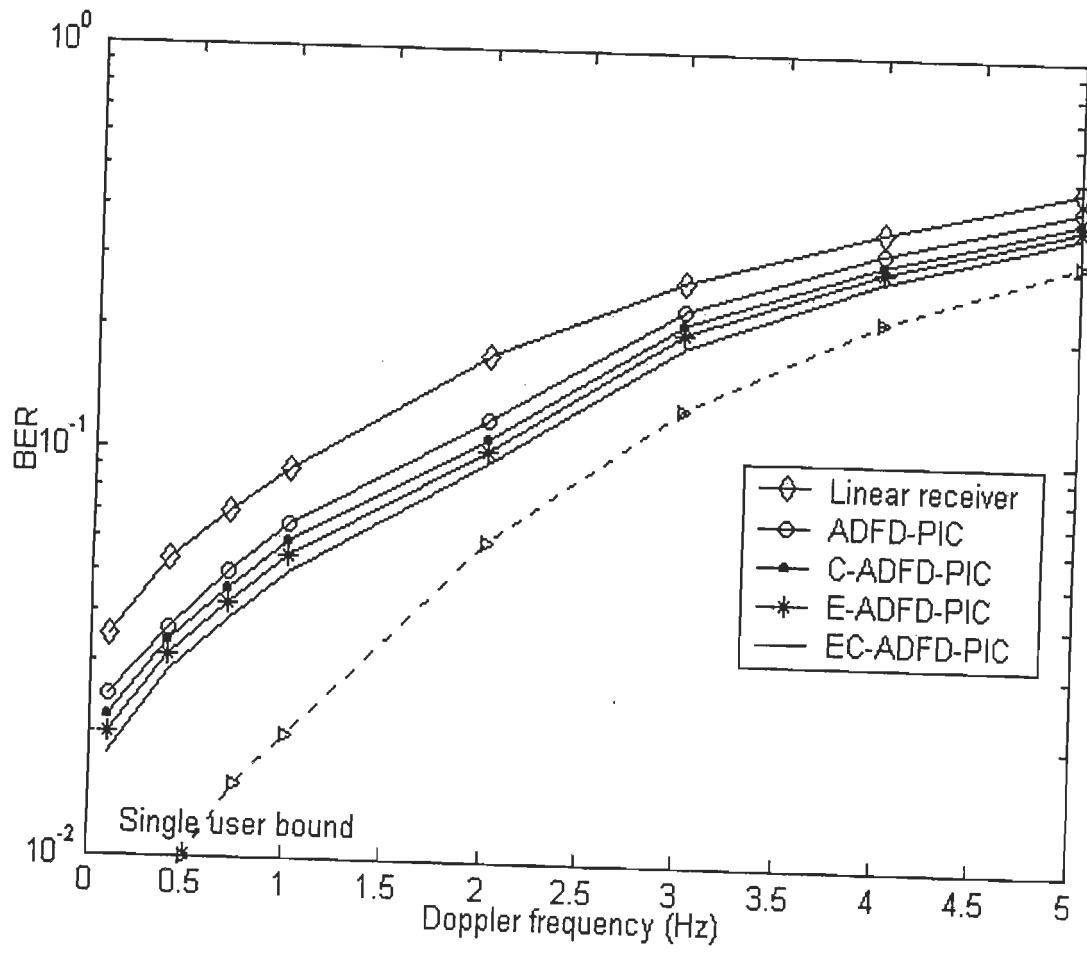


Fig. 5.10: BER vs Doppler frequency for adaptive EC-ADFD-PIC.

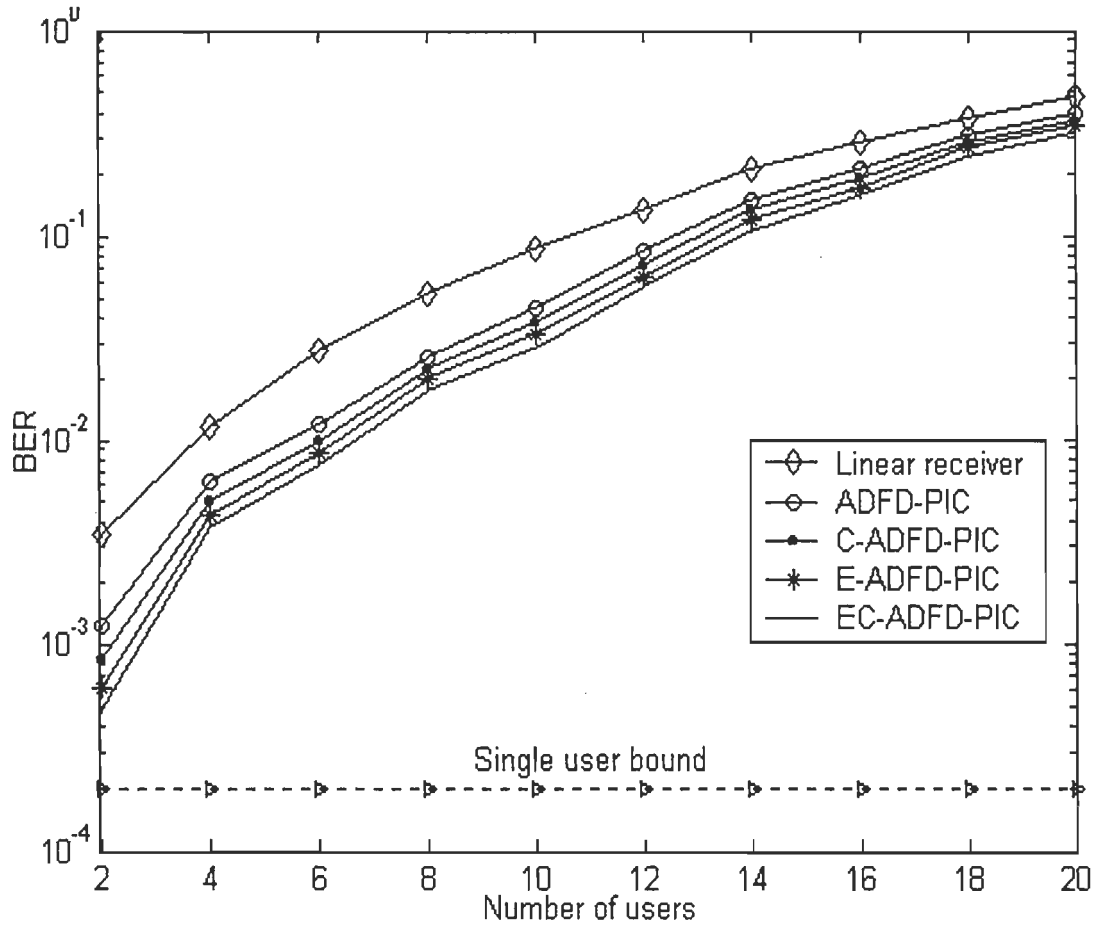


Fig. 5.11: BER vs the number of users for adaptive EC-ADFD-PIC.

It is clear from results shown in Fig. 5.11 that the proposed receiver may handle slightly higher load than the linear MMSE multiuser receiver. The *BER* performance of the ADFD-PICs degrade due to the increasing load factor because we have used the linear multiuser filter (F_{lin}) in its design (as shown in Fig. 5.4), which limits the performance gain due to the feedback of wrong tentative decisions under the practical conditions. The performance gain of the EC-ADFD-PIC receiver over the linear multiuser detector reduces with the increasing number of users.

However in both cases, the EC-ADFD-PIC supersedes other detectors in the multiuser detection scenario due to the improved interference suppression strategy.

5.7 Concluding remarks

In this chapter, we have introduced a novel erasure algorithm to control the effects of error propagation in the conventional adaptive MMSE DFE receivers. Over slowly time-varying frequency-selective multipath fading channel, this technique provides improvement by reducing the bit error rate in the asynchronous DS-CDMA system. Simulation results show that the adaptive E-DFE outperforms the C-DFE for both the near-far and high loading environments. However as loading factor approaches unity, the performance of E-DFE is comparable to the C-DFE. The proposed adaptive non-linear receiver (equalizer) also proves to be effective under the conditions like sudden changes in the signal-to-noise ratio of the desired user, where the error rate is high. The simulation results have evidenced the superior performance of the proposed erasure algorithm.

Next, we have proposed an adaptive decision feedback detector based on the parallel interference cancellation scheme for the DS-CDMA system, which uses the channel estimator and E-slicer. The estimated multiuser channel response is used to cancel ISI due to the past data bits of all the active users. The ISI due to the chip waveforms of present data bit and

MAI are suppressed first by the linear MMSE feedforward filter, and then the residual MAI, ISI and other-cell interference are cancelled using the feedback filter. The effects of error propagation are controlled by incorporating the erasure algorithm in the feedback unit. The EC-ADFD-PIC provides approximately $3dB$ performance advantage relative to the linear MMSE multiuser receiver under the smoothly time-varying multipath fading channel. Moreover, the adaptive implementation using LMS algorithm eliminates the requirement of the estimation of covariance matrix of the received signal vector under the time-varying environment. The simulation results depict that the proposed receiver may be used efficiently for the slow moving mobile users.

Since the S-DFDs based on successive interference cancellation approach are known to provide better performance than the P-DFDs, therefore we focus on the development of multistage (iterative) ADFDs using both parallel and successive interference cancellation schemes in the next chapter.

TWO-STAGE MMSE MULTIUSER DECISION FEEDBACK DETECTORS FOR DS-CDMA SYSTEMS

Multistage multiuser decision feedback detectors have emerged as a way to increase the spectral efficiency of code division multiple access systems and to circumvent the deleterious effects of error propagation in the conventional single-stage non-linear detection techniques [129]. In this chapter, we propose a novel two-stage minimum mean square error multiuser decision-feedback-detector (DFD), which can handle higher load under the low signal-to-noise ratio conditions.

In section 6.1, we first briefly review the single-stage and multistage DFDs used for the multiuser detection. In section 6.2, we describe the DS-CDMA system model for the frequency-selective fading channel (see [101], [102]). It includes details about the successive interference cancellation technique. The noise-predictive successive multiuser DFD based on MMSE criterion is presented in section 6.3. We also present an optimum detection ordering scheme *i.e.*, sorting algorithm. In section 6.4, we next propose a two-stage MMSE multiuser DFD for the DS-CDMA systems working in the multipath Rayleigh fading environment. The first stage of the proposed cascaded structure is the noise-predictive successive-DFD (NP-S-DFD), in which the active users are detected successively using the MMSE Bell-Labs-Layered-Space-Time (BLAST) ordering criterion. The second stage includes an adaptive successive/parallel-DFD (SP-DFD), which uses the tentative decisions obtained at the first stage for the successive multiuser interference cancellation and data detection. Therefore, the proposed two-stage DFD may be called the noise-predictive successive-SP-DFD (NP-S-SP-DFD). Section 6.5 includes the simulation results to reveal the BER performance of the

proposed NP-S-SP-DFD. Finally, conclusions are given in section 6.6.

6.1 Introduction

Decision feedback detection is a popular strategy used in a wide range of MIMO applications [110], [135], [140]. Duel-Hallen [109], [111] has incorporated this scheme for multiuser detection in the DS-CDMA system, which is similar to the decision feedback equalizer employed in the single user channels with intersymbol interference. Different decision feedback strategies have also been proposed in [10], [14], [116] and [121] for MAI and ISI cancellation. For practical implementations, the non-linear multiuser detectors using the successive-interference-cancellation (SIC) approach have been subject to most attention. Hui and Letaief [163] have presented a method for successive co-channel interference cancellation using the estimated channel parameters, which improves the system performance by regenerating estimates of the interfering signal and then subtracting those reconstructed interference signals from the input of the desired receiver. This process is performed in a cascaded fashion in such a way that the “strong” interfering signals are cancelled. However in SIC scheme [164], the magnitude of the matched filter output can be used as the received amplitude estimate of the detected user for reconstructing the interfering signal. A generalized SIC algorithm presented in [165] can also be applied for the multiuser delay and channel estimation in the DS-CDMA system.

A low complexity successive intra-cell interference cancellation scheme using the orthogonal spreading is proposed in [166]. The mobile receiver estimates the effective spreading codes of the interfering users regardless of their spreading factors using the fast Walsh transform correlators, and uses this information to suppress the intra-cell multiuser interference. The performance of the SIC receiver significantly deteriorates due to the lack of variance in the received signal powers [167]. Since the SIC detector orders cancellation based

on the average power criterion, the performance of signal detected early in the cancellation process suffers due to the inefficient interference suppression.

In [168], the author calculates the received power distribution required to obtain the equal BER performance for all the links in a DS-CDMA system employing a linear SIC receiver. It has been shown that the variance of the decision statistic of the linear SIC receiver can be formulated in a non-recursive manner that allows calculation of the power profile necessary to obtain equal signal-to-noise-plus-interference ratio for all the received signals, when the cancellation order is determined based on the average power.

A linear SIC approach using the matrix algebra has been presented in [169], which can be performed on the received chip-matched filtered signal vector without explicitly performing the interference cancellation. Based on this approach, it is realized that both single-stage and multistage linear SIC schemes correspond to a one-shot linear matrix filtering. In an adaptive approach, Cho and Lee [170] have proposed a MMSE detection technique in combination with the SIC, which provides superior performance in comparison to the conventional adaptive linear multiuser detectors in terms of the asymptotic multiuser efficiency and BER.

However, previous work on the MMSE multiuser decision feedback detectors for combined interference suppression and data detection depict that the DFDs exhibit higher spectral efficiency in comparison to the linear multiuser detectors under the high SNR conditions for the high load values [73], [128]. Two conventional decision feedback detectors are (i) S-DFD (Successive–), which uses the successive interference cancellation architecture based on the linear prediction of noise and (ii) P-DFD (Parallel–), which uses the parallel interference cancellation architecture for simultaneous suppression of MAI using the tentative decisions obtained from the conventional detectors [111]. In decorrelating S-DFD, a white noise model is obtained by factoring the positive definite matrix of the cross-correlation

matrix using the Cholesky-decomposition algorithm. The MAI is eliminated by processing the vector output of matched filter bank; and subsequently detection is performed using the maximum-likelihood criterion. The S-DFD achieves the sum capacity of the synchronous DS-CDMA channel with additive white Gaussian noise [133]. It outperforms the P-DFD at the cost of additional processing delay. However on the reverse link, both detectors require information about the multipath channel or received amplitude level of all the active users at the receiver end. But, the P-DFD suffers due to the error propagation effect under the low signal-to-noise ratio conditions.

Duel-Hallen [111] has also explored two-stage detectors with decision feedback in the second stage. Decisions made by the first stage detector are used for cancellation of interference due to the future inputs. This approach was previously proposed in [19], where the conventional matched filter first stage was studied. In [111], the author has modified the structure of two-stage DFD by replacing the conventional matched filter with the decorrelator at the first stage, in which the weaker users utilize decisions made by the strong users in the same time frame. In particular, the decorrelating S-DFD has a low bit error rate and is stable in the presence of interferers with various energy distributions. The weaker user derives the greatest benefit from this two-stage detector *i.e.*, its performance is close to the single-user bound when interferers are strong. The performance of two-stage detector with decision feedback in the second stage is determined by the choice of the first stage. When the first stage is conventional matched filter, substantial degradation in the BER performance is observed. Although it approaches the single-user bound in a two-user system when the interferer is strong, its bit error rate remains high in a system with more than two users. The incorporation of decorrelator at the first stage provides performance gain in comparison to the convention matched filter detector.

To circumvent the deleterious error propagation effects, Woodward *et al.* [129] have

presented multistage (iterative) DFD; which is a cascaded configuration using the successive and non-adaptive successive/parallel-DFDs (S-SP-DFD) with hard-decision feedback. The first stage of S-SP-DFD is a S-DFD because it is observed from the numerical comparisons that the error propagation effects can be mitigated by using the successive interference cancellation and detection rather than the parallel interference cancellation. The second stage is a non-adaptive SP-DFD (the order of users is reversed from the first stage), which subsequently refines the received signal by interference cancellation using the tentative decisions obtained at the first stage.

The two-stage S-SP-DFD approaches the single-user bound in the absence of error propagation [129]. The first user at the first stage avails the maximum benefit of interference cancellation because it is detected last in the second stage. It is apparent from the simulation results presented in [129] that for the high load factor, the bit error rate performance of first user with S-SP-DFD improves as compared to the S-DFD. However the performance degradation is observed for the small number of users *i.e.*, for the low load factor, the error propagation severely affects the BER performance of S-SP-DFD.

In the conventional successive decision feedback detection techniques [109], [111], all the active users are detected in the descending order according to the received power level *i.e.*, the strongest user is detected first at the first stage. Since the received composite signal is corrupted due to the presence of noise, multiple access interference and intersymbol interference under the multipath fading channel, therefore the above brute force approach for determining the detection order may enhance bit error rate due to the inaccurate detection order.

For MIMO applications, the performance of DFD is strongly impacted by the order in which the inputs are detected. Unfortunately, optimizing the detection order is a difficult problem that often dominates the overall receiver complexity. The commonly used optimal

detection order is known as the BLAST ordering [171], which maximizes the worst-case post-detection SNR and approximately minimizes the joint error probability of the DFD. In [134], Waters *et al.* have proposed the NP-S-DFD, which consists of a linear detector followed by a linear prediction mechanism that reduces the noise variance before making a decision. It uses MMSE criterion for the V-BLAST (Vertical-Bell-Labs-Layered-Space-Time [140]) ordering with lower computational complexity. However, the performance degradation due to the residual ISI and noise is unavoidable in case of the conventional single-stage detectors. The symbol error rate performance evaluation of V-BLAST system is presented in [172] by taking into account the error propagation effect, which deteriorates substantially with the increasing channel estimation errors. However, there is no significant degradation due to the sub-optimal sub-stream detection order caused by the channel estimation errors. The analogy between DFDs used for the V-BLAST and DS-CDMA facilitates the usage of NP-S-DFD with MMSE detection ordering in the multiuser systems [143].

In the present work, a novel two-stage NP-S-SP-DFD is proposed using the NP-S-DFD and adaptive SP-DFD at the first and second stages respectively; in which the output of NP-S-DFD (tentative hard-decisions) at the first stage is fed to the adaptive SP-DFD at the second stage for the parallel interference cancellation and multiuser data detection. The incorporation of MMSE detection ordering at the first stage of the presented NP-S-SP-DFD provides performance gain over the available non-adaptive S-SP-DFD [129]. Simulation results are presented to demonstrate the substantial improvement in the bit error rate performance of NP-S-SP-DFD over the conventional single-stage and cascaded DFDs. It may be inferred that the proposed DFD provides an additional performance gain, when the order in which the users are detected is optimized according to the BLAST ordering based on MMSE criterion.

6.2 Successive interference cancellation scheme

For the k th user, the received signal vector $\hat{r}_k(i)$ consists of N consecutive stacked samples, where i is the data symbol index *i.e.*, $\hat{r}_k(i) = [\hat{r}_k(iN) \ \hat{r}_k(iN+1) \ \dots \ \hat{r}_k(iN+N-1)]^T$. The received composite signal vector may be written as:

$$\hat{r}(i) = \sum_{k=1}^K \hat{r}_k(i) + \hat{z}(i) \quad (6.1)$$

where, $\hat{z}(i) = [z(iN) \ z(iN+1) \ \dots \ z(iN+N-1)]^T$ denotes the zero-mean noise sample vector with variance σ^2 . Without loss of generality, we assume that K active users are transmitting at the same signal power level *i.e.*, $A_1 = A_2 = \dots = A_K = 1$, and the number of multipaths L is considered equal for all the intra-cell users. For a multiuser system model under the multipath fading environment (see section 4.2), we can define the $N \times L$ dimensional signature sequence matrices C^k , \tilde{C}^k , and $L \times 1$ dimensional channel coefficient vector $\bar{h}_k(i)$ for the k th user's i th data symbol as:

$$C^k = \begin{bmatrix} c_0^k & \dots & 0 \\ c_1^k & \dots & 0 \\ \vdots & \dots & \vdots \\ c_{N-1}^k & \dots & c_{N-L}^k \end{bmatrix} \quad \tilde{C}^k = \begin{bmatrix} 0 & c_{N-1}^k & c_{N-L+1}^k \\ 0 & 0 & \vdots \\ \vdots & \vdots & \vdots \\ 0 & 0 & \dots & 0 \end{bmatrix}$$

, and $\bar{h}_k(i) = [h_{0k}(i) \ h_{1k}(i) \ \dots \ h_{(L-1)k}(i)]^T$. Using (6.1), we can define the data symbol detection equation as:

$$\hat{r}(i) = C(i)H(i)b(i) + \tilde{C}(i)H(i-1)b(i-1) + \hat{z}(i) \quad (6.2)$$

where $C(i) = [C^1 \ C^2 \ \dots \ C^K]$, $\tilde{C}(i) = [\tilde{C}^1 \ \tilde{C}^2 \ \dots \ \tilde{C}^K]$, $H(i) = \text{diag}[\bar{h}_1(i), \bar{h}_2(i), \dots, \bar{h}_K(i)]$, and $b(i) = [b_1(i) \ b_2(i) \ \dots \ b_K(i)]^T$. At the receiver end, we consider the estimated channel

coefficient matrix $H(i|i)$ known with small scale ambiguities ($\Delta H(i) = H(i|i) - H(i)$ is a zero-mean process). In (6.2), the intersymbol interference term may be cancelled using the estimated multiuser channel response $H(i-1|i-1)$ and estimated past data symbols $b_e(i-1)$.

Under no error propagation situation *i.e.*, $b(i-1) = b_e(i-1)$,

$$\hat{r}_{eq}(i) = \hat{r}(i) - \tilde{C}(i)H(i-1|i-1)b(i-1) = C(i)H(i)b(i) - \tilde{C}(i)\Delta H(i-1)b(i-1) + \hat{z}(i) \quad (6.3a)$$

Assuming small number of multipaths and small scale channel estimation errors, the residual ISI due to past data bits $\tilde{C}(i)\Delta H(i-1)b(i-1)$ is neglected in the above equation. It follows that

$$\hat{r}_{eq}(i) = H_c(i)b(i) - \Delta H_c(i)b(i) + \hat{z}(i) \quad (6.3b)$$

where, $H_c(i) = C(i)H(i|i)$ and $\Delta H_c(i) = C(i)\Delta H(i)$ are the $N \times K$ dimensional complex matrices.

The above described model for the DS-CDMA system is similar to the MIMO model used in [134], in which the columns of matrix $H_c(i)$ are linearly independent with $N \geq K$ (the maximum permissible value of the load factor is kept lower than unity [73]). For MIMO and V-BLAST architectures, the well-known detection strategy is zero-forcing (ZF) decision feedback detection using a typical QR-decomposition of the channel matrix. In this chapter, we consider the QR-decomposition of matrix $H_c(i)$ for the detection of K users in a DS-CDMA system. For i th data bit interval, we may write

$$H_c = Q_c D_c M_c \quad (6.4)$$

where Q_c is a $N \times K$ dimensional matrix with orthonormal columns (q_{ck} is the k th column), D_c is a $K \times K$ dimensional real diagonal matrix with positive elements, and M_c is a lower triangular matrix with ones on its main diagonal (m_{kj} and d_{kj} are the k th row and

j th column elements of the matrices M_c and D_c respectively). Similar to the decorrelating DFD presented in [109], we feed $N \times 1$ dimensional vector \hat{r}_{eq} into the matrix filter $D_c^{-1}Q_c^H$ (sometimes referred to as the whitened-matched filter) as shown in Fig. 6.1. The output vector of this conventional S-DFD based on ZF criterion is

$$y_c = D_c^{-1}Q_c^H \hat{r}_{eq} \quad (6.5a)$$

The above equation can be simplified using (6.3b) and (6.4) as:

$$y_c = M_c b - D_c^{-1}Q_c^H \Delta H_c b + D_c^{-1}Q_c^H \hat{z} \quad (6.5b)$$

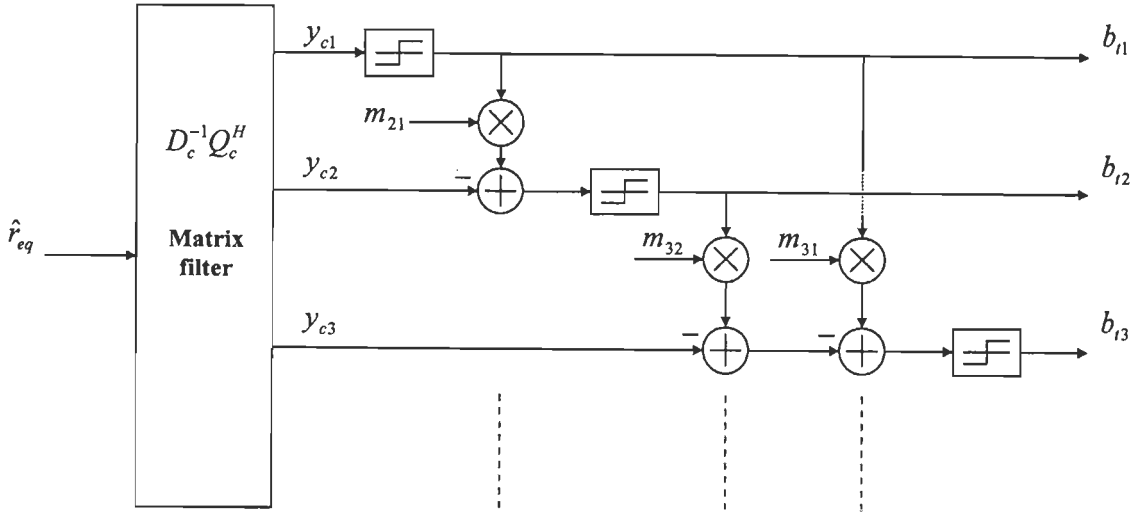


Fig. 6.1: Decision feedback detector using the successive interference cancellation scheme.

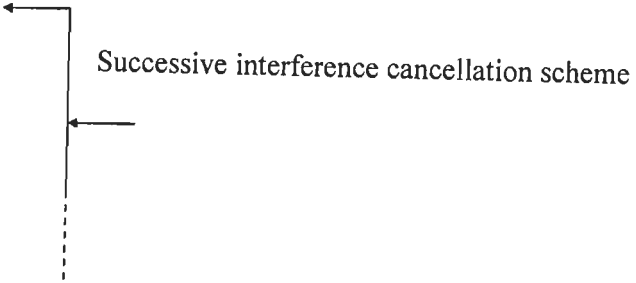
The k th element of $y_c = [y_{c1} \ y_{c2} \ \dots \ y_{cK}]^T$ is defined as:

$$y_{ck} = b_k + \sum_{j < k} m_{kj} b_j - \frac{\Delta_{ck} b}{d_{kk}} + \frac{q_{ck}^H \hat{z}}{d_{kk}} \quad (6.6)$$

where, Δ_{ck} is the k th row of the matrix $Q_c^H \Delta H_c$. The iterative procedure for the successive decision feedback detection is

$$b_{ik} = \text{sgn} \left\{ y_{ck} - \sum_{j < k} m_{kj} b_{ij} \right\} \quad (6.7)$$

where, $\text{sgn}\{\bar{x}\}$ represents the quantization of \bar{x} to the nearest symbol in the alphabet b i.e., $+1$ or -1 . In the above equation, b_{ik} is the output data bit corresponding to the k th user (as shown in Fig 6.1), which may be considered as tentative decision for the next stage. It is apparent from (6.7) and Fig. 6.1 that

$$\begin{aligned} b_{i1} &= \text{sgn}\{y_{c1}\} \\ b_{i2} &= \text{sgn}\{y_{c2} - m_{21}b_{i1}\} \\ b_{i3} &= \text{sgn}\{y_{c3} - m_{31}b_{i1} - m_{32}b_{i2}\} \end{aligned}$$


Thus, the interference due to the present data bits of all the detected users is cancelled successively using the ZF criterion. Note that the first user is detected using the decorrelation approach only, and is not having the additional advantage of SIC scheme.

However, the MMSE decision feedback detection scheme supersedes the zero-forcing criterion based approach in the presence of noise [15]. In the next section, we present NP-S-DFD using the MMSE criterion for multiuser detection.

6.3 Noise-predictive successive DFD

6.3.1 NP-S-DFD using MMSE criterion

Since the channel estimation errors are assumed to be small in comparison to the noise, therefore the linear transformation used for the linear MMSE MUD may be written as:

$$O_{MMSE} = R_c^{-1} H_c^H \quad (6.8)$$

where, $R_c = H_c^H H_c + \sigma^2 I_K$ and I_K is a $K \times K$ dimensional identity matrix. The output of linear MMSE MUD receiver is

$$y_{cl} = O_{MMSE} \hat{r}_{eq} \quad (6.9a)$$

The above equation can be simplified using (6.3b) and (6.8) to give

$$y_{cl} = b - (\sigma^2 R_c^{-1} I_K + O_{MMSE} \Delta H_c) b + O_{MMSE} \hat{z} \quad (6.9b)$$

where, $y_{cl} = [y_{cl1} \ y_{cl2} \ \dots \ y_{clK}]^T$ is the soft output vector of linear MMSE MUD receiver. The corresponding $K \times 1$ dimensional linear error vector is $\varepsilon_{cl} = y_{cl} - b$ with ε_{clj} denoting the j th element. The linear transformation O_{MMSE} minimizes the trace of error covariance matrix $\Gamma_{cl} = E\{\varepsilon_{cl} \varepsilon_{cl}^H\}$, where $E\{\}$ is the ensemble average operator. It is apparent that the linear error vector ε_{cl} contains the residual ISI and noise, which may be “predicted and successively cancelled” by using a recursive strategy similar to the successive interference cancellation (SIC) scheme (6.7). Let $y_{cs} = [y_{cs1} \ y_{cs2} \ \dots \ y_{csK}]^T$ be the soft output vector of NP-S-DFD. For the detection of k th user, the NP-S-DFD based on MMSE criterion is modelled as:

$$y_{csk} = y_{clk} - \sum_{j < k} p_{kj} \varepsilon_{clj} \quad (6.10)$$

where, p_{kj} is the k th row and j th column element of a lower triangular “prediction filter” matrix P with zeros on its main diagonal. The error vector at the output of NP-S-DFD is $\varepsilon_{cs} = (I - P)\varepsilon_{cl}$. Its error covariance matrix is defined as:

$$\Gamma_{cs} = E\{\varepsilon_{cs} \varepsilon_{cs}^H\} = (I - P) \Gamma_{cl} (I - P^H) \quad (6.11)$$

which implicitly depends on

$$\Gamma_{cl} = \sigma^2 R_c^{-1} + R_c^{-1} H_c^H R_\Delta H_c R_c^{-1} \quad , \text{ where } R_\Delta = E\{\Delta H_c \Delta H_c^H\} \quad (6.12)$$

Since the channel is assumed to be known with small scale ambiguities, therefore $R_c^{-1} H_c^H R_\Delta H_c R_c^{-1}$ may be neglected in comparison to $\sigma^2 R_c^{-1}$ (noise term) in (6.12).

Consequently $O_{MMSE} \Delta H_c b$ term can be neglected in (6.9b), which leads to

$$\Gamma_{cl} \approx \sigma^2 R_c^{-1} \quad (6.13a)$$

$$\text{and } \varepsilon_{cl} \approx -\sigma^2 R_c^{-1} b + O_{MMSE} \hat{z} \quad (6.13b)$$

The above equation can be rewritten as:

$$\Gamma_{cl} \approx \sigma^2 G G^H, \quad \text{where } G = \begin{bmatrix} O_{MMSE} & \sigma R_c^{-1} \end{bmatrix} \quad (6.14)$$

For further simplification of (6.13a), the Hermitian and positive definite matrix R_c is decomposed using the Cholesky factorization as:

$$R_c = F_L F_U, \quad \text{where } F_U = F_L^H = \overline{Q}_c \overline{D}_c \overline{M}_c \quad (6.15)$$

Substitution of the above equation in (6.13a) and the application of matrix inversion property [162] results in

$$\Gamma_{cl} \approx \sigma^2 \left[\overline{M}_c^H \overline{D}_c^H I_K \overline{D}_c \overline{M}_c \right]^{-1} = \sigma^2 (\overline{M}_c^{-1}) \overline{D}_c^{-2} (\overline{M}_c^{-1})^H \quad (6.16)$$

where, \overline{M}_c^{-1} is a lower triangular matrix with diagonal elements of one and \overline{D}_c^{-2} is a real diagonal matrix with positive diagonal elements. Using (6.11) and (6.16), we may define the error covariance matrix of NP-S-DFD as:

$$\Gamma_{cs} = \sigma^2 (I - P) (\overline{M}_c^{-1}) \overline{D}_c^{-2} (\overline{M}_c^{-1})^H (I - P^H) \quad (6.17)$$

Defining the cost function as the trace of matrix Γ_{cs} , the optimum error prediction filter is determined by differentiating the cost function *w.r.t.* P and equating it to zero [160]. The optimum error prediction filter is thus

$$P_{opt} = I_K - \overline{M}_c \quad (6.18)$$

It is also shown in [86] that the optimum $(I - P)$ cancels \overline{M}_c^{-1} in (6.17). Under optimum conditions, we calculate the optimum value of the coefficient p_{kj} from the matrix P_{opt} , and the soft output of NP-S-DFD is obtained using (6.9b) and (6.10) as:

$$y_{cs} = b - (I - P_{opt}) \left(\sigma^2 R_c^{-1} I_K + O_{MMSE} \Delta H_c \right) b + (I - P_{opt}) O_{MMSE} \hat{z} \quad (6.19)$$

It is clear that the effective forward filter is $(I - P_{opt}) O_{MMSE} = \overline{M}_c R_c^{-1} H_c^H = \overline{D}_c^{-2} (\overline{M}_c^{-1})^H H_c^H$,

which suppresses noise during the successive data detection process.

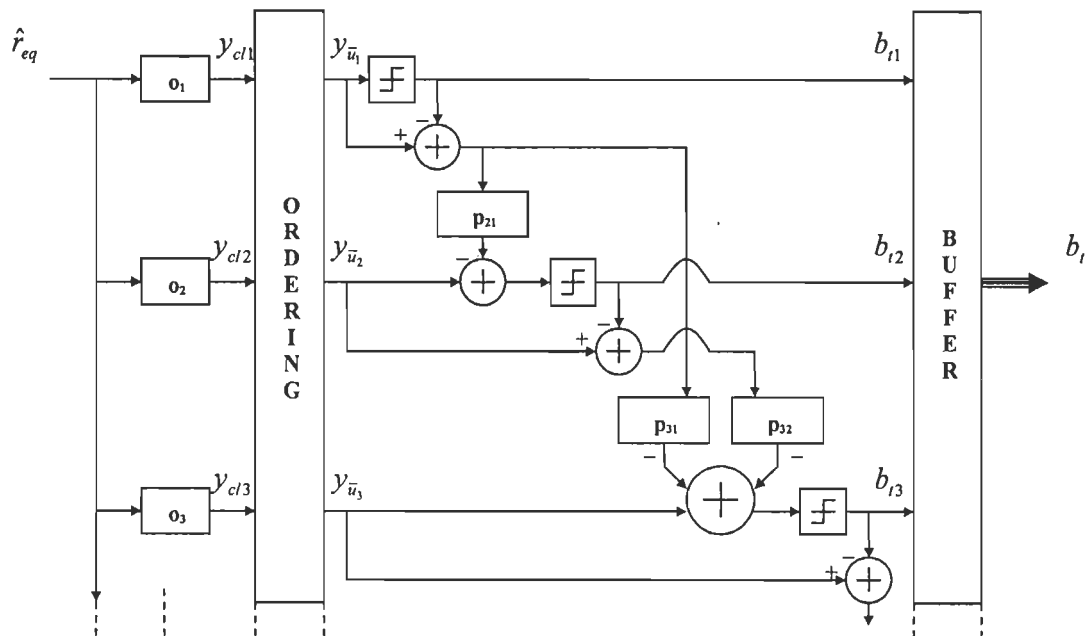


Fig. 6.2: Single-stage noise-predictive successive DFD.

(o_k is the k th row of linear transformation matrix O_{MMSE})

The above described scheme for NP-S-DFD is applicable on the reverse link of DS-SS-CDMA systems for the multiuser detection (as shown in Fig. 6.2). However, it requires the knowledge of multipath channel coefficients of all the active users along with their respective signature sequences. Fig 6.2 depicts that at each stage in the noise-predictive successive interference cancellation scheme, the interference is cancelled using the prediction filter coefficient p_{kj} and the linear error $\varepsilon_{clj} = y_{clj} - b_j$ for $j < k$.

In the successive detection procedure, the detection ordering of the active users is another key parameter, which provides improvement at the cost of additional computational burden. The k th user \bar{u}_k is positioned in the optimum detection queue $\{\bar{u}_1, \bar{u}_2, \dots, \bar{u}_K\}$ by using the detection ordering algorithm, which is discussed in the next subsection. Therefore, the output of linear MMSE filter is reordered as $\{y_{\bar{u}_1}, y_{\bar{u}_2}, \dots, y_{\bar{u}_K}\}$ in Fig. 6.2. Note that we use the reordered $K \times 1$ dimensional vector y_{cl} in the successive detection procedure governed by the equation (6.10). The corresponding output data bit vector is $b_l = \text{sgn}(y_{cl}) = [b_{l1} \ b_{l2} \ \dots \ b_{lK}]^T$, which may be used as the tentative decision vector in the multistage detection.

6.3.2 Detection ordering using MMSE criterion

In the conventional SIC procedure [111], the strongest user is detected first, and then other users are detected successively according to their received power level arranged in the descending order. In the multipath fading environment, the soft output of linear MMSE MUD receiver is used to determine the detection order, which contains the noise as well as the residual ISI (6.9b). The erroneous detection order may lead to error propagation in the successive interference cancellation process. However the following MMSE noise-predictive sorting algorithm may be used to determine the optimal detection order, which is implemented using the modified Gram-Schmidt or Householder orthogonalization

procedure [134], [173].

Let g_k be the k th row of matrix G in (6.14). We choose the first user corresponding to that row, which accounts for the minimum MSE *i.e.*,

$$\bar{u}_1 = \arg \min [g_k g_k^H] \quad , \quad k \in \{1, \dots, K\} \quad (6.20)$$

Let us assume that the tentative decision b_{i_1} corresponding to the user \bar{u}_1 in the detection queue is correct, o_k and r_{ck} be the k th rows of matrices O_{MMSE} and R_c^{-1} respectively. Next,

the MSE for the second user's data symbol is defined by using $\varepsilon_{cs} = (I - P)\varepsilon_{cl}$ as:

$$E|\varepsilon_{c\bar{u}_2} - p_{21}\varepsilon_{c\bar{u}_1}|^2 = E|o_{\bar{u}_2}\hat{z} - \sigma^2 r_{c\bar{u}_2}b - p_{21}o_{\bar{u}_1}\hat{z} + \sigma^2 p_{21}r_{c\bar{u}_1}b|^2 \quad (6.21a)$$

$$= \sigma^2 \|o_{\bar{u}_2} - p_{21}o_{\bar{u}_1}\|^2 + \sigma^4 \|r_{c\bar{u}_2} - p_{21}r_{c\bar{u}_1}\|^2 \quad (6.21b)$$

$$= \sigma^2 \|g_{\bar{u}_2} - p_{21}g_{\bar{u}_1}\|^2 \quad (6.21c)$$

$$= \sigma^2 \|g_{\bar{u}_2} - \hat{g}_{\bar{u}_2}\|^2 \quad (6.21d)$$

where, $\hat{g}_{\bar{u}_2}$ is the projection of $g_{\bar{u}_2}$ on to the subspace spanned by $g_{\bar{u}_1}$ under the optimum condition (6.18). Therefore, the decision criterion for selecting the next user in the detection order is

$$\bar{u}_2 = \arg \min \|g_k - \hat{g}_k\|^2 \quad , \quad k \neq \bar{u}_1 \quad (6.22)$$

For selection of other users in the optimally ordered queue, the recursive sorting algorithm may be stated as:

$$\bar{u}_K = \arg \min \|g_k - \hat{g}_k\|^2 \quad , \quad k \notin \{\bar{u}_1, \dots, \bar{u}_{K-1}\} \quad (6.23)$$

where, \hat{g}_k denotes the projection of g_k onto the span of $\{g_{\bar{u}_1}, \dots, g_{\bar{u}_{K-1}}\}$ under the minimum MSE condition. Thus, the above described optimal BLAST ordering scheme is used to generate the detection ordering queue $\{\bar{u}_1, \bar{u}_2, \dots, \bar{u}_K\}$ for SIC scheme in the multiuser detection scenario.

The NP-S-DFD using the MMSE criterion considered above may be converted to the NP-S-DFD based on ZF criterion (ZF-NP-S-DFD) by using $\sigma^2 = 0$ in the linear transformation O_{MMSE} . Similarly, the sorting algorithm may be used in the ZF mode by considering $\sigma = 0$ in (6.14). However the ZF linear transformation includes the matrix pseudo inversion operation, which is computationally complex. The ZF-NP-S-DFD cancels the interference completely at the cost of noise amplification, which leads to the performance degradation under the high noise conditions. On the contrary, the NP-S-DFD based on MMSE criterion finds optimal balance between the interference cancellation and the noise reduction [15]. Therefore, the proposed NP-S-DFD with optimal detection ordering using the MMSE criterion is expected to perform better than the other existing single-stage DFDs.

6.4 Two-stage NP-S-SP-DFD

In NP-S-DFD, the first user is detected using the linear MMSE detection because the “noise-prediction and cancellation” process starts from the second user (see (6.10) for $k = 1$). Subsequently, other users are detected using the SIC approach. Therefore, the performance of NP-S-DFD depends on the detection of first user in the optimal detection ordering queue. In case of wrong decision feedback, its performance suffers due to the error propagation effect. This motivates the development of a novel two-stage NP-S-SP-DFD, in which the parallel interference cancellation approach is used to detect the first user at the second stage by using the tentative decisions obtained from the first stage (as shown in Fig. 6.3a).

As the NP-S-DFD supersedes other single-stage DFDs (as shown by simulations in the next section), its output *i.e.*, hard-decisions may be used as tentative decisions at the second stage (adaptive successive/parallel DFD) of the proposed NP-S-SP-DFD (as shown in Fig. 6.3a). The adaptive SP-DFD at second stage cancels the noise and interference by using the tentative data bit vector b_i .

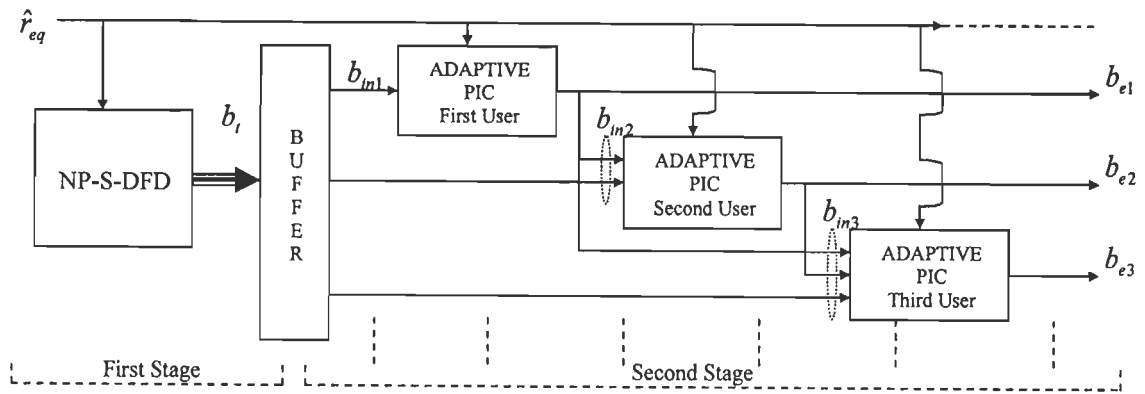


Fig. 6.3a: Two-stage NP-S-SP-DFD with adaptive successive/parallel DFD at the second stage.

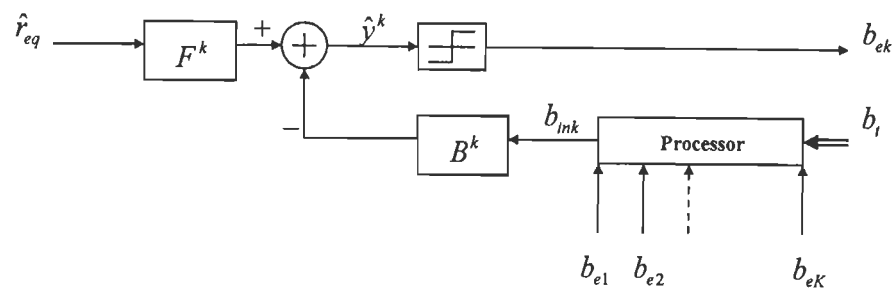


Fig 6.3b: Adaptive parallel interference canceller.

The adaptive SP-DFD uses the parallel-interference-cancellers (PICs) arranged in the successive detection order. The structure of adaptive PIC is similar to the adaptive equalizer described in section 5.2. But in the presented PIC, we feed the tentative decisions about the present data bits of all the intra-cell users (interferers) to the feedback filter for interference cancellation. For the detection of k th user, let the input vectors to the $N \times 1$ dimensional feedforward filter F^k and $(K-1) \times 1$ dimensional feedback filter B^k be \hat{r}_{eq} and $b_{ink} = [b_{e1} \dots b_{ek-1} b_{ik+1} \dots b_{iK}]^T$ respectively.

Considering the case of a single undetected user, we may define the input to decision device (slicer) of the k th adaptive PIC as $\hat{y}^k = \tilde{F}^{kH} \hat{r}_{dfe}$ (as shown in Fig. 6.3b); where $\tilde{F}^k = [F^{kT} \ -B^{kT}]^T$, $\hat{r}_{dfe} = [\hat{r}_{eq}^T \ b_{ink}^T]^T$ and the corresponding error is $e_{dfe}^k = b_k - \hat{y}^k$ in the training mode. During the decision directed mode, b_k is replaced by $b_{ek} = \text{sgn}(\hat{y}^k)$. The feedforward and feedback filters are updated recursively using the LMS adaptive algorithm. It follows that

$$\tilde{F}^k(i+1) = \tilde{F}^k(i) + \mu \hat{r}_{dfe} e_{dfe}^{k*} \quad (6.24)$$

where μ is the step size, which controls the convergence and stability of the LMS algorithm [43].

At the second stage of NP-S-SP-DFD, the first user is detected using the adaptive PIC based on MMSE criterion. The first user uses $b_{m1} = [b_{i2} \ b_{i3} \ \dots \ b_{iK}]^T$ in the feedback unit for simultaneous cancellation of interference using the adaptive algorithm (6.24) for $k=1$. Similarly the input vector $b_{m2} = [b_{e1} \ b_{i3} \ \dots \ b_{iK}]^T$ is fed to the feedback filter of the second (next) user, where b_{e1} is the estimated data bit corresponding to the first user. The improved detection of first user mitigates the error propagation effects at successive stages. The update of input vector b_{in} at each successive PIC results in the improved parallel interference

cancellation. The BER performances of the proposed two-stage and single-stage DFDs are compared by computer simulations in the next section.

6.5 Simulation results

We shall investigate first the performance of a single-stage NP-S-DFD in the multiuser interference cancellation and data detection scenario. We next evaluate the BER performance of the proposed NP-S-SP-DFD based on MMSE criterion for the frequency-selective multipath fading channel. For simulating the DS-CDMA system, the Gold-sequences of length $N = 31$ are generated. The LMS algorithm is used in each adaptive PIC as shown in Fig. 6.3a, in which the step size is adjusted to control the convergence and stability. The presented results are based on an ensemble average of 100 independent simulation runs with different “3 path” channel realizations [14], where the “1 path” channel is a flat fading channel. In all the simulation examples, we have considered the multipath channel coefficient matrix known. We have shown the average bit error rate for each detector, which is defined as $BER = \sum_{k=1}^K BER_k / K$. The BER performances of the single-stage and the two-stage DFDs are compared in the following examples.

Example 6.1: In this simulation, the effects of the ZF and the MMSE criterion based sorting algorithms on the performance of NP-S-DFD are analysed. For a twenty-user cellular system, we consider a three-tap frequency-selective multipath fading channel model *i.e.*, $K = 20$ and $L = 3$. The simulation results are presented in Fig. 6.4 for the different values of SNR. It may be inferred that the single-stage NP-S-DFD with the MMSE criterion based detection ordering outperforms the ZF based approaches. At the target $BER = 0.001$, the NP-S-DFD (MMSE-ordering) gives approximately 1.2dB performance gain over the NP-S-DF (ZF-ordering). It provides 2dB performance advantage over the S-DFD under similar conditions.

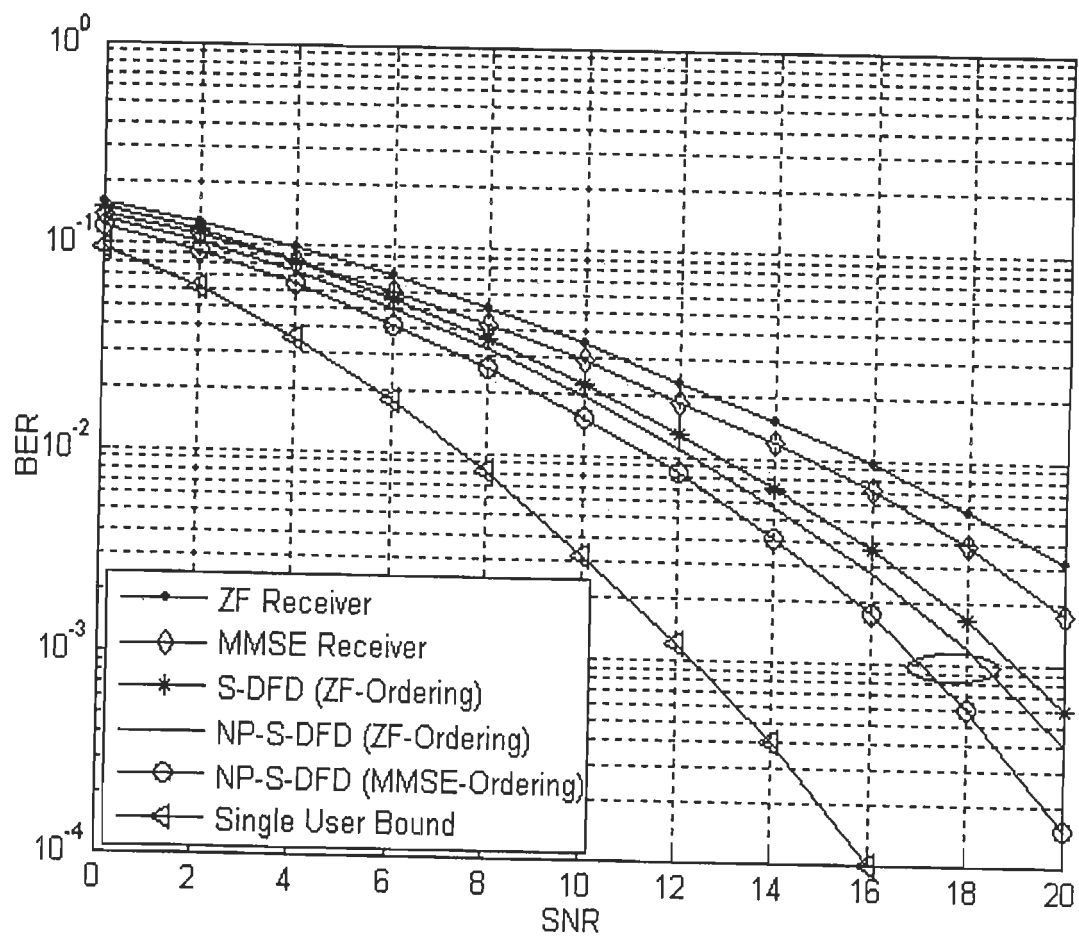


Fig. 6.4: Performance comparison of single-stage DFDs using the different detection ordering criteria.

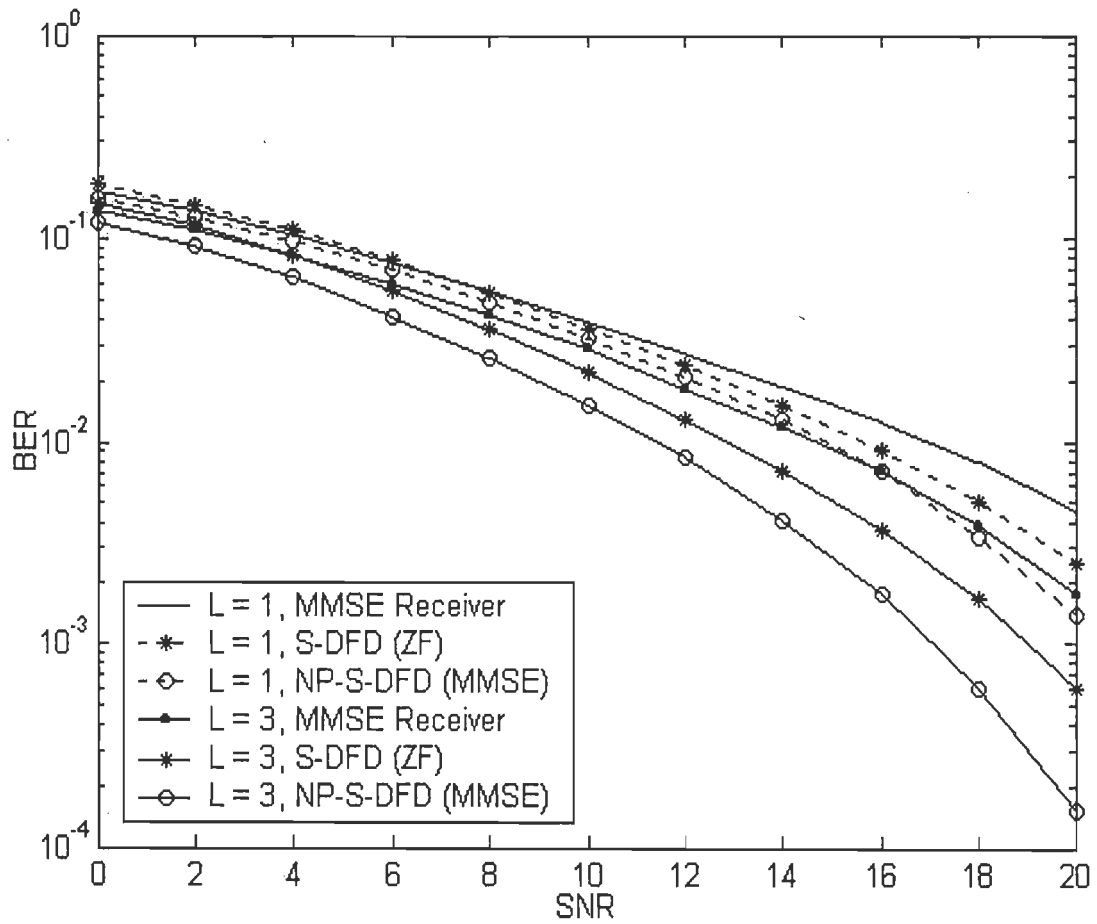


Fig. 6.5: Multipath channel effects on the performance of NP-S-DFD, (SNR in dB).

However, the performance gap between the NP-S-DFD (MMSE-ordering) and single user bound is 4.8dB. The NP-S-DFD with ordering based on MMSE criterion provides 4dB performance gain over the linear MMSE receiver at the $BER = 0.002$. This performance advantage increases with the increasing value of SNR. Thus, it supersedes the ZF MUD and MMSE MUD by providing lower BER.

We further compare the BER performances of the single-stage DFDs with $L = 1$ and $L = 3$. The simulation results shown in Fig. 6.5 demonstrate that the use of more number of multipaths provides diversity gain by enhancing the SNR. At the target $BER = 0.002$, the NP-S-DFD (MMSE) with $L = 3$ provides approximately 3.5dB performance improvement over the NP-S-DFD (MMSE) with $L = 1$. This performance advantage is due to the diversity gain. At $BER = 0.01$, the NP-S-DFD with $L = 3$ provides approximately 3.2dB performance gain over the linear MMSE receiver with $L = 3$. The NP-S-DFD with $L = 1$ outperforms the S-DFD (ZF) by giving approximately 1dB performance advantage at the $BER = 0.003$. This demonstrates the advantage of the MMSE criterion over the ZF approach in successive interference cancellation technique. However, it may be inferred from Fig 6.5 that the NP-S-DFD performs better than other single-stage DFDs.

Example 6.2: We next consider the performance comparison of the last user's detection with the NP-S-DFD (MMSE) and S-DFD at $K = 31$ and $L = 3$. For the target $BER = 0.03$, the performance gain of NP-S-DFD over the linear MMSE receiver (MUD) increases significantly with load (as shown in Fig. 6.6) because the latter receiver does not favour the high load values [73]. The S-DFD outperforms the linear MMSE receiver when the BER is less than approximately 0.07 because at high BER , the error propagation effect deteriorates the performance of SIC process. However, the simulation results in Fig. 6.6 clearly show that the BER performance of last user with NP-S-DFD is superior to S-DFD.

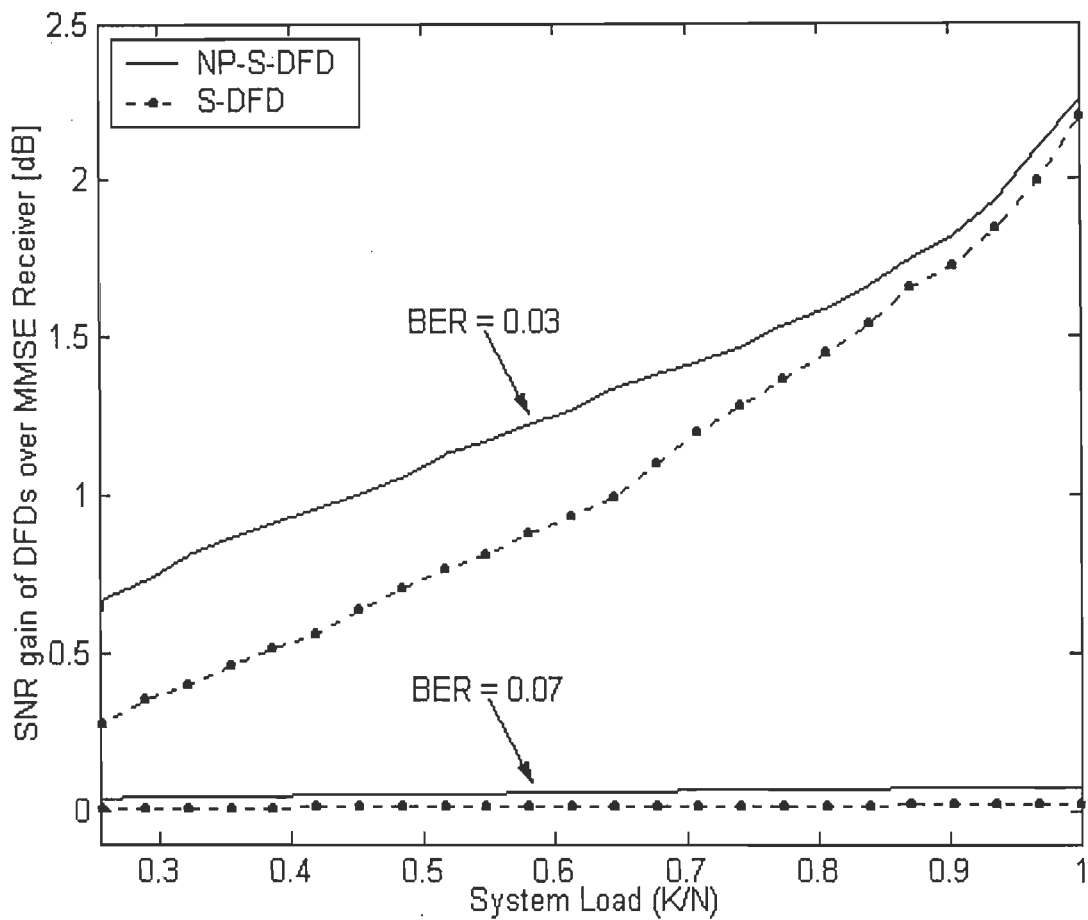


Fig. 6.6: Gain of the last detected NP-S-DFD and S-DFD user relative to the linear MMSE user.

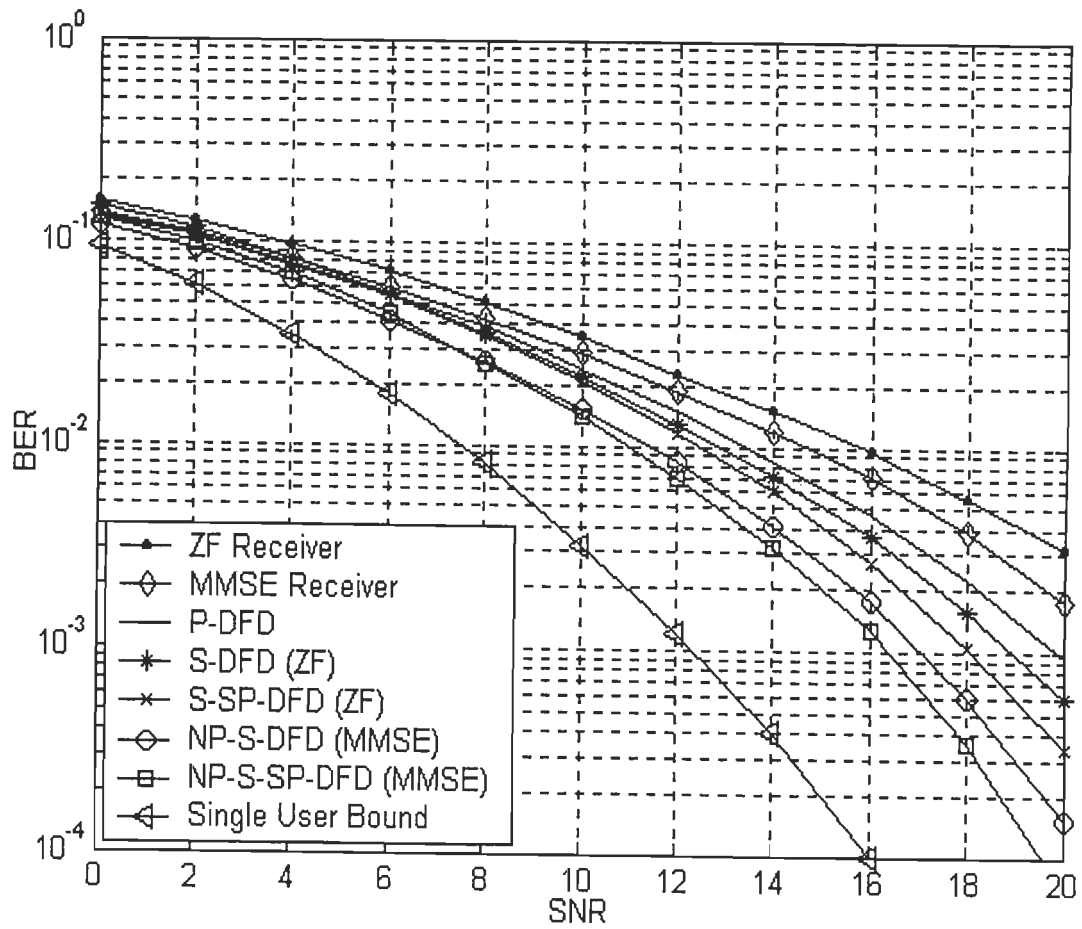


Fig. 6.7: Performance comparison of the two-stage NP-S-SP-DFD with other detectors, (SNR in dB).

Further for the load factor fixed at $K/N = 0.6452$ (a twenty-user system) and $L = 3$, the BER performance of the proposed two-stage NP-S-SP-DFD is evaluated, and the performance comparison of the NP-S-SP-DFD with single-stage and other two-stage DFDs is presented in Fig. 6.7. At $BER = 0.05$, the NP-S-DFD gives 0.3dB performance gain over the NP-S-SP-DFD. This BER performance degradation in case of the presented NP-S-SP-DFD is observed due to the error propagation effect under the low SNR conditions.

However it is apparent that at high SNR, the NP-S-SP-DFD with the MMSE based detection ordering outperforms other DFDs at the different values of SNR. The performance of NP-S-SP-DFD is approximately 4.5dB better than the linear MMSE receiver at the $BER = 0.002$. For the target $BER = 0.001$, It provides 1.7dB and 2.7dB performance advantage over the S-SP-DFD and S-DFD respectively. Under similar conditions, the performance gap between the NP-S-SP-DFD and single user bound is 4.1dB. It may further be observed that at high SNR values, this performance gap reduces significantly.

6.6 Concluding remarks

In this chapter, we have presented a two-stage NP-S-SP-DFD, in which the first stage is a NP-S-DFD and the second stage is an adaptive successive/parallel DFD. All the active users are ordered in the optimum detection queue using the noise-predictive sorting algorithm, which is incorporated in the NP-S-DFD. At the second stage *i.e.*, adaptive SP-DFD, the adaptive PICs are used in the successive order. Under the low SNR conditions, significant degradation in the BER performance of NP-S-SP-DFD is observed due to the error propagation effect. On the other hand, its performance substantially improves under the high SNR conditions. The first user is detected using the linear MMSE transformation in NP-S-DFD, which may lead to the error propagation at successive stages due to the wrong detection of data symbol corresponding to the first user. However at the second stage of NP-S-SP-

DFD, the first user is detected using the parallel interference cancellation approach, which results in the improved BER performance. The presented computer simulation results demonstrate that the proposed NP-S-SP-DFD based on MMSE criterion outperforms the conventional single-stage and two-stage DFDs.

CONCLUDING REMARKS

In this work, we have studied adaptive decision feedback techniques based on minimum mean square error criterion for the suppression of multiple access interference and intersymbol interference in the code division multiple access systems for multiuser detection. In the following, we summarize important results of our study and also give suggestions for further investigations.

7.1 Conclusions

We have first considered the decorrelating and MMSE linear sub-optimum multiuser detectors in the presence of background Gaussian noise and have analysed their performances, by using the leakage coefficients and Kullback-Leibler divergence theorem under the near-far situation. It may be noted that the MAI is inevitable due to the non-orthogonal properties of signature sequences. The MAI-plus-noise mixture at the output of linear MMSE MUD is Binomially distributed for a small number of users, and the Chernoff upper bound on the probability of error in MMSE multiuser detection increases with the increasing number of users due to the high value of residual MAI. The two-user case is shown to have maximum non-Gaussian MAI-plus-noise mixture. However, the MAI-plus-noise mixture at the output of linear MMSE MUD is asymptotically Gaussian for a large number of users. For joint MMSE multiuser detection and interference cancellation under the near-far scenario, the signal-to-noise ratio of the desired user should be more than the minimum bounded value, which depends on the number of users and the value of signature sequence normalized cross-correlation value. We have derived the optimum NCC ranges for $K > 2$ users, in which the error probability of linear MMSE MUD minimizes. It is shown

that the MMSE multiuser detector outperforms the decorrelating detector by exhibiting the lower error probability only if the value of signature sequence NCC is less than or equal to the upper bounded value under worst conditions.

We have next proposed the use of two-step LMS-type adaptive algorithms for the tracking of smoothly time-varying channels. We have presented a modified version of the two-step LMS-type algorithm (MG-LMS) motivated by the work of Gazor (G-LMS in [60]), and have also described its nonstationary adaptation characteristics. We have incorporated a control parameter in addition to a smoothing parameter used in the G-LMS algorithm, which provides stability to the MG-LMS algorithm by controlling its oscillatory behaviour in the convergence mode. The proposed modification reduces the initial learning period in comparison to the G-LMS algorithm. It is shown that the tracking performances of the LMS and NLMS algorithms suffer due to the lag noise, which consequently increases the total misadjustment. However the MG-LMS algorithm purges a large amount of the lag noise, and reduces the lag-misadjustment at the cost of slight increase in the gradient-misadjustment.

For system identification problem, the first-order Markovian model has been used to derive the analytical results for the lag-misadjustment corresponding to the MG-LMS adaptive algorithm, which mainly depend on the values of control and smoothing parameters. It may be inferred that the smoothing parameter controls the tracking speed of the MG-LMS algorithm, and the lag-misadjustment reduces with its increasing value. On the other hand, the control parameter provides stability in the convergence mode and also reduces the lag-misadjustment when its value is kept less than a threshold value. It has been shown that the complex poles induce oscillations (resulting in high output MMSE) when the value of control parameter is more than the threshold value. Therefore, its value should be kept less than the threshold value. The decoupling theorem and direct-averaging method have been used to derive the optimum value of control parameter at which the lag noise (lag-misadjustment)

minimizes.

Simulation results depict that the output mean square error decreases with the increasing value of control parameter and starts increasing again when the value of control parameter is more than the optimum value. Under the smoothly time-varying channel, the NLMS algorithm provides approximately 2.5dB performance advantage over the conventional LMS algorithm at 20dB SNR. Like the previously reported results in [60], the G-LMS algorithm gives approximately 11dB performance gain over the LMS algorithm. Under similar conditions, the performance of the presented MG-LMS algorithm improves by approximately 14dB over the LMS algorithm at the optimum values of control parameter, step size and smoothing parameter. The MG-LMS algorithm outperforms the LMS, NLMS and G-LMS algorithm in tracking the smoothly time-varying channels by combating the lag noise, and thus provides less output MMSE. The simulation results validate the derived analytical results for tracking, convergence and lag-misadjustment behaviour. Moreover the conventional LMS algorithm is a special case of the proposed MG-LMS adaptive algorithm, which signifies its flexibility.

We then present the application of a novel two-step reduced Kalman/LMS algorithm in the adaptive multiuser decision feedback equalization and data detection for the DS-CDMA systems working over the smoothly time-varying channels. It has been designed by exploiting the Kalman filtering algorithm, which leads to the reduction in computational complexity as compared to the commonly used adaptive multiuser DFE receiver using the Kalman algorithm. Its design includes the incorporation of LMS algorithm for the prediction of first-order weight increment vector, which updates the *a priori* estimate of tracking weight vector. We have also analysed and discussed the tracking and convergence characteristics of the multiuser channel estimator using RK-LMS algorithm under the time-varying environment, and have derived operating ranges for the control parameter, smoothing parameter and step

size. Similar to MG-LMS algorithm, it may be inferred from analytically derived results that the tracking speed of the presented channel estimator can be increased by increasing the value of smoothing parameter, but it enhances the oscillatory behaviour of adaptive algorithm in the convergence mode. However the amplitude of oscillations can be controlled by adjusting the value of control parameter, which provides stability to the RK-LMS algorithm. The proposed two-step adaptive algorithm supersedes the conventional LMS algorithm by suppressing the lag noise during channel tracking and by combating the nonstationarity introduced due to the time-variations in multipath channel response.

We have used the channel estimates obtained from the RK-LMS adaptive algorithm based multiuser channel estimator to cancel the intersymbol interference due to the chip waveforms corresponding to the past data bits of all the active users in a particular cell. The probability of error analysis of the presented adaptive multiuser DFE receiver demonstrates that the application of two-step reduced/Kalman algorithm exhibits less probability of error than the conventional LMS algorithm based approach. In this analysis, we have considered the residual MAI component as Gaussian distributed for a large number of users.

Simulation results depict that at 20dB SNR, the RK-LMS algorithm gives approximately 3dB performance gain over the conventional LMS algorithm for the fading rate $f_D T_b = 0.0001$ due to better tracking performance under the smoothly time-varying channels. Under similar conditions, this performance gap reduces to 1.5dB for the fading rate $f_D T_b = 0.001$ due to the increasing value of lag noise. The performance advantage of the RK-LMS algorithm over the conventional LMS algorithm reduces with the increasing number of users because for a large number of users, the magnitude of residual MAI increases. This performance advantage also reduces due to the increasing number of multipaths because the value of SNR per path reduces, which deteriorates the channel tracking performance.

The BER performance of the proposed multiuser DFE receiver degrades with the

increasing speed of mobile users as we have incorporated the conventional LMS algorithm to estimate the first-order weight increment vector used in the RK-LMS adaptive algorithm, which can not follow the fast time-variations in the multipath channel response. On the other hand, as the load factor increases, its BER performance deteriorates due to the increasing value of the residual MAI and ISI. However for a small number of multipaths, the BER performance of presented multiuser receiver improves because of diversity gain through multipath reception. On the contrary, for a large number of multipaths, its performance degrades due to the channel estimation errors. It is also observed that the error propagation effect due to the overwhelming nature of residual MAI, ISI and channel estimation errors results in the BER performance degradation under the low SNR conditions. It is apparent from different simulation examples that the configuration consisting of RK-LMS algorithm based adaptive channel estimator in the feedback unit for intersymbol interference suppression and RK-LMS algorithm based forward filter for MAI, ISI and noise cancellation outperforms the conventional LMS algorithm based approaches.

We have further proposed an adaptive decision feedback equalizer receiver using the erasure algorithm, which not only combats the inter-cell and intra-cell interference in the multiuser systems but also controls the error propagation effect. The received composite signal is over-sampled to tackle the problem of asynchronous reception. The feedback filter of the presented MMSE DFE receiver is fully connected, which uses the past decisions of all the active users to cancel the intra-cell interference. However the fractionally spaced feedforward filter suppresses the inter-cell interference, MAI and noise, and also acts like RAKE by providing the diversity gain. The erasure algorithm based soft-slicer erases the highly unreliable signals and assigns weight to each detected data bit according to the level of uncertainty in the estimated value of symbol. The assigned value of the weight decreases with the increasing value of error between the estimated symbol and data symbol, which reduces

the error propagation in the non-linear detection techniques (using decision feedback). The conventional DFE receiver is a special case of E-DFE when the value of assigned weight is constrained to unity.

Under erroneous conditions like sudden changes in the signal-to-noise ratio value of the desired user, high load factor and near-far situation, the proposed adaptive E-DFE outperforms the C-DFE due to the error control. For the value of load factor more than 0.645, the residual MAI limits the BER performance of the multiuser system. But, the E-DFE performs marginally better than the C-DFE for the high load conditions. It also provides approximately 2.5dB performance improvement over the C-DFE at the target $BER = 0.01$ when the interferers are kept at 20% higher power level than the desired user's power level.

We have next proposed the application of erasure algorithm in the multiuser adaptive decision feedback detector using the partial parallel interference cancellation scheme, in which the erasure algorithm is used to generate the time-variable partial cancellation factors depending on the soft-output of linear MMSE multiuser filter. Previously reported results in [128] depict that the P-DFD offers approximately 2dB gain relative to the linear MMSE multiuser receiver. But the filter coefficients are obtained by using the covariance matrix of the received signal vector, which is difficult to compute in the time-varying environment. However the presented adaptive EC-ADFD-PIC provides approximately 3dB performance advantage over the linear MMSE multiuser receiver at the $BER = 0.04$, in which the erasure algorithm is used to control the error propagation effect and the channel estimator is used to cancel the intersymbol interference due to the past data bits of all the active intra-cell users. Moreover, the requirement of the covariance matrix of the received signal vector is eliminated by updating the recursive filter coefficients using the conventional LMS adaptive algorithm. Simulation results demonstrate that the proposed multiuser receiver can handle higher load in comparison to other multiuser detectors. As the speed of mobile users

increases, the BER performance of the EC-ADFD-PIC degrades due to the inability of LMS algorithm to adapt in the fast time-varying environment. However, it is observed that the EC-ADFD-PIC supersedes the linear MMSE multiuser receiver and other detectors under the slow time-varying channels.

We have next proposed a novel two-stage MMSE multiuser decision feedback detector for the DS-CDMA system. An adaptive successive/parallel DFD has been used at the second stage, which uses the tentative hard-decisions obtained from the noise-predictive successive DFD at the first stage for parallel interference cancellation and multiuser data detection. At the first stage (NP-S-DFD), we have used the MMSE noise-predictive sorting algorithm for determining the user detection order. Simulation results reveal that the use of MMSE noise-predictive ordering in NP-S-DFD gives approximately 1.2dB performance advantage over the conventional zero-forcing BLAST ordering scheme at the $BER = 0.001$ under typical conditions. However, the NP-S-DFD (MMSE-ordering) provides 4dB performance gain over the linear MMSE receiver at the target $BER = 0.002$, which increases with the increasing value of SNR. It is also noted that the use of more number of multipaths enhances the SNR, and thus provides the diversity gain. The presented NP-S-DFD with MMSE detection ordering provides approximately 3.5dB additional gain at the $BER = 0.002$ when the number of multipaths are increased from one to three. It is apparent from different simulation examples that the successive interference cancellation scheme using the MMSE criterion supersedes the ZF criterion based approaches. But, the error propagation severely affects the performance of SIC process. Therefore under high BER conditions, the linear MMSE multiuser receiver outperforms the S-DFD based on ZF criterion.

At second stage, the successively arranged adaptive parallel interference cancellers using the LMS algorithm use the output of NP-S-DFD as the tentative decisions. It provides approximately 4.5dB performance improvement relative to the linear MMSE multiuser

receiver at the target $BER = 0.002$. The first user at the second stage is detected using the parallel interference cancellation technique, which was previously detected using the conventional MMSE approach at the first stage (NP-S-DFD). The improved detection of the early detected users reduces the error propagation at subsequent stages of SIC scheme. It may be concluded that under the high SNR conditions, the proposed cascaded structure using the NP-S-DFD and adaptive successive/parallel DFD outperforms other single-stage and two-stage DFDs.

7.2 Suggestions for further work

In this study, we have seen that the linear MMSE multiuser detector outperforms the decorrelating detector in the multiuser system using the non-orthogonal signature sequences. But, the presented analysis is only confined to the AWGN channels. It is worthwhile to investigate the probability of error analysis of linear multiuser detectors under the multipath fading channels and to compare their performances under the asymptotic conditions. Bounds on the probability of error and the corresponding value of normalized cross-correlation of the signature sequences can be derived under the near-far situation. This work can be extended to the performance evaluation of the non-linear sub-optimum multiuser detection techniques and to analyse the behaviour of MAI-plus-noise mixture at their output.

We have considered the two-step MG-LMS adaptive algorithm for tracking the smoothly time-varying channels, where the conventional LMS and NLMS algorithms fail to perform well. The application of MG-LMS algorithm in nonstationary environments suggests a number of interesting avenues for further research. The MG-LMS algorithm can be used to develop a set of new adaptive algorithms using the variable step size approach considered in [174]. Its performance needs to be evaluated for the fourth generation wireless OFDM systems for the tracking of time-varying channels. Space-time coding for the multiple

transmit and receive antenna systems (MIMO channels) rely on the knowledge of channel coefficient matrix. Therefore the MG-LMS adaptive channel tracking algorithm can be used to estimate the MIMO channel coefficient matrix in the time-varying environment, thus reducing the computational complexity of the receiver which uses the Kalman algorithm for parameter estimation.

It is observed that the adaptive E-DFE outperforms the C-DFE by controlling the error propagation effect. Using the previously presented work on the erasure DFE for PAM signalling scheme in [80], the probability of error evaluation of E-DFE for the DS-CDMA system is a topic for further research. The application of the erasure algorithm in the adaptive space-time feedforward/feedback architectures presented in [9] and [10] for the multiuser detection in the high data rate wireless DS-CDMA networks can also be considered.

Another area for further research includes the development of multistage multiuser DFDs using the adaptive parallel and successive interference cancellation approaches (see [129]), which can provide BER performance close to the single-user bound. The use of convolutional codes provides substantial coding gain over the uncoded systems at the cost of additional bandwidth. However with the trellis coded modulation, the performance gain is achieved without increasing the bandwidth. The use of the trellis coded modulation in place of the convolutional codes for obtaining additional coding gain needs further investigation.

From a communication theorist's point of view, "iterative (turbo)" processing is a way to approach the Shannon limit on channel capacity, while "space-time" processing is a way to increase the possible capacity by exploiting the rich multipath nature of the fading wireless environments. Combining the two concepts provides a practical way to both increase and approach the possible wireless channel capacity. It will be interesting to use the adaptive iterative MMSE multiuser decision feedback structures for the multicarrier CDMA systems in combination with the space-time coding for multiple transmit and receive antenna systems.

The presented work on the time-varying channel tracking and the use of non-linear decision feedback structures in the equalization, interference suppression and multiuser detection can also be extended to the hybrid OFDM/CDMA wireless systems.

APPENDIX – A

Determination of the time constant

In $\beta_{threshold} < \beta < \beta_{upper}$ domain, the poles are complex conjugate *i.e.*, $P_1 = P_2^*$. From (3.45), the maximum permissible pole magnitude is

$$|P_1| = |P_2| = |P_{max}| = \sqrt{(1 + 2\alpha\mu\lambda_p)\beta_{upper}} \quad (A.1)$$

The maximum value of the time constant is thus defined as:

$$Max(\tau_p) = [1 - |P_{max}|]^{-1} \quad (A.2)$$

The inequality in (3.45) may be rewritten as:

$$(1 + 2\alpha\mu\lambda_p)\beta_{upper} < 1 \quad (A.3)$$

Let us assume that $(1 + 2\alpha\mu\lambda_p)(\beta_{upper} + x) \cong 1$. It follows that

$$(1 + 2\alpha\mu\lambda_p)\beta_{upper} \cong 1 - (1 + 2\alpha\mu\lambda_p)x \quad (A.4)$$

For $x \ll 1$, (A.1) and (A.4) are used to give

$$|P_1| = |P_x| = \sqrt{1 - (1 + 2\alpha\mu\lambda_p)x} \cong 1 - (1 + 2\alpha\mu\lambda_p)(x/2) \quad (A.5)$$

Thus, the time constant in operating range is

$$\tau_p = [1 - |P_x|]^{-1} \cong (2/x)(1 + 2\mu\lambda_p)^{-1} \quad (A.6)$$

Example 1: For $x = \mu\lambda_p \ll 1$, the resultant approximate time constant is

$$\tau_p \approx 2/\mu\lambda_p = 2(\tau_{LMS}) \quad (A.7)$$

It illustrates that under typical conditions, the time constant for the MG-LMS is double of the conventional LMS algorithm. The derived result matches with the analysis of Gazor in [60].

However for the real poles, its value is

$$\tau_p = [1 - (X + Y)/2]^{-1} = 2[(1 + 2\mu\lambda_p) - (\beta + Y)]^{-1} \quad (\text{A.8})$$

where, $X = 1 + \beta - 2\mu\lambda_p$ and $Y = \sqrt{(1 + \beta - 2\mu\lambda_p)^2 - 4\beta(1 + 2\alpha\mu\lambda_p)}$

Example 2: Under a typical condition *i.e.*, $\alpha = \beta = 0$, the MG-LMS reduces to the conventional LMS algorithm with poles located at $P_1 = (1 - 2\mu\lambda_p)$ and $P_2 = 0$. It leads to [equation (75), 57] *i.e.*,

$$\tau_p \approx 1/2\mu\lambda_p \quad (\text{A.9})$$

APPENDIX – B

Equations for estimated weight error

From subsection 4.4.2, the received composite signal vector is

$$\hat{r}(i) = \hat{D}(i)\hat{h}_o(i) + \hat{z}(i) \quad (\text{B.1})$$

The substitution of (4.20) and (4.21) in (4.24) leads to

$$\hat{h}(i|i) - \hat{h}_o(i) = \hat{h}(i|i-1) + \mu\hat{D}^T(i)[\hat{r}(i) - \hat{D}(i)\hat{h}(i|i-1)] - \hat{h}_o(i) \quad (\text{B.2})$$

Using (B.1) and (B.2), we can solve the above equation as:

$$\Delta\hat{h}(i) = [I - \mu\hat{D}^T(i)\hat{D}(i)]\Delta\hat{h}(i|i-1) + \mu\hat{D}^T(i)\hat{z}(i) \quad (\text{B.3})$$

$$\text{where, } \Delta\hat{h}(i|i-1) = \hat{h}(i|i-1) - \hat{h}_o(i) \quad \text{with } \hat{h}_o(i-1) = \hat{h}_o(i) - \hat{h}_o(i-1) \quad (\text{B.4})$$

The equation (B.4) can be simplified by using (4.22) in terms of the first-order weight increment vector as:

$$\Delta\hat{h}(i|i-1) = \Delta\hat{h}(i-1) + \Delta\dot{\hat{h}}(i-1) - (1 - \beta)\dot{\hat{h}}(i-1|i-1) \quad (\text{B.5})$$

The first-order weight increment error vector is defined using (4.20), (4.23) and (4.24) as:

$$\dot{\hat{h}}(i|i) - \dot{\hat{h}}_o(i) = \dot{\hat{h}}(i-1|i-1) + \alpha\mu\hat{D}^T(i)[\hat{r}(i) - \hat{r}_e(i)] - \dot{\hat{h}}_o(i) \quad (\text{B.6})$$

Using (B.1) and (B.6), we can solve the above equation as:

$$\Delta\dot{\hat{h}}(i) = \dot{\hat{h}}(i-1|i-1) - [\alpha\mu\hat{D}^T(i)\hat{D}(i)]\Delta\hat{h}(i|i-1) - \dot{\hat{h}}_o(i) + \alpha\mu\hat{D}^T(i)\hat{z}(i) \quad (\text{B.7})$$

The equation (B.7) can be simplified in terms of the first-order and second-order weight increment vectors as:

$$\Delta\dot{\hat{h}}(i) = \Delta\dot{\hat{h}}(i-1) - [\alpha\mu\hat{D}^T(i)\hat{D}(i)]\Delta\hat{h}(i|i-1) - \ddot{\hat{h}}_o(i-1) + \alpha\mu\hat{D}^T(i)\hat{z}(i) \quad (\text{B.8})$$

In the above equation, we have considered $\ddot{\hat{h}}_o(i-1) = \dot{\hat{h}}_o(i) - \dot{\hat{h}}_o(i-1)$. The results (B.3), (B.5) and (B.8) can be written in the matrix form to define the recursive vector $\Phi(i)$ i.e., (4.25).

Determination of the partial cancellation factor

Let the i th data symbol of k th user be b_k with amplitude A_k . The estimated value of the data symbol at the output of F_{lin} is $\hat{x}_{lin,k}$. The corresponding error is $e_{lin}^k = b_k - \hat{x}_{lin,k}$. The erasure algorithm (see subsection 5.2.2) is stated as:

$$\begin{cases} |\hat{x}_{lin,k}| > |2A_k| \text{ or } 1 - \left(|e_{lin}^k|^2 / |A_k|^2 \right) < 0 \longrightarrow w_{pcf}^k = 0 \\ 0 < |\hat{x}_{lin,k}| \leq |2A_k| \longrightarrow w_{pcf}^k = 1 - \left(|e_{lin}^k|^2 / |A_k|^2 \right) \end{cases}$$

We replace b_k with the tentative decision $b_{ik} = \text{sgn}(\hat{x}_{lin,k})$ in the decision directed mode. The output of E-slicer is $w_{pcf}^k b_{ik}$. The proposed partial PIC system is equivalent to the “Brute Force” interference canceller [116], if we let $w_{pcf}^k(i) = 1$. Note that we have considered $A_k = 1$ for $k = 1, 2, \dots, K$ in the generation of PCFs.

REFERENCES

- [1] R. L. Pickholtz, D. L. Schilling, and L. B. Milstein, "Theory of spread spectrum communications – A tutorial," *IEEE Trans. Commun.*, vol. 30, no. 5, pp. 855 – 884, May 1982.
- [2] G. L. Stuber, *Principles of Mobile Communications*, 2nd ed., Kluwer Academic Publishers, 2001.
- [3] L. B. Milstein, "Wideband code division multiple access," *IEEE J. Select. Areas Commun.*, vol. 18, no. 8, pp. 1344 – 1354, Aug. 2000.
- [4] B. Melis and G. Romano, "UMTS W-CDMA: Evaluation of radio performance by means of link level simulations," *IEEE Personal Commun.*, vol. 7, no. 3, pp. 42 – 49, June 2000.
- [5] E. Dahlman, B. Gudmundson, Mats Nilsson, and J. Skold, "UMTS/IMT-2000 based on wideband CDMA," *IEEE Commun. Mag.*, pp. 70 – 79, vol. 36, no. 9, Sept. 1998.
- [6] F. Adachi, M. Sawahashi, and H. Suda, "Wideband DS-CDMA for next-generation mobile communication systems," *IEEE Commun. Mag.*, vol. 36, no. 9, pp. 56 – 69, Sept. 1998.
- [7] D. Koulakiotis and A. H. Aghvami, "Data detection techniques for DS/CDMA mobile systems: A review," *IEEE Personal Commun.*, vol. 7, no. 3, pp. 24 – 34, June 2000.
- [8] S. L. Miller, M. L. Honig, and L. B. Milstein, "Performance analysis of MMSE receivers for DS-CDMA in frequency-selective fading channels," *IEEE Trans. Commun.*, vol. 48, no. 11, pp. 1919 – 1929, Nov. 2000.
- [9] J. E. Smee and S. C. Schwartz, "Adaptive space-time feed-forward/feedback detection for high data rate CDMA in frequency-selective fading," *IEEE Trans. Commun.*, vol. 49, no. 9, pp. 317 – 328, Feb. 2001.
- [10] J. E. Smee and S. C. Schwartz, "Adaptive feedforward/feedback architectures for multiuser detection in high data rate wireless CDMA networks," *IEEE Trans. Commun.*, vol. 48, no. 6, pp. 996 – 1011, June 2000.
- [11] G. L. Turin, "The effects of multipath and fading on the performance of Direct-Sequence CDMA systems," *IEEE J. Select. Areas Commun.*, vol. 43, no. 2/3/4, pp. 1746 – 1755, Feb./Mar./Apr. 1995.
- [12] S. Verdú, "Minimum probability of error for asynchronous Gaussian multiple-access

- channels,” *IEEE Trans. Inform. Theory*, vol. 32, no. 1, pp. 85 – 96, Jan. 1986.
- [13] S. Moshavi, “Multiuser detection for DS-CDMA communications,” *IEEE Commun. Mag.*, vol. 34, no. 10, pp. 124 – 136, Oct. 1996.
- [14] M. Abdulrahman, A. U. H. Sheikh, and D. D. Falconer, “Decision feedback equalization for CDMA in indoor wireless communications,” *IEEE J. Select. Areas Commun.* vol. 12, no. 4, pp. 698 – 706, May 1994.
- [15] C. A. Belfiore and J. H. Park, “Decision-feedback equalization,” *Proc. IEEE*, vol. 67, no. 8, pp. 1143 – 1156, Aug. 1979.
- [16] R. Kohno, H. Imai, and M. Haroti, “Cancellation techniques for co-channel interference in asynchronous spread spectrum multiple access systems,” *Electron. Commun. Jpn.*, vol. 66, no. 5, pp. 20 – 29, May 1983.
- [17] R. Lupas and S. Verdú, “Near-far resistance of multiuser detectors in asynchronous channels,” *IEEE Trans. Commun.*, vol. 38, no. 4, pp. 496 – 508, Apr. 1990.
- [18] R. Lupas and S. Verdú, “Linear multiuser detectors for synchronous code-division-multiple-access channels,” *IEEE Trans. Inform. Theory*, vol. 35, no. 1, pp. 123 – 136, Jan. 1989.
- [19] Z. Xie, R. T. Short, and C. K. Rushforth, “A family of sub-optimum detectors for coherent multiuser communications,” *IEEE J. Select. Areas Commun.*, vol. 8, no. 4, pp. 683 – 690, May 1990.
- [20] M. K. Tsatsanis and G. B. Giannakis, “Optimal decorrelating receivers for DS-CDMA systems: A signal processing framework,” *IEEE Trans. Signal Processing*, vol. 44, no. 12, pp. 3044 – 3054, Dec. 1996.
- [21] M. Honig, U. Madhow, and S. Verdú, “Blind adaptive multiuser detection,” *IEEE Trans. Inform. Theory*, vol. 41, no. 4, pp. 944 – 960, July 1995.
- [22] M. S. Pinsky, V. V. Prelov, and S. Verdú, “Sensitivity of channel capacity,” *IEEE Trans. Inform. Theory*, vol. 41, no. 6, pp. 1877 – 1888, Nov. 1995.
- [23] A. McKellips and S. Verdú, “Worst case additive noise for binary-input channels and zero-threshold detection under constraints of power and divergences,” *IEEE Trans. Inform. Theory*, vol. 43, no. 4, pp. 1256 – 1264, July 1997.
- [24] A. M. Monk, M. Davis, L. B. Milstein, and C. W. Helstrom, “A noise-whitening approach to multiple access noise rejection – Part I: Theory and background,” *IEEE J. Select. Areas Commun.*, vol. 12, no. 5, pp. 817 – 827, June 1994.
- [25] M. B. Pursley, “Performance evaluation for phase-coded spread spectrum multiple-access communication – Part I: System analysis,” *IEEE Trans. Commun.*, vol. 25, no.

- 8, pp. 795 – 799, Aug. 1977.
- [26] E. A. Geraniotis and M. B. Pursley, “Error probability for direct-sequence spread-spectrum multiple-access communications – Part II: Approximations,” *IEEE Trans. Commun.*, vol. 30, no. 5, pp. 985 – 995, May 1982.
- [27] H. V. Poor and S. Verdú, “Probability of error in MMSE multiuser detection”, *IEEE Trans. Inform. Theory*, vol. 43, no. 3, pp. 858 – 871, May 1997.
- [28] B. R. Saltzberg, “Intersymbol interference error bounds with applications to ideal bandlimited signals,” *IEEE Trans. Inform. Theory*, vol. IT-14, no. 4, pp. 563 – 568, **July 1968**.
- [29] G. V. Moustakides and H. V. Poor, “On the relative error probabilities of linear multiuser detectors,” *IEEE Trans. Inform. Theory*, vol. 47, no. 1, pp. 450 – 456, Jan. 2001.
- [30] M. L. McCloud and L. L. Scharf, “Asymptotic analysis of the MMSE multiuser detector for nonorthogonal multipulse modulation,” *IEEE Trans. Commun.*, vol. 49, no. 1, pp. 24 – 30, Jan. 2001.
- [31] A. Lampe and M. Breiling, “Asymptotic analysis of widely linear MMSE multiuser detection – complex vs. real modulation,” *IEEE Inform. Theory Workshop*, Sept. 2001, pp. 55 – 57.
- [32] S. Verdú and S. Shamai, “Spectral efficiency of CDMA with random spreading,” *IEEE Trans. Inform. Theory*, vol. 45, no. 2, pp. 622 – 640, Mar. 1999.
- [33] S. Buzzi, M. Lops, and A. M. Tulino, “MMSE multiuser detection in multipath fading channels,” *Proc. ICASSP’99, IEEE International Conference on Acoustics, Speech and Signal Processing*, vol. 5, Mar. 1999, pp. 2715 – 2718.
- [34] S. Verdú, “Optimum multiuser asymptotic efficiency,” *IEEE Trans. Commun.*, vol. 34, no. 9, pp. 890 – 897, Sept. 1986.
- [35] J. Zhang, K. P. Chong, and N. C. David, “Output MAI distributions of linear MMSE multiuser receivers in DS-CDMA systems,” *IEEE Trans. Inform. Theory*, vol. 47, no. 3, pp. 1128 – 1144, Mar. 2001.
- [36] Y. Wang, J. Wu, Z. Du, and W. Wu, “Performance of MMSE multiuser detection for downlink CDMA,” *Proc. ICC’2000, IEEE Int. Conf. on Commun.*, June 2000, pp. 919 – 923.
- [37] Y. Wang, J. Wu, Z. Du, and W. Wu, “Performance analysis of MMSE multiuser detection,” *Proc. WCC-ICCT’2000, Int. Conf. on Commun. Tech.*, Aug. 2000, pp. 1341–1346.

- [38] U. Madhow and M. L. Honig, "MMSE interference suppression for direct sequence spread spectrum CDMA," *IEEE Trans. Commun.*, vol. 42, no. 12, pp. 3178 – 3188, Dec. 1994.
- [39] S. L. Miller, "An adaptive direct-sequence code-division multiple-access receiver for multiuser interference rejection," *IEEE Trans. Commun.*, vol. 43, no. 2/3/4, pp. 1746 – 1755, Feb./Mar./Apr. 1995.
- [40] S. L. Miller, "Training analysis of adaptive interference suppression for direct-sequence code-division multiple-access systems," *IEEE Trans. Commun.*, vol. 44, no. 4, pp. 488 – 495, Apr. 1996.
- [41] U. Madhow, "MMSE interference suppression for timing acquisition and demodulation of DS-CDMA signals," *IEEE Trans. Commun.*, vol. 46, no. 8, pp. 1065 – 1075, Aug. 1998.
- [42] P. B. Rapajic and D. K. Borah, "Adaptive MMSE maximum likelihood CDMA multiuser detection," *IEEE J. Select. Areas Commun.*, vol. 17, no. 12, pp. 2110 – 2121, Dec. 1999.
- [43] S. Haykin, *Adaptive Filter Theory*, 4th ed., Person Education Inc., 2002.
- [44] B. C. Banister and J. R. Zeidler, "Tracking performance of the RLS algorithm applied to an antenna array in a realistic fading environment," *IEEE Trans. Signal Processing*, vol. 50, no. 5, pp. 1037 – 1050, May 2002.
- [45] S. Haykin, A. H. Sayed, J. R. Zeidler, P. Yee, and P. C. Wei, "Adaptive tracking of linear time-variant systems by extended RLS algorithms," *IEEE Trans. Signal Processing*, vol. 45, no. 5, pp. 1118 – 1128, May 1997.
- [46] A. H. Sayed and T. Kailath, "A state-space approach to adaptive RLS filtering," *IEEE Signal Processing Mag.*, vol. 11, no. 3, pp. 18 – 60, July 1994.
- [47] L. Davis, I. Collings, and R. Evans, "Coupled estimators for equalization of fast-fading mobile channels," *IEEE Trans. Commun.*, vol. 46, no. 10, pp. 1262 – 1265, Oct. 1998.
- [48] J. Chen and Y. Wang, "Adaptive MLSE equalizers with parametric tracking for multipath fast-fading channels," *IEEE Trans. Commun.*, vol. 49, no. 4, pp. 655 – 663, Apr. 2001.
- [49] A. M. Sayeed and B. Aazhang, "Joint multipath-Doppler diversity in mobile wireless communications," *IEEE Trans. Commun.*, vol. 47, no. 1, pp. 123 – 132, Jan. 1999.
- [50] A. M. Sayeed, A. Sendonaris, and B. Aazhang, "Multiuser detection in fast fading multipath environments," *IEEE J. Select. Areas Commun.*, vol. 16, no. 9, pp. 1691 –

1701, Dec. 1998.

- [51] R. A. Iltis, "An EKF-Based joint estimation for interference, multipath, and code delay in a DS spread-spectrum receiver," *IEEE Trans. Commun.*, vol. 42, no. 2/3/4, pp. 1288 – 1299, Feb./Mar./Apr. 1994.
- [52] R. A. Iltis and L. Mailaender, "An adaptive multiuser detector with joint amplitude and delay estimation," *IEEE J. Select. Areas Commun.*, vol. 12, no. 5, pp. 774 – 785, June 1994.
- [53] L. Lindbom, M. Sternad, and A. Ahlén, "Tracking of time-varying mobile radio channels – Part I: The Wiener LMS algorithm," *IEEE Trans. Commun.*, vol. 49, no. 12, pp. 2207 – 2217, Dec. 2001.
- [54] A. Ahlén, L. Lindbom, and M. Sternad, "Analysis of stability and performance of adaptation algorithms with time-invariant gains," *IEEE Trans. Signal Processing*, vol. 52, no. 1, pp. 103 – 116, Jan. 2004.
- [55] L. Lindbom, M. Sternad, A. Ahlén, and M. Falkenström, "Tracking of time-varying mobile radio channels – Part II: A case study," *IEEE Trans. Commun.*, vol. 50, no. 50, pp. 156 – 167, Jan. 2002.
- [56] H. S. Wang and P. Chang, "On verifying the first-order Markovian assumption for a Rayleigh fading channel model," *IEEE Trans. Veh. Tech.*, vol. 45, no. 2, pp. 353 – 357, May 1996.
- [57] B. Widrow, J. M. McCool, M. G. Larimore, and C. R. Johnson, "Stationary and nonstationary learning characteristics of the LMS adaptive filter," *Proc. IEEE*, vol. 64, no. 8, pp. 1151 – 1162, Aug. 1976.
- [58] B. Widrow and E. Walach, "On the statistical efficiency of the LMS algorithm with nonstationary inputs," *IEEE Trans. Inform. Theory*, Special Issue on Adaptive Filtering, vol. IT-30, no. 3, pp. 211 – 221, Mar. 1984.
- [59] A. Benveniste, "Design of one-step and multi-step adaptive algorithms for the tracking of time-varying systems," *Rapport de Recherche, INRIA, IRISA*, no. 340, Sept. 1984.
- [60] S. Gazor, "Predictions in LMS-Type adaptive algorithms for smoothly time-varying environments," *IEEE Trans. Signal Processing*, vol. 47, no. 6, pp. 1735 – 1739, June 1999.
- [61] B. Farhang-Borojeny, *Adaptive Filters: Theory and Applications*, London, U.K.: Wiley, 1998.
- [62] B. Farhang-Borojeny and S. Gazor, "Performance of LMS-based adaptive filter in

- tracking a time-varying plant,” *IEEE Trans. Signal Processing*, vol. 44, no. 11, pp. 2868 – 2871, Nov. 1996.
- [63] Y. Xue and X. Zhu, “Second-order LMS based wireless channel tracking: Implementation under imperfect carrier synchronization,” *Signal Processing*, vol. 83, no. 1, pp. 199 – 212, Jan. 2003.
- [64] O. Macchi, “Optimization of adaptive identification for time-varying filters,” *IEEE Trans. Automat. Contr.*, vol. AC-31, no. 3, pp. 283 – 287, Mar. 1986.
- [65] O. M. Macchi and N. J. Bershad, “Adaptive recovery of a chirped sinusoid in noise, Part I: Performance of the RLS algorithm,” *IEEE Trans. Signal Processing*, vol. 39, no. 3, pp. 583 – 594, Mar. 1991.
- [66] N. J. Bershad and O. M. Macchi, “Adaptive recovery of a chirped sinusoid in noise, Part II: Performance of the LMS algorithm,” *IEEE Trans. Signal Processing*, vol. 39, no. 3, pp. 595 – 602, Mar. 1991.
- [67] O. M. Macchi, *Adaptive Processing: The LMS Approach with Applications in Transmission*, New York: Wiley, 1995.
- [68] D. A. George, R. R. Bowen, and J. R. Storey, “An adaptive decision feedback equalizer,” *IEEE Trans. Commun.*, vol. 19, no. 3, pp. 281 – 293, June 1971.
- [69] P. Mosen, “MMSE equalization of interference on fading diversity channels,” *IEEE Trans. Commun.*, vol. COM-32, no. 1, pp. 5 – 12, Jan. 1984.
- [70] B. Mulgrew and S. Chen, “Adaptive minimum-BER decision feedback equalizers for binary signalling,” *Signal Processing*, vol. 81, pp. 1479 – 1489, July 2001.
- [71] S. R. Chaudhary and A. U. H. Sheikh., “Performance of a dual rate DS-CDMA DFE in an overlaid cellular system,” *IEEE Trans. Veh. Tech.*, vol. 48, no. 3, pp. 683 – 695, May 1999.
- [72] A. Klein, G. K. Kaleh, and P. W. Baier, “Zero forcing and minimum mean square error equalization for multiuser detection in code division multiple access channels,” *IEEE Trans. Veh. Tech.*, vol. 45, no. 2, pp. 276 – 287, Feb. 1996.
- [73] P. B. Rapajic and B. S. Vucetic, “Adaptive receiver structures for asynchronous CDMA systems,” *IEEE J. Select. Areas Commun.*, vol. 12, no. 4, pp. 685 – 697, May 1994.
- [74] G. Woodward and B. S. Vucetic, “Adaptive detection for DS-CDMA,” *Proc. IEEE*, vol. 86, no. 7, pp. 1413 – 1434, July 1998.
- [75] M. Honig and M. K. Tsatsanis, “Adaptive techniques for multiuser CDMA receivers: Enhanced signal processing with short spreading codes,” *IEEE Signal Processing*

Mag., vol. 17, no. 3, pp. 49 – 61, May 2000.

- [76] Y. Gu and T. Le-Ngoc, “Adaptive combined DFE/MLSE techniques for ISI channels,” *IEEE Trans. Commun.*, vol. 44, no. 7, pp. 847 – 857, July 1996.
- [77] T. F. Wong, Q. Zhang, and J. S. Lehnert, “Decision-feedback MAP receiver for time-selective fading CDMA channels,” *IEEE Trans. Commun.*, vol. 48, no. 5, pp. 829 – 840, May 2000.
- [78] Y. Lee and D. C. Cox, “MAP selection diversity DFE for indoor wireless data communication,” *IEEE J. Select. Areas Commun.*, vol. 16, no. 8, pp. 1376 – 1384, Oct. 1998.
- [79] M. Chiani, “Analysis of error propagation in decision feedback equalizers with erasures,” Univ. of Bologna, Bologna, Italy, DEIS Tech. Rep., Dec. 1994.
- [80] M. Chiani, “Introducing erasures in decision-feedback equalization to reduce error propagation,” *IEEE Trans. Commun.*, vol. 45, no. 7, pp. 757 – 760, July 1997.
- [81] M. Torlak and G. Xu, “Blind multiuser channel estimation in asynchronous CDMA systems,” *IEEE Trans. Signal Processing*, vol. 45, no. 1, pp. 137 – 147, Jan. 1997.
- [82] L. Tong, G. Xu, and T. Kailath, “Blind identification and equalization based on second-order statistics: A time domain approach,” *IEEE Trans. Inform. Theory*, vol. 40, no. 2, pp. 340 – 349, Apr. 1994.
- [83] C. B. Papadias and A. Paulraj, “Decision-feedback equalization and identification of linear channels using blind algorithms of the Bussgang type,” *Proc. IEEE Int. Conf. Asilomar-29*, 1996, pp. 335 – 340.
- [84] D. Gesbert, J. Sorelius, P. Stoica, and A. Paulraj, “Blind multiuser MMSE detector for CDMA signals in ISI channels,” *IEEE Commun. Letters*, vol. 3, no. 8, Aug. 1999.
- [85] X. Wang and H. V. Poor, “Blind equalization and multiuser detection in dispersive CDMA channels,” *IEEE Trans. Commun.*, vol. 46, no. 1, pp. 91 – 103, Jan. 1998.
- [86] R. T. Causey and J. R. Barry, “Blind multiuser detection using linear prediction,” *IEEE J. Select. Areas Commun.*, vol. 16, no. 9, pp. 1702 – 1710, Dec. 1998.
- [87] S. N. Diggavi, B. C. Ng, and A. Paulraj, “An interference suppression scheme with joint channel-data estimation,” *IEEE J. Select. Areas Commun.*, vol. 17, no. 11, pp. 1924 – 1939, Nov. 1999.
- [88] D. S. Chen and S. Roy, “An adaptive multiuser receiver for CDMA systems,” *IEEE J. Select. Areas Commun.*, vol. 12, no. 5, pp. 808 – 816, June 1994.
- [89] L. Chen, B. Chen, and W. S. Hou, “Adaptive multiuser DFE with Kalman channel estimation for DS-CDMA systems in multipath fading channels,” *Signal Processing*,

- vol. 81, no. 4, pp. 713 – 733, Apr. 2001.
- [90] M. S. Grewal and A. P. Andrew, *Kalman Filtering: Theory and Practice*, Englewood Cliffs, NJ: Prentice-Hall, 1993.
 - [91] D. Godard, “Channel equalization using a Kalman filter for fast data transmission,” *IBM J. Res. Develop.*, vol. 18, pp. 267 – 273, May 1974.
 - [92] R. E. Lawrence and H. Kaufman, “The Kalman filter for the equalization of a digital communication channel,” *IEEE Trans. Commun. Tech.*, vol. 19, no. 6, pp. 1137 – 1141, Dec. 1971.
 - [93] B. W. Kozminchuk and A. Sheikh, “A Kalman filter-based architecture for interference excision,” *IEEE Trans. Commun.*, vol. 43, no. 2/3/4, pp. 574 – 580, Feb./Mar./Apr. 1995.
 - [94] T. J. Lim and L. K. Rasmussen, “Adaptive symbol and parameter estimation in asynchronous multiuser CDMA detector,” *IEEE Trans. Commun.*, vol. 45, no. 2, pp. 213 – 220, Feb. 1997.
 - [95] T. J. Lim, “An asynchronous multiuser CDMA detector based on the Kalman filter,” *IEEE J. Select. Areas Commun.*, vol. 10, no. 9, pp. 1711 – 1722, Dec. 1998.
 - [96] T. J. Lim and Y. Ma, “The Kalman filter as the optimal linear minimum mean-squared error multiuser CDMA detector,” *IEEE Trans. Inform. Theory*, vol. 46, no. 7, pp. 2561 – 2566, Nov. 2000.
 - [97] S. McLaughlin, “Adaptive equalization via Kalman filtering techniques,” *Proc. IEE*, vol. 138, no. 4, pp. 388 – 396, Aug. 1991.
 - [98] R. E. Kalman, “A new approach to linear filtering and prediction problems,” *Trans. ASME, Series D., J. Basic Eng.*, vol. 82, pp. 34 – 45, 1960.
 - [99] R. E. Kalman and R. S. Bucy, “New results in linear filtering and prediction,” *Trans. ASME, Series D., J. Basic Eng.*, vol. 83, pp. 95 – 108, 1961.
 - [100] B. Mulgrew, “Kalman filter techniques in adaptive filtering,” *Proc. IEE*, vol. 134, pp. 239 – 243, June 1987.
 - [101] L. Chen and B. Chen, “A robust adaptive DFE receiver for DS-CDMA system under multipath fading channels,” *IEEE Trans. Signal Processing*, vol. 49, no. 7, pp. 1523 – 1532, July 2001.
 - [102] B. Chen, C. Tsai, and C. Hsu, “Robust adaptive MMSE/DFE multiuser detection in multipath fading channel with impulse noise,” *IEEE Trans. Signal Processing*, vol. 53, no. 1, pp. 306 – 317, Jan. 2005.
 - [103] P. H. Wu and A. Duel-Hallen, “Multiuser detectors with disjoint Kalman channel

- estimators for synchronous CDMA mobile radio channels,” *IEEE Trans. Commun.*, vol. 48, no. 5, pp. 752 – 757, May 2000.
- [104] C. Komninakis, C. Fragouli, A. H. Sayed, and R. D. Wesel, “Multi-input multi-output fading channel tracking and equalization using Kalman estimation,” *IEEE Trans. Signal Processing*, vol. 50, no. 5, pp. 1065 – 1076, May 2002.
- [105] P. A. Bello, “Characterisation of randomly time-variant linear channels,” *IEEE Trans. Commun.*, vol. CS-11, no. 4, 360 – 393, Dec. 1963.
- [106] R. R. Müller, and S. Verdú, “Spectral efficiency of low-complexity multiuser detectors,” *Proc. IEEE Inter. Symposium on Inform. Theory*, June 2000, pp. 25 – 30.
- [107] R. R. Müller, “Power and bandwidth efficiency of multiuser systems with random spreading,” Ph.D. Dissertation, Univ. of Erlangen-Nürnberg, 1999.
- [108] P. B. Rapajic, M. L. Honig, and G. K. Woodward, “Multiuser decision-feedback detection: Performance bounds and adaptive algorithms”, *Proc. IEEE Int. Symp. Inform. Theory*, Boston, MA, p. 34, Aug. 1998.
- [109] A. Duel-Hallen, “Decorrelating decision-feedback multiuser detector for synchronous code-division multiple-access channel,” *IEEE Trans. Commun.*, vol. 41, no. 2, pp. 285 – 290, Feb. 1993.
- [110] A. Duel-Hallen, “Equalizers for multiple input/multiple output channels and PAM systems with cyclostationary input sequence,” *IEEE J. Select. Areas Commun.*, vol. 10, no. 3, pp. 630 – 639, Apr. 1992.
- [111] A. Duel-Hallen, “A family of multiuser decision-feedback detectors for asynchronous code-division multiple-access channels,” *IEEE Trans. Commun.*, vol. 43, no. 2/3/4, pp. 421 – 434, Feb./Mar./Apr. 1995.
- [112] A. J. Viterbi, “Very low rate convolutional codes for maximum theoretical performance of spread spectrum multiple access channels,” *IEEE J. Select. Areas Commun.*, vol. 8, no. 4, pp. 641 – 649, May 1990.
- [113] R. Kohno, H. Imai, M. Haroti, and S. Pasupathy, “Combination of an adaptive array antenna and a canceller of interference for direct-sequence spread-spectrum multiple-access system,” *IEEE J. Select. Areas Commun.*, vol. 8, no. 4, pp. 675 – 682, May 1990.
- [114] P. Patel and J. Holtzman, “Performance comparison of a DS/CDMA system using interference cancellation (IC) scheme and a parallel IC scheme under fading,” *Proc. ICC’94*, New Orleans, LA., May 1994, pp. 510 – 514.
- [115] P. Patel and J. Holtzman, “Analysis of a simple successive interference cancellation

- scheme in a DS/CDMA system,” *IEEE J. Select. Areas Commun.*, vol. 12, no. 5, pp. 796 – 806, June 1994.
- [116] D. Divsalar, M. K. Simon, and D. Raphaeli, “Improved parallel interference cancellation for CDMA,” *IEEE Trans. Commun.*, vol. 46, no. 2, pp. 258 – 268, Feb. 1998.
- [117] R. M. Buehrer and S. P. Nicoloso, “Comments on partial parallel interference cancellation for CDMA,” *IEEE Trans. Commun.*, vol. 47, no. 5, pp. 658 – 661, May 1999.
- [118] P. G. Renucci and B. D. Woerner, “Analysis of soft cancellation to minimize BER in DS-CDMA interference cancellation,” *Proc. Int. Conf. Telecommun.*, 1998.
- [119] X. Guo and C. Li, “Performance of partial parallel interference cancellation in DS-CDMA system with delay estimation errors,” *Proc. 11th Int. Symp. Personal, Indoor, Mobile Radio Commun.*, London, U. K., Sept. 2000, pp. 724 – 727.
- [120] G. Xue, J. Weng, T. Le-Ngoc, and S. Tahar, “Adaptive multistage parallel interference cancellation for CDMA,” *IEEE J. Select. Areas Commun.*, vol. 17, no. 10, pp. 1815 – 1827, Oct. 1999.
- [121] S. R. Kim, I. Choi, S. Kang, and J. G. Lee, “Adaptive weighted parallel interference cancellation for CDMA systems,” *Electronics Letters*, vol. 34, no. 22, pp. 2085 – 2086, Oct. 1998.
- [122] Y. Li, M. Chen, and S. Cheng, “Determination of cancellation factors for soft-decision partial PIC detector in DS/CDMA systems,” *Electronics Letters*, vol. 36, no. 3, pp. 239 – 241, Feb. 2000.
- [123] M. Ghotbi and M. R. Soleymani, “Multiuser detection of DS-CDMA signal using partial parallel interference cancellation in satellite communications,” *IEEE J. Select. Areas Commun.*, vol. 22, no. 3, pp. 584 – 593, Apr. 2004.
- [124] W. Hou, L. Chen, and B. Chen, “Adaptive narrowband interference rejection in DS-CDMA systems: A scheme of parallel interference cancellers,” *IEEE J. Select. Areas Commun.*, vol. 19, no. 6, pp. 1103 – 1114, June 2001.
- [125] Y. Hsieh and W. Wu, “Optimal two-stage decoupled partial PIC receiver for multiuser detection,” *IEEE Trans. Wireless Commun.*, vol. 4, no. 1, pp. 112 – 127, Jan. 2005.
- [126] W. Hou and Bor-Sen Chen, “Adaptive detection in asynchronous code-division multiple-access system in multipath fading channels,” *IEEE Trans. Commun.*, vol. 48, no. 5, pp. 863 – 873, May 2000.

- [127] A. Host-Madsen and K. Cho, "MMSE/PIC multiuser detection for DS/CDMA with inter- and intra-cell interference," *IEEE Trans. Commun.*, vol. 47, no. 2, pp. 291 – 299, Feb. 1999.
- [128] R. Ratasuk, G. Woodward, and M. L. Honig, "Adaptive multiuser decision-feedback for asynchronous cellular DS-CDMA," *Proc. Annu. Allerton Conf. Commun. Control and Computing*, Monticello, IL., Sept. 1999, pp. 1236 – 1245.
- [129] G. Woodward, R. Ratasuk, M. L. Honig, and P. B. Rapajic, "Minimum mean-squared error multiuser decision-feedback detectors for DS-CDMA", *IEEE Trans. Commun.*, vol. 50, no. 12, pp. 2104 – 2111, Dec. 2002.
- [130] M. K. Varanasi and B. Aazhang, "Multistage detection for asynchronous code-division multiple-access communications," *IEEE Trans. Commun.*, vol. 38, no. 4, pp. 509 – 519, Apr. 1990.
- [131] M. K. Varanasi and B. Aazhang, "Optimally near-far resistant multiuser detection in differentially coherent synchronous channels," *IEEE Trans. Inform. Theory*, vol. 37, no. 4, pp. 1006 – 1018, July 1991.
- [132] M. K. Varanasi and B. Aazhang, "Near-optimum detection in synchronous code-division multiple-access systems," *IEEE Trans. Commun.*, vol. 39, no. 5, pp. 725 – 736, May 1991.
- [133] M. K. Varanasi and T. Guess, "Optimum decision feedback multiuser equalization with successive decoding achieves the total capacity of the Gaussian multiple-access channel," *Proc. 31st Asilomar Conf. Signals, Systems and Computers*, Monterey, CA., Nov. 1997, pp. 1405 – 1409.
- [134] D. W. Waters and J. R. Barry, "Noise-predictive decision-feedback detection for multiple-input multiple-output channels," *IEEE Trans. Signal Processing*, vol. 53, no. 5, pp. 1852 – 1859, May 2005.
- [135] J. M. Cioffi and G. D. Forney et al., "Generalized decision-feedback equalization for packet transmission with ISI and Gaussian noise," in *Communication, Computation, Control and Signal Processing*, A. Paulraj et al., Eds. Boston, MA: Kluwer, 1997, ch. 4, pp. 79 – 127.
- [136] G. Ginis and J. M. Cioffi, "On the relation between V-BLAST and the GDFE," *IEEE Commun. Letters*, vol. 5, no. 9, pp. 364 – 366, Sept. 2001.
- [137] N. A. Dhahir and J. M. Cioffi, "MMSE decision feedback equalizers: Finite length results," *IEEE Trans. Inform. Theory*, vol. 41, no. 4, pp. 961 – 975, July 1995.
- [138] J. M. Cioffi, G. P. Dudevoir, M. V. Eyuboglu, and G. D. Forney, "MMSE decision

- feedback equalizers and coding-part I: Equalization results,” IEEE Trans. Commun., vol. 43, no. 10, pp. 2582 – 2594, Oct. 1995.
- [139] N. Al-Dhahir and A. H. Sayed, “The finite-length multi-input multi-output MMSE-DFE,” IEEE Trans. Signal Processing, vol. 48, no. 10, pp. 2921 – 2936, Oct. 2000.
- [140] G. J. Foschini, G. D. Golden, R. A. Valenzuela, and P. Wolniansky, “Simplified processing for wireless communication at high spectral efficiency,” IEEE J. Select. Areas Commun., vol. 17, no. 11, pp. 1841 – 1852, Nov. 1999.
- [141] G. D. Golden, C. J. Foschini, R. A. Valenzuela, and P. W. Wolniansky, “Detection algorithm and initial laboratory results using V-BLAST space-time communication architecture,” Electronics Letters, vol. 35, no. 1, pp. 14 – 16, Jan. 1999.
- [142] W. Wai, C. Tsui, and R. S. Cheng, “A low complexity architecture of the V-BLAST system,” Proc. IEEE Wireless Commun. Networking Conf., vol. 1, 2000, pp. 310 – 314.
- [143] S. Verdú, *Multiuser Detection*, Cambridge, U.K.: Cambridge Univ. Press, 1998.
- [144] M. B. Pursley and D. V. Sarwate, “Performance evaluation for phase-coded spread spectrum multiple-access communication – Part II: Code sequence analysis,” IEEE Trans. Commun., vol. 25, no. 8, pp. 800 – 803, Aug. 1977.
- [145] M. B. Pursley, D. V. Sarwate, and W. E. Stark, “Error probability for direct-sequence spread-spectrum multiple-access communications – Part I: Upper and lower bounds,” IEEE Trans. Commun., vol. 30, no. 5, pp. 975 – 984, May 1982.
- [146] D. K. Borah and P. B. Rapajic, “Optimal adaptive multiuser detection in unknown multipath channels,” IEEE J. Select. Areas Commun., vol. 19, no. 6, pp. 1115 – 1127, June 2001.
- [147] D. R. Anderson and P. A. Wintz, “Analysis of a spread-spectrum multiple-access system with a hard limiter,” IEEE Trans. Commun., vol. 17, pp. 285 – 290, Apr. 1969.
- [148] J. C. Vanelli and N. M. Shehadeh, “Computation of bit-error probability using the trapezoidal integration rule,” IEEE Trans. Commun., vol. 22, no. 8, pp. 331 – 334, Mar. 1974.
- [149] T. Kailath, *Linear Systems*, Englewood Cliffs, NJ.: Prentice-Hall, 1980.
- [150] J. G. Proakis, *Digital Communications*, 3rd ed., McGraw-Hill Inc., 1995.
- [151] S. Haykin and T. K. Bhattacharya, “Modular learning strategy for signal detection in nonstationary environment,” IEEE Trans. Signal Processing, vol. 45, no. 6, pp. 1619 – 1637, June 1997.

- [152] H. J. Kushner, *Approximation and Weak Convergence Methods for Random Process with Applications to Stochastic System Theory*, Cambridge, MA.: MIT Press, 1984.
- [153] A. V. Oppenheim and R.W. Schaffer, *Discrete Time Signal Processing*, Englewood Cliffs, NJ: Prentice-Hall, 2001.
- [154] W. C. Jakes, *Microwave Mobile Communications*, New York: McGraw-Hill, 1994.
- [155] H. Wu and A. Duel-Hallen, "On the performance of coherent and noncoherent multiuser detectors for mobile radio CDMA channels," Proc. 5th IEEE Int. Conf. on Universal Personal Commun., Oct. 1996, pp. 76 – 80.
- [156] B. D. O. Anderson and J. B. Moore, *Optimal Filtering*, Englewood Cliffs, NJ: Prentice-Hall, 1979.
- [157] K. J. Kim and R. A. Iltis, "Joint detection and channel estimation algorithm for QS-CDMA signals over time-varying channels," IEEE Trans. Commun., vol. 50, no. 5, pp. 845 – 855, May 2002.
- [158] J. Choi, S. R. Kim, and C. Lim, "Receivers with chip-level decision feedback equalizer for CDMA downlink channels," IEEE Trans. Wireless Commun., vol. 3, no. 1, pp. 300 – 314, Jan. 2004.
- [159] C. Cao, L. Xie, H. Zhang, and S. Xie, "A robust channel estimator for DS-CDMA systems under multipath fading channels," IEEE Trans. Signal Processing, vol. 54, no. 1, pp. 13 – 22, Jan. 2006.
- [160] H. L. Van Trees, *Optimum Array Processing*, New York: Wiley-Interscience, 2002.
- [161] H. L. Van Trees, *Detection, Estimation, and Modulation Theory – Part I*, New York: John Wiley & Sons Inc., 2002.
- [162] G. Yen and A. N. Michel, "A learning and forgetting algorithm in associative memories: Results involving pseudo-inverses," IEEE Trans. Circuit and Systems, vol. 38, no. 10, pp. 1193 – 1205, Oct. 1991.
- [163] A. L. C. Hui and K. B. Letaief, "Successive interference cancellation for multiuser asynchronous DS/CDMA detectors in multipath fading links," IEEE Trans. Commun., vol. 46, no. 3, pp. 384 – 391, Mar. 1998.
- [164] K. Lai and J. J. Shynk, "Analysis of the linear SIC for DS/CDMA signals with random spreading," IEEE Trans. Signal Processing, vol. 52, no. 12, pp. 3417 – 3428, Dec. 2004.
- [165] R. A. Iltis and S. Kim, "Geometric derivation of expectation-maximization and generalized successive interference cancellation algorithms with applications to CDMA channel estimation," IEEE Trans. Signal Processing, vol. 51, no. 5, pp. 1367 –

1377, May 2003.

- [166] M. F. Madkour, S. C. Gupta, and Y. E. Wang, "Successive interference cancellation algorithms for downlink W-CDMA communications," *IEEE Trans. Wireless Commun.*, vol. 1, no. 1, pp. 169 – 177, Jan. 2002.
- [167] R. M. Buehrer, N. S. Mendoza, and B. D. Woerner, "A simulation comparison of multiuser receivers for cellular CDMA," *IEEE Trans. Veh. Tech.*, vol. 49, no. 4, pp. 1065 – 1085, July 2000.
- [168] R. M. Buehrer, "Equal BER performance in linear successive interference cancellation for CDMA systems," *IEEE Trans. Commun.*, vol. 49, no. 7, pp. 1250 – 1258, July 2001.
- [169] L. K. Rasmussen, T. J. Lim, and A. Johansson, "A matrix-algebraic approach to successive interference cancellation in CDMA," *IEEE Trans. Commun.*, vol. 48, no. 1, pp. 145 – 151, Jan. 2000.
- [170] Y. Cho and J. H. Lee, "Analysis of an adaptive SIC for near-far resistant DS-SS-SSA," *IEEE Trans. Commun.*, vol. 46, no. 11, pp. 1429 – 1432, Nov. 1998.
- [171] P. W. Wolniansky, G. J. Foschini, G. D. Golden, and R. A. Valenzuela, "V-BLAST: An architecture for realizing very high data rates over rich-scattering wireless channel," *Proc. Int. Symp. Signals Syst., Electron.*, Oct. 1998, pp. 295 – 300.
- [172] R. Narasimhan, "Error propagation analysis of V-BLAST with channel-estimation errors," *IEEE Trans. Commun.*, vol. 53, no. 1, pp. 27 – 31, Jan. 2005.
- [173] G. H. Golub and C. F. Van Loan, *Matrix Computations*, 3rd ed., Baltimore, MD: Johns Hopkins Univ. Press, 1996.
- [174] T. Aboulnasr and K. Mayyas, "A robust variable step-size LMS-type algorithm: Analysis and simulations," *IEEE Trans. Signal Processing*, vol. 45, no. 3, pp. 631 – 639, Mar. 1997.

PUBLICATIONS BASED ON THIS WORK

International journals

1. Amit Kumar Kohli and D. K. Mehra, "Adaptive MMSE decision feedback equalizer for asynchronous CDMA with erasure algorithm," *Digital Signal Processing*, Elsevier, vol. 15, no. 6, pp. 621 – 630, Nov. 2005.
2. Amit Kumar Kohli and D. K. Mehra, "New results for probability of error performance in MMSE multiuser detection for CDMA," *Digital Signal Processing*, Elsevier, In Press.
3. Amit Kumar Kohli and D. K. Mehra, "Tracking of time-varying channels using two-step LMS-type adaptive algorithm," *IEEE Trans. Signal Processing*, In Press. (To appear in Aug. 2006)
4. Amit Kumar Kohli and D. K. Mehra, "Adaptive DFE multiuser receiver for CDMA systems using reduced Kalman/LMS algorithm – An equalization approach," *Digital Signal Processing*, Elsevier, Under Review.
5. Amit Kumar Kohli and D. K. Mehra, "A two-stage MMSE multiuser decision feedback detector using successive/parallel interference cancellation," *Digital Signal Processing*, Elsevier, Under Review.
6. Amit Kumar Kohli and D. K. Mehra, "Adaptive multiuser decision feedback detector – A novel parallel interference canceller," *IEEE Communication Letters*, Under Review.

International conference

7. Amit Kumar Kohli and D. K. Mehra, "Bounds on MMSE multiuser detection for CDMA," *Proceeding of Inter. Conf. on Signal Processing and Communications*, IEEE, I.I.Sc., Bangalore, India, Dec. 2004, pp. 101 – 105.

National conference

8. Amit Kumar Kohli and D. K. Mehra, "Adaptive multiuser decision feedback detection using erasure algorithm based partial parallel interference cancellation," *Proceeding of National Conference on Communications*, I.I.T.D., Delhi, India, Jan. 2006.

Page	Line	Existing form	Correction
ii	11	in the BER performance.	in the BER performance at low SNR.
3	09	more affective than	more effective than
3	14	are considered to solve	have been considered to solve
5	12	MUD technique supersedes	MUD technique supercedes
9	12	into a Weiner filtering problem.	into a Wiener filtering problem.
10	04	It supersedes the conventional	It supercedes the conventional
17	11	when ever the power profile changes.	whenever the power profile changes.
124	10	by considering MAI as noise	by considering MAI due to intra-cell users as noise
170	22	NP-S-DF (ZF-ordering)	NP-S-DFD (ZF-ordering)

G 13009